GIS-BASED STUDIES FOR ARTIFICIAL GROUNDWATER RECHARGE IN WESTERN GANGA PLAINS

A THESIS

Submitted in partial fulfilment of the requirements for the award of the degree of

DOCTOR OF PHILOSOPHY

in

EARTH SCIENCES

By

RATAN KUMAR SAMADDER

DEPARTMENT OF EARTH SCIENCES
INDIAN INSTITUTE OF TECHNOLOGY ROORKEE
ROORKEE-247 667 (INDIA)

MARCH, 2008

INDIAN INSTITUTE OF TECHNOLOGY ROORKEE
ROORKEE

CANDIDATE'S DECLARATION

I hereby certify that the work is being presented in the thesis entitled **GIS-BASED STUDIES FOR ARTIFICIAL GROUNDWATER RECHARGE IN WESTERN GANGA PLAINS** in partial fulfilment of the requirements for the award of the degree of Doctor of Philosophy and submitted in the Department of Earth Sciences of the Indian Institute of Technology Roorkee, Roorkee is an authentic record of my own work carried out during a period from July 2004 to March 2008 under the supervision of Dr. R. P. Gupta, Professor and Head, Department of Earth Sciences, Indian Institute of Technology Roorkee, Roorkee and Dr. Sudhir Kumar, Scientist E1, National Institute of Hydrology, Roorkee.

The matter presented in this thesis has not been submitted by me for the award of any other degree of this or any other Institute.

Ratan Kr Samadder

(RATAN KUMAR SAMADDER)

This is to certify that the above statement made by the candidate is correct to the best of our knowledge.

Sudhir Kr.

(Sudhir Kumar)
Supervisor

(R. P. Gupta)
Supervisor

Date: 25/3/08

The Ph. D. viva voce examination of **Mr. Ratan Kumar Samadder**, Research Scholar, has been held on _____.

Signature of Supervisors

Signature of External Examiners

Abstract

The Indo-Gangetic Plains, the land where our civilization has been nurtured, is a land of fertile soil, moderate climate and abundant water. These factors have combined to make this a region of plenty for human settlement. Groundwater is a major source of water available for consumption in this area. However, over the years due to swelling population, increasing industrialization and expanding agriculture, the demand of water has increased manifold. Simultaneously, the available per-capita water resource has been reduced due to generally declining groundwater table. Hence, there is a tremendous need to take up augmentation measures.

In the present work, a systematic study has been taken up for developing a strategy to replenish groundwater artificially in the study area, lying in the western part of the Indo-Gangetic Plains. The main objectives of the research work are: (a) application of Remote Sensing — GIS techniques to map spatial distribution of porous and permeable stretches, which happen to be parts of paleochannels of the Ganga river, (b) evaluation of hydrogeological characteristics of the paleochannel-aquifers and also the adjacent alluvial plains, (c) estimation of allowable recharge volume of the rechargeable aquifer, and (d) estimation of source water availability and planning for artificial recharge.

The study area (between latitudes $29^0 10'$N to $29^0 50'$N and longitudes $77^0 30'$E to $78^0 10'$E) exhibits the characteristics of a river flood plain. The area slopes gently from north to south, at an average gradient of less than 0.38 m km^{-1}. Hydrogeologically it comprises extensive, multiple alluvial aquifer systems, composed of unconsolidated to

semi-consolidated deposits of sand, clay and calcium carbonate concretions that constitute a good groundwater reservoir system.

The following datasets have been used for the study: (a) Remote Sensing data: IRS-1B LISS-II multi-spectral; (b) Survey of India toposheets at 1:50,000 scale; (c) Soil map from National Bureau of Soil Survey and Land Use Planning, (d) other data such as specific yield, storage coefficient etc. collected from various sources, and (e) field data. The remote sensing data has been processed by using ERDAS Imagine-8.7 software. The GIS analysis has been carried out using ILWIS-3.3, ARCVIEW-3.2 and R2V software. Litholog data analysis is carried out by using ROCKWORKS-2006 software.

A base map has been prepared from the Survey of India topographic maps by scanning, geo-referencing, mosaicking and digitizing. All the data layers have been co-registered with the base map. Point data obtained from field and laboratory experiment are properly placed on the base map and finally various information have been obtained using GIS tools.

The IRS-1B LISS-II multispectral data have been co-registered with the base map, and corrected for atmospheric path radiance and striping, and enhanced for improving interpretability. The IRS-1B-LISS-II sensor data has been used as the primary data source to implement the supervised classification for generating landuse/landcover (LULC) map. Six LULC classes - agricultural land, paleochannel, dry streams, water body, built-up area, and marshy land, have been chosen and a LULC map has been generated with an overall accuracy of 87.9% using Maximum Likelihood Classifier (MLC). Finally, integrating information from colour infra-red composites and LULC map, a paleochannel map has been generated. The existence of paleochannels has also been cross-checked from litholog data and field observations.

In the study area, three major paleochannels characterized by serpentine and meandering pattern, have been deciphered. The paleochannels are located to the west of the present day course of the river Ganga. Most of the paleochannels are very wide (2-5 km) suggesting their formation by a large river. Thus, it can be inferred that the Ganga river has gradually shifted from the west to the east. Field observations have revealed that the soils in the paleochannels are generally coarse sand. Rather sparse vegetation and low surface moisture over the paleochannel areas are indicative of highly permeable, porous, coarse grained materials possessing high infiltration rate. This is amply indicated by the spectral characteristics such as, very light tone in NIR band, and yellowish-white colour in CIR composites.

The litholog data have been analysed to determine aquifer depth and lithological details. It has been observed that the paleochannel aquifer mainly consists of coarse sand occasionally mixed with pebbles, and boulders of varying sizes. On the other hand, the aquifers of adjacent alluvial plains are mainly composed of medium to fine grained sand along with clay and kankar beds.

Construction of subsurface lithological cross-section, construction of paleochannel aquifer geometry and its inter-connectivity with the adjacent alluvial plains aquifer has been done by aggregating and synthesizing all the information, such as the lithological information, the base map, the CIR composite image, paleochannel map, well location map, and the DEM. The first aquifer (≈ 25-30 m thick) in the alluvial plains is unconfined and consists of fine to medium sand with several lenses of clay and kankar. The second aquifer is confined in nature and mainly consists of fine to medium grained sand along with some lenses of kankar. The paleochannel aquifer is unconfined and is mainly composed of coarse sandy material along with boulder and pebbles beds. This

paleochannel aquifer extends upto a depth of about 65 m and is well inter-connected with the adjacent alluvial aquifers.

A series of 17 observation wells systematically sited on the paleochannel and its either flanks have been drilled and sampling has been carried out for collecting lithological information at different depths. Grain size analysis has been conducted for 82 samples. Based on grain-size analyses and the use of the Hazen (1911) equation, the bulk hydraulic conductivity for selected core samples at different depths has been estimated. It is found that the value of hydraulic conductivity ranges from 30 to 75.3 m/day for samples falling in the paleochannel, and that between 13.5 to 22.3 m/day for the alluvial plain aquifers.

The natural groundwater recharge rate due to precipitation has been estimated using tritium tagging technique. Comparison of recharge rates and hydrogeologic characteristics in different landforms indicates that: (a) paleochannel area have coarse grained soil (sandy loam) and high recharge rate of 18.9 to 28.7%, and (b) the alluvial plains have medium to fine grained soil (silty loam) and relatively lower recharge rate (6.3 to 8.9 %).

Stable isotopes of groundwater samples from the first unconfined aquifer of the study area have been analysed using Dual Inlet Mass Spectrometer. The study indicates that the alluvial plains aquifers get recharged dominantly by canal and/or rainfall. The data also indicates that the influence of canal water to groundwater recharge decreases away from the canal, where rainfall recharge component relatively increases. It is also inferred that rainfall/precipitation constitute the dominant source for groundwater recharge in paleochannel aquifers.

Groundwater levels have been monitored at 37 locations (12 on the paleochannel aquifers and 25 on the adjacent alluvial plains aquifer) over 2 years (2005-2006) for both pre- and post-monsoon period. The precise locations (x, y, z co-ordinates) have been

determined through differential GPS. Interpretation have been made by combining information of paleochannel map, reduced water level contour map and flow direction map. It has been observed that groundwater flows away from the paleochannel in both pre- and post-monsoon period, which is related to the high hydraulic conductivity and porosity of the paleochannel aquifer. This further indicates that recharging of groundwater through paleochannels would lead to gradually recharging of the aquifers in the alluvial plains.

For estimating the rainfall runoff in the three watersheds in the study area, the Soil Conservation Service Curve Number (SCS-CN) method has been used. Further, for planning artificial recharge of the paleochannel aquifer, its storage potential has been estimated, and the value is found to be 89.5×10^6 m^3. On the other hand, the volume of water required for arresting the decline of groundwater table over the three watersheds is estimated as 34.6×10^6 m^3. Sources of water considered for artificial recharge are rainfall runoff and the canal water. A flow accumulation has been generated from DEM in GIS. Considering the various aspects, an integrated three-stage planning using rainfall runoff water and barely 1% of canal discharge in the lean water demand period (July-September), has been suggested – that would be sufficient to meet the requirement of artificial recharge and arrest the declining groundwater table in the area.

Acknowledgement

First and foremost, I would like to express my sincere gratitude to my supervisors **Dr. R. P. Gupta**, Professor and Head, Department of Earth Sciences, IIT Roorkee and **Dr. Sudhir Kumar**, Scientist E1, National Institute of Hydrology, Roorkee for motivating me towards this area of research and their able guidance. **Professor Gupta** will forever remain my creditor for his caring attitude and emotional backing at every stage in this work. The amount of freedom to think and coping up with problems that inevitably arise in the course of research given by him deserve a special mention. On the other hand, I have learnt the nuances and fruits produced by hard work from **Dr. Kumar**, who has graduated in my relationship with him from a guide to a caring friend. He always encouraged me by giving innovative ideas and friendly help.

I am grateful to **Professor V. N. Singh**, former Head, **Professor B. Prakash**, Emiritus Profesor and Ex-Professor, **Professor R. G. S. Sastri**, Department of Earth Sciences, IIT Roorkee for providing research facilities during the course of this work. I would especially like to thank **Professor A. K Awasthi**, Ex-Dean, PGS & R, for administrative help at different stages in my Ph.D. tenure.

I would like to thank **Dr. Bhishm Kumar**, Scientist F and **Mr. S. K. Verma**, Scientist C, National Institute of Hydrology, Roorkee for their help at different stages of the thesis.

I sincerely thank **Mr. S. K. Malhotra**, Engineer, Groundwater Department, Uttar Pradesh for providing the hydrological and meteorological data.

This is also an opportunity for me to convey a special word of thanks to **Dr. M. K. Arora**, Professor, Department of Civil Engineering, IIT Roorkee for extending help, support and facilities during the course of this research work.

The financial assistance provided by the **Ministry of Human Resource Development** (MHRD), New Delhi, India, in the form of Research Fellowships, is duly acknowledged.

I cannot but express my heartfelt thanks to the people of Muzzaffarnagar and surrounding areas for their help during the field data collection.

I am grateful to **Lekhraj, Ashish Misra, Nisha** and other research scholars of the Remote Sensing Lab., Department of Earth Sciences, IIT Roorkee for their enthusiastic help and ready assistance whenever and whichever way I sought it.

The help extended by **Mr. Sarvesh Sharma, Mr. M. Nair** and other technical and non-technical staff of the Department of Earth Sciences, IIT Roorkee is duly acknowledged.

Finally, my heart goes on a spin when I think of the contribution by my **Parents** and **brothers** towards whatever little or much I have been able to achieve. Without their blessing and emotional strength, I would have never seen this day. I cannot express my feeling towards my wife **Beauty**. Without her company and mental support; this research would never gained the shape as it has now.

Ratan Kumar Samadder

Contents

	Page No.
Abstract	i
Acknowledgement	vii
Contents	ix
List of Figures	xiii
List of Tables	xvii
Chapter 1: Introduction	1
1.1 Introduction	1
1.2 Study Area	3
1.2.1 Location and Extent	3
1.2.2 Physiography	3
1.2.3 Climate	4
1.3 Geology	4
1.3.1 Regional Set Up	4
1.3.2 Regional Hydrogeology	11
1.3.3 Regional Landforms	12
1.3.4 Tectonic Faults	13
1.4 Soil Types and Crops	13
1.5 Drainage	14
1.6 Rationale of the Present Study	14
1.7 Research Objectives	20
1.8 Organization of the Thesis	21
Chapter 2: Artificial Recharge – a Brief Overview	23
2.1 Introduction	23
2.2 Factors Governing Artificial Recharge	24
2.3 Data Types/Studies Needed for Planning Artificial Recharge	26
2.3.1 Detailed Studies for Site Selection	27

	Page No.
2.3.2 Estimation of Sub-surface Potential for Groundwater Recharge	32
2.3.3 Recharge Methods/ Site-specific Mechanisms	32
2.4 Role of Remote Sensing – GIS in Artificial Recharge Studies	33
2.4.1 Role of Remote Sensing	34
2.4.2 Role of GIS	42
2.4.3 Remote Sensing - GIS in Artificial Groundwater Studies	45
Chapter 3: Data Sources and Methodology-Overview	49
3.1 Introduction	49
3.2. Remote Sensing Data	50
3.3 Ancillary Data	51
3.4 Field Data	52
3.4.1 Collection of Existing Lithologs	52
3.4.2 Drilling Operations	53
3.4.3 Soil Sample Collection	59
3.4.3.1 Collection of Samples	59
3.4.3.2 Laboratory Analysis of Soil Samples	60
3.4.4 Groundwater Level Data Collection	63
3.4.5 Groundwater Sample Collection	64
3.4.6 Tracer Studies	64
3.5 Software Used	65
3.6 Methodology-Overview	66
Chapter 4: Mapping of Major Paleochannels from Remote Sensing Data	69
4.1 Introduction	69
4.2 Major Landform/Landcover (LULC) Classes	70
4.3 Pre-Processing of Remote Sensing Data	76
4.4 Processing of Remote Sensing Data	81
4.4.1 Image Classification	81
4.4.2 Post-classification Filtering	86
4. 5 Paleochannel Mapping	86

	Page No.
4.6 Distribution of Major Paleochannel	91
Chapter 5: Hydrogeological Characteristics	93
5.1 Introduction	93
5.2 Soil Texture	94
5.3 Vertical Hydraulic Conductivity	99
5.4 Recharge Source Identification	111
5.5 Groundwater Flow	122
Chapter 6: Delineation of Paleochannel Aquifer Geometry	129
6.1 Introduction	129
6.2 Methodology	130
6.3 Litholog Data Analysis	130
6.4 Data Integration and Interpretation	132
6.5 Interpretation and Construction of Aquifer Geometry	149
Chapter 7 : Natural Groundwater Recharge Estimation by Tracer Technique	155
7.1 Introduction	155
7.2 Tritium Tagging	157
7.2.1 Site Selection	157
7.2.2 Injection of Tritium at the Selected Sites	157
7.2.3 Soil Sampling	158
7.3 Laboratory Experiments	158
7.3.1 Soil moisture content	158
7.3.2 Water Extraction from Soil Sample	162
7.3.3Tritium Activity Measurement with LSC	162
7.4 Determination of Recharge to Groundwater	167
7.5 Particle Size Analysis	172
7.6 Estimation of Specific Yield	173
7.7 Results	176
ANNEXURE-I	177
ANNEXURE-II	189

	Page No.
Chapter 8 : Source Water Availability and Recharge Planning	193
8.1 Introduction	193
8.2 Flow Accumulation Map Generation	195
8.3 Estimation of Surface Runoff through SCS-CN Method	195
8.3.1 Database Generation	196
8.3.1.1 Landuse/Landcover	196
8.3.1.2 Hydrological Soil Group	203
8.3.2 SCS Curve Number Method for Runoff Estimation	205
8.3.3 Spatial Intersection and Derivation of Curve Number	206
8.3.4 Estimation of Antecedent Moisture Condition (AMC)	210
8.3.5 Runoff Estimation for the Watersheds	211
8.4 Estimation of Actual Allowable Recharge for the Paleochannel Aquifer	213
8.5 Planning for Artificial Recharge	215
Chapter 9 : Summary and Conclusions	219
References	233

List of Figures

Figure No.	Title	Page No.
Figure 1.1:	Location map of the study area. Selected well locations are also marked.	5
Figure 1.2:	Monthly variation in rainfall data averaged for 18 years (1985-2002).	7
Figure 1.3:	Geological map of the study area (Pandy et al., 1963).	9
Figure 1.4:	Variation of groundwater level in different wells during 1995-2004. The locations of these wells are shown in Figure 1.1.	15
Figure 1.5:	The increasing trend of population in the study area (data for the years 1991 and 2001).	19
Figure 1.6:	Three-year moving average of area, production and productivity of rice and wheat in Uttar Pradesh. (a) Rice and (b) Wheat.	20
Figure 2.1:	Diagram of different artificial recharge methods in different hydrogeological environments (Gale et al., 2002).	35
Figure 2.2:	Flow chart showing data flow for site selection of artificial recharge by integrated remote sensing and GIS technique.	47
Figure 3.1:	Sample of one 'Strata Chart' collected from Tube Well Division of Uttar Pradesh.	55
Figure 3.2:	Drilling conducted on the paleochannel near Berla village. (a) Machine operated 'Bukki System' and (b) Different parts of 'Bukki System'.	57
Figure 3.3:	Flow diagram showing the broad methodology adopted in this study.	67
Figure 4.1:	Field photographs. (a) Paleochannel near Barla village (note the scant vegetation and agricultural activity and presence of coarse sand); (b) Agricultural field in the alluvial plains and (c) Trace of Fault/Scarp near Harinagar village.	71

Figure No.	Title	Page No.
Figure 4.2:	Colour infra-red composite of LISS-II image (NIR band coded in red colour; Red band codded in green colour and Green band coded in blue colour) showing various LULC classes (AG-Agricultural lands; P-Paleochannel; BL- Built-up areas; ML-Marshy lands; WB-Water body DS-Dry stream/flood plains and F-F: Fault scarp).	73
Figure 4.3:	Flow diagram showing image processing techniques adopted in the study.	77
Figure 4.4:	Supervised classification approach adopted in this study.	83
Figure 4.5:	Landcover map possessing accuracy of 87.9% generated from band combination 4, 1, 2,3 (i.e. NIR, Red, Green and Blue bands of LISS-II image). A post-classification filtering has been applied.	87
Figure 4.6:	Major paleochannels of the study area.	89
Figure 5.1:	Location map of soil samples and drilling sites.	95
Figure 5.2:	Soil samples plotted on USDA soil textural triangle.	97
Figure 5.3a:	Grading curves of samples falling within the paleochannel (see Figure 5.1 for locations).	101
Figure 5.3b:	Grading curves of samples falling within the paleochannel (see Figure 5.1 for locations).	103
Figure 5.4a:	Grading curves of samples falling within the alluvial plains (see Figure 5.1 for locations).	105
Figure 5.4b:	Grading curves of samples falling within the alluvial plains (see Figure 5.1 for locations).	107
Figure 5.5:	Location map of water samples for stable isotope analysis. Also paleochannel, Ganga Canal and major distributaries are shown on the background.	117
Figure 5.6:	Variation of $\delta^{18}O$ in groundwater and precipitation water of Roorkee.	119
Figure 5.7:	$\delta^{18}O$ and δD characterization of the recharging sources and groundwater.	119
Figure 5.8:	(a) Location map of wells; (b) Pre-monsoon reduced groundwater level contour and flow direction map.	125

Figure No.	Title	Page No.
Figure 5.9:	Post-monsoon reduced groundwater level contour and flow direction map.	127
Figure 6.1:	Flow diagram showing methodology for constructing aquifer geometry.	131
Figure 6.2:	Well location marked on the Colour Infra-red Composite (R: NIR band; G: Red band; B: Green band), generated from the IRS-LISS-II (November, 1998) image data. Major locations, paleochannels and fault-scarp are also marked on the background.	133
Figure 6.3:	(a) Lithologic description of wells 19M, 18M, 20M, 59M and 3PKJ. (b) Interpreted geological section along A-A′ through well Nos. 19M, 18M, 20M, 59M and 3PKJ (for section orientation see Figure 6.2). Note the paleochannel.	135
Figure 6.4:	(a) Lithologic description of wells 32M, 47M, 70M, 49M, 84M and 43M. (b) Interpreted geological section along B-B′ through well Nos. 32M, 47M, 70M, 49M, 84M and 43M (for section orientation see Figure 6.2). Note the paleochannel.	137
Figure 6.5:	(a) Lithologic description of wells 84M, 43M, 14M, 69M and 10JG. (b) Interpreted geological section along C-C′ through well Nos. 84M, 43M, 14M, 69M and 10JG (for section orientation see Figure 6.2). Note the paleochannel.	139
Figure 6.6:	(a) Interpreted geological section along D-D′ through well Nos. 19M, 28M, 32M, and 25M. (b) Interpreted geological section along E-E′ through well Nos. 59M, 61M, 84M and 40M. Line of section and well locations are shown in Figure 6.2.	141
Figure 6.7:	(a) Lithologic description of wells 67M, 73M, 49JG, 33JG and 78JG. (b) Interpreted geological section along F-F′ through well Nos. 67M, 73M, 49JG, 33JG and 78JG (for section orientation see Figure 6.2). Note the paleochannel.	143
Figure 6.8:	Interpreted geological section along G-G′ through well Nos. 21M, 20M, 53M, 70M and 49M (for section orientation see Figure 6.2).	145
Figure 6.9:	(a) Lithologic description of wells 6M, 40M, 45M and 54JG. (b) Interpreted geological section along H-H′ through well Nos. 6M, 40M, 45M and 54JG (for section orientation see Figure 6.2). Note the paleochannel.	147

Figure No.	Title	Page No.
Figure 7.1:	Location of tritium injection sites in paleochannels and alluvial plains, marked on the colour infra-red composite of IRS-LISS-II image data (NIR band coded in red colour; Red band coded in green colour; and Green band coded in blue colour).	159
Figure 7.2:	Flow diagram showing methodology adopted for estimating natural groundwater recharge using tritium tagging technique.	161
Figure 7.3:	Systematic diagram of injection layout for artificial tritium injection at test sites (NIH).	163
Figure 7.4:	(a) Tritium injection at selected site. (b) Soil sampling during field investigation. (c) Liquid scintillation counter at NIH (Model: WALLAC 1409). (d) Soil moisture extraction set up.	165
Figure 7.5:	Movement of tritium peak and soil moisture for location T1-T4.	169
Figure 7.6:	Movement of tritium peak and soil moisture for location T5-T8.	170
Figure 7.7:	Movement of tritium peak and soil moisture for location T9-T12.	171
Figure 7.8:	Relationship between average sand content (%) and corresponding recharge rate (%).	173
Figure 7.9:	Relationship between water table fluctuation and corresponding recharge rate (%).	174
Figure 8.1:	Flow diagram showing methodology adopted for source water estimation and planning for artificial recharge.	194
Figure 8.2:	Digital Elevation Model (DEM) of the study area.	197
Figure 8.3:	Flow accumulation map over the study area.	199
Figure 8.4:	Combined map of landuse/landcover and hydrological soil group for three watersheds.	201
Figure 8.5:	Hydrological soil group map of the study area.	207

List of Tables

Table No.	Title	Page No.
Table 1.1:	Regional geological set up and stratigraphy.	7
Table 1.2:	Pre-monsoon water table depth (m) from the year 1995 to 2004 for different locations.	17
Table 1.3:	Post-monsoon water table depth (m) from the year 1995 to 2004 for different locations.	18
Table 1.4:	Population and water demand of Muzzaffarnagar, Saharanpur and Haridwar district (Census, 1991, 2001).	19
Table 2.1:	Overview of different artificial recharge schemes (Gale et al., 2002).	37
Table 2.2:	Salient physical features of the landscape used for assessing groundwater condition from remote sensing data (Todd, 1980; Todd and Mays, 2005).	43
Table 3.1:	Salient characteristics of the satellite sensor data used.	51
Table 3.2:	Ancillary data used in this study.	52
Table 3.3:	Field data types and their purposes.	53
Table 3.4:	Pipette withdrawal times calculated from Stokes' law (Carver, 1971).	63
Table 4.1:	Characteristics of landcover/landuse classes.	75
Table 4.2:	Properties of map projection system used.	78
Table 4.3:	Number of training pixels for each LULC class used in classification.	84
Table 4.4:	Error matrix of the classified image obtained from classification of data with 1, 2, 3, 4 band combinations of LISS-II data.	86
Table 5.1:	Sand, silt and clay percent of soil samples falling in paleochannel.	99
Table 5.2:	Sand, silt and clay percent of soil samples falling in alluvial plains.	99

Table No.	Title	Page No.
Table 5.3:	Values for the coefficient 'C' (Fetter, 1994).	100
Table 5.4:	D_{10} and hydraulic conductivity (K) values for locations falling in the paleochannel aquifer.	109
Table 5.5:	D_{10} and hydraulic conductivity (K) values for locations falling in the alluvial plains aquifer.	110
Table 5.6:	Isotopic data of precipitation data at NIH, Roorkee.	116
Table 5.7:	Isotopic data of canal water from Dhanauri, Roorkee.	116
Table 5.8:	Isotope data of groundwater samples over the study area.	121
Table 5.9:	Groundwater level data used in the present study.	124
Table 7.1:	The percentage recharge to groundwater at various experimental sites due to monsoonal rain.	172
Table 7.2:	Specific yield estimated from tritium tracer technique.	174
Table 8. 1:	LULC and their corresponding CN values for different soil groups (Antecedent moisture condition II and Ia = 0.2S) (based on USDS-SCS, 1985).	203
Table 8.2:	Criteria for classification of hydrological soil group (Chow et al., 1988; Viessman et al., 1989).	204
Table 8.3:	Area of different soil group in watersheds.	205
Table 8.4:	Values of weighted curve number, retention parameter and initial abstraction for different watersheds.	209
Table 8.5:	Number of events generating surface runoff for different watersheds.	210
Table 8.6:	Antecedent moisture condition classification (USDS-SCS, 1985).	211
Table 8.7:	Average runoff depth for different landuse/landcover – soil group estimated by SCS–CN weighted method.	212
Table 8.8:	Average annual runoff for paleochannel and alluvial plains for different watersheds.	212
Table 8.9:	Annual average runoff volume for different locations.	216

Chapter 1

Introduction

1.1 Introduction

Groundwater is a precious natural resource of limited extent and volume. With the increasing use of groundwater for agricultural, municipal and industrial needs, the annual extraction of groundwater happens to be generally far in excess of its net average natural recharge. Additionally, interventions in hydrological regime and climate change have impact on natural recharge. Consequences of overexploitation of groundwater include alarming fall of water table widely observed all over the world, which may result in lower agricultural productivity, sea water intrusion in coastal aquifer, land subsidence, droughts etc. (Clarke, 1991; Falkenmark and Lundqvist, 1997; de Villiers, 2000; Tsakiris, 2004). Scientists, technocrats and planners have unanimously agreed and understood that replenishing the groundwater artificially is possibly the only remedial measure to arrest such aggressive falling groundwater tables. Therefore, artificial recharge or managed

recharge of aquifer is becoming an important aspect of studies all over the world (Barksdae and Debuchanne, 1946; Beeby-Thomson, 1950; Todd, 1959, Wright and Toit, 1996; Romani, 1998).

Broadly, the artificial recharge may be defined as a method of modifying the natural hydrological cycle and thereby providing groundwater in excess of that is available by natural processes. It is accomplished by augmenting the natural infiltration or precipitation or surface water into underground formations by some method of construction, by ponding or spreading of water, or by artificially changing the natural conditions (Bouwer, 2002; Raghunath, 2003). The main objectives of artificial recharge of groundwater may be summarized as (Tzimopoulos, 1989; CGWB, 2000):

a) To enhance the sustainable yield in areas where over-development has depleted the aquifer.
b) Conservation and storage of excess surface water for future requirements, since these requirements often change within a season or a period.
c) To modify/ improve the groundwater quality.
d) Creation of underground water barriers to halt salt water intrusion or penetration of other undesirable water into aquifer, and also to restore and restitute the contaminated aquifer.

The Indo-Gangetic Plains, the land where our civilization has been nurtured, is a land of fertile soil, moderate climate and abundant water. These factors have combined to make this a region of plenty for human settlement. Groundwater is a major source of water available for consumption in this area. However, over the years due to swelling population, increasing industrialization and expanding agriculture, the demand of water has increased manifold. Simultaneously, the available per-capita water resource has been reduced due to

generally declining groundwater table. Hence, there is a tremendous need to take up remedial/augmentation measures and plan management strategies for proper utilization of groundwater in this region and artificial recharge is an important aspect in this context.

1.2 Study Area

The western Gangetic Plains form a region of high agricultural productivity with the prevalent two to three-crop per annum system and the intensive use of groundwater for irrigation. The region forms the granary of India – a population of $1/5^{th}$ of the world. A region covering parts of Saharanpur – Muzzaffarnagar districts of Uttar Pradesh has been selected for the present study.

1.2.1 Location and Extent

The area under investigation is a part of the vast Indo–Gangetic Plains and lies between latitudes $29^0 10'N$ to $29^0 50'N$ and longitudes $77^0 30'E$ to $78^0 10'E$ with total geographic area of approximately 3000 square km. Administratively, the study area covers parts of district Saharanpur and Muzzaffarnagar of Uttar Pradesh, India. It is covered by the Survey of India Toposheets No. 53G and 53K on the scale 1: 50,000 and bound by the Ganga river on the east and Hindon river on the west (Figure 1.1).

1.2.2 Physiography

The Indo-Gangetic Plains are almost devoid of any significant relief features and are composed of unconsolidated alluvial deposits. The alluvium has been derived from the Himalayan ranges by fluvial action, which has been subsequently deposited southwards in a depression – called the Indo–Gangetic trough (Sinha et al., 2002; Jain and Sinha, 2003; Tandon et al., 2006). The area slopes down gently from north to south, at an average

gradient of less than 0.38 m per km. The physiography of the area is marked by the following landforms which are characteristics of a river flood plain: (a) the river channel, b) ox-bow lake, and (c) point bars.

A few slightly raised mounds and elongated stretches rising to a height of about 3 to 5 m above the ground surface are present at a few places in the area. These are composed of brownish coarse to medium sand and locally known as 'Bhurs' and are interpreted to be related to paleochannels.

1.2.3 Climate

The study area has a moderate to sub-tropical monsoon climate. The rainy season (monsoon) extends from 15th June to 15th September. The average annual rainfall of the study area is about 1000 mm, of which about 85% is received during the monsoon season (Figure 1.2). From October to the end of June next, generally dry condition prevails except for a few light showers received from the westerly depression coming across the Middle East. The region experiences higher temperatures during the month of May and June, with average maximum of 40 °C. The temperatures drop during the month of December and January, with minimum average of 5 °C.

1.3 Geology

1.3.1 Regional Set Up

Regionally, the study area forms a part of the Indo-Gangetic Plains lying to the south of the Siwaliks ranges that represent the molasse deposits of the Himalayas. The Indo-Gangetic Plains have been traditionally divided into three parts namely Bhabar, Tarai, and the Gangetic alluvium from north to south (Table 1.1, Figure 1.3) (Taylor, 1959;

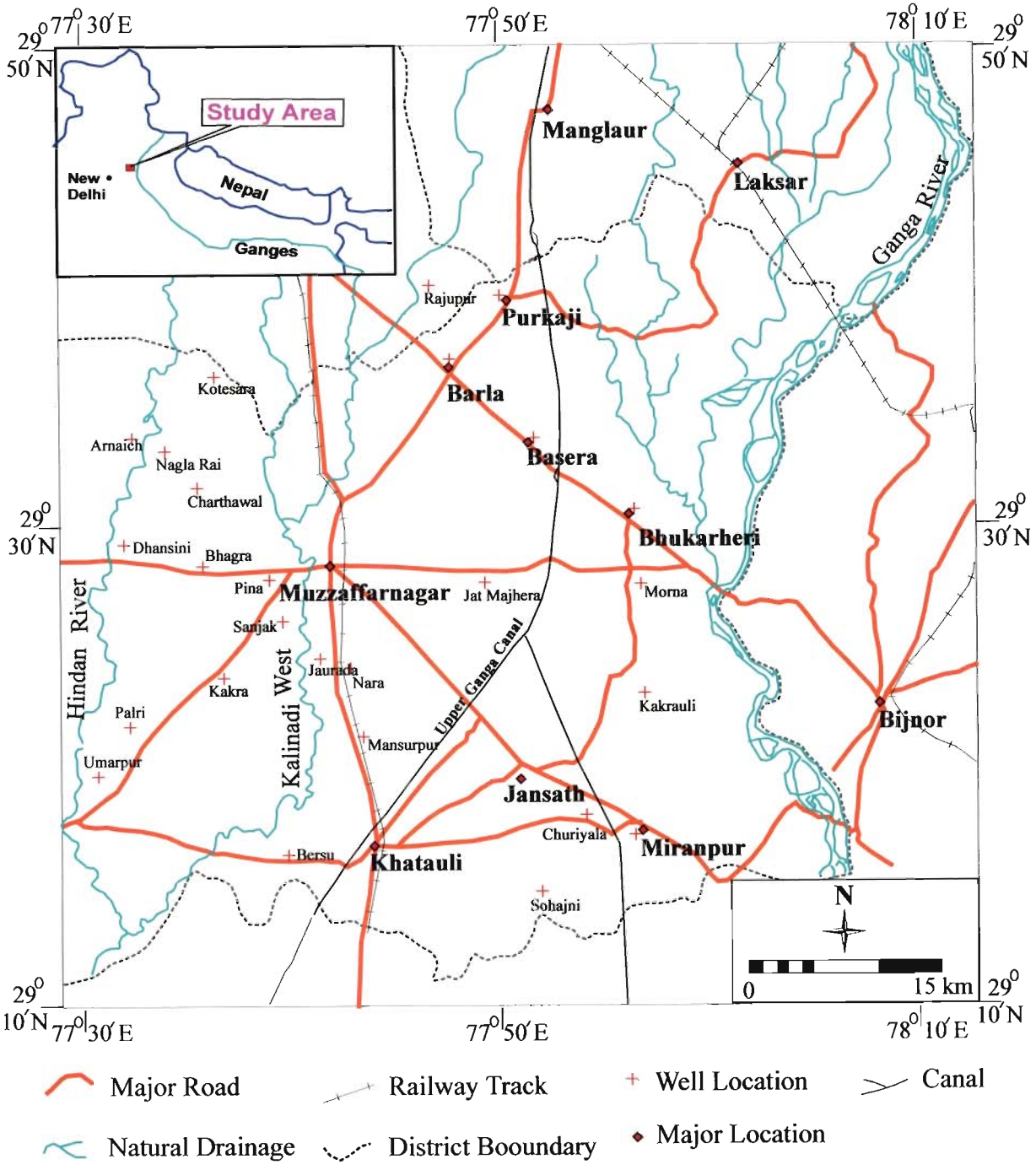

Figure 1.1: Location map of the study area. Selected well locations are also marked.

Mithal et al., 1973; Kumar et al., 1996).

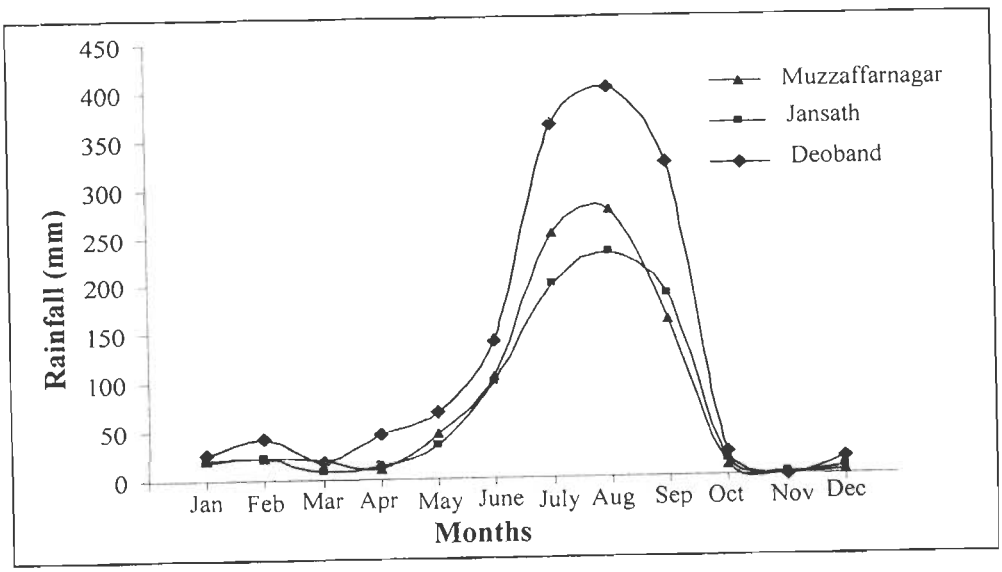

Figure 1.2: Monthly variation in rainfall data averaged for 18 years (1985-2002).

Table 1.1: Regional geological set up and stratigraphy.

AGE	FORMATION	LITHOLOGY
Recent	Bhabar Deposits	Alluvial fan deposits essentially constituted of sand boulders, clay boulders beds with gravel.
	Tarai Deposits	Sand, sandy clay, clay with gravels and pebbles
	Gangetic Alluvium	Sand, silts, clay and kankars with occasional gravel beds
Mio-Pliocene (Siwaliks)	Upper	Pebbles, boulders, conglomerates and sand rocks, green and maroon clay.
	Middle	Massive sand rocks, light gray sandstone associated with clay and calcareous beds.
	Lower	Massive hard gray to brown sandstone, gray to maroon clays

Bhabar and Tarai Belt: The Bhabar is a 9-12 km wide belt along the foothills of the Siwaliks. It is mainly made up of the unconsolidated sand boulders and clay boulder bed. The topography is normally characterized by badlands (high undulations, non-cohesive soils and sparse vegetation). The sediment matrix of Bhabar therefore, exhibits high porosity and permeability. Considerable amount of groundwater recharge takes place in this zone through direct infiltration of precipitation. Within the Gangetic alluvial basin, the water table in the Bhabar zone occurs at relative higher elevations, and represents the maximum recharge head available to the various aquifer systems occurring within the plains (Pandy et al., 1963). The northern boundary of the Bhabar belt is in contact with the Siwaliks ranges and the southern limit generally is the spring line which demarcates the northern boundary of the Tarai Belt. The Tarai Belt is a belt of 6-16 km width parallel to the Bhabar zone (Figure 1.3), and has been formed by the deposition of the finer outwash of Bhabars. It is relatively flat as compared to Bhabar, and is composed chiefly of clays with kankar, coarse sand with pebbles (~20%), little amount of fine sand and sandy clay, and occasionally thin beds of granules. The southern limit of the Tarai is not clearly defined and is generally taken as the zone where flowing conditions cease to exist in the tube wells which indicates beginning of the plains (Pandy et al., 1963). Tarai receives groundwater recharge by downward percolation and through lateral southward flow from the Bhabar belt.

Gangetic Alluvial Plains: The lower slope of Tarai merges imperceptibly with the further southward lying Gangetic alluvium, which comprises the bulk of the alluvium laid by larger streams of the Ganga and Brahmaputra system. Lithologically, it is composed of

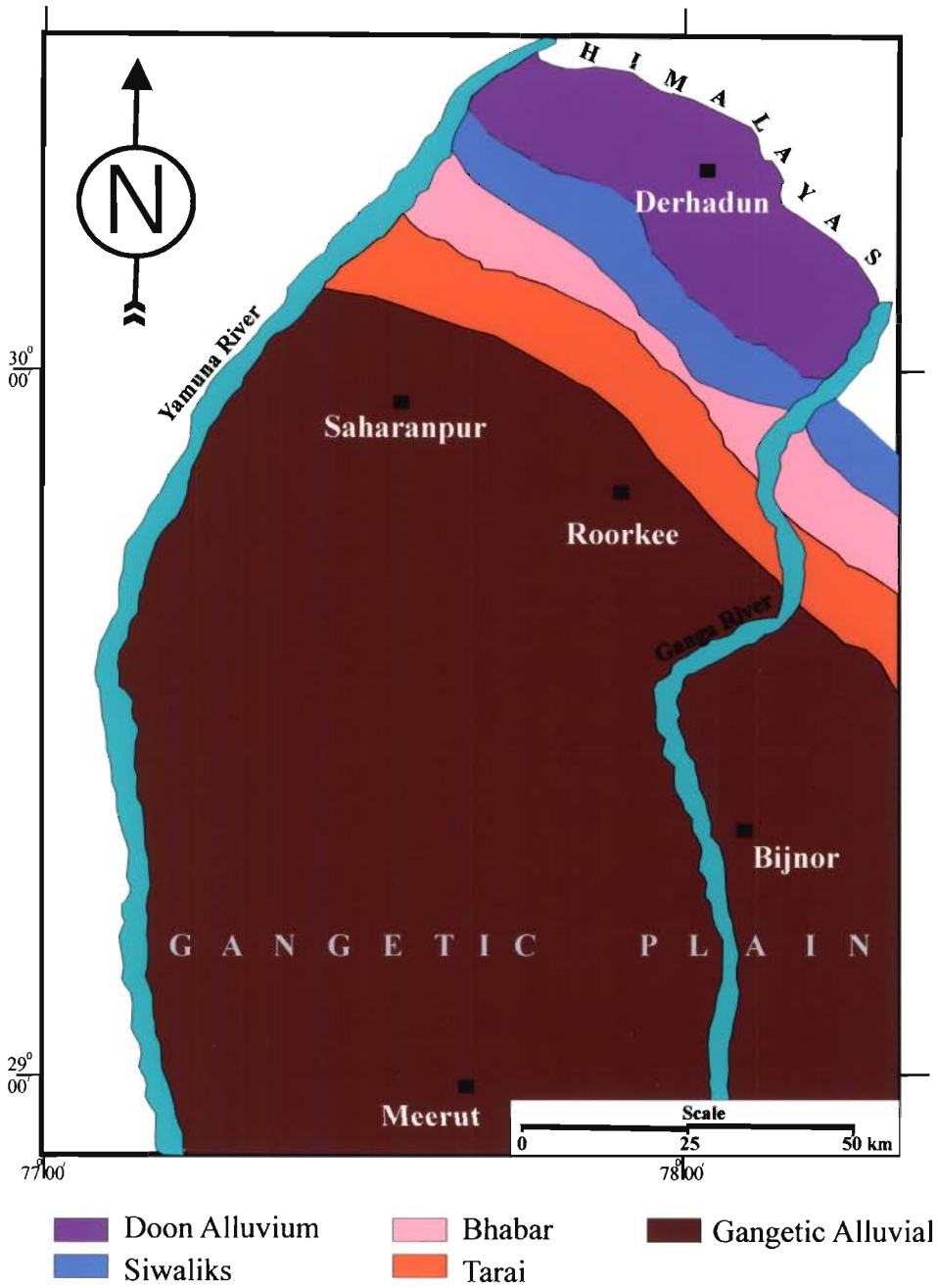

Figure 1.3: Geological map of the study area (Pandy et al., 1963).

unconsolidated and semi–consolidated deposits of sand, clay and kankar that provide a good groundwater reservoir (Panday et al., 1963). The total thickness of the alluvium is not definitely known. However, the thickness of the alluvium is variable going up to around 7 km (Kumar et al., 1996).

1.3.2 Regional Hydrogeology

The Indo-Gangetic Plains comprise extensive, multiple alluvial aquifer systems. It is mainly a vast asymmetric trough with maximum thickness of Tertiary sediments occurring in the northern ridges (thickness about 10 km) that thin out to the south. From various studies (Sastri et al., 1971; Rao, 1973; Raiverman et al., 1983; Kamal, 1999), it has been widely observed that the groundwater conditions in this alluvial part are dominantly influenced by the varying lithology of the formations. Within the Indo-Gangetic Plains, the strata are found to exhibit significant variations, both vertically and horizontally, and this heterogeneity of aquifer system leads to wide variation of groundwater availability in the area (Taylor, 1959; Singhal and Gupta, 1966; Mithal et al., 1973; Samadder et al., 2007). From the study of lithologs and water table fluctuations, two major aquifer systems have been delineated in this region. The upper one is the shallow unconfined aquifer extending to a depth of about 25 m, and the deeper one is confined to semi-confined in nature and is located between 30 to 140 m below ground level and separated by 3 to 4 aquitards located at variable depths (Singh et al., 1983). However, on a regional scale, aquifers are interconnected and hydraulically continuous throughout the plains. The main source of water which sustains groundwater body in fine to coarse grained sands is rainfall; other sources of groundwater replenishment are infiltration from river, return seepage from irrigation and inflow from neighbouring areas. Regarding the occurrence of groundwater, the principal groundwater reservoir in this region is the unconsolidated alluvial deposits

consisting mainly of interbeded as well as lenticular sand. The water level gradient is generally towards south-west in the Yamuna sub-basin and towards south-east in Ganga basin. The depth of water table varies from 3 to 18 m below ground level in the top unconfined aquifer.

1.3.3 Regional Landforms

The study area is a part of the vast Indo-Gangetic Plains, which is mainly composed of alluvium sediments transported by rivers from the Himalayas. Morphologically, four major landforms — piedmonts, plains associated with rivers, interfluves and aeolian plains have been recognized (Mohindra et al. 1992; Kumar et al. 1996; Sinha et al. 2000, Sinha et al., 2005). Within each landform, a number of soil-geomorphic units with soil character varying within small ranges are present. The major landforms are described below:

Piedmont: It is a steeply sloping, narrow (10-25 km wide), and elongated landform, drained by many parallel or sub-parallel streams. Within the piedmont zone, two soil-geomorphic units –(i) younger piedmont, and (ii) older piedmont have been recognized. The younger piedmont is overlain by poorly developed soils and sediments deposited from many braided streams traversing the area. The older piedmont is overlain by well developed soils.

Plains associated with rivers: The plains are overlain by poorly to well develop soils and their clear association with some rivers. These include Ganga Plains, Ganga-Solani Plains and Ganga-Yamuna Plains. Among them, Ganga-Yamuna Plain is the large soil geomorphic unit, gently sloping towards south (slope < 0.1m/km) and marked by numerous paleochannel of the Ganga and Yamuna rivers forming an anastomosing pattern. Most of the paleochannels are very wide (3-6 km) and are easily identified on satellite images, suggesting their formation by a large river.

Interfluves: Interfluves are upland areas and occur at highest level with respect to river floodplain levels in the adjoining areas and are overlain by moderately to strongly developed soils. The Ganga-Yamuna interfluve lies in the southern part of the study area and has been earlier called the Yamuna upland. The soil geomorphic unit in this area is often salt affected subunit. The Ganga-Ramganga interfluves have a width of 20-25 km and covered with heavy loamy soils.

1.3.4 Tectonic Faults

The Himalayan frontal fault trending NW-SE separates the geomorphic system of Siwalik hills and Gangetic Plains, and has been mapped by several workers. Besides, there are other tectonic features present, namely Solani fault, Ganga faults, Meerut fault and Balawali fault, which have also been mapped in the study area (Meijerink, 1974; Nakata, 1982; Sinhai et al., 1991; Mohindra et al., 1992; Kumar et al., 1996).

1.4 Soil Types and Crops

The soils in this region are generally deep and loamy developed on alluvium soil. The soils in general are neutral in reaction and have moderate clay and low organic carbon content. Traditionally, rain fed and irrigated agriculture is common. The main crops grown are rice, maize, pigeonpea, sorghum, pearl millet, moong beans during 'kharif' and wheat, Bengal gram, green peas, rapeseed and mustard and lentil during 'rabi' season. Sugarcane is the main cash crop. Rice–wheat cropping system is more predominant. Amongst the fruit crops, mango and guava, and amongst the vegetable crops potato, onion, brinjal, tomato, cauliflower and cabbage are widespread.

1.5 Drainage

The region, in general, is a part of well integrated drainage system of the Ganga river. Almost all the streams follow a south-eastward course, concomitant with the regional slope of the land (Figure 1.1). The extremely gentle gradient almost all over the region restricts the gradational activities of the streams resulting in the nearly parallel courses and acute angle junctions of the tributaries with their master stream. This feature imparts the region a pinnate drainage, an extreme case of the dendritic pattern on macro-level. Hindon river and Kali Nadi (west) are also another group of the stream. The Hindon river, a tributary of Yamuna near Gaziabad, originates in the Siwalik and flows almost linearly from Saharanpur to its point of confluence with the river Yamuna, covering a distance of about 200 km while the river Kali Nadi (west) is entirely the alluvial plain river.

The Ganga is only the Himalayan river which carries sufficient water all round the year, though with seasonal fluctuations, while Hindon river and Kali Nadi remaining dry most of time but carry large flows in rainy seasons (Mithal et al., 1973).

Besides the above natural drainage courses, the important irrigation system in the area is formed by the Upper Ganga canal which is more than 150 years old.

1.6 Rationale of the Present Study

As mentioned earlier, the present study has been taken up in parts of Saharanpur and Muzzaffarnagar district lying in the western Gangetic Plains. In this region, it has been reported that many wells are showing declining groundwater levels. The locations of important water level recording stations are shown in Figure 1.1, and plots of water level versus years are shown in Figure 1.4. The corresponding water level data obtained from the Groundwater Division Muzzaffarnagar, Uttar Pradesh, are also given in Table 1.2 and

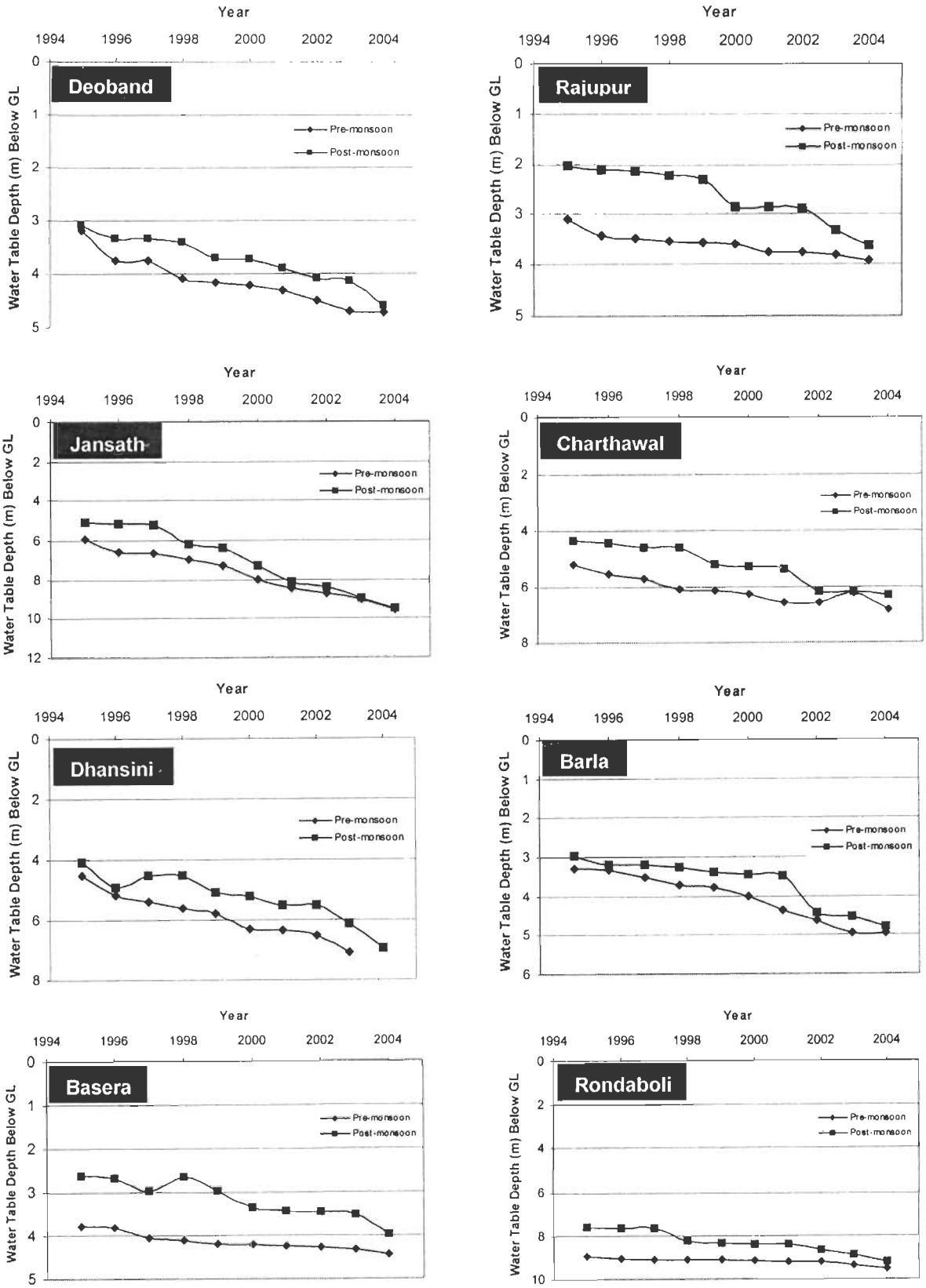

Figure 1.4: Variation of groundwater level in different wells during 1995-2004. The locations of these wells are shown in Figure 1.1.

Table 1.3. From the water level data analysis, it is obvious that many parts of the study area exhibit declining water level over the years. It has been also observed that many of the observation wells have dried during the last few years.

Population density of Uttar Pradesh as a whole is very high (689/km^2 as compared to 324/km^2 at national level) and about 79% of total population is living in the rural areas and is dependent on agriculture (Census, 2001). The average growth rate of population is estimated as 1.03% per year (Figure 1.5, Table 1.4). The study area falls on the western part of the Indo-Gangetic Plains and has highest land productivity in the state. About 70% land is under agriculture and another 5% under forest. A progressive positive trend of growth in productivity (rice: 0.3%; wheat: 1.6%), area (rice: 0.7% wheat: 1.2 %), production (rice: 1.0% wheat 2.8%) has been observed over the year (Figure 1.6) (Narang and Virmani, 2001). For sustaining higher agricultural productivity, most of the farmers take two crops a year, and some with assured irrigation also take third crop during summer. Thus, due to increasing population, agricultural activity, the water demand has increased. To meet out this ever-increasing demand in the near future, artificial recharge becomes very much important to sustain the growth in the area.

Table 1.2: Pre-monsoon water table depth (m) from the year 1995 to 2004 for different locations.

Hydrograp -hic Station	Latitude/ Longitude	Pree-monsoon water table depth (m) below ground level									
		1995	1996	1997	1998	1999	2000	2001	2002	2003	2004
Deoband	29.69/77.68	3.2	3.75	3.75	4.1	4.18	4.21	4.32	4.5	4.7	4.72
Bhayala		Dry	4.48	5.21	5.5	Dry	Dry	Dry	Dry	Dry	Dry
Nihal		dry	5.37	5.47	Dry	Dry	Dry	5.56	5.75	6.45	Dry
Rajupur	29.67/77.79	3.09	3.42	3.48	3.52	3.56	3.6	3.74	3.75	3.8	3.9
Churiyala	29.3/77.9	5.28	5.85	6	Dry	6.18	6.4	6.45	6.62	6.62	6.81
Kakrauli	29.39/77.93	5.94	6.61	6.68	6.99	7.3	8.02	8.5	8.71	9.05	9.58
Miranpur	29.27/77.85	9.58	9.28	9.21	8.78	7.33	8.45	9.34	9.49	8.93	8.66
Ramraj		16.4	13.61	17.1	Dry	Dry	Dry	Dry	16.7	17.1	17.2
Arnaich	29.56/77.55	Dry	Dry	5.87	5.83	Dry	8.47	5.53	6.75	7.3	6.3
Charthawal	29.55/77.6	5.19	5.54	5.72	6.09	6.15	6.3	6.59	6.6	6.22	6.84
Nagla Rain	29.55/77.57	6.5	6.15	5.43	Dry	Dry	5.84	5.68	5.96	6.18	6.15
Dhansini	29.48/77.54	4.51	5.19	5.39	5.63	5.79	6.3	6.33	6.52	7.07	Dry
Pina	29.47/77.64	8	7.38	6.43	6.05	5.3	5.96	Dry	Dry	7.11	7.58
Sanjak	29.43/77.64	Dry	Dry	Dry	Dry	Dry	Dry	6.9	Dry	7.82	7.63
Barla	29.61/77.8	3.29	3.33	3.52	3.71	3.78	4.02	4.36	4.63	4.95	4.97
Basera	29.56/77.86	3.79	3.82	4.06	4.11	4.18	4.21	4.25	4.26	4.32	4.42
Purkaji	29.49/77.88	2.25	3.35	3.39	3.93	4.18	4.19	4.23	4.39	5.95	6.3
Rondabali		8.93	9.02	9.08	9.09	9.1	9.12	9.18	9.21	9.33	9.5
Kakra	29.37/77.55	9.63	9.77	11.1	Dry	Dry	Dry	Dry	Dry	Dry	Dry
Umarpur	29.33/77.51	11.6	12.46	Dry	Dry	Dry	Dry	Dry	Dry	Dry	Dry
Palri	29.36/77.53	Dry	Dry	Dry	Dry	Dry	Dry	9.34	9.93	10.1	10.5
Sojani		Dry	Dry	Dry	Dry	Dry	Dry	7.07	7.56	7.85	7.99
Barsu	29.26/77.67	Dry	3.79	2.85	3.64	5.53	Dry	5.29	5.49	5.79	4.3
Mansurpur	29.35/77.72	6.5	6.48	5.82	5.7	5.37	5.56	5.8	5.91	5.3	7.63
Baruk	29.51/77.83	5.88	5.44	Dry	5.67	5.11	6.52	6.65	Dry	Dry	Dry
Bhakaraheri	29.51/77.94	Dry	13.87	Dry	13.6	13.6	14	14.5	14.6	14.6	Dry
Morna	29.46/77.94	Dry	14.72	Dry	13.6	13.9	14.6	15.2	15.5	Dry	Dry
Jat Majhera	29.46/77.81	5.67	5.88	5.75	Dry	Dry	Dry	Dry	Dry	Dry	Dry

Table 1.3: Post-monsoon water table depth (m) from the year 1995 to 2004 for different locations.

Hydrograp -hic Station	Latitude/ Longitude	Post-monsoon water table depth (m) below ground level									
		1995	1996	1997	1998	1999	2000	2001	2002	2003	2004
Deoband	29.69/77.68	3.1	3.35	3.35	3.41	3.7	3.72	3.9	4.1	4.15	4.6
Bhayala		3.81	4.38	5.1	Dry	Dry	Dry	Dry	Dry	Dry	Dry
Nihal		Dry	3.43	Dry	Dry	Dry	Dry	5.37	5.22	Dry	Dry
Rajupur	29.67/77.79	2.05	2.12	2.15	2.24	2.31	2.84	2.84	2.88	3.31	3.61
Churiyala	29.3/77.9	Dry	4.03	4.61	Dry	4.77	4.8	5.19	Close	5.29	5.34
Kakrauli	29.39/77.93	5.1	5.14	5.22	6.17	6.38	7.33	8.13	8.43	9	9.5
Miranpur	29.27/77.85	8.72	8.75	8.38	6.05	7.17	8.19	8.14	8.4	7.6	8.43
Ramraj		14.7	11.98	15.4	Dry	Dry	Dry	Dry	16.03	15.6	Dry
Arnaich	29.56/77.55	Dry	Dry	5.21	4.8	5.75	5.02	4.95	6.15	6.16	6.38
Charthawal	29.55/77.6	4.35	4.43	4.59	4.6	5.19	5.29	5.37	6.18	6.21	6.31
Nagla Rain	29.55/77.57	5.24	4.34	4.2	3.94	5	5.15	5.05	5.25	4.79	6.77
Dhansini	29.48/77.54	4.1	4.9	4.51	4.52	5.08	5.2	5.51	5.52	6.12	6.96
Pina	29.47/77.64	6.72	5.24	4.19	2.39	4.61	5.84	Dry	Dry	5.5	7.16
Sanjak	29.43/77.64	Dry	Dry	Dry	Dry	Dry	Dry	6.29	Dry	5.67	7.49
Barla	29.61/77.8	2.98	3.2	3.21	3.26	3.4	3.46	3.48	4.44	4.52	4.78
Basera	29.56/77.86	2.62	2.68	2.98	2.66	2.97	3.35	3.42	3.45	3.52	3.96
Purkaji	29.49/77.88	2.2	3.15	3.28	3.7	3.81	3.94	4.01	4.21	4.6	6.88
Rondabali		7.58	7.62	7.66	8.23	8.31	8.37	8.39	8.67	8.85	9.19
Kakra	29.37/77.55	8.61	8.9	10.3	Dry	Dry	Dry	Dry	Dry	Dry	5.46
Umarpur	29.33/77.51	10.08	10.67	Dry	Dry	Dry	Dry	Dry	Dry	Dry	Dry
Palri	29.36/77.53	Dry	Dry	Dry	Dry	Dry	Dry	7.73	8.23	8.36	9.99
Sojani		Dry	Dry	Dry	Dry	Dry	Dry	6.11	6.16	6.44	7.27
Barsu	29.26/77.67	Dry	Dry	Dry	3.22	3.33	Dry	4.11	Dry	Dry	4.26
Mansurpur	29.35/77.72	4.69	4.54	4.68	2.17	4.57	5.18	4.96	4.79	3.5	5.33
Baruk	29.51/77.83	4.34	Dry	Dry	Dry	4.98	6.22	6.7	Dry	Dry	Dry
Bhakaraheri	29.51/77.94	Dry	13.23	Dry	Dry	13.45	13.8	13.8	Dry	Dry	13.8
Morna	29.46/77.94	10.51	13.9	Dry	Dry	13.8	14.1	14.1	14.35	Dry	14.9
Jat Majhera	29.46/77.81	4.73	Dry	4.5	Dry	Dry	Dry	Dry	Dry	Dry	Dry

Table 1.4: Population and water demand of Muzzaffarnagar, Saharanpur and Haridwar district (Census, 1991, 2001).

District	Area (km^2)	Population		Population Density (person/ km^2)		Drinking water demand (44 litre/day; Indian standard)	
		1991	*2001*	*1991*	*2001*	*1991*	*2001*
Haridwar	1872	1, 124,400	1,444,213	600	772	49473600	63545372
Saharanpur	3721	2,309,029	2, 848,152	620	765	101597276	125318688
Muzzaffarnagar	4008	2,842,543	3, 541,952	709	884	125071892	155845888

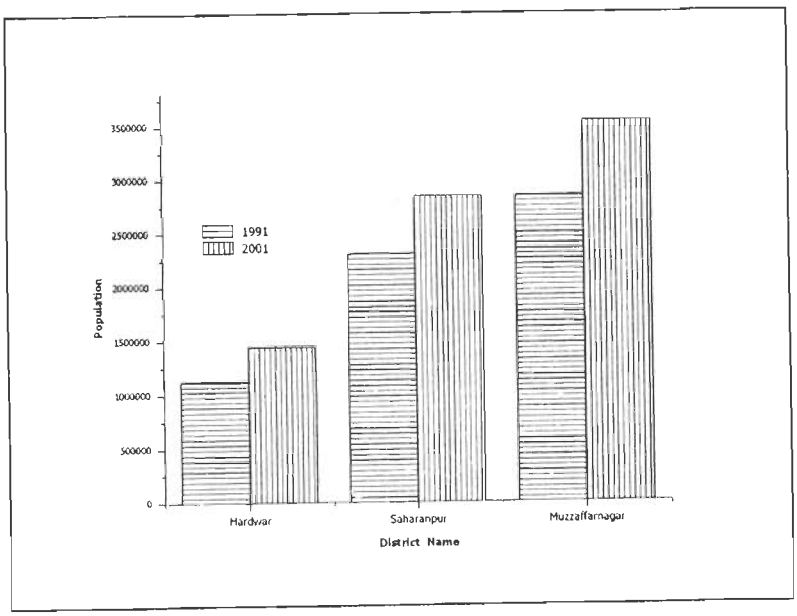

Figure 1.5: The increasing trend of population in the study area (data for the years 1991 and 2001).

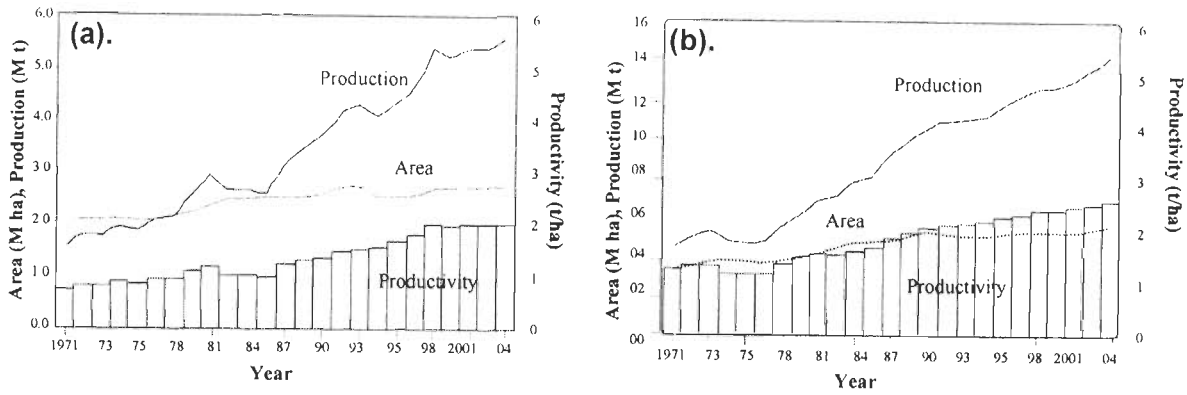

Figure 1.6: Three-year moving average of area, production and productivity of rice and wheat in Uttar Pradesh. (a) Rice and (b) Wheat.

1.7 Research Objectives

In the present work, a systematic study has been taken up for developing a strategy to replenish groundwater artificially in the study area, lying in the western part of the Indo-Gangetic Plains. Such a work with the above specific objective not has been taken up in the area hitherto. The main objectives of the research work are as follows:

a) Application of Remote Sensing — GIS techniques to map spatial distribution of porous and permeable stretches which happen to be parts of paleochannels of the Ganga river.

b) Evaluation of hydrogeological characteristics of paleochannel-aquifers and also the adjacent alluvial plains.

c) Estimation of allowable recharge volume of the rechargeable aquifer.

d) Estimation of source water availability and planning for artificial recharge.

1.8 Organization of the Thesis

In this chapter, after a general introduction and relevant details of the study area, the rationale of the study objectives have been set out. The main emphasis is on using geo-spatial data generated by remote sensing, various field and laboratory techniques and integrating the data in GIS environment. Chapter 2 provides a brief review of artificial groundwater recharge, particularly emphasising the role of modern Remote Sensing — GIS techniques. Data sources and methodology overview have been described in Chapter 3.

Chapter 4 deals with the delineation of major landforms (paleochannels) from remote sensing and field data and this chapter also describes the dimensional characteristics of the paleochannels. A description on remote sensing image processing and different field monitoring programmes adopted in this study is also presented in this chapter.

Detailed hydrogeological studies - such as soil texture analysis, groundwater level and groundwater flow analysis, litholog data analysis, rainfall runoff and water availability for artificial recharge, vertical hydraulic conductivity and recharge rate due to precipitation, which are very important for artificial groundwater recharge studies, have been carried out for the aquifers formed by the paleochannels and the adjacent alluvial plains.

Chapter 5 deals with the estimation of hydrogeological characteristics (such as soil texture, vertical hydraulic conductivity, recharge source, and groundwater flow direction) of the aquifers formed by the paleochannels and the adjacent alluvial plains.

A systematic study has been presented in Chapter 6 to construct aquifer geometry and assess interconnectivity of paleochannel aquifer with the adjacent aquifers by integrating the well-log and remote sensing data.

Chapter 7 describes estimation of natural groundwater recharge by tritium tagging technique. Chapter 8 deals with estimation of total allowable recharge of the paleochannel aquifer, estimation of source water availability and finally planning/water budgeting for artificial recharge.

Finally, chapter 9 provides a brief summary and conclusions of the present research work.

Chapter 2

Artificial Recharge – a Brief Overview

2.1 Introduction

Forced massive mining of groundwater for mankind has resulted in alarming fall of groundwater table all over the world. To address such concerns, considerable emphasis is being given to the augmentation of natural recharge by both traditional and modern techniques. As a result, artificial recharge as a means to boost the natural supply of groundwater is becoming increasingly important in groundwater management and many government and academic institutions from all over the world have embarked upon studies dealing with artificial recharge (Bhowmic, 1992; CGWB, 2000; Gale et al., 2002).

The artificial recharge needs study and analysis of a variety of spatial data sets. Most of the studies so far conducted are of rather conventional type. However, in the recent years, Remote Sensing – GIS techniques have emerged as very potential tools for generating and interpreting geo-spatial data sets. In this study, a major emphasis has been

placed on Remote Sensing – GIS techniques, as mentioned earlier. In this chapter, first a review of the need of artificial recharge is given followed by scope of multidisciplinary studies for artificial recharge planning, the methodologies of artificial recharge, and finally the role of Remote Sensing – GIS in artificial recharge is reviewed.

Need of artificial recharge: The need of artificial recharge may arise due to one or more of the following reasons (CGWB, 2000; Ramasamy and Anbazhagan, 1997):

a) Lowering of water table and reduced water supply (due to overpumping, increased socio-economic needs etc.).
b) Higher cost of pumping due to lowered groundwater levels.
c) Coastal water encroachment.
d) Water quality deterioration in pumping wells due to up coning of saline water.
e) For improving the insitu quality of aquifer water by recharging better quality water.
f) Waste water utilization, and
g) Improving the quality and discharge of groundwater and tube-wells by river bank infiltration (induced recharge).

The most common need for artificial groundwater recharge in India is generally due to the declining groundwater levels, though in coastal areas, salt water intrusion may be also an important reason to take up artificial recharge.

2.2 Factors Governing Artificial Recharge

Groundwater development by artificial recharge is very difficult and delicate task as it involves sensitive environmental and cost effective issues. A number of factors need to be taken into consideration for any project on artificial recharge (Gale et al., 2002):

(a) Climatic factors: Climatic factors include rainfall, evaporation losses and climatological features which influence the applicability of artificial recharge methods, as they will determine the quantities of water that will be available for storage. An overall understanding is best gained from a quantification of the components of a water balance, broadly – precipitation, evaporation, surface flow and change in groundwater storage. These components need to be viewed not only on an average annual basis but also in time and space.

(b) Topography: Topography is an important factor to be considered with regards to recharge site selection. It permits or retards runoff, thus influencing recharged water infiltration rates and amounts. Specific attention is needed in the case of recharge to unconfined aquifers, where water tables will rise during recharge and may intersect the ground surface. This is especially important in cases where groundwater flow paths are difficult to predict, e.g. in fractured or karstic limestone formations (Australian Water Resources Council, 1982). Groundwater levels tend to form a surface that is sub-parallel to the topography; greater depth to water at the interfluves than in the valleys. Hence, the depth to groundwater is also generally related to topography, the water table being shallower in areas of low relief and hence less available storage. Areas of low topographic relief therefore tend to have very low groundwater gradients compared to areas with higher relief. This factor needs to be considered in relation to movement of water away from the location where it is recharged artificially.

(c) Hydrogeological characteristics: The physical success of an artificial recharge scheme depends largely on the local hydrogeological conditions. These determine the ability of the recharge water to percolate through the unsaturated zone and the ability of the aquifer to

store the recharge water. In particular, the features, parameters and data to be considered are:

a) Hydrogeological parameters of the aquifer and the overlying formation such as storage capacity, porosity, hydraulic conductivity, transmissivity etc.

b) Natural discharge of springs.

c) Water resources available for recharge.

d) Depth of aquifer, physical and hydraulic boundaries of the aquifer, features such as lineaments, shear zones, geomorphic features etc.

(d) Source of water: A prerequisite for artificial recharge of groundwater is the availability of a source of water of suitable quality in sufficient quantity. Several sources of water can be considered for using recharge water, namely surface water, runoff water, waste water etc.

2.3 Data Types/Studies Needed for Planning Artificial Recharge

Development of an appropriate scientific strategy/methodology for artificial groundwater recharge involves study and analysis of a variety of data sets. The investigations include site selection, volume estimation of rechargeable formation, detection of site specific mechanism, estimation of allowable recharge, source water availability etc. Definite and fool-proof methodologies are yet to be developed for designing artificial recharge schemes, not only in hard rock areas, but also in sedimentary tracts, deltaic aquifers, beach dunes aquifers etc. The broad methodology for developing an artificial recharge scheme may include the following:

a) Detailed studies for site selection.

b) Estimation of sub-surface potential, and

c) Recharge methods/site-specific mechanism.

2.3.1 Detailed Studies for Site Selection

The artificial recharge projects are site specific and even the replication of the techniques from similar areas are to be based on the local hydrogeological and hydrological environments. The first step in planning for artificial recharge is to demarcate the suitable sites/areas for recharge. A number of researchers have discussed criteria for site selection for artificial recharge (Ramasamy and Anbazhagan, 1997).

The artificial recharge of groundwater is normally applied in following areas: (a) areas where groundwater levels are declining on regular basis, (b) areas which are hydrogeologically and socio-economically suitable, (c) areas where substantial amount of aquifer has already been desaturated, (d) areas where availability of groundwater is inadequate in lean months, and (e) areas where salinity ingress is taking place.

In order to plan the artificial recharge schemes following studies are needed:

(a) Hydrometeorological studies: These are undertaken to decipher the rainfall pattern, evaporation losses and climatological features. These can bring out the extent of evaporation losses in post monsoon period which would be helpful in designing the storages of particular capacity with a view to have minimum evaporation losses. In semi-arid regions of India, evaporation losses are significant after January hence the stored water should percolate to groundwater reservoir by this period. The data on rainfall intensity, number of rain-days etc. help in deciding the capacity and design of the artificial recharge structures.

(b) Soil infiltration studies: The infiltration rate or the recharge rate over the study area helps to design suitable artificial recharge structures and to assess the extent of recharge from these structures. It has also an important impact on the site selection. Areas with high

infiltration/recharge rate are more suitable for artificial recharge. Hence, infiltration/recharge rate studies are very much important for artificial groundwater recharge. Infiltration capacity depends on many factors such as soil type, landuse conditions, moisture content, organic matter, vegetative cover, season, air entrapment, formation of surface seals or crusts etc. Of the soil characteristics affecting infiltration, non-capillary porosity is perhaps the most important. Porosity determines storage capacity and also effects resistance to flow. Thus, infiltration tends to increase with porosity. Vegetal cover increases infiltration as compared with barren soil because (i) it retards surface flow giving the water additional time to enter the soil, (ii) the root system make the soil more pervious, and (iii) the foliage shields the soil from raindrop impact and reduces rain packing of surface soil. Surface conditions have a marked effect on the infiltration process and the formation of surface seals or crusts which forms under the influence of external forces such as rain drop impact and mechanical compaction or through staking reduces the rate of infiltration.

In order to know infiltration rates of soils, infiltration tests are carried out. Cylinder or flood infiltro-meters are common type of instruments which measure the infiltration as the rate of water leaving the device. The recent trend is to use artificial tracer to estimate infiltration rate/recharge rate.

(c) Hydrogeological studies: A correct understanding of hydrogeology of an area is of prime importance in successful implementation of any artificial recharge scheme. A desirable first step is to synthesize all the available data on hydrogeology from different agencies. The regional geological maps, which indicate the location of different geological strata, their geological age, sequence, boundaries/contacts of individual formations and the structural expressions like strike, dip, faults, folds, flexures, intrusive bodies etc. are very

much important to artificial recharge studies. These maps also bring out correlation of topography and drainage to geological contacts. The map providing information on regional hydrogeological rock units, their groundwater potential and general pattern of groundwater flow and chemical quality of water in different aquifers are necessary. Satellite images are of great importance in this regards as they provide useful data on geomorphic, lineaments and surface moisture conditions which govern the occurrence and movement of groundwater (Gupta, 2003). A detailed hydrogeological study besides the regional picture of hydrogeological set up available is therefore imperative to know precisely the promising hydrogeological units for recharge and correctly decide on the location and type of structures to be constructed in the field. The hydrogeological factors that are important for artificial groundwater studies have already been discussed in section 2.2.

The purpose of hydrogeological information is to present the following information which facilitate in the analysis of the groundwater regime and its suitability to artificial recharge schemes.

a) Demarcation of hydrogeological units on the basis of their water bearing capabilities, both at shallow and deeper levels.

b) Analysis of water level data to determine the form of the water table and the hydraulic connection of groundwater with rivers, canals etc.

c) Depths to the water table are usually compiled for the periods of the maximum, minimum and mean annual position of water table.

d) The amplitudes of groundwater level fluctuations and the maximum position of the water table of considerable importance for artificial recharge studies.

e) Piezometric head in deeper aquifers and their variations with time.

f) Estimation of groundwater potential of different hydrogeological units and the level of groundwater development.

g) Information on chemical quality of groundwater in different aquifers.

The usefulness of all the above interpretative maps is additive, i.e. their conjunctive usage allows greater knowledge and understanding of an area.

(a) Geophysical studies: The main purpose of applying geophysical methods for the selection of appropriate site for artificial recharge studies is mostly to help and assess the unknown sub-surface hydrogeological conditions adequately and unambiguously. Generally the prime task is to compliment the exploratory programme. Mostly it is employed to narrow down the target zone, pinpoint the probable site for artificial recharge structure and its proper design. Nevertheless, the application of geophysical methods is to bring out a comparative picture of the sub-surface litho-environment, surface manifestation of such structures, and correlate them with the hydrogeological setting. Besides defining the sub-surface structure and lithology, it can identify the brackish/fresh groundwater interface, contaminated zone (saline) and the area prone to seawater intrusion.

There are common geophysical methods such as seismic, resistivity, gravity methods which are very much applicable to groundwater studies. Using certain common geophysical methods (such as seismic and resistivity method), it is possible to model the

i) Stratification of aquifer system and spatial variability of hydraulic conductivity of the characteristic zone, suitable for artificial recharge.

ii) Negative or non-productive zones of low hydraulic conductivity in unsaturated and saturated zones.

iii) Vertical hydraulic conductivity discontinuities, such as dyke and fault zone.

iv) Moisture movement and infiltration capacity of the unsaturated zone.

v) Direction of groundwater flow under natural/artificial recharge processes.

vi) Salinity ingress, trend and short duration depth salinity changes in the aquifers due to varied abstraction or recharge.

The application of proper techniques, plan of survey and suitable instruments will definitely yield better understandable results, but, of indirect nature.

(e) Hydrological studies for source water supply: Before undertaking any artificial recharge project, it is a basic prerequisite to ascertain the availability of source water for the purpose of recharging the groundwater reservoir. For determining the source water availability for artificial recharge, hydrological investigations are required to be carried out in the watershed/sub-basin/basin where the artificial recharge schemes are envisaged. Four types of source water may be available for artificial recharge viz.

(i) In situ precipitation on the watershed.

(ii) Surface (canal) supplies from large reservoirs located within basin.

(iii) Surface supplies through trans basin water transfer.

(iv) Treated municipal and industrial wastewaters.

'In situ' precipitation will be available almost at every location but may or may not be adequate to cause artificial recharge but the runoff going unutilised outside the watershed/basin can be stored/transmitted through simple recharge structures at appropriate locations. In addition none, one or both of the other two sources may be available in any of the situations; the following information will be required:

a) The quantity that may be diverted for artificial recharge.

b) The time for which the source water will be available.

c) The quality of source water and the pre-treatment required.

d) Conveyance system required to bring the water to the recharge site.

Mainly, hydrological studies are undertaken to work out surplus monsoon runoff which can be harnessed as source water for artificial recharge.

(f) Chemical quality of source water: Problem which arise as a result of recharge to groundwater are mainly related to the quality of raw waters that are available for recharge and which are generally require some sort of treatment before being used is recharge installations. They are also related to the changes in the soil structure and the biological phenomena which take place when infiltration begins, to the changes brought to the environmental conditions. The chemical and bacteriological analysis of source water besides that of groundwater is therefore essential.

2.3.2 Estimation of Sub-surface Potential for Groundwater Recharge

Estimation of volume of the rechargeable formation is very important so as to design artificial recharge schemes according to the volume of such rechargeable containers. The aquifers best suited for artificial recharge are those that can hold large quantities of water and do not release them quickly. Based on the hydrogeological/geophysical surveys/ or litholog data analysis, the thickness of potential unsaturated zone for recharge should be worked out to assess the potential for artificial recharge in terms of volume of water which can be accommodated in this zone vis-à-vis source water availability. The studies should bring out the potential of unsaturated zone in terms of total volume which can be recharged. Hence, study on aquifer geometry is very much important for developing artificial recharge schemes.

2.3.3 Recharge Methods/ Site-specific Mechanisms

It is also very important to suggest the suitable techniques/methods for recharging the reservoir artificially. The site specific mechanism for a particular site is largely depend

on topographic and other factors (such as slope, drainage pattern, water level, and other hydrological and socio-economic parameters of the artificial recharge zones). There are numerous mechanisms/ schemes to artificially recharge groundwater (Figure 2.1), which are mostly site specific and varied as the ingenuity of those involved in their construction and operation. A summary on various artificial recharge schemes, their general characteristics, hydrogeological settings, methodology etc. is given in Table 2.1. Broadly, the various techniques of artificial recharge can be grouped into the following:

a) Spreading methods.

b) Open wells and shafts.

c) Drilled wells and boreholes.

d) Bank infiltration.

e) Sand storage dams.

f) Roof-top rainwater harvesting.

Details on these types of schemes, e.g. construction, restoration, operation etc. are described by United Nations (1975), O'Hare et al.(1982), Huisman and Olsthoorn (1983), National Institute of Hydrology (1998), Ponce (1999), Central Groundwater Board (2000), CGWB/UNESCO (2000), and American Society of Civil Engineers (2001). Various studies on this aspect of the individual schemes are also described by many authors (Pyne, 1995; Bouwer, 1996; Batchelor et al., 2000; Bouwer, 2002).

2.4 Role of Remote Sensing – GIS in Artificial Recharge Studies

The complex interaction of all factors (both physical and socio-economic factors) will determine the degree of success, which itself can be viewed from a variety of perspectives. Artificial recharge studies have been carried out in the earlier years by using

various conventional (field-based) methods for data collection and analysis (Karanth, 1963; Bourgeosis, 1972; Cochran, 1981; Bhowmick, 1992; Abu-Taleb, 1999). However, the conventional methods have some limitations in such type of geo-spatial studies, whereas the modern remote sensing – GIS tools have revolutionized data collection and analysis.

2.4.1 Role of Remote Sensing

Remote sensing with its advantages of spatial, spectral and temporal availability of data covering large and inaccessible areas within short time has become a very handy tool in exploring, evaluating, and managing vital groundwater resources (Navalgund and Kasturirangan, 1983; Ghosh et al., 1993; Sanjeevi, 1996; Sanjeevi et al., 2001; Shanmugam and Sanjeevi, 2002; Chowdhury et al., 2003; Shanmugam et al., 2003; Jha and Peiffer, 2006; Srivastava et al., 2006). Many of the hydrogeological factors that control artificial groundwater recharge can be obtained directly or indirectly through remote sensing data due to the following advantages (Saraf and Chaudhury, 1998; Lillesand and Kiefer, 1999; Navalgund, 2001; Gupta, 2003): (a) synoptic overview of the terrain, (b) repetitive coverage of the area, (c) unbiased recording of events, (d) data availability in digital form, (e) cost-effective technology, (f) multi-spectral information, and (g) stereoscopic viewing and 3-dimensional capability.

Apart from the above advantages, modern high resolution image data, computing facilities and advanced digital enhancement and image processing techniques of satellite data result in extraction of maximum information and increased interpretability (Gupta, 2003). The hydrogeologic interpretation of satellite data have been proved to be a valuable survey tool in areas of the world where little geologic and cartographic information exists

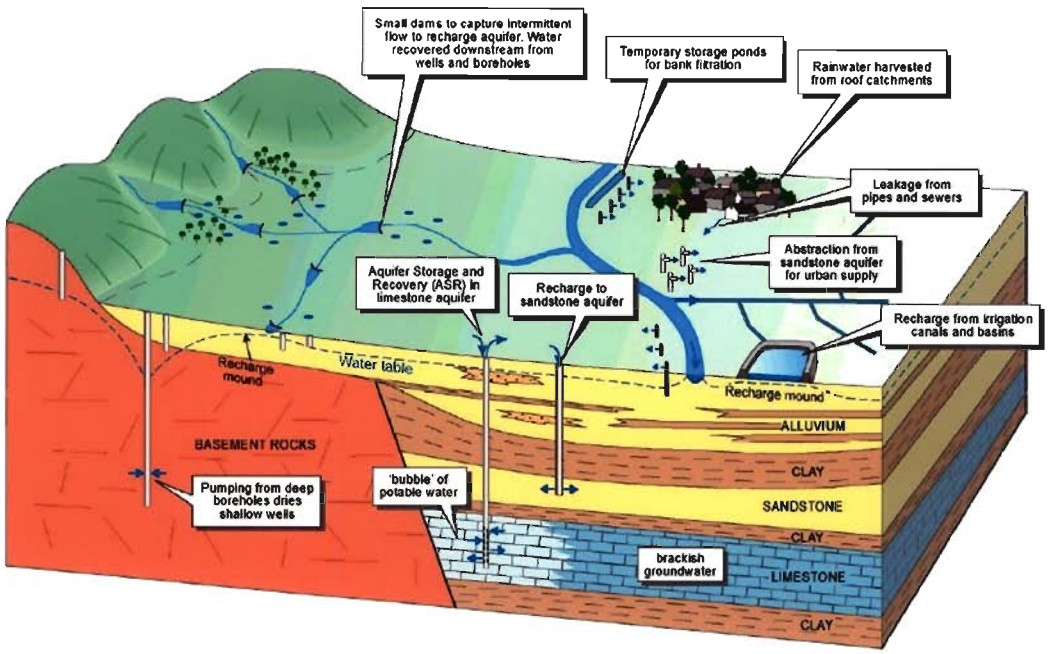

Figure 2.1: Diagram of different artificial recharge methods in different hydrogeological environments (Gale et al., 2002).

Table 2.1: Overview of different artificial recharge schemes (Gale et al., 2002).

	ALLUVIAL AQUIFERS	ALLUVIUM OVER FRACTURED HARD ROCK AQUIFERS	FRACTURED HARD ROCK WITH THIN SOIL/WEATHERED ZONE	CONSOLIDATED SANDSTONE AQUIFERS	CARBONATE AQUIFERS
EXAMPLES OF ARTIFICIAL RECHARGE SCHEMES	Terai region, Nepal and adjacent area in Uttar Pradesh, India Phoenix, Arizona, USA Atlantis, S. Africa	Alwar, Rajasthan, India Meshana District, Gujarat, India	Saurashtra, Gujarat, Coimbatore, Tamil Nadu Andhra Pradesh, India Karnataka, India Maharasthra, India	Loftsome Bridge, Yorkshire, UK	Lytchett Minster, England, UK Israel
GENERAL CHARACTERISTICS	Fluvial, marine and lacustrine deposits ranging in thickness from a few tens of metres to kms. Layered sequence of clays, sands and gravels as well as some calcareous layers. Lower reaches of rivers forming flood plains, so low relief.	Fluvial and colluvial deposits in upper reaches of rivers. Deposits are sandy to coarse and form aquifers a few tens of metres thick. Underlying aquifer is fractured igneous and metamorphic rocks, usually in hydraulic connectivity with the overlying alluvium	Aquifer is the fractured bedrock comprising igneous, metamorphic and volcanic rocks. Soil/weathered zone is too thin to store water other than at a very local scale.	Aquifers with a matrix of sand grains held together by a cement (e.g. calcite silica) or indurated by metamorphic processes. This results in a wide range of porosity/fracture ratios and hence hydraulic properties	Aquifers with hydraulic propertied controlled by the solubility of the rock. Solution enhanced fractures can result in karstic flow.
HYDROGEOLOGY PHREATIC OR CONFINED	Phreatic if permeable layer at surface, becoming more confined with depth. Layered aquifers with variable connectivity.	Coarse nature of alluvium usually results in phreatic conditions, the hard-rock aquifer being in hydraulic connectivity.	Usually phreatic in the hard-rock aquifers, depending on interconnection of fractures.	Phreatic where there is no alluvial cover or a confining clay layer.	Phreatic where there is no alluvial cover or a confining clay layer.

Table 2.1: Overview of different artificial recharge schemes (Gale et al., 2002).

	ALLUVIAL AQUIFERS	ALLUVIUM OVER FRACTURED HARD ROCK AQUIFERS	FRACTURED HARD ROCK WITH THIN SOIL/WEATHERED ZONE	CONSOLIDATED SANDSTONE AQUIFERS	CARBONATE QUIFERS
POROSITY AND STORAGE	Porosity high but effective storage restricted to sand and coarse layers.	High porosity and storage in the alluvium, only limited by the thickness. Low storage capacity in fractures in the hard-rock but drainage from the alluvium can maintain well yields.	Low storage capacity in fractures. If this storage is depleted through overdraft then additional storage can be created, to be filled in subsequent wet season.	Proportion of storage in the matrix of these aquifers will be determined by the porosity and degree consolidation and fracturing.	Proportion of storage in the matrix of these aquifers will be determined by the porosity and degree consolidation and solution-enhancement of fractures.
PERMEABILITY AND FLOW	Flow mainly in coarser horizons so their inter-connectivity, as well as the connectivity to the recharge zones will determine the flow paths. Low hydraulic gradients will result in slow groundwater flow.	Flow in alluvium will drain towards streams rapidly, depleting resources. Hard-rock aquifers will generally have low fracture permeability, except in large fracture zones.	Flow to wells in hard-rock will be in fractures; the greater the number the greater the yield and speed of refilling the well.	Permeability and flow will be determined by the porosity and degree consolidation and fracturing.	Permeability and flow will be determined by the porosity, the degree of consolidation and solution-enhancement of fractures.
GROUNDWATER LEVEL FLUCTUATIONS	Because of high storage capacity, fluctuations will small; a few metres. If water table is near the surface then there is limited scope for recharge. Pumped drawdown can create additional storage if managed carefully.	If water-table is in the hard-rock aquifer then it will generally respond quickly to pumping and recharge, but within a restricted radius due to the low permeability. When the water table is in the alluvium then the same arguments apply as discussed in the box to the left.	Groundwater levels will rise and fall rapidly in response to recharge and pumping.	Where the porosity of the aquifer is high, the groundwater fluctuations will be relatively subdued in response to pumping and recharge.	Where the fractures provide the main porosity, groundwater fluctuations will be rapid.

Table 2.1: Overview of different artificial recharge schemes (Gale et al., 2002).

	ALLUVIAL AQUIFERS	ALLUVIUM OVER FRACTURED HARD ROCK AQUIFERS	FRACTURED HARD ROCK WITH THIN SOIL/WEATHERED ZONE	CONSOLIDATED SANDSTONE AQUIFERS	CARBONATE AQUIFERS
INFILTRATION CAPACITY	High if surface layer is sandy but low if there is a high clay content. Coarse material needed for full zone of recharge. A clay, or other low-permeability layer, at a shallow depth will restrict recharge.	Good in sandy alluvium, which can store water and hence facilitate infiltration into the underlying fractured rock.	Capacity limited by the number of open fractures so runoff can be large.	Very high where there is no cover and the soil has developed from the sandstone.	Very high where there is no cover. Soil development is usually very thin and surface runoff minimal.
QUALITY ISSUES	Groundwater quality good in active flow zones but can deteriorate where flow is slow or from saline intrusion. Where there is little natural groundwater movement, the concentrations of elements such as iron, magnesium, arsenic and fluoride can exceed acceptable limits. Artificial recharge can improve water quality by dilution or displacement. Vulnerability to pollution depends on the permeability of the surface layers.	Groundwater quality is goodin active flow zones. Permeable alluvium will be vulnerable to pollution.	Groundwater quality good in active flow zones but vulnerable to rapid pollution through fracture flow. Thin soil cover will only provide limited protection.	Very good quality groundwater where actively recharged but susceptible to contamination, particularly where soil cover is thin.	Very good quality groundwater where actively recharged but extremely susceptible to contamination.

Table 2.1: Overview of different artificial recharge schemes (Gale et al., 2002).

	ALLUVIAL AQUIFERS	ALLUVIUM OVER FRACTURED HARD ROCK AQUIFERS	FRACTURED HARD ROCK WITH THIN SOIL/WEATHERED ZONE	CONSOLIDATED SANDSTONE AQUIFERS	CARBONATE AQUIFERS
METEOROLOGY RAINFALL INTENSITY	Surface flow will occur if infiltration rate is exceeded or soil is at capacity. Widespread flooding will result in flood plain deposition.	Rapid runoff from adjacent bedrock during intense rainfall may cause erosion of alluvium and soil.	Rapid runoff during intense rainfall may cause erosion of soil.	Infiltration capacity likely to be high so natural infiltration and recharge likely to be high also. Extreme events may cause soil erosion and provide potential water for artificial recharge.	All but the most extreme events will infiltrate. Thin soils are easily eroded.
EVAPOTRANSPIRATION	Rainfall and evaporation will vary considerably in both time and space. Annual variability of rainfall is high, so average figures need to be used accordingly. The components of the water balance in three watersheds in Karnataka that follow are given as examples only and cannot be applied widely (Batchelor et al., 2000). Long-term annual average rainfall is 520 mm and Penman potential evapotranspiration of 1750 mm. Indicative estimates of the water balance at the field scale in non-irrigated areas are: evapotranspiration from the soil, 45%; evapotranspiration from cropped areas, 25%; surface runoff, 10%; and recharge to groundwater, 10%. Open water evaporation will occur at full potential rate for standing water bodies, about 2000 mm/year (5.5 mm/day). Evaporative losses from tanks can be reduced by increasing the depth of water; hence reducing the surface area/volume ratio. Underground storage through artificial recharge will obviously reduce evaporative losses to zero, once infiltrated.				

or is not accurate (Engman and Gurney, 1991). Observation from satellite data is not only used for extraction of valuable information but also for improving/updating the existing available maps.

Excellent reviews of remote sensing applications in groundwater hydrology are presented in Waters et al. (1990), Engman and Gurney (1991) and Meijerink (2000). However, there is less efforts to use remote sensing derivatives in artificial groundwater recharge studies. Satellite data provide quick and useful baseline information about the factors controlling the occurrence, movement and artificial recharge of groundwater like geology, lithology, geomorphology, soils, land use/cover, drainage patterns, lineaments, etc. (Bobba et al., 1992; Meijerink, 2000; Gupta, 2003). Other features like sedimentary strata (i.e., alluvial deposits and glacial moraines) or certain rock outcrops may indicate potential aquifers. The presence of ox-bow lakes and old river channels are good indicators of alluvial deposits. These may be easily identified from remote sensing data. Shallow groundwater could also be inferred by soil moisture measurements and by changes in vegetation types and pattern (Nefedov and Popova, 1972).

In arid regions, vegetation characteristics may indicate groundwater depth and quality. Groundwater recharge and discharge areas in drainage basins can be detected from soils, vegetation, and shallow/perched groundwater (Todd, 1980). Furthermore, differences in surface temperature (resulting from near-surface groundwater) measured by remote sensing have also been used to identify alluvial deposits, shallow groundwater, and springs or seeps (Mayers and Moore, 1972; Heilman and Moore, 1981; van de Griend et al., 1985). van de Griend et al. (1985) suggested that if surface temperature measurements were made using thermal infrared sensors after a long period without rain, it should be possible to map the regions of shallow water table and infer groundwater recharge and discharge.

The important physical features of the landscape which can be derived from satellite imagery or aerial photographs and used for assessing groundwater conditions (i.e., occurrence, depth, flow patterns, quantity, or quality) and artificial groundwater recharge studies under a variety of hydrogeologic settings are summarized in Table 2.2. However, all the controlling factors responsible for artificial groundwater recharge have rarely been studied together because of the non-availability of data, integrating tools and/or modelling techniques.

2.4.2 Role of GIS

The geographic information system (GIS) has emerged as an effective tool for handling spatial data and decision making in several areas including engineering, environmental fields (Stafford, 1991; Goodchild, 1993) and also in artificial groundwater recharge studies due to the following advantages:

a) GIS is able to perform convergent analysis of spatial data from diverse sources. Using multi-disciplinary data, the number of attributes or channels of information are increased and this should correspondingly enhance the capability of discrimination, identification or categorization. The collateral data also usually include ground truth and this should enable proper labelling of categories. Interpretation of all the data sets collectively should result in a coherent analysis.

b) GIS facilitates integrated and conjunctive analysis of large volume of multi-disciplinary data both spatial and non-spatial, within the same georeferencing schemes (Aronoff, 1989; Saraf and Chaudhury, 1998).

Table 2.2: Salient physical features of the landscape used for assessing groundwater condition from remote sensing data (Todd, 1980; Todd and Mays, 2005).

Surficial feature	Information obtained
• Topography	The local and regional relief setting gives an idea about the general direction of groundwater flow and its influence on groundwater recharge and discharge.
Low slope (0–5.)	Presence of high groundwater potential.
Medium slope (5–20.)	Presence of moderate to low groundwater potential.
High slope (>20.)	Presence of poor groundwater potential.
• Natural vegetation	Dense vegetation indicates the availability of adequate water where groundwater may be close to the land surface.
Phreatophytes	Shallow groundwater under unconfined conditions.
Xerophytes	Appreciably deep groundwater under confined or unconfined conditions.
Halophytes	Shallow brackish or saline groundwater under unconfined conditions.
• Geologic landforms	
Modern alluvial terraces, alluvial plains, floodplains, and glacial moraines.	Favorable sites for groundwater storage.
Sand Dunes	Give an idea about the presence of underlying sandy glacio-fluvial sediments, which indicate the presence of groundwater.
Rock outcrops	Presence of potential aquifer.
Thick weathered rocks	Moderate groundwater potential.
Rocks with fractures/fissures	Very good or excellent potential of groundwater.
Rocks without fractures/fissures	Unfavorable sites for groundwater occurrence.
Hillocks, mounds and residual hills	Unfavorable sites for groundwater existence
• Lakes and streams	
Ox-bow lakes and old river channels	Favorable sites for groundwater extraction
Perennial rivers, and small perennial and intermittent lakes.	High to moderate potential of groundwater.
Drainage density	High drainage density indicates unfavorable site for groundwater existence. Moderate drainage density indicates moderate groundwater potential and less/no drainage density indicates high groundwater potential.
Drainage pattern	Gives an idea about the joints and faults in the bedrock which in turn indicates the presence or absence of groundwater.
• Springs Types (tentatively inferred from RS data)	
Depression springs, contact springs, and artesian springs	Presence of potential aquifer.
Moist depressions, seeps, and marshy environment	Presence of shallow groundwater under unconfined conditions.
• Lineaments (Applicable to rocky terrains)	Give an idea about the underground faults and fractures, and thereby indicate the occurrence of groundwater.

c) The Geographic Information system and advanced computing facilities also offer advantages in multi-geodata handling, such as storage of large quantities of data in cost-effective and efficient digital formats and their fast retrieval, ability to perform complex spatial analysis rapidly, usefulness in planning and decision-making (Aronoff, 1989).

d) GIS has been found to be the most powerful technique in assessing the suitability based on the spatial variability of the hydrological parameters.

e) It offers many tools to extract the information regarding hydrogeology, geomorphology, deep geophysical response, soil, lithology, landuse, drainage and other relevant parameters. Statistical methods such as krigging, inverse method etc. are common features of the most GIS and can be applied to interpolate hydrogeological parameters such as the surface elevation, aquifer thickness, hydraulic conductivity map etc. In case of limited number of basic data, extrapolation of hydrogeological parameters is also possible.

Remotely sensed data are one of the main sources for providing information on land and water related subjects. These data being digital in nature, can be efficiently interpreted and analyzed using various kinds of software packages (e.g., PCI, ENVI, ERDAS IMAGINE, etc.). It is easy to feed such information into a GIS environment for integration with other types of data and then do analyses (Faust et al., 1991; Hinton, 1996).

A brief review on GIS applications in hydrology and water management has been presented by several researchers such as Zhang et al. (1990), DeVantier and Feldman (1993), Ross and Tara (1993), Schultz (1993), Deckers and Te Stroet (1996), Tsihrintzis et al. (1996), and Jha et al., (2006). Several workers (such as Bobba et al., 1992; Salama et al., 1994; Kamaraju et al., 1995; Teeuw, 1995; Krishnamurthy et al., 1996; Sander et al.,

1996; Edet et al., 1998; Travaglia and Ammar, 1998; Goyal et al., 1999; Musa et al., 2000; Lachassagne et al., 2001; Shahid and Nath, 2002; Singh and Prakash, 2002; Singh et al., 2002; Hadithi et al., 2003; Sikdar et al., 2004; Srivastava, 2005) used GIS and remote sensing data for groundwater exploration. Most of the workers used remote sensing data for geological and/or geomorphological interpretations and GIS for image processing and data integration. There is also combined use of remote sensing and GIS as a valuable tool for the analysis of voluminous hydrogeologic data and for the simulation modeling of complex sub-surface flow and transport processes under saturated and unsaturated conditions (e.g. Watkins et al., 1996; Loague and Corwin, 1998; Gogu et al., 2001; Gossel et al., 2004). Undoubtedly, the GIS technology allows for swift organization, quantification, and interpretation of a large volume of hydrologic and hydrogeologic data with computer accuracy and minimal risk of human errors.

2.4.3 Remote Sensing - GIS in Artificial Groundwater Studies

Application of remote sensing and GIS in artificial groundwater studies, particularly for selecting suitable/favourable site for artificial recharge has been practiced by several researchers (e.g. Elango and Arrikkat, 1998; Krishnamurthy and Srinivas, 1995; Saraf and Choudhury, 1998; Anbazhagan et al., 1999; Anbazhagan et al., 1997; Ramlingam and Santhakumar, 2002; Vasanthakumaran et al., 2002; Anbazhagan et al., 2005). They basically determined appropriate areas for artificial recharge through weighting-rating method using several thematic data layers (such as geomorphology, geology, soil, slope, land use, drainage density, lineament density, runoff isolines, depth to weathered zone, depth to basement, groundwater level fluctuations , water quality etc.) which were prepared using both remotely sensed and conventional data. It was concluded

that remotely sensed data, conventional data, and GIS tools provide a powerful and practical approach to identify suitable sites for artificial recharge.

Most of the work mainly involve only site selection for artificial recharge by integrating very limited number of information layers (such as landuse/landcover, vegetation index, water table map, hydraulic conductivity, aquifer thickness map, lithological map, soil map, lineament density map, drainage density map, slope and aspect map etc.) obtained by using several tools (such as Krigging, Inverse Interpolation method, etc and different mathematical function in GIS) through simple Boolean logic or Index overlay methods or combination of both. Besides the site selection, remote sensing and GIS in combination of other field data together may help in site specific mechanism, water budgeting/source water availability, aquifer geometry study etc. due to their novel advantages. The general methodology for the identification of suitable sites for artificial recharge or rainwater harvesting is illustrated in Figure 2.2.

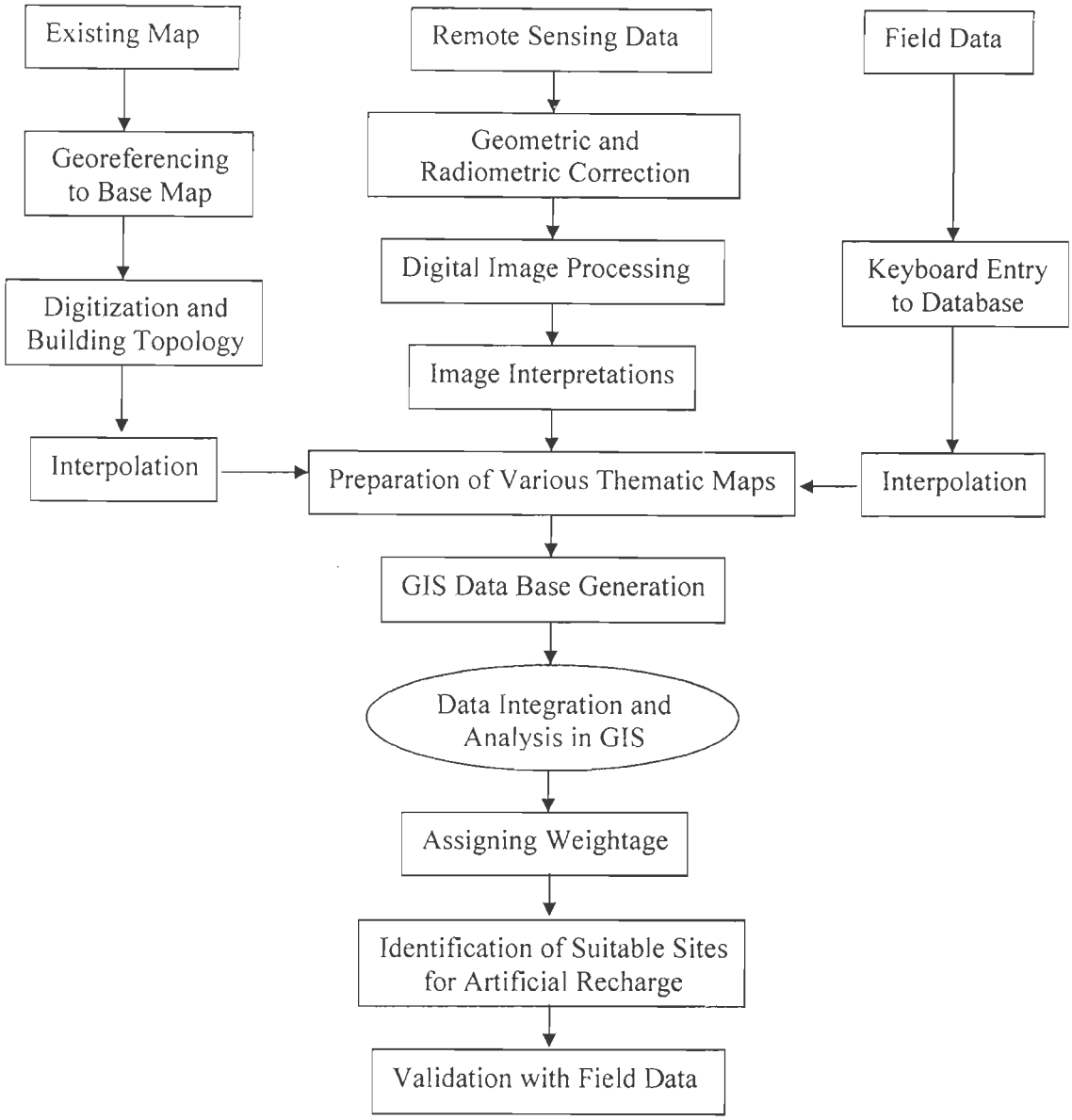

Figure 2.2: Flow chart showing data flow for site selection of artificial recharge by integrated remote sensing and GIS technique.

Chapter 3

Data Sources and Methodology-Overview

3.1 Introduction

A broad overview of various factors affecting artificial groundwater recharge has been given in section 2.2. The present study area is a small region located in the Indo-Gangetic plains, and posses gentle topographic slope, and is mainly composed of alluvial material. Further, the first unconfined aquifer only is considered for artificial recharge. Therefore, landform, soil, and hydrogeological characteristics have greater importance for artificial groundwater recharge studies, than other factors, such as relief, lineaments etc. In this chapter, an overview of data used and methodology is presented.

The data used in this study can be broadly categorized into three main groups - (a) remote sensing data, (b) ancillary data, and (c) field data.

3.2. Remote Sensing Data

The study has mainly utilised remote sensing data from Indian Remote Sensing (IRS) satellite mission acquired from National Remote Sensing Agency (NRSA), Hyderabad, India. The IRS uses pushbroom scanning system based on Charge-Coupled Device (CCD), the sensors being called Linear Imaging Self Scanner (LISS-I and LISS-II). IRS-1B-LISS-II (www.nrsa.gov.in) data has been used for extracting information on geomorphology, vegetation cover, lineaments and paleochannel mapping in the research study. Selected sensors specifications of IRS-1B-LISS-II are given in Table 3.1. The IRS data have widely been used in recent times in a variety of applications – in geosciences, landuse/landcover mapping, hydrogeological mapping, urban planning, biodiversity characterization, disaster management etc (e.g. Navalgund, 2001; Gupta, 2003). The main characteristics of wavelength bands of IRS-1B-LISS-II are as follows:

Blue (band 1): Very strong absorption by vegetation, good water penetration; high scattering by suspended atmospheric fine particles.

Green (band 2): Some vegetation reflectance; good water penetration; good scattering by atmospheric particles.

Red (band 3): Very strong absorption by vegetation; good water penetration; fair scattering by atmospheric particles.

NIR (band 4): High reflectance by vegetation; total absorption by water; general high reflectance by most dry materials.

Pre-processing, processing and interpretation of the remote sensing data has been discussed in Chapter 4.

Table 3.1: Salient characteristics of the satellite sensor data used.

Satellite/Sensor	IRS-1B, LISS-II
Date of acquisition	November, 1998
Path/Row	29-46B1
Spatial resolution	36.25 m
Quantization	8-bit
No. of bands	4
Spectral resolution	Band1 (Blue) : 0.46-0.52μm Band2 (Green) : 0.52-0.59μm Band3 (Red) : 0.62-0.68μm Band4(NIR) : 0.77-0.86μm
Swath width	74 km
Format	Band Interleaved by Line (BIL)
Repeat Cycle	22 days

3.3 Ancillary Data

A brief description of ancillary data, namely – topographic maps, soil maps collected from various sources and used in the study has been given in Table 3.2.

Toposheets of Survey of India have been used for generation of base map of the study area. Various types of information e.g., contours and point elevations, drainage network and roads have been extracted from the topographic map. Soil map obtained from National Bureau of Soil Survey and Land Use Planning (1999) has been used for obtaining information on soil characteristics of the study area. Data such as specific yield, storage coefficient etc. are collected from various reports and existing literature. These data have been used for obtaining hydrogeological characteristics of the aquifer.

Table 3.2: Ancillary data used in this study.

Data type	Specification	Source
Topographic Maps	Scale 1: 50,000 (Toposheet Nos. 53G/9, 53G/13, 53G/14, 53G/15, 53K/1, 53K/2, 53K/3)	Survey of India, Dehradun
Soil Map	Scale 1: 500,000 (Sheet No.1; Soil Map of Uttar Pradesh)	National Bureau of Soil Survey and Land Use Planning (ICAR), 1999
Other Data (soil texture, specific yield, storage coefficient etc.)	----	Groundwater Division Uttar Pradesh and various published Journals, reports and maps

3.4 Field Data

Collection of field data is very important for any remote sensing and GIS based study. Extensive field work has been carried out during July 2004 to July 2007 for collecting various field data. The types and main purposes of field data collected from various sources have been given in Table 3.3. Field photographs and details of the field data have been incorporated at relevant places in subsequent chapters.

3.4.1 Collection of Existing Lithologs

A large number (more than 100) of vertical bores have been drilled by the Tube Well Division of Uttar Pradesh (earlier including the present Uttarakhand state also) in the study area. Well-log data of these bore wells are available in the form of tables, representing depth of strata below ground level, strata numbers, nature and thickness of strata, along with village/location name (Figure 3.1). These well-logs pertaining to the

Table 3.3: Field data types and their purposes.

Data type	Purposes	Source
Litholog data	To construct aquifer geometry, and to estimate vertical hydraulic conductivity	Tube Well Division of Uttar Pradesh Dedicated field drilling operation
GPS data (Differential GPS)	To determine latitudes, longitudes and ground height (from mean sea level) of water level recording stations where ground levels were not available	Hand held GPS survey Differential GPS survey
Groundwater level data	To estimate unsaturated aquifer thickness and ground water flow direction	Groundwater Division Uttar Pradesh Water level monitoring programme
Rainfall data	To estimate surface runoff and recharge rate	Groundwater Division Uttar Pradesh
Tracer data (Tritium injection)	To find out recharge rate and specific yield	Dedicated field work
Ground water sample	To obtain information on recharge source through stable isotope analysis	Dedicated field work
Soil samples	To obtain soil textural information	Dedicated field work

study area have been collected from the Tube Well Division of Hardwar (Uttarakhand), Saharanpur and Muzzaffarnagar (U. P).

3.4.2 Drilling Operations

The most of the bore logs collected from the Tuble Well Division of Uttar Pradesh are pertained to non-paleochannel area. They also have a large variation in strata penetrated, level of details, and lithological description. So, few bores were drilled both on the paleochannel and the alluvial plains to fill up gaps and also to rectify the collected

lithologs with respect to the drilling observations. Sampling has been carried out for collecting lithological information at different depths. Firstly, paleochannels have been mapped from remote sensing data analysis. These paleochannels have been traced and displayed on the base map by GIS and sites are selected systematically for drilling. A series of 17 observation wells systematically sited on the paleochannel and the alluvial plains have been drilled. Both shallow (depth upto 20 m) and deep (depth upto 80 m) bore wells were constructed. The details about the location of drilling wells and their lithological interpretation have been given in Chapter 6.

Drilling Method - Local *"Bukki System"*

A variety of drilling methods such as cable-tool method, forward (direct) rotary method, reverse circulation drilling, bailer method etc. have been developed over time to account for many geologic conditions. As the study area is a part of the Indo-Gangatic plains and is mainly composed of unconsolidated alluvial deposits, a machine operated local drilling technique called 'Bukki System' has been used for collecting the lithological information. 'Bukki System' is quite similar with the mechanism of cable-tool drilling method.

The 'Buki System' has two main parts (Figure 3.2)-

(i) The 'Bukki'- a hollow pipe having 4 inch diameter; length of about 7 ft, weight of about 60-70 kg and a valve at the lower portion.

(ii) An outer pipe of about 5 inch diameter which acts as a casing material.

The 'Bukki' is lowered by a cable within the outer pipe. And the 'Bukki' is moved up and down by motor operated cable (Figure 3.2). When the 'Bukki' moves downward, the valve on the lower portion is opened and the material cut by it is entered within hollow space of the 'Bukki'. When it moves upward, the valve is closed and thus the cutting

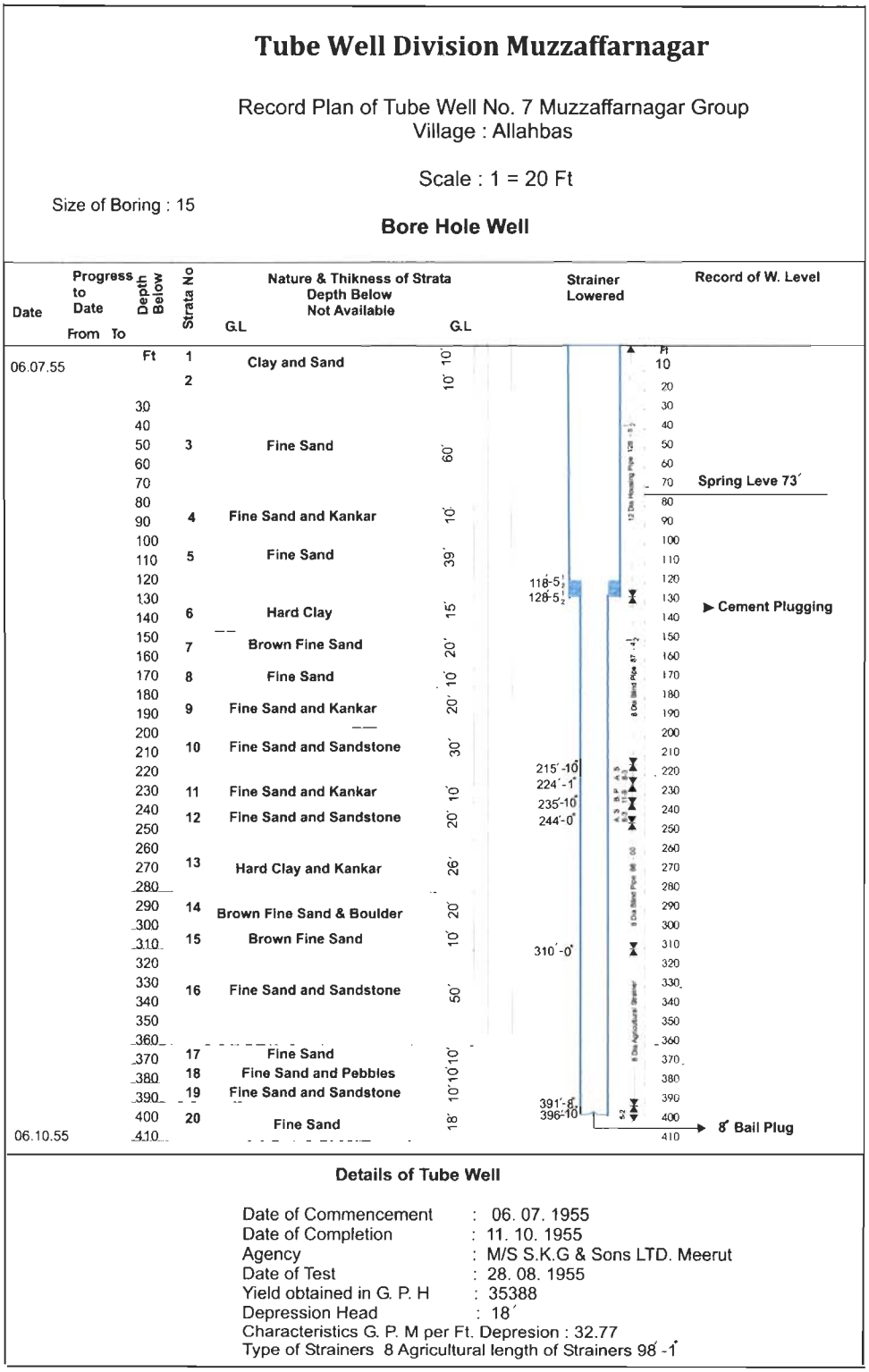

Figure 3.1: Sample of one 'Strata Chart' collected from Tube Well Division of Uttar Pradesh.

Figure 3.2: Drilling conducted on the paleochannel near Berla village. (a) Machine operated 'Bukki System' and (b) Different parts of 'Bukki System'.

materials are caught within the 'Bukki'. Thus, by subsequent up and down movement of the 'Bukki', the formation materials are cut and filled within the hollow portion of the 'Bukki' and at the same time the outer pipe is lowered down by pressure. After cutting 2-3 ft of material, the 'Bukki' is taking out and samples are collected. Thus, automatically the outer pipe is lowered by pressure subsequently restricts the side material from entering into the inner portion of the already bored hole. When drilling is completed up to the desired depth, a PVC pipe of 4 inch diameter along with filter (according to requirement) are lowered through the outer pipe and then the outer pipe is removed. The constructed wells are used as observation wells for groundwater monitoring and sample collection. It is found that this system is economic and very much useful for drilling in unconsolidated alluvial deposit. Most of the villagers have used this local 'Bukki System' for constructing production wells due to its cheap rate and nominal labour cost.

3.4.3 Soil Sample Collection

3.4.3.1 Collection of Samples

Soil samples were collected from different types of land use, using hand auger from a depth ranging up to 50 cm and stored in clean self-sealing plastic bags before transportation from the sits. The soil samples were air-dried in the laboratory, and passed through a 2 mm sieve, after they had been disaggregated with a porcelain pestle and mortar. Subsequently, samples were stored in clean self-sealing plastic bags for further analysis.

3.4.3.2 Laboratory Analysis of Soil Samples

Soil texture is a term commonly used to designate the proportionate distribution of different sizes of mineral particles in a soil. It dose not include any organic matter (Brown, 1990). Preparation of the samples for textural analysis consisted of the following steps (Carver, 1971):

(i) Breaking all clumps and mashing with fingers.

(ii) Mixing sample thoroughly and splitting.

(iii) Coning and Quartering the sample.

(iv) Taking 50-100 gm sample chunk, removing carbonates by adding in1N HCl with stirrer and rim washing, followed by decanting HCI.

(v) Removing organic matter by adding 6% to 30% H_2O_2, stirring and rim washing.

(vi) Adding distilled water and heating on hot plate for 12 hours (at 40°C temperature).

(vii) Removing Iron Oxide by adding distilled water, aluminium foil and 15 gm Oxalic acid with stirrer and heating on hot plate for 10 to 25 minutes followed by decanting excess clear water.

(viii) Drying and weighing.

Mechanical analysis by wet sieving: Evaluation of the distribution of particle sizes can be accomplished by mechanical analysis. This involves sieving particles coarser than 0.05 mm and measuring rates of settlement for smaller particles in suspension by the wet analysis (Todd, 1980). In the present study, size analysis was conducted by wet sieving as per the procedure suggested by Carver (1971):

Approximately 80 gm of soil sample was weighed. The sieve rack employing a 62 micron sieve was set up and the pan was attached to the bottom of the sieve rack. Sieving and washing was done using distilled water and washing was continued until

nearly all fines were washed through screen. The sediments (silt and clay) that passed through the screen were collected along with the sand collected on sieve. The sand and finer sediments (silt and clay) were dried and weighed. Finally, the percentage of sand in the sample was calculated.

Mechanical analysis by pipette: Sedimentation is based upon Stokes' law where the terminal velocity of a spherical particle settling in a fluid of a given density and viscosity, under the influence of gravity, is proportional to the square of the particle's radius (Hillel, 1982). Thus, the larger particles settle faster. If a soil sample is completely dispersed and suspended and then allowed to settle, the sand size particles will settle past the sample zone (within the top 10 cm) in 30 seconds, while the silt size particles will take up to 8 hours. There are two methods of particle fractionation based upon Stokes' law (Carver, 1971):

(a) *The Pipette Method:* The pipette method of analysis depends upon the premise that after a particular time, all particles greater than a specific diameter would have settled below a certain depth. If a pipette is inserted into the liquid at this depth, the sample will only contain particles of diameter smaller than this size.

(b) *The Hydrometer Method:* For the hydrometer method, the depth to which a hydrometer sinks when placed in a suspension is dependent on the suspension density. As the larger particles settle beyond the depth at which the hydrometer is suspended, the liquid density becomes lower and the hydrometer drops giving lower readings.

In the present study, the Pipette method has been used for soil samples for the grain size smaller than 62 micron (Carver, 1971). The method is described in the following paragraph.

About 10 to 20 gm of the soil sample (silt and clay) was placed in a beaker, moistened with a little distilled water and transferred to a larger container. Thereafter, 300 ml of distilled water and 15 ml (10%) Calgon solutions were added. Stirring was done for 15 minutes to disperse the aggregates in the soil. The sample was then transferred to a 1000 ml graduated measuring cylinder, and the volume up to the 1000 ml mark was made up with distilled water. The stem of a 25 ml pipette was marked exactly 20 cm from its tip. The measuring cylinder was placed in a sink filled with water to maintain the temperature near a constant value. The suspension was vigorously stirred for about half a minute so that the soil got evenly distributed throughout the cylinder, care was taken to avoid introducing air bubbles into the suspension. The temperature of the suspension was noted and then stirring was done again for 30 seconds. The timer (stop watch) was started as soon as the stirrer was withdrawn. Samples were withdrawn in the marked pipette from 20 cm depth after 20 seconds and from 5 cm depth as per the Table 3.4 depending upon the water temperature. The pipetted samples were transferred to a weighed crucible. The crucible was placed in an oven, evaporated to dryness, cooled and weighed again. Subsequently the total weight of the evaporation dish plus its contents was recorded on the data sheet, and the weight of the clean evaporation dish (ED) and the weight of dispersant (DS) were subtracted from the total. The weight of the dispersant (DS) in the evaporation dish was calculated as follows:

DS = [(molecular weight of dispersant)×(molarities of dispersant in 1000 ml cylinder)]/ 50

After subtracting ED and DS, the remainder was SC, the weight of the silt and clay in the evaporation dish. Because SC values was estimated from a sample volume of 20

ml (or 1/50 of the original volume of the 1000 ml cylinder), it was multiplied by 50 to get the net total weight in the cylinder (Carver, 1971).

Table 3.4: Pipette withdrawal times calculated from Stokes' law (Carver, 1971).

Diameter in ϕ finer than	Diameter in Microns Finer than	Withdrawal Depth (cm)	Elapsed time for withdrawal of sample in hours (h), minutes (m) and second (s)			
			22^0	23^0	24^0	25^0
4.0	62.5	20	20s	20s	20s	20s
9.0	1.95	5	3h, 52m	3h, 46m	3h, 41m	3h, 36m

ϕ = particle size in ϕ units
= $- \log_2 d$; where, d = diameter of particle in mm

3.4.4 Groundwater Level Data Collection

Groundwater level data forms mandatory parameters in artificial groundwater recharge study. The zone of deeper water levels indicates maximum thickness of unsaturated zone and hence forms suitable sites for artificial recharge. Also water level data analysis along with other factors is of great importance to analysis the necessity of artificial recharge over the study area. During the feasibility study, the monitoring of groundwater level greatly help in identifying the method of artificial recharge. The depth of water table at post monsoon period is vital for estimating the thickness available for recharge. Ground water flow direction map is helpful because it determines whether the groundwater will flow away from the location where it is recharges artificially or not. If the groundwater flow direction is away from the location where it is recharged artificially, more water can be added / supplied for recharge. Hence, those sites are very important for artificial recharge.

Groundwater levels have been monitored at 37 locations (12 on the paleochannel aquifers and 25 on the adjacent alluvial plains aquifer) over 2 years (2005-2006) for both pre- and post-monsoon period. The precise locations (x, y, z co-ordinates) have been determined through differential GPS. Groundwater levels were measured using a survey-grade groundwater level indicator. Also, groundwater level data (pre- and post-monsoon) are collected from Groundwater Division, Uttar Pradesh for over 10 years (1994-2004). The detail about the water level data analysis has been presented in Section 1.6 and Section 5.5.

3.4.5 Groundwater Sample Collection

The groundwater samples were collected in clean polypropylene bottles from the first unconfined aquifer in the study area from shallow hand pumps and open wells. For sampling from open wells, the water sample was collected from some depth from the groundwater level. Before the collection of the groundwater sample, the hand pump was purged to remove any stagnant water to ensure that the water sample is representative of the aquifer formation being sampled. As a rule of thumb, a minimum of three to five well volumes of water were purged (Harter, 2003). The water samples were collected immediately after purging. All sample bottles were filled completely, capped, and labelled. These water samples were subjected to stable isotopes analysis for obtaining information on recharge source (Chapter 5).

3.4.6 Tracer Studies

The infiltration rate or the recharge rate over the study area also helps to design suitable artificial recharge structures and to assess the extent of recharge from these structures. Areas with high infiltration/recharge rate are more suitable for artificial

recharge. So, it is very much essential for estimating recharge rate/infiltration rate for artificial groundwater recharge studies. Here, recharge rate due to precipitation have been estimated using tritium tagging technique along with remote sensing and rainfall data. The technique of estimation of recharge rate by using artificial tritium method was first applied by Zimmerman et al. (1967 a, b) in West Germany. The basic principle of this technique assumes that the soil water in the unsaturated zone moves downward "layer by layer" similar to a piston flow. Since the lateral molecular diffusion mixes the percolating water rather fast, this assumption is probably valid in most natural situations e.g. in the alluvial formations, except where the alluvial cover is too thin and the basement rock is at a shallow depth or where the" fissures and/or discontinuities are present in the soil profile (NIH,1986 and 2000). On the basis of this assumption, if fresh water tagged with tritium enters the top of the soil below the active root zone, and is not affected by evaporation, the tagged tritium will be mixed with the soil moisture available at that depth and act as an impermeable sheet. In this case, if any water is further added at the top of the soil surface, it will be infiltrated into the ground by pushing down the older water, thus the shift in the tritium peak can be observed after some time (say after lapse of one season). Recharge rate has been calculated from the tritium peak shit, rainfall and grain size analysis. The detailed methodologies have been described in Chapter 7.

3.5 Software Used

The remote sensing data has been processed by using ERDAS Imagine-8.7 software. The GIS analysis has been carried out using ILWIS-3.3, ARCVIEW-3.2 and R2V software. Litholog data analysis is carried out by using ROCKWORKS-2006 software.

3.6 Methodology-Overview

The broad methodology adopted in the present study has been outlined in Figure 3.3. Details of methodologies employed in the procurement and analysis of the different data sets have been discussed separately at relevant places in the succeeding chapters.

In this work, particular emphasis has been placed on using remote sensing – GIS technology for the study aimed artificial groundwater recharge in the area. The entire study has been carried out in GIS environment. A base map has been prepared by scanning, geo-referencing, mosaicking and digitizing the Survey of India (SOI) topographic maps. The various data layers have been co-registered with the base map. Point data obtained from field and laboratory experiment are properly placed on the base map and finally various information have been obtained using GIS tools.

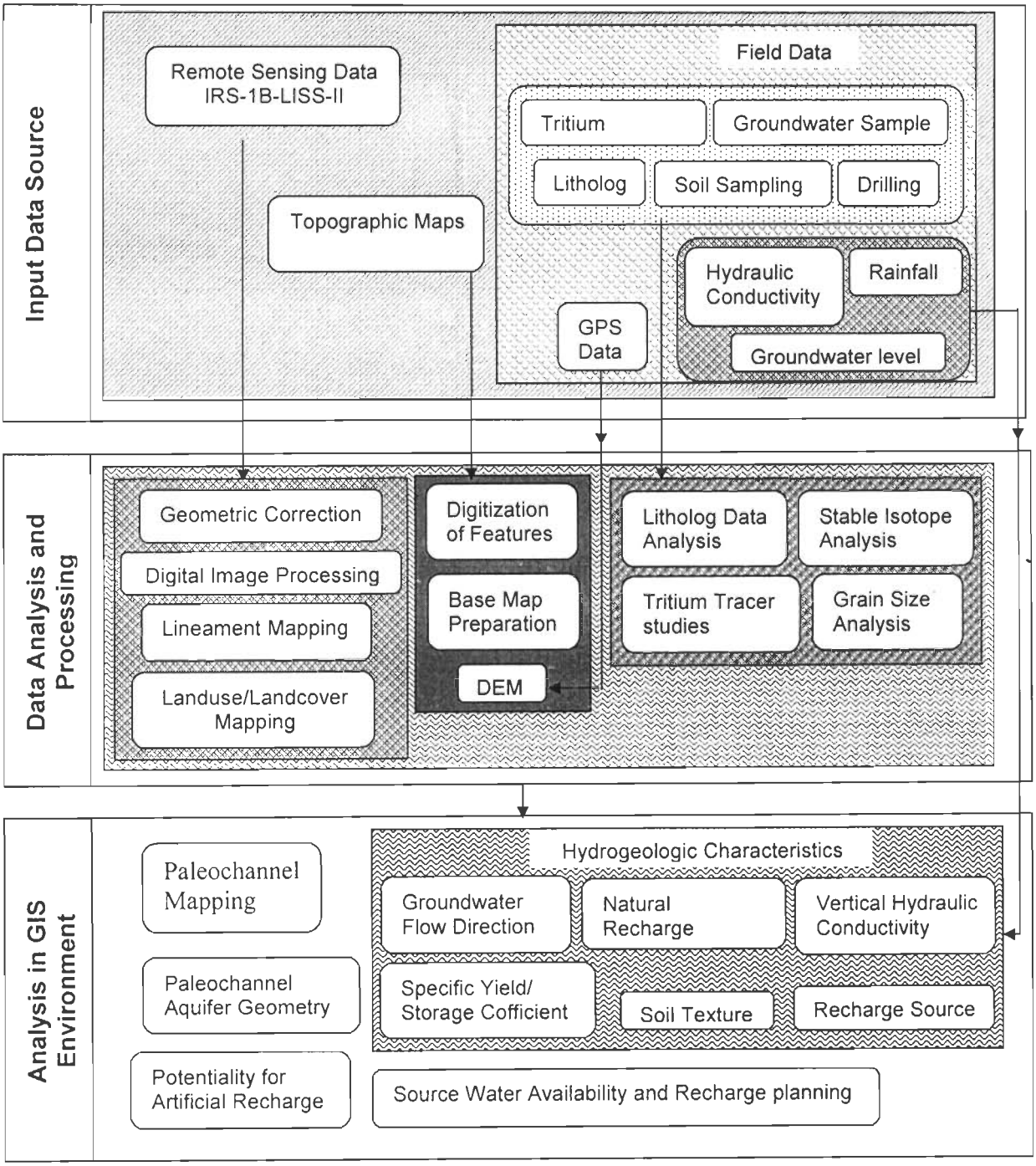

Figure 3.3: Flow diagram showing the broad methodology adopted in this study.

Chapter 4

Mapping of Major Paleochannels from Remote Sensing Data

4.1 Introduction

In this study, the major emphasis is on artificial groundwater recharge, for which in the first stage site selection is required. The study area is a part of the Indo-Gangetic plains and is quite devoid of any significant relief features and physiographically exhibits the typical characteristics of a river flood plain. The various major physiographic/landform units are – (a) vast stretches of alluvial plains, (b) dry streams, (c) paleochannels, and (d) marshy land (Kumar et al., 1996; Sammdder et al., 2007). The river paleochannel deposits are significantly different from the vast alluvial deposits being composed of coarse sand with pebbles, boulder, cobbles etc. and have been came from well developed regionally extensive earlier river systems. The landcover types are closely related to the landform

units. Therefore, as a first step, landcover/landform mapping has been carried out using remote sensing data.

In this chapter, first a description of landcover/landform classes is given. This is followed by description of pre-processing and processing of remote sensing data and its interpretation. Finally, an over view of major paleochennels present in the area is presented.

4.2 Major Landform/Landcover (LULC) Classes

Due to synoptic view, map like format and repetitive coverage, satellite remote sensing imagery is a viable source of gathering quality LULC information at local, regional and global scales (Csaplovics, 1998; Gupta, 2003; Foody, 2002). In this study, six LULC classes have been identified. These are – agricultural land, paleochannel, dry streams, water body, built-up area, and marshy land. Pre-processing and processing of remote sensing data has been discussed in the subsequent section to follow. Detailed characteristics of all the classes along with their interpretative characteristics on each band as well as on the colour infrared composite of LISS-II image are given below (Figure 4.1, Figure 4.2, Table 4.1):

Agricultural lands: The agricultural lands having sparse vegetation and high agricultural activity appear as dull red colour in CIR composite. In red band it appears as medium to dark due to high absorption. This landform unit occupies most of the study area.

Paleochannel: The paleochannels on the NIR band appear as very light tone implying extremely low surface soil moisture. In Red band they also appear as very light tone indicating complete absence of vegetation. They are marked by sinuous/serpentine shape with high permeability and appeared as pale-white zones on colour infra-red composite.

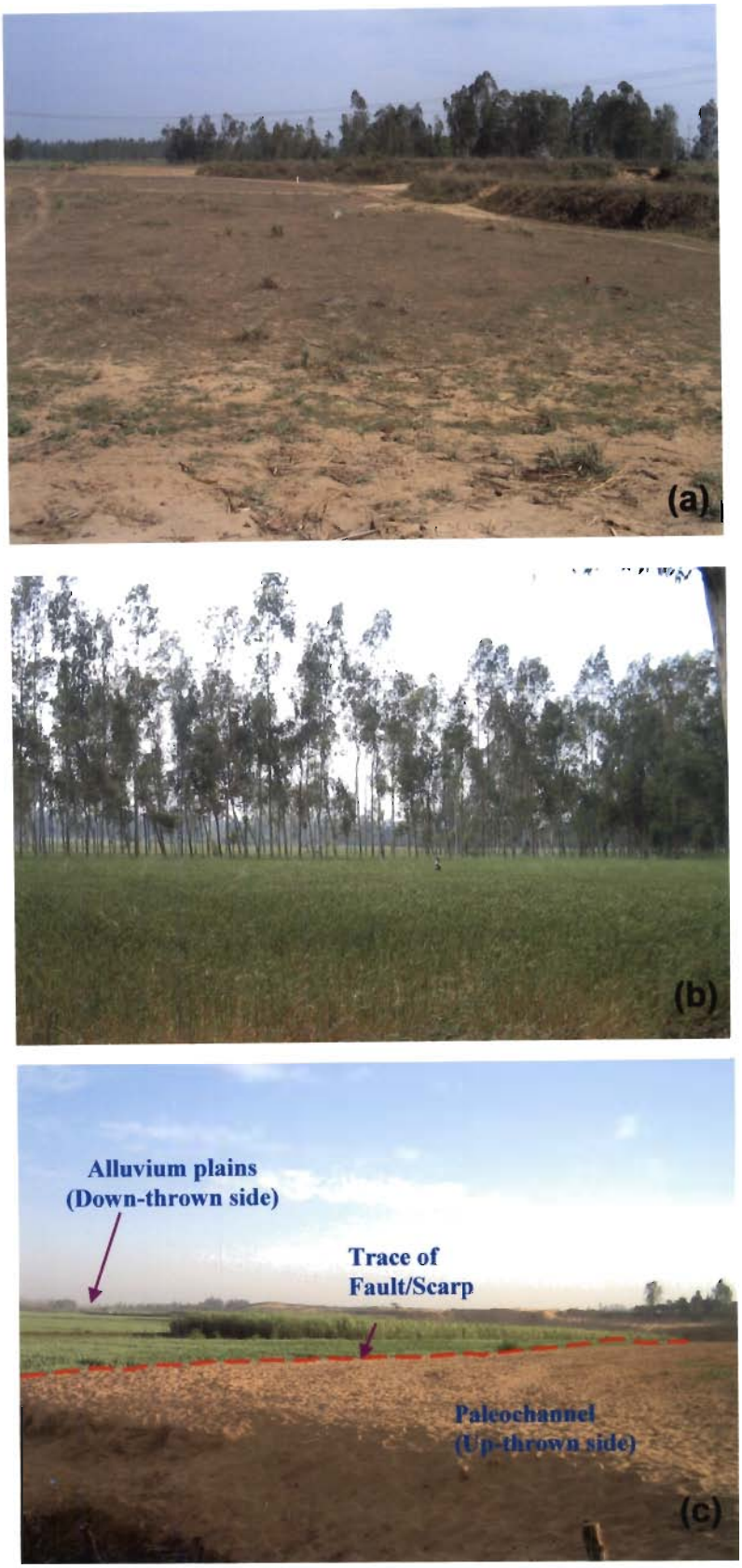

Figure 4.1: Field photographs. (a) Paleochannel near Barla village (note the scant vegetation and agricultural activity and presence of coarse sand); (b) Agricultural field in the alluvial plains and (c) Trace of Fault/Scarp near Harinagar village.

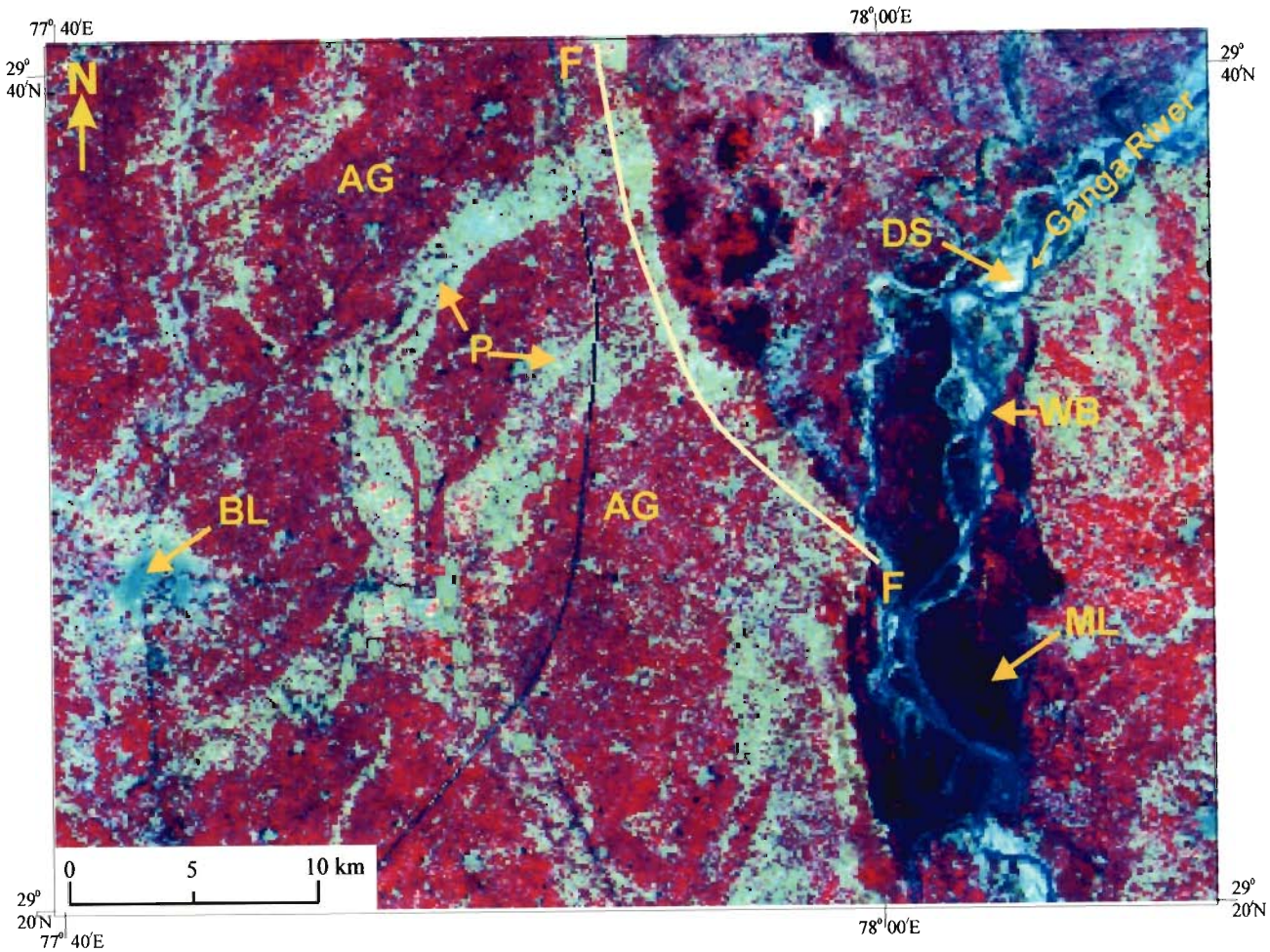

Figure 4.2: Colour infra-red composite of LISS-II image (NIR band coded in red colour; Red band codded in green colour and Green band coded in blue colour) showing various LULC classes (AG-Agricultural lands; P-Paleochannel; BL- Built-up areas; ML-Marshy lands; WB-Water body DS-Dry stream/flood plains and F-F: Fault scarp).

Table 4.1: Characteristics of landcover/landuse classes.

Landcover classes	Description	Blue Component Green Band	Green Component Red band	Red Component NIR band	CIR composite
Agricultural Land	Sparse vegetation, agricultural activity	Dark	Very dark	Medium to dark	Dull red
Water body	River, Ponds etc.	Light	Light	dark	Cyanish blue to Blue
Paleochannel	Very low vegetation density, agricultural activity, fallow land	Grey	Light	light	Yallowish-white
Marshy land	Low lying land stagnant with shallow depth water throught the year	Very dark	Very dark	Medium to dark	Black
Built-up area	Town and villages; block like appeaence	Light grey	Grey	Darker	Bluish grey
Dry stream/flood plains	Dry sand appear in the bank of river	Dark gray	Dark	Dark	Cyanish-white

Drainages: The drainages appear bluish-white colour in CIR composite and dark in NIR band. The Ganga River and its tributaries are incorporated into this class.

Dry streams: Numerous dry streams appear as cyanish-white in CIR composite. They have light tone in red band.

Marshy land: It is low lying land stagnant with shallow depth water throughout the year and appears as black on CIR composite. These appear on the bank of the Ganga River.

Built-up area: The cities and villages were identified by its blocky appearance. The CIR composite shows bluish gray colour for built-up areas.

4.3 Pre-Processing of Remote Sensing Data

A digital image is a two-dimensional data array of brightness values representing spectral response of the scene captured. It typically comprises of small equal-sized areas called pixels (picture elements), which form the ground resolution cell. A digital image often contains distortions with respect to its geometry and radiometry (e.g., atmospheric effects). Therefore, the data needs to be pre-processed to rectify for various distortions. The rectified image is then subjected to a number of image processing operations, such as contrast enhancement, image ratioing, classification, etc. for extracting useful information related to the Earth's environment. An overall framework of various digital image processing operations adopted here for various task is shown in Figure 4.3.

(a) Geometric Correction

The digital images acquired from remote sensing satellites are fraught with geometric distortions, which render them unusable, as these may not be directly correlated to ground locations (Gupta, 2003). The geometric distortions in images may occur due to several reasons, such as Earth's curvature, panoramic distortion, etc. Geometric correction involves the process of assigning map coordinate information to the image data so that the geometric integrity of the map in the image is achieved.

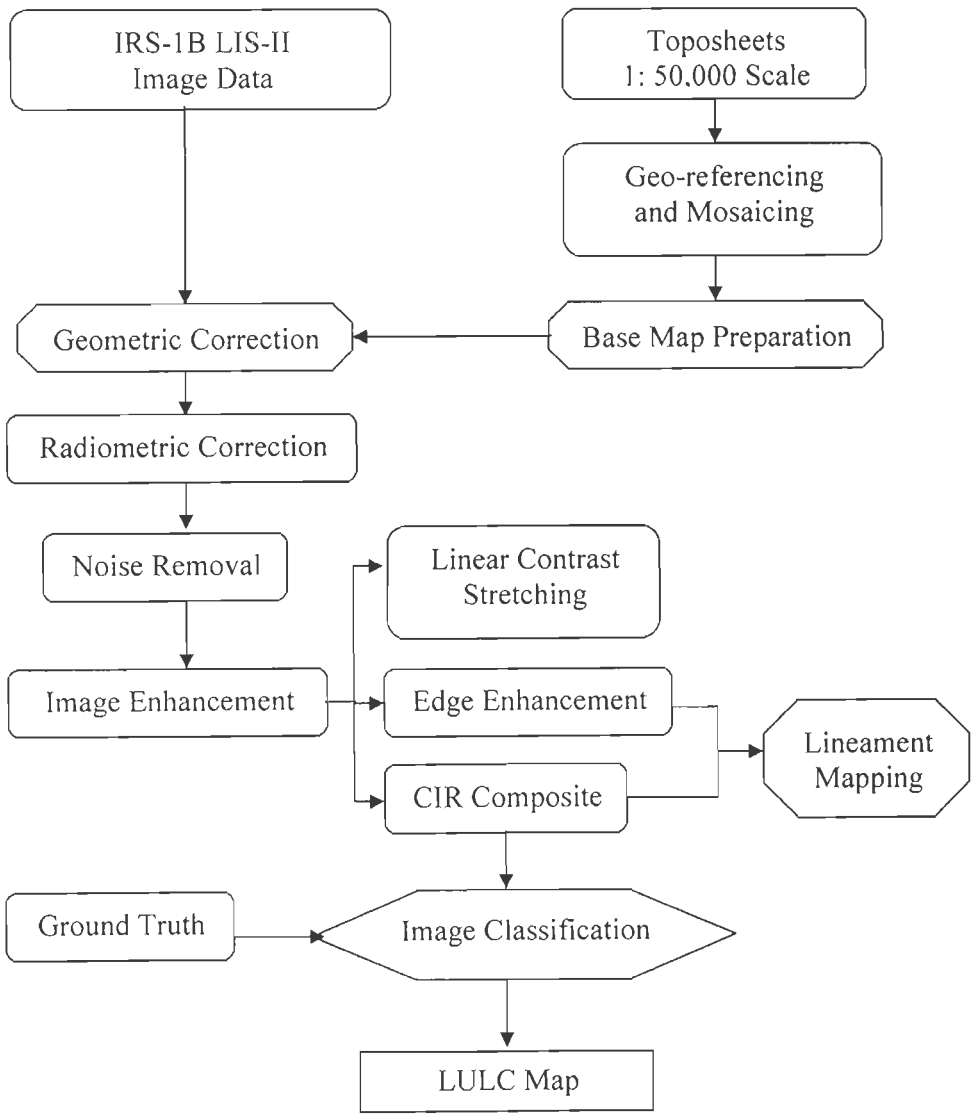

Figure 4.3: Flow diagram showing image processing techniques adopted in the study.

Geo-referencing is commonly performed using the method of rubber-sheet stretching that has been explained in many standard texts (e.g., Mather, 1999; Gupta, 2003). A number of ground control points (GCPs) distributed uniformly over the entire area are collected such that they can be easily located on both the image to be rectified and the reference map, such as a toposheet. A GPS survey is often carried out for accurate determination of coordinates of the GCPs.

In this study, the geometric correction of remote sensing data (IRS-1B-LISS-II image) using the above procedure has been performed on ERDAS Imagine. In the first step, Survey of India toposheets (53G/9, 53G/13, 53G/14, 53G/15,53K/1, 53K/2, 53K/3 at 1: 50,000 scale) have been scanned to convert the paper maps into digital format. The scanned toposheets have been geo-coded using the latitude and longitude information of the graticule intersections and reprojected to Polyconic projection system with Everest 1956 spheroid and India-Nepal as datum (Table 4.2). A mosaic of these geo-coded toposheets has been generated and used as reference map or "master" for geometric rectification of satellite images and geological maps.

Table 4.2: Properties of map projection system used.

Projection	Polyconic
Spheroid	Everest 1956
Datum	India-Nepal
Longitude of Central Meridian	$77^0 44' 59.32'' E$
Latitude of Origin	$29^0 45' 0.13'' N$
False Easting	5,00000.0
False Northing	5,00000.0

Remote sensing data (IRS-1B-LISS-II) have been geo-referenced with reference to the base or master map by taking input GCPs from LISS-II image and the reference GCPs from topographic (master) map. A large number of well distributed points (like intersection of roads, road and canals, bifurcation of canal etc.) identified both on the image and the reference map have been taken as GCPs in view of the absence of other distinct features in the area.

As this is a plain area, eighteen GCPs are found to be enough for adequate geometric correction of remote sensing data. A Root Mean Square (RMS) control point error of 0.252 pixel has been obtained by using 2^{nd} order polynomial model, which is well within the acceptable limit of one pixel for such type of study. The nearest-neighbour resampling method has been adopted to generate the final geo-referenced LISS-II image, as this preserves the original brightness values in the output image (Gupta, 2003).

(b) Radiometric Correction

The optical remote sensing data invariably contains the atmospheric haze components due to atmospheric interaction. In the visible – near infrared region of the electromagnetic spectrum, scattering is the most dominant process leading path radiance. This has an additive role and affects the brightness values (Jensen, 1996). The remote sensing data, therefore, need to be corrected for removing atmospheric haze components. Although there are many techniques to perform this correction, the most widely used 'dark-object subtraction' technique (Chavez, 1988; Gupta, 2003) has been adopted here to correct such atmospheric haze effect. This is a simple, fast to implement, empirical procedure. The method is based on the assumption that in every image there should be at least a few pixels completely dark (0% reflectance); they may correspond to areas of deep, clear, open water bodies, deep shadows etc. Ideally, these pixels should have DN values of zero; however,

because of the atmospheric haze, they record non-zero values. This characteristic is used in empirically for estimating the haze component. In practice, the method involves first locating clear, open and deep water bodies or completely shadowed (dark) areas (where ground reflectance can be considered to be null and the DN-values in infrared channels are also generally nearly zero). The minimum DN-value in each channel over such pixels is taken as the path radiance and is subtracted from all other pixel values in the respective channel.

(c) Noise Removal

An efficient method to remove noise from digital image is through Fourier analysis. Strippings are seen on the LISS image, which have been removed through Fourier filtering. Initially, First Fourier Transformation is calculated which gives the Fourier spectrum of the raw image. The Fourier spectrum shows the different anomalous high frequencies that are responsible for different type of noises. So, initially a low pass filter is applied on the image to block the high frequencies. The corresponding IFT (Inverse Fourier Transform) is calculated. Then the wedge filter is applied in the direction of the axis and the abnormal patches in the spectrum are blocked by using symmetrical rectangular and circular filters. These filters are used carefully because application of such filtering may block certain important frequencies which may results in complete black-out of the image. Application of wedge filters and corresponding transformation through IFT gives an image where the noises are removed.

(d) Image Enhancement

The purpose of image data enhancement is to render the set of digital image data more interpretable. Various standard digital image processing techniques can be applied to remote sensing data to extract information on geology, geomorphology, land use, structural

features and vegetation cover (Jensen, 1996; Gupta, 2003). In this study, the following types of image enhancement techniques have been applied on rectified LISS-II image:

Edge Enhancement and Linear Contrast Stretching: Individual spectral bands have been edge enhanced to emphasize high frequency variations and subsequently these enhanced bands have been used to generate Colour Infra-red composite (CIR composite). Various features like transport network, boundaries of water bodies, paleochannel boundaries etc. get very distinct on edge enhanced image. In the present case, edge enhancement followed by linear contrast stretching of individual bands of LISS-II data set have been applied for improving interpretability.

CIR composite : As the near infrared band gives information on surface moisture and the red band on vegetation, further interpretability is improved by making CIR composite using the enhanced NIR, Red, and Green bands (coded in red, green and blue colour respectively) (Figure 4.2).

4.4 Processing of Remote Sensing Data

4.4.1 Image Classification

A classification scheme defines the number of LULC classes to be considered to perform remote sensing image classification. Sometimes, a standard classification scheme, such as Anderson's LULC classification system (Anderson et al., 1976) may be used, while at other times the number of LULC classes may be chosen according to the requirements of the specific project for a particular application. In this study, six LULC classes have been chosen. Their detail description has been given in Section 4.2. Supervised classification scheme is applied for generating LULC map over the study area using - (a) LISS-II Colour

Infra-red composite (base map), and (b) field data (ground truth). The preparation of reference data has been ably supported with field surveys and previous knowledge of the study area. The GPS survey has been carried out to obtain accurate location of LULC classes for their easy demarcation on geo-rectified LISS-II image. All the processing steps have been implemented in ERDAS Imagine and ILWIS software.

The classification has been performed using the most widely used Maximum Likelihood Classifier (MLC) (Figure 4.4). The MLC assumes that spectral values of the training pixels are statistically distributed according to a multi-variate normal probability density function. For each set of spectral input values, the distance towards each class mean is calculated using Mahalanobis distance. The algorithm for calculating the distance to class means is

$$D_i(x) = \ln |V_i| + y^T V_i^{-1} y$$

Where, D_i = Distance between spectral input x and class mean based on probabilities

x = Spectral input (feature vector)

y = Distance towards a class mean.

y^T = Transpose of y

V_i = M × M variance-covariance matrix of a class, M is number of bands

$|V_i|$ = Determinant of V_i

The distance to class means thus computed is used to define the class name of the input pixel. The class name with the shortest distance to mean is assigned to the input pixel if this distance is smaller than a user defined threshold value; else an undefined value is assigned.

Selection of Training Data Set: In this step, a certain number of pixels are collected from relatively homogeneous areas consisting of the LULC classes. In case of doubt in

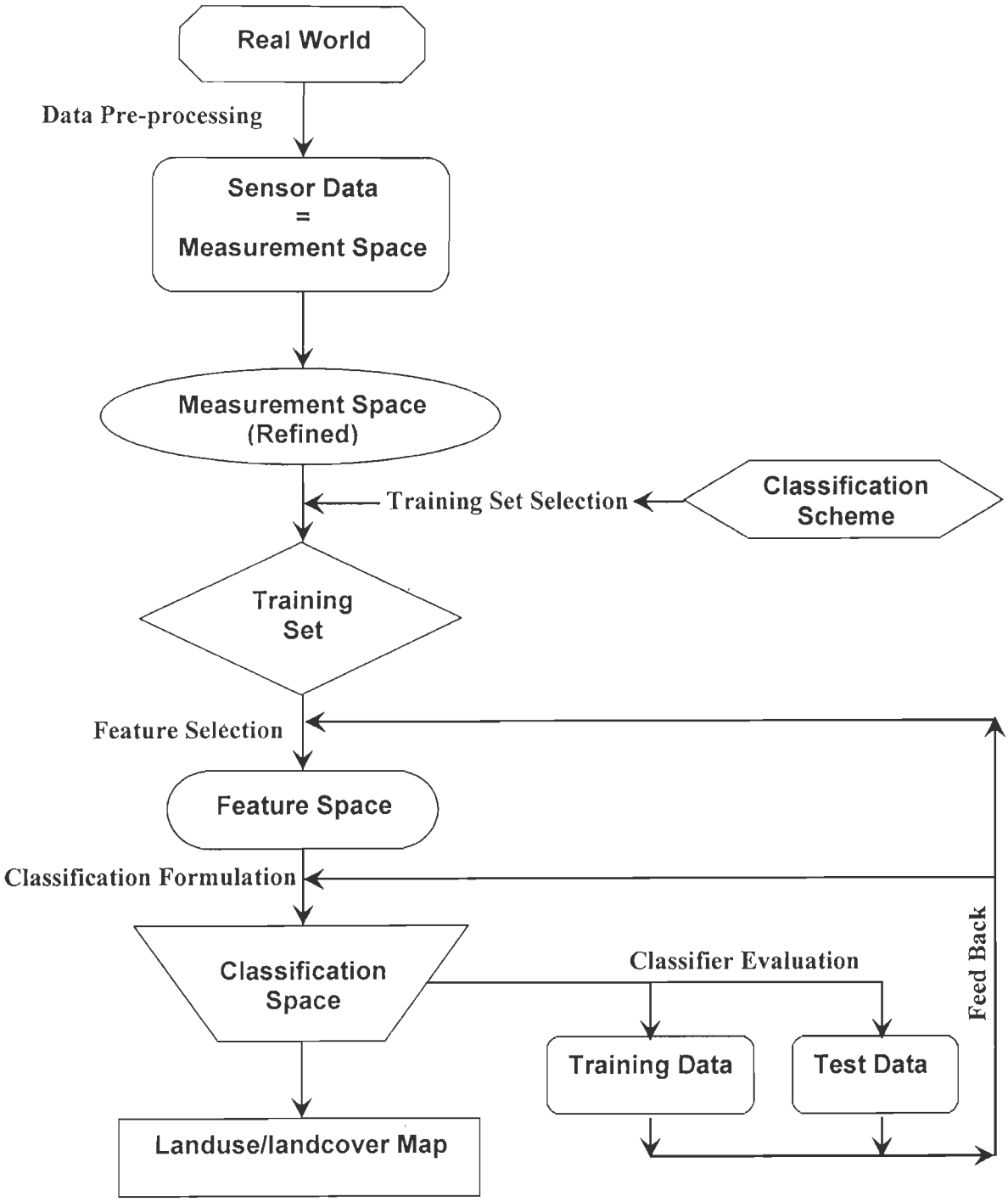

Figure 4.4: Supervised classification approach adopted in this study.

identifying the classes, field verification, and GPS survey have been carried out. These set of sample is known as training sample set. For each class, the number of training pixels has been adopted in accordance with the proportion of the area covered by the respective classes on the ground (Table 4.3).

Table 4.3: Number of training pixels for each LULC class used in classification.

Landuse/landcover class	Number of training pixels
Agriculture	1280
Settlements	287
Water body	210
Dry streams	205
Paleochannel	786
Marshy land	203
Total	2971

Thus, for the agricultural area 1280 pixels and for paleochannel 786 pixels have been selected due to their importance, while only 205 pixels have been selected for dry channels due to the very small area occupied by it. The pixels have been selected such that they are well distributed over the entire area. The histogram plot of majority of training areas shows normal distribution, which is a requirement of the maximum likelihood classifier used in this study.

Allocation Stage: Each pixel in the image, in this step, is assigned to a class depending upon the training set data statistics using a decision rule or image classifiers. Numerous image classifiers have been developed and applied for remote sensing data, each having their own merits and demerits in terms of efficiency and accuracy. The Maximum

likelihood classifier (MLC) has been found to be the most accurate and commonly used classifier, when data-distribution assumptions are met. This classifier is based on the decision rule that the pixels of unknown class membership are allocated to those classes with which they have the highest likelihood of membership (Foody et al., 1992). The detailed formulation of this classifier may be found in Richards and Jia (1999). A classified map thus generated by MLC is shown in Figure 4.5.

Testing/Classification Accuracy Assessment: No image classification is said to be complete unless its accuracy has been assessed. To determine the accuracy of classification, a sample of testing pixels is selected on the classified image and their class identity is compared with the reference data (ground truth). The choice of a suitable sampling scheme and the determination of an appropriate sample size for testing data play a significant role in the assessment of classification accuracy (Arora and Agarwal, 2002). The pixels of agreement and disagreement are generally compiled in the form of an error matrix. It is a $c \times c$ matrix (c is the number of classes), the elements of which indicate the number of pixels in the testing data.

The columns of the matrix depict the number of pixels per class for the reference data, and the rows show the number of pixels per class for the classified image (Table 4.4). From this error matrix, a number of accuracy measures, such as average accuracy, average reliability and overall accuracy. The overall accuracy is used to indicate the accuracy of whole classification (*i.e.,* number of correctly classified pixels (diagonal element of the error matrix) divided by the total number of pixels in the error matrix). The classification based only on spectral data of LISS-II image has produced an accuracy of 87.9%, which is more than the minimum accuracy criterion of 85% overall accuracy, as reported in USGS LULC classification system (Anderson et al., 1976).

Table 4.4: Error matrix of the classified image obtained from classification of data with 1, 2, 3, 4 band combinations of LISS-II data.

Classes in the classified image	Classes on reference data						
	1	2	3	4	5	6	Row total
1. Agriculture	**189**	0	0	1	6	1	197
2. Settlements	0	**128**	7	3	0	0	138
3. Water body	2	24	**147**	0	0	2	175
4. Dry streams	1	0	1	**132**	35	0	169
5. Paleochannel	3	0	0	28	**185**	0	216
6. Marshy land	1	8	0	1	0	**123**	133
Column total	196	160	155	165	226	126	**1028/1028**

4.4.2 Post-classification Filtering

Some stray pixels always occur in a LULC classification produced from remote sensing data. To remove these stray pixels and to generate a smooth image, a 3 × 3 pixels majority filter has been applied, which assigns the most dominant class to the central pixel (Figure 4.5).

4. 5 Paleochannel Mapping

Finally, integrating information from CIR composites, LULC map, and extensive field observations, paleochannels have been traced and a paleochannel map has been generated (Figure 4.6). The existence of paleochannels has also been cross-checked from litholog data and field observations. It has been observed from field observation that in the

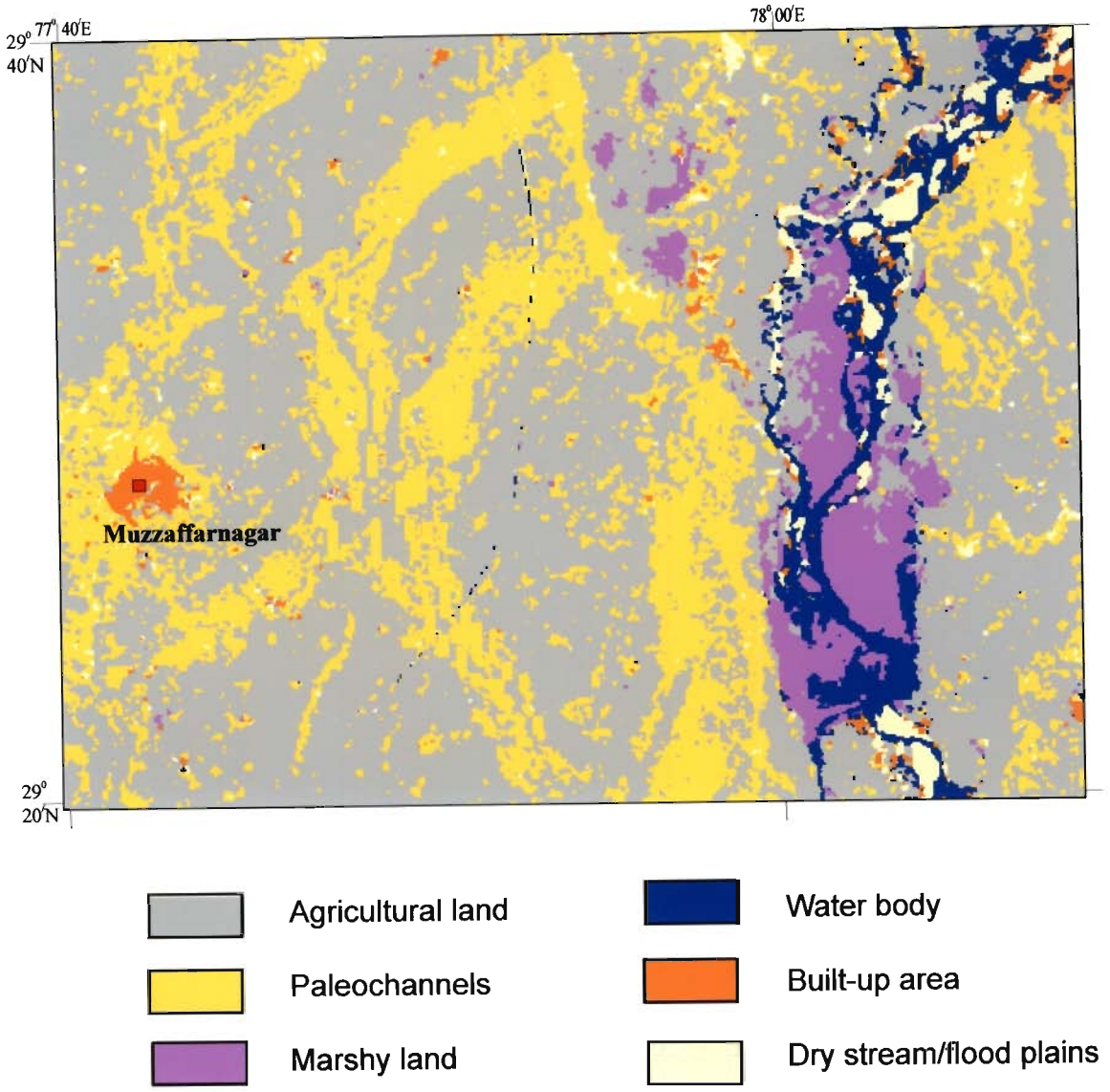

Figure 4.5: Landcover map possessing accuracy of 87.9% generated from band combination 4, 1, 2,3 (i.e. NIR, Red, Green and Blue bands of LISS-II image). A post-classification filtering has been applied.

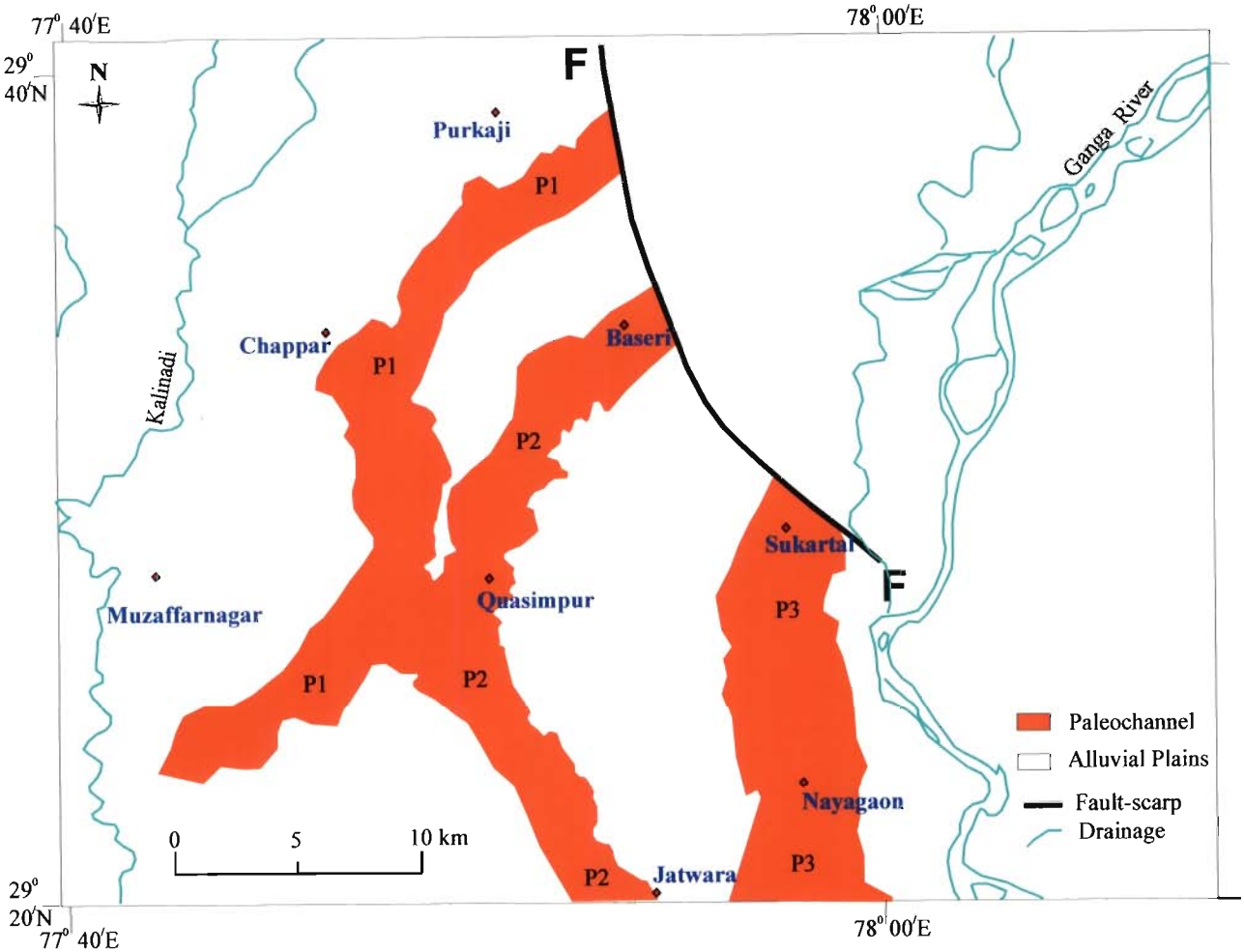

Figure 4.6: Major paleochannels of the study area.

northern upper part, paleochannels are suddenly cut by one fault-scarp (Figure 4.2, Figure 4.1c). The fault-scarp appears as narrow zones having similar signature like paleochannel. The south-western side of the fault-scarp is up-thrown and north-eastern side is down-thrown. The ground height difference between up-thrown and down-thrown is about 5 m. So, for preparation of paleochannel map, this falt-scrap is also taken into consideration.

4.6 Distribution of Major Paleochannel

In the study area, three major paleochannels exhibiting broadly successive shifting and meandering pattern have been deciphered (Figure 4.6). Some of the paleochannels when extended northwards meet the point, where the Yamuna and Ganga rivers debouch from the Siwalik Hills, into the plains, indicating that these rivers were active on this unit in the past, which is upland in nature presently. The characteristics of the major paleochannels over the study area are described below:

Paleochannel 1: It runs from east of Purkaji to near Chappar and then turns westward upto Muzzaffarnagar (marked as P1 in Figure 4.6). The trend of this paleochannel is NNE-SSW. The width varies from 2.3 km to 3.8 km, average being 3.0 km. The length is about 35 km. The areal extent is 105 square km.

Paleochannel 2: The second main paleochannel (marked as P2 in Figure 4.6) starts from near Baseri village through Quasimpur upto Jatwara. The average width of this paleochannel is 3.2 km. The length is about 30 km and the areal extent is 103.5 square km.

Paleochannel 3 (marked as P3 in Figure 4.6): This paleochannel starts from Sukratal through Mirahpur and extends southward parallel to the Ganga river upto Hastinapur. The width of the paleochannel is about 4.2 km. The length is more than 40 km.

All of these paleochannels in this study area are broadly N–S trending and are located to the west of the present day course of the river Ganga. So, it can be inferred that the Ganga River has been shifted successively from the west to the east. Most of the paleochannels are very wide (2-5 km) suggesting their formation by large river. A field work to the area has been carried out. It has been found during the field observation that the soils on the paleochannels are coarse sand or at times it appears pure sand (Figure 4.1a). Scant agricultural activity and mostly devoid of vegetation on the paleochannels are indicative of high permeable, porous, coarse grained materials possessing high infiltration rate.

Chapter 5

Hydrogeological Characteristics

5.1 Introduction

In the foregoing chapter, we have presented the results of landform mapping in the area. It has been shown that the area comprises of dominantly vast stretches of alluvial plains within which there are major paleochannels. From the point of view of artificial recharge of groundwater, the paleochannels hold distinct promise. Therefore, it is important to study the hydrogeologic characteristics of both the landforms, viz. the paleochannels and the adjacent alluvial plains, their recharge rate and hydrogeologic mutual interconnectivity, groundwater flow pattern, recharge sources, rainfall runoff etc., in order to asses the suitability of these units for artificial groundwater recharge.

In this chapter, first, the results of soil texture analysis are given which describe the compositional characteristics of the soils of the two landform regions. This is followed by results of computed vertical hydraulic conductivity values based on soil texture data. Then,

the present-day recharge sources of groundwater are discussed. Finally, based on groundwater level data, groundwater flow analysis is presented.

The litholog data analysis and aquifer geometry construction, recharge rate and rainfall runoff of the paleochannel and the adjacent alluvial plains have been presented in Chapter 6, Chapter 7, and Chapter 8 respectively.

5.2 Soil Texture

Tweenty (20) surface soil samples, collected from sites located on both the paleochannels and alluvial plains, have been subjected to grain size analysis to yield information on soil texture. From the mechanical analysis of soil samples in the laboratory (Section 3.4.3), the percentage for each of the soil fractions (sand, silt and clay) were determined. The percent of each the soil fractions (sand, silt and clay) are plotted on the USDA textural triangle (Brown, 1990; Bouwer, 2002). From this plot, textural class of the soil sample were determined. The location map of soil samples is given in Figure 5.1. The triangular plot is shown in Figure 5.2 and the overall summery of grain size analysis is given in Table 5.1 and Table 5.2.

From this soil textural analysis, the following observations have been made:

(a) It has been observed that in the area of paleochannels, the percentage of sand varies from 58.3 to 78.6 and that of silt and clay varies between 7.0 to 29.1 and 7.3 to 16.3 respectively. On the other hand, in the areas of alluvial plains, the sand percent varies between 15.1 to 28.8, whereas silt and clay percentage is between 51.9 to 69.3 and 11.8 to 24.2 respectively.

(b) This shows that the paleochannels comprise dominantly sandy loam type of soil, on the other hand, the alluvial plains are characterised by silty loam type of soil (Figure 5.2, Table 5.1, Table 5.2).

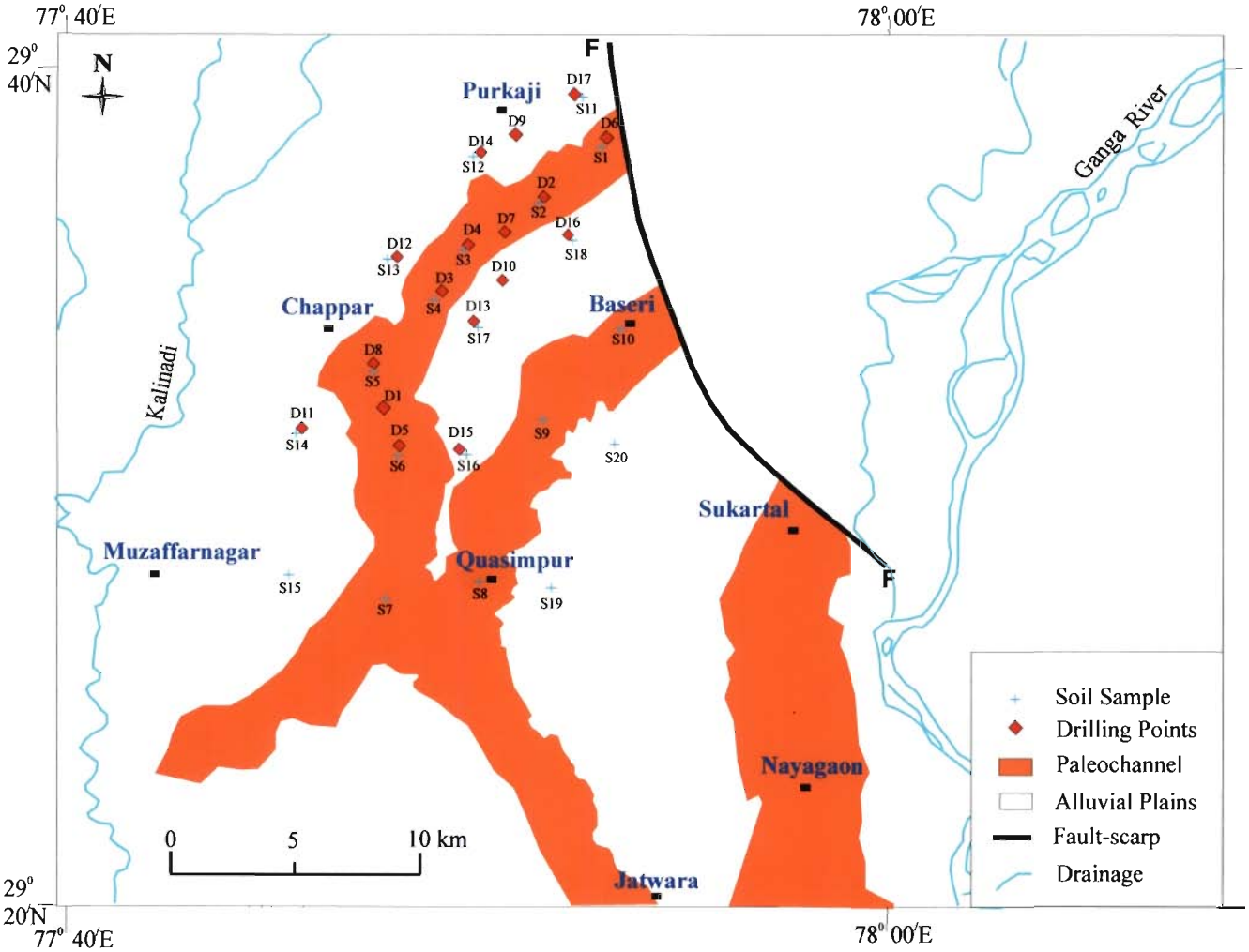

Figure 5.1: Location map of soil samples and drilling sites.

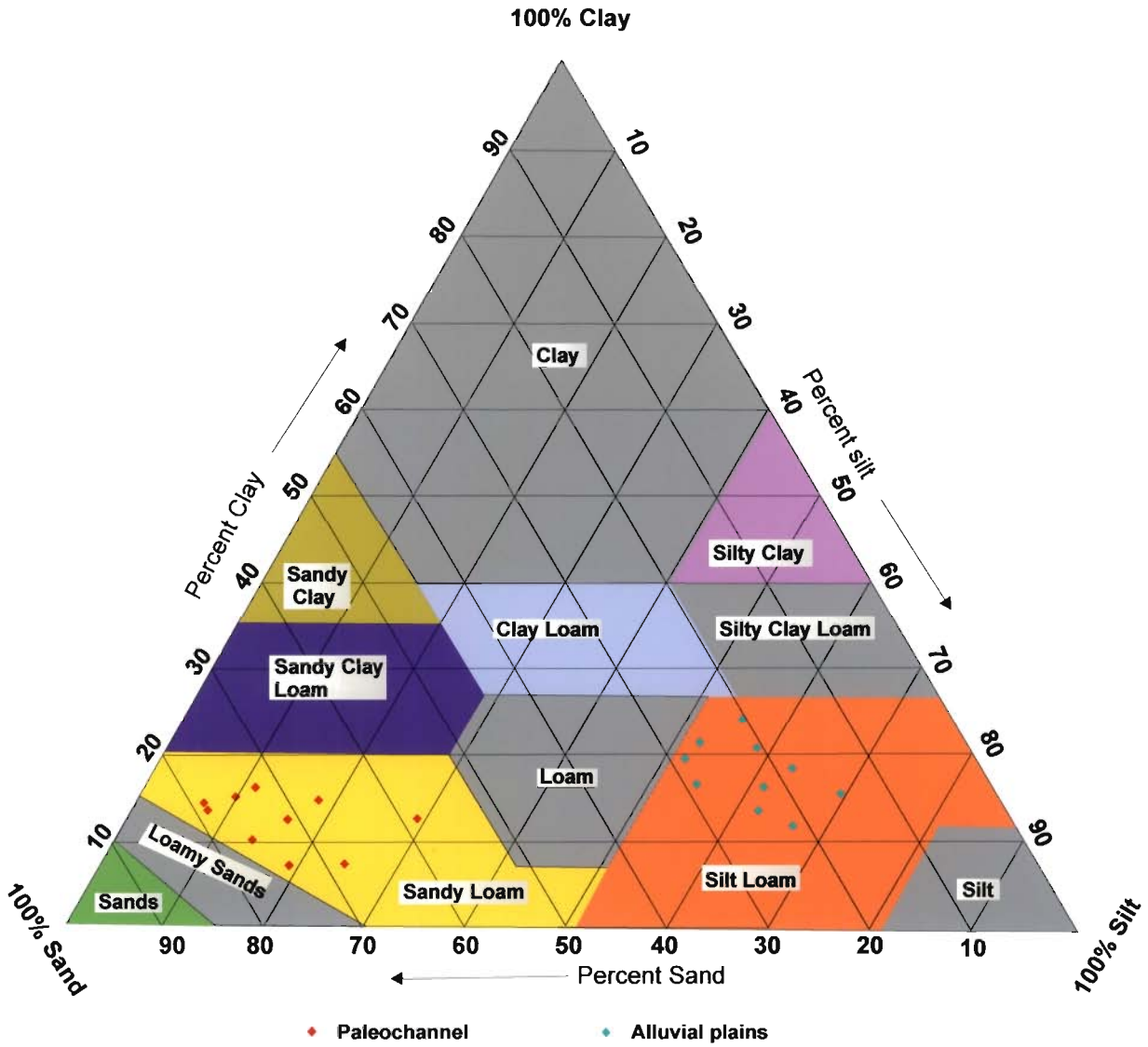

Figure 5.2: Soil samples plotted on USDA soil textural triangle.

Table 5.1: Sand, silt and clay percent of soil samples falling in paleochannel.

Location Name	Sand%	Silt%	Clay%
S1	72.5	11.2	16.3
S2	67	18.3	14.7
S3	68.2	24.4	7.4
S4	58.3	29.1	12.6
S5	75.1	9.8	15.1
S6	78.5	7	14.5
S7	73.6	19.1	7.3
S8	71.11	16.29	12.6
S9	76	13.75	10.25
S10	78.6	7.8	13.6

Table 5.2: Sand, silt and clay percent of soil samples falling in alluvial plains.

Location Name	Sand%	Silt%	Clay%
S11	20.5	55.3	24.2
S12	26	52.5	21.5
S13	22.3	61.4	16.3
S14	15.1	69.3	15.6
S15	28.8	54.7	16.5
S16	18.3	63.2	18.5
S17	21.7	66.5	11.8
S18	20.7	58.5	20.8
S19	28.6	51.9	19.5
S20	24.2	62.2	13.6

5.3 Vertical Hydraulic Conductivity

A series of 17 observation wells systematically sited on the paleochannel and its either flanks have been drilled (Figure 5.1) and sampling has been carried out for collecting lithological information at different depths (Section 3.4.2). Grain size analysis has been carried out for all the 82 samples collected from different locations and at various depths during drilling. The grain size distributions have been plotted on lognormal graph paper to

obtain grading curve for each sample. D_{10} has been calculated for each sample form the grading curve and subsequently bulk hydraulic conductivity has been determined using Hazen (1911) equation. The D_{10} is the grain size (in millimeters) at which 10 percent by weight of the sample has been retained and 90 percent of the sample has passed. The Hazen approximation was used to estimate bulk hydraulic conductivity where the D_{10} is between 0.1 and 0.3 mm (Hazen, 1911; Fetter, 1994). The Hazen (1911) equation is as follow:

$$K=C\ (D_{10})^2$$

Where, K is bulk hydraulic conductivity (centimeters per second) and C is a coefficient assigned to the sample based on the characteristics of the D_{10} (centimeters). The following table shows values for the coefficient C:

Table 5.3: Values for the coefficient 'C' (Fetter, 1994).

Soil characteristics	Values of C
Very fine sand, poorly sorted	40–80
Fine sand with appreciable fines	40–80
Medium sand, well-sorted	80–120
Coarse sand, poorly sorted	80–120
Coarse sand, well sorted, clean	120–150

The grading curves for different samples are shown in Figure 5.3 and Figure 5.4. The estimated D_{10} and bulk hydraulic conductivity values for different samples at different depth are detailed in Table 5.4 and Table 5.5.

In paleochannel aquifer, the D_{10} value ranges from 0.21 to 0.33 mm, whereas, in alluvial plains, it is 0.14 to 0.18 mm. The value of hydraulic conductivity ranges from 30 to

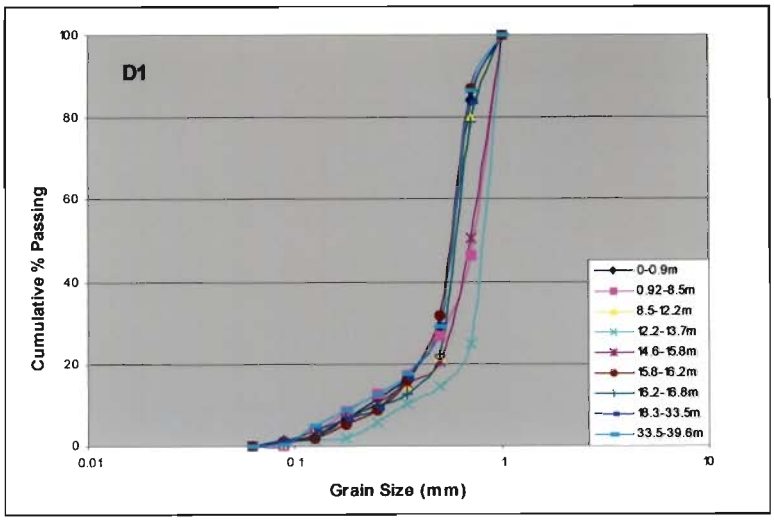

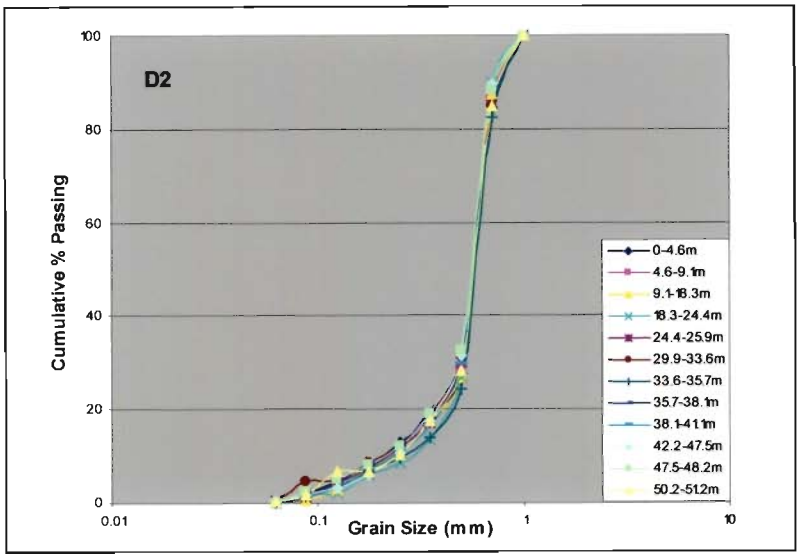

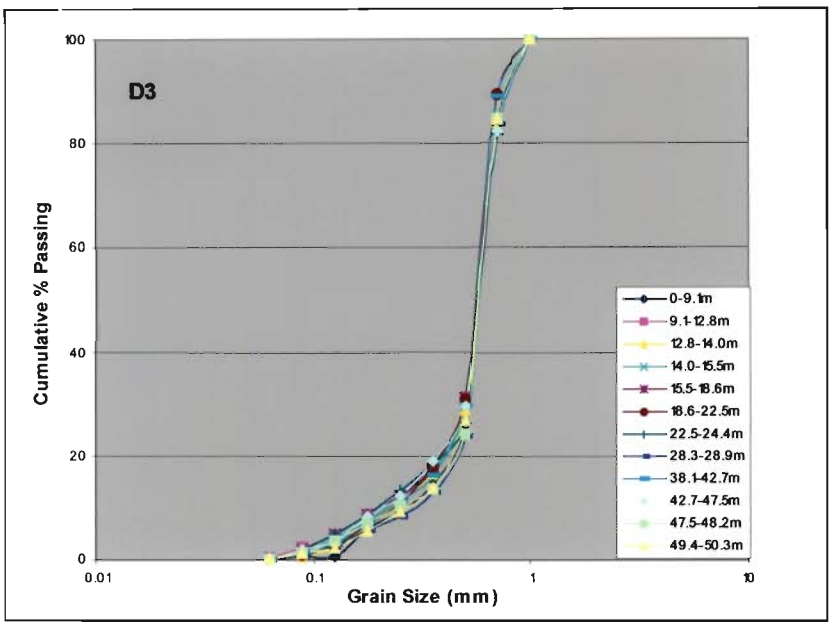

Figure 5.3a: Grading curves of samples falling within the paleochannel (see Figure 5.1 for locations).

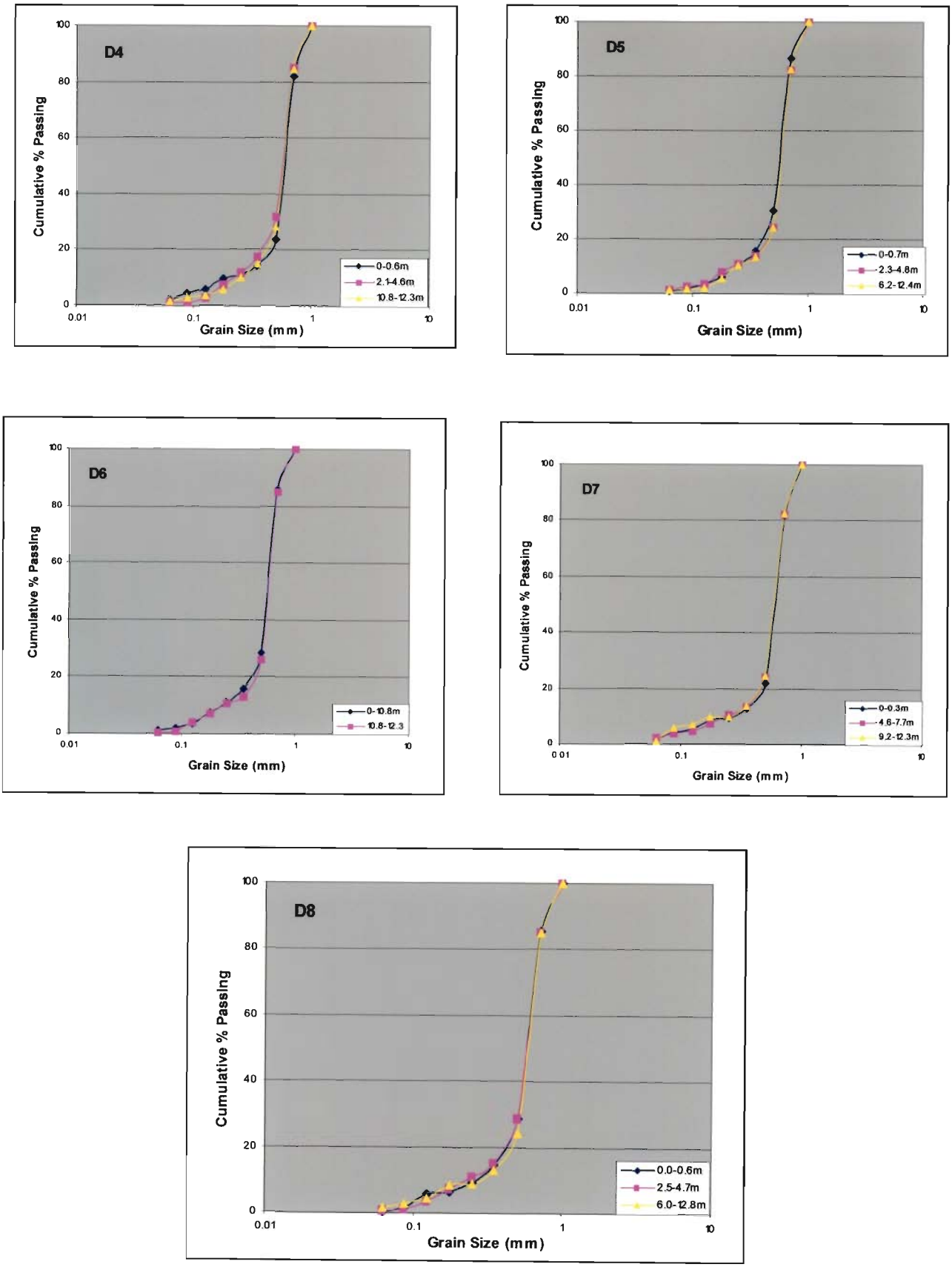

Figure 5.3b: Grading curves of samples falling within the paleochannel (see Figure 5.1 for locations).

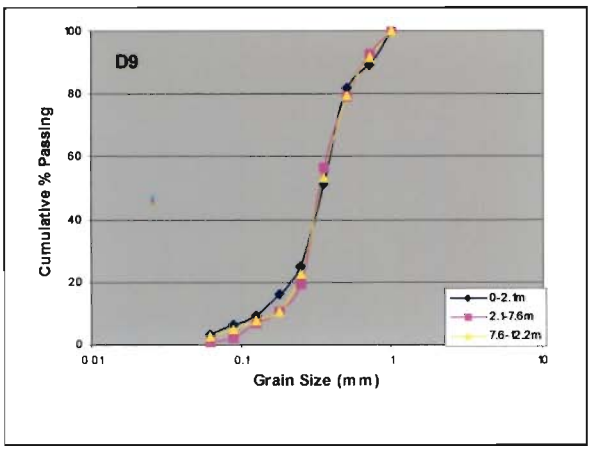

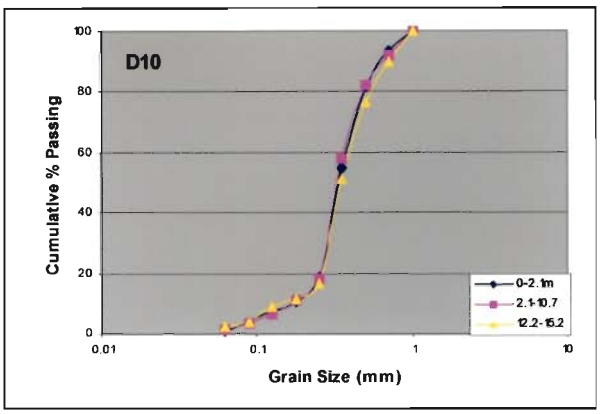

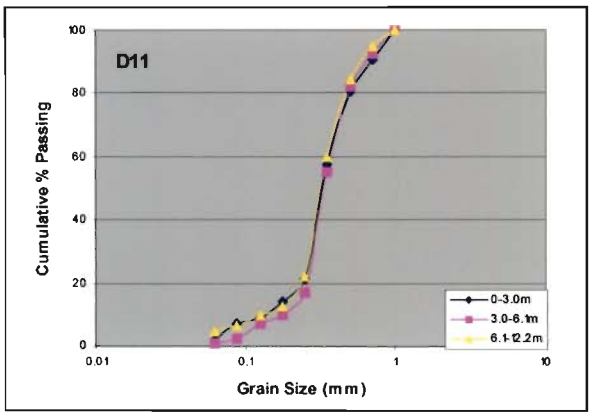

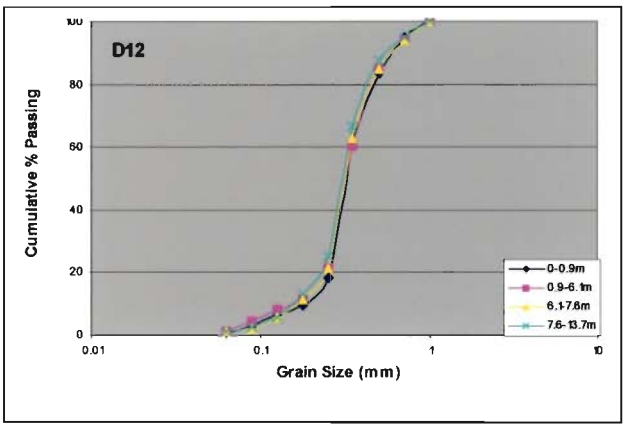

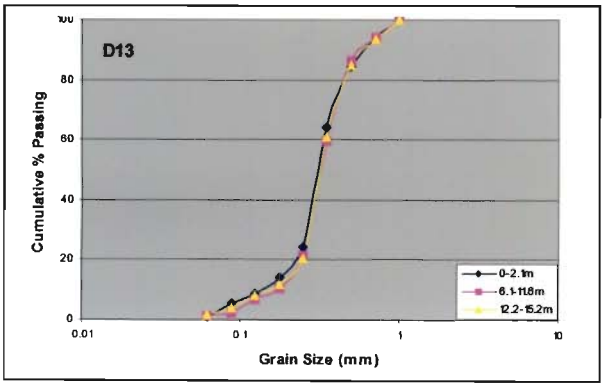

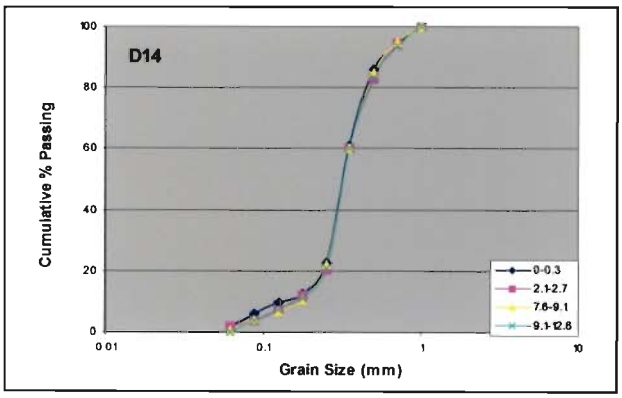

Figure 5.4a: Grading curves of samples falling within the alluvial plains (see Figure 5.1 for locations).

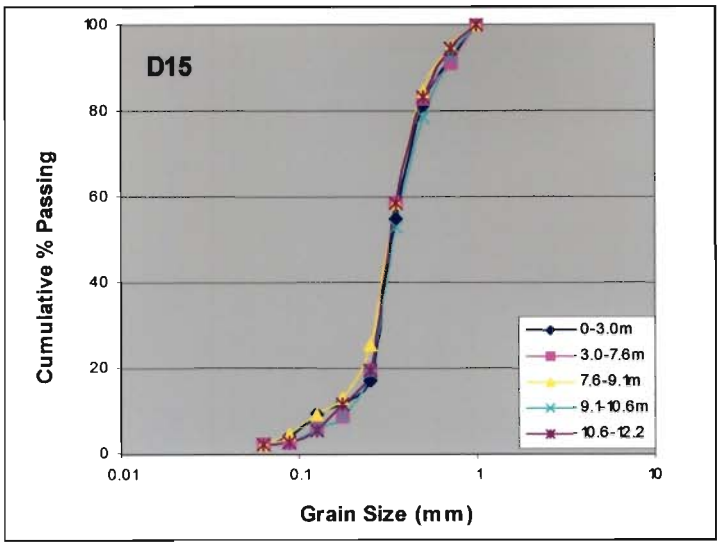

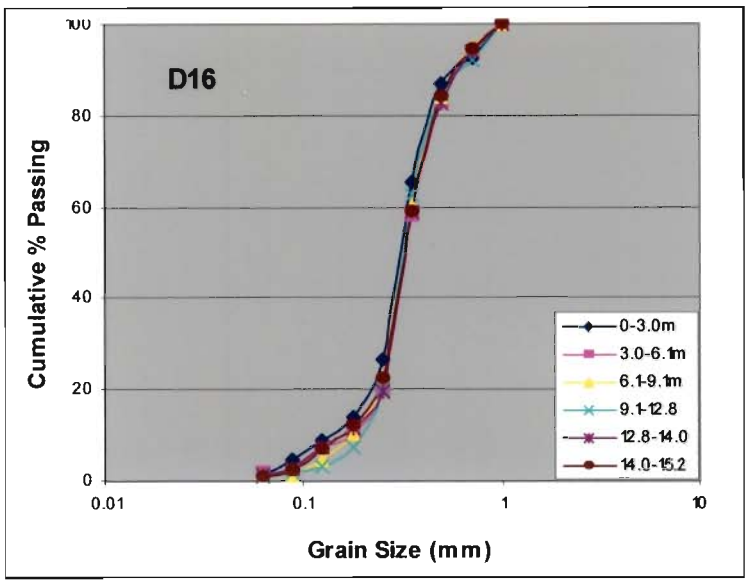

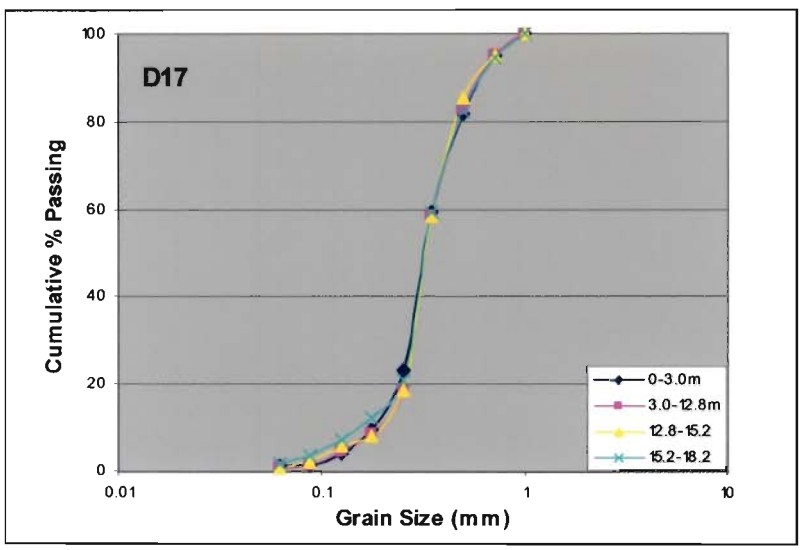

Figure 5.4b: Grading curves of samples falling within the alluvial plains (see Figure 5.1 for locations).

Table 5.4: D_{10} and hydraulic conductivity (K) values for locations falling in the paleochannel aquifer.

Location Name	Sample No	Depth (m)		D10 (mm)	K (m/day) (Hazen, 1911)
		From	To		
D1	S1	0.0	0.9	0.23	36.5
	S2	0.9	8.5	0.21	30.5
	S3	8.5	12.2	0.22	33.5
	S4	12.2	13.7	0.33	75.3
	S5	13.7	14.6	Pebble	> 100
	S6	14.6	15.8	0.24	39.8
	S7	15.8	16.2	0.25	43.2
	S8	16.2	16.8	0.24	39.8
	S9	16.8	18.3	Pebble	> 100
	S10	18.3	33.5	0.24	39.8
	S11	33.5	39.6	0.21	30.5
D2	S1	0.0	4.6	0.21	30.5
	S2	4.6	9.1	0.23	36.5
	S3	9.1	18.3	0.24	39.8
	S4	18.3	24.4	0.25	43.2
	S5	24.4	25.9	0.22	33.45
	S6	25.9	28.9	Pebble	> 100
	S7	28.9	29.9	Pebble	> 100
	S8	29.9	33.6	0.21	30.5
	S9	33.6	35.7	0.25	43.2
	S10	35.7	38.1	0.21	30.5
	S11	38.1	41.1	0.23	36.5
	S12	41.1	42.2	Pebble	> 100
	S13	42.2	47.5	0.24	39.8
	S14	47.5	48.2	0.21	30.5
	S15	48.2	49.4	Pebble	> 100
	S16	49.4	50.2	Pebble	> 100
	S17	50.2	51.2	0.23	36.5
D3	S1	0.0	9.1	0.25	43.2
	S2	9.1	12.8	0.21	30.5
	S3	12.8	14.0	0.23	36.5
	S4	14.0	15.5	0.22	33.4
	S5	15.5	18.6	0.21	30.5
	S6	18.6	22.5	0.23	36.5
	S7	22.5	24.4	0.21	30.5
	S8	24.4	28.3	Pebble	> 100
	S9	28.3	28.9	0.27	50.38
	S10	28.9	38.1	Pebble	> 100
	S11	38.1	42.7	0.23	36.56
	S12	42.7	47.5	0.21	30.5
	S13	47.5	48.2	0.23	36.5
	S14	48.2	49.4	Pebble	> 100
	S15	49.4	50.3	0.26	46.7

Table 5.4: (continued from last page)

Location Name	Sample No	Depth (m)		D10 (mm)	K (m/day) (Hazen, 1911)
		From	To		
D4	S1	0.0	0.6	0.21	30.5
	S2	2.1	4.6	0.21	30.5
	S3	10.8	12.3	0.24	39.8
D5	S1	0.0	0.7	0.24	39.8
	S2	2.3	4.8	0.23	36.5
	S3	6.2	12.4	0.25	43.2
D6	S1	0.0	10.8	0.23	36.56
	S2	10.8	12.3	0.23	39.8
D7	S1	0.0	0.3	0.25	43.2
	S2	4.6	7.7	0.23	35.5
	S3	9.2	12.3	0.21	30.5
D8	S1	0.0	0.6	0.26	46.7
	S2	2.5	4.7	0.25	43.2
	S3	6.0	12.8	0.27	50.38

Table 5.5: D_{10} and hydraulic conductivity (K) values for locations falling in the alluvial plains aquifer.

Location Name	Sample No	Depth (m)		D10 (mm)	K (m/day) (Hazen, 1911)
		From	To		
D9	S1	0.0	2.1	0.14	13.5
	S2	2.1	7.6	0.16	17.7
	S3	7.6	12.2	0.16	17.7
D10	S1	0.0	2.1	0.16	17.7
	S2	2.1	10.7	0.16	17.7
	S3	12.2	15.2	0.15	15.6
D11	S1	0.0	3.0	0.14	13.5
	S2	3.0	6.1	0.17	19.9
	S3	6.1	12.2	0.14	13.5
D12	S1	0.0	0.9	0.16	17.7
	S2	0.9	6.1	0.15	15.6
	S3	6.1	7.6	0.16	17.7
	S4	7.6	13.7	0.15	15.6
D13	S1	0.0	2.1	0.14	13.5
	S2	6.1	11.6	0.16	17.7
	S3	12.2	15.2	0.15	15.6
D14	S1	0.0	0.3	0.14	13.5
	S2	2.1	2.7	0.16	17.7
	S3	7.6	9.1	0.16	17.7
	S4	9.1	12.6	0.15	15.6

Table 5.5: (continued from last page)

Location Name	Sample No	Depth (m)		D10 (mm)	K (m/day) (Hazen, 1911)
		From	To		
D15	S1	0.0	3.0	0.14	13.5
	S2	3.0	7.6	0.17	19.97
	S3	7.6	9.1	0.14	13.5
	S4	9.1	10.6	0.18	22.3
	S5	10.6	12.2	0.16	17.7
D16	S1	0.0	3.0	0.14	13.5
	S2	3.0	6.1	0.17	19.97
	S3	6.1	9.1	0.17	19.97
	S4	9.1	12.8	0.17	19.97
	S5	12.8	14.0	0.16	17.7
	S6	14.0	15.2	0.15	15.6
D17	S1	0.0	3.0	0.17	19.97
	S2	3.0	12.80	0.18	22.3
	S3	12.8	15.2	0.18	22.3
	S4	15.2	18.2	0.15	15.6

75.3 m/day for samples falling in the paleochannel, and that between 13.5 to 22.3 m/day for the alluvial plain aquifers.

5.4 Recharge Source Identification

Isotopes are the atoms of the same element with different atomic mass. The isotope, which do not decay with time or take infinite time to decay are called stable isotopes, for example ^{1}H and ^{2}H. On the other hand, those isotopes spontaneously disintegrate by giving out alpha (α), beta (β) particles and/or gamma (γ) radiation etc. and transform into another type of atom are called radioactive isotopes like ^{3}H. Due to disintegration or the property of giving out radiation, the unstable isotopes are also called radioactive isotopes.

Stable isotopes of H, C, N, O and S occur naturally through the atmosphere, hydrosphere, lithosphere and biosphere. Each element has a dominant light isotope with

nominal atomic weight (^{12}C, ^{14}N, ^{16}O, ^{32}S, ^{1}H), and one or two heavy isotopes (^{13}C, ^{15}N, ^{17}O, ^{18}O, ^{33}S, ^{34}S, ^{2}H), with a natural abundance of a few percent or less.

The natural isotope abundance ratios show significant and characteristic variations when measured very precisely (Libby, 1946; Urey, 1947, Sinha et al., 2000). It was observed that isotopes of same element differ in chemically identical materials of different materials or produced by different processes. However, isotopes of the same element take part in the same chemical reactions but they do so at different rates. Therefore, Chemical reactions and physical processes such as evaporation and condensation discriminate against heavy isotopes. This results in fractionation of products, which are isotopically lighter (containing less of the heavy isotope) than their starting materials. Thus stable isotopes have found wide application in various areas of hydrology such as climate studies using measurements of temperature-dependent oxygen and carbon isotope ratios in for a minerals; rock age dating using radiogenic isotopes of elements such as lead, neodymium or strontium; and source determinations using carbon isotope, deuterium, and oxygen isotope ratios.

In the present study, the stable isotopes of groundwater samples are analysed using Dual Inlet Mass Spectrometer at National Institute of Hydrology, Roorkee (India). The main functional parts of the Dual Inlet Mass Spectrometers are Ion Source, analyzer and detector. The ion source is a small chamber in which reference and sample gas molecules are converted into ions. An analyzer is a flight tube/magnet and has the ability to separate ions. It bends ion beam when passes through the field of a magnet installed over the flight tube. Here, the beam separated into spectrum of masses according to the isotopes present. After the ions are formed and separated according to their m/z values, the Faraday cups detect the ion beams. The universal collector consists of three Faraday cups, each with a

different width of resolving slit. By collecting two or three ion beams simultaneously, the ion current can be expressed in mass ratios. Ion Currents from the collectors pass out of the vacuum envelope through insulated ceramic-to-metal seals electrically connected to "head" amplifiers and pre- amplifiers mounted on a vacuum flange. Thus, the measurement process completes.

The measurement is in terms of isotopes ratios of less abundant to more abundant isotope, i.e. ^{2}H /^{1}H and ^{18}O /^{16}O. Thus measurements of ratio of stable isotopes are done with reference to international standards. Natural abundance data are nearly always reported as delta values,δ, in units of per mil ("mil= 1000), written ‰. Delta values are calculated from measured isotope ratios as -

$$\delta = (R_{sample} - R_{standard})\ 1000/\ R_{standard}$$

Where, R_{sample} is the ratio of the heavy to the light isotope measured for the sample and $R_{standard}$ is the equivalent ratio for the standard. Thus, δ units are calculated relative to an internationally recognized standard, which is arbitrarily set to 0‰. For water sample analysis there are three International Standards that are distributed by the IAEA (International Atomic Energy Agency, Analytical Quality Control Services, Agency's Laboratory, Seibersdorf, P.O.Box 100, A-1400 Vienna, Austria). These are: V-SMOW (Vienna Standard Mean Ocean Water and Standard Light Antarctic Precipitation), SLAP ((Standard Light Antarctic Precipitation) and GISP (Greenland Ice Sheet Precipitation). The absolute isotope ratios of D/H, $^{18}O/^{16}O$ and $^{17}O/^{16}O$ in these two water standards are known. For oxygen isotope ratio, the δ values are defined as:

$$\delta\ ^{18}O = \{[(^{18}R/^{16}R)_{sample} / (^{18}R/^{16}R)_{standard}] - 1\} \times 1000 \text{ (in per mil)}$$

In normal practice, a given laboratory obtains the two water standards from IAEA by a written request and paying a small amount. These are supplied in sealed glass vials.

The laboratory, on its own is required to make two water standards that are different in δ-values so that the calibration can be done properly by correction of any possible non-linearity of analytical procedures. The laboratory water standards (called internal standards) are then calibrated against the V-SMOW and SLAP whose values are: V-SMOW: 0.00, 0.00 (by definition) and SLAP: $\delta D = -428.0$ and $\delta^{18}O = -55.5$ per mil relative to V-SMOW. For regular use, the internal water standards (secondary) are used along with the samples in routine runs. Craig (1961a, b) obtained the isotopic relation between oxygen and hydrogen for Global precipitation water as:

$$\delta D = 8\,\delta\,18O + 10$$

The line represented by this equation in the δD versus δ18O plot is also known as Global Meteoric Water Line (GMWL). It provides a base line for the interpretation of hydrological data at global/regional scale. Similar to the GMWL, NIH has developed Regional Meteoric Water Line (RMWL) and sub-regional meteoric water lines and the Local Meteoric Water Line (LMWL) for its station at Roorkee. These characteristic lines provide a base line for the interpretation hydrological data at regional, sub-regional or local scale. Here, MWL ($\delta D = 7.28\,\delta^{18}O + 5.93$) developed by NIH for its station at Roorkee is used for interpretation.

In the present study, samples were collected from three different sources namely, precipitation (at NIH), groundwater (from 11 sites- 5 in the paleochannel and 6 in the alluvial plains aquifer, Figure 5.5), and the adjacent Ganga Canal. The $\delta^{18}O$, D of such samples are tabulated in Table 5.6 to Table 5.8. Monthly variation of isotopic signatures of these sources is plotted in the Figure 5.6 and the relationship between the $\delta^{18}O$ and δD of groundwater, precipitation and canal water is shown in Figure 5.7.

Results and interpretations: Interpretation has been made by integrating all the informations i.e. isotopic data, sample location map along with major distributary and

canal, (Table 5.6 to Table 5.8, Figure 5.5 to Figure 5.7). The following conclusions are drawn:

i) Isotopic characteristic of precipitation data shows highest fluctuation over a year (±5.5‰) followed by canal water (±1.5‰).

ii) The inter-comparison of the annual average isotopic shows most enriched isotopic values for precipitation water (-4‰ (not normalized to the monthly rainfall amount)) and with the most depleted isotopic content in the canal water (-9.7‰). Minor fluctuations in isotopic values of canal water may indicate its major composition arising from its constant background reservoir source as melt water of high altitude origin.

iii) The isotopic differences between these water types reduce to minimum level in the months from Mid of July to September which are the monsoon months of the year.

iv) Between the months October to May, $\delta\ ^{18}O$ of precipitation shows enrichment to -1‰ probably due to evaporative enrichment of rain drop as these are the periods when rainfall amount is low. The precipitation during few showers in the monsoon months show high depletion which probably indicates local re-circulation of lighter re-circulating vapor of local origin.

v) Canal water anti-correlates with the precipitation peaks. This may be due to fact that at the time of low rainfall, the canal carries glacial melt water which are depleted and during these periods any weak showers that occurs gets enriched in isotopic content due to evaporation process.

Table 5.6: Isotopic data of precipitation data at NIH, Roorkee.

Sampling Date	$\delta^{18}O$	D
8.2003	-5.89	-35.3
1.2004	-0.1	5.2
2.2004	-1.84	-7.5
3.2004	-1.12	-2.2
4.2004	-0.56	0.5
5.2004	0.26	7.3
6.2004	-3.85	-22.53
7.2004	-2.32	-9.4
8.2004	-6.26	-38.5
10.2004	-3.97	-22.9

Table 5.7: Isotopic data of canal water from Dhanauri, Roorkee.

Sampling Date	$\delta^{18}O$	DO
Jan'04	-10.43	-67.00
Feb'04	-9.09	-59.90
20.03.2004	-8.13	-59.30
18.04.2004	-9.69	-65.30
16.05.2004	-10.68	-70.90
20.06.2004	-11.20	-75.20
04.07.2004	-8.42	-55.10
18.07.2004	-9.85	-63.20
01.08.2004	-8.07	-49.60

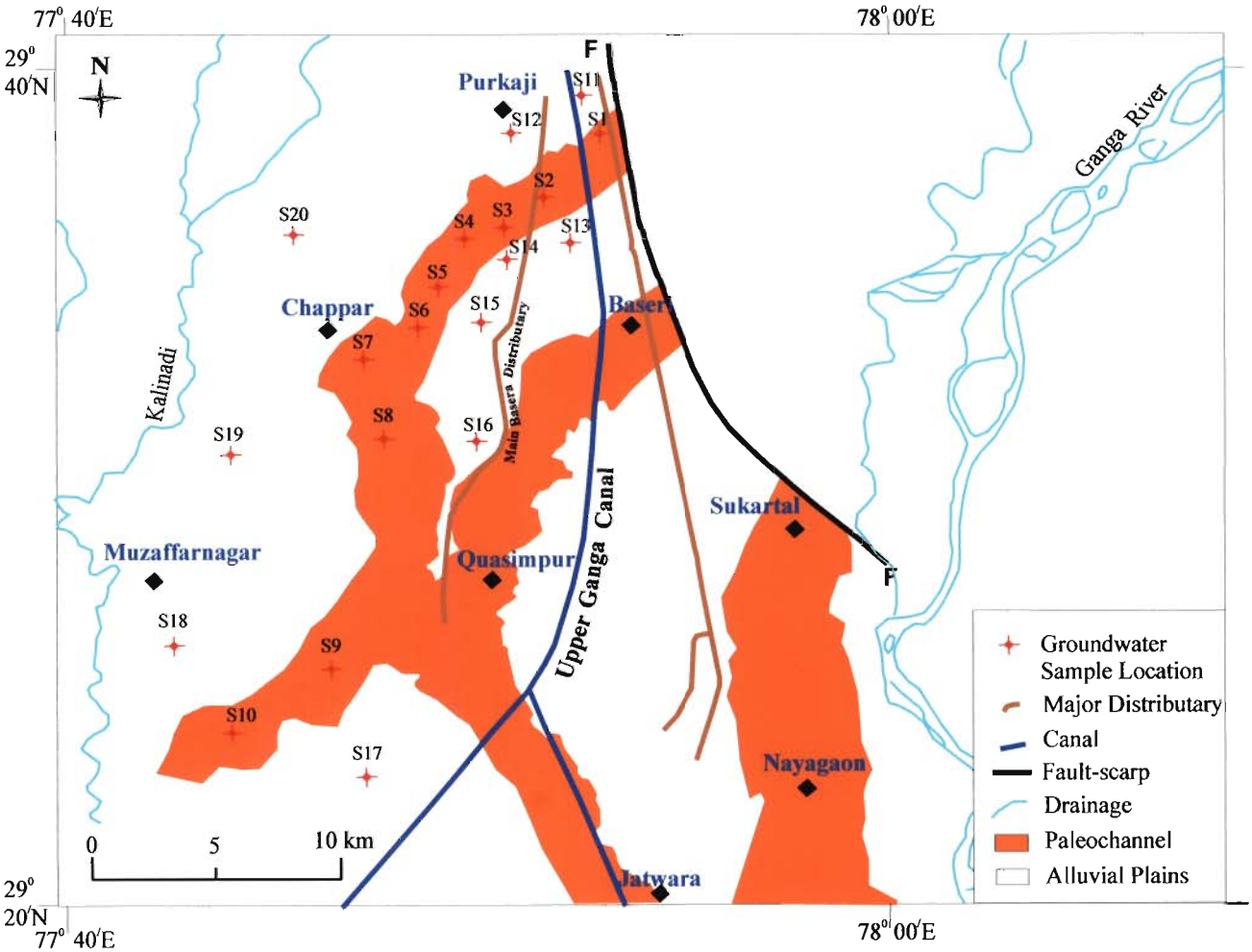

Figure 5.5: Location map of water samples for stable isotope analysis. Also paleochannel, Ganga Canal and major distributaries are shown on the background.

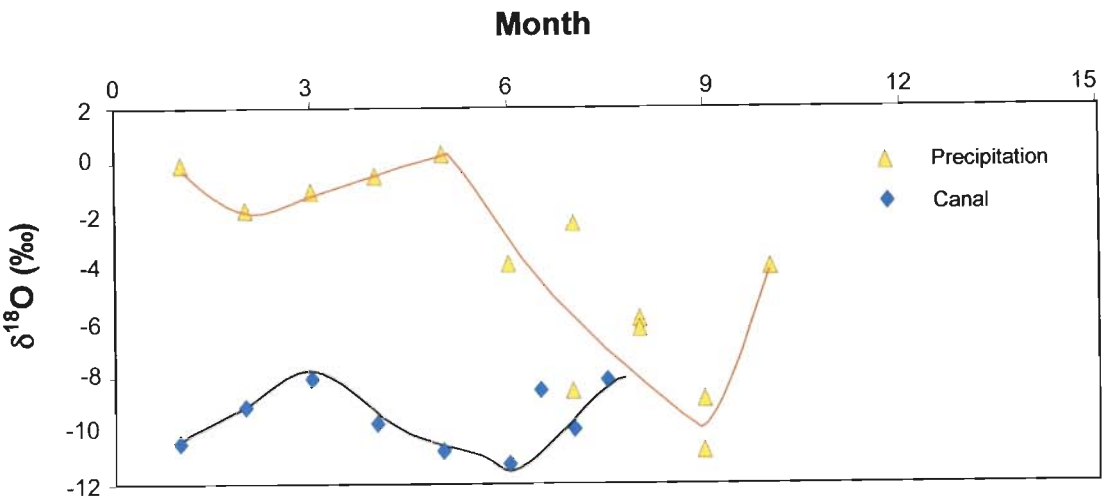

Figure 5.6: Variation of δ ^{18}O in groundwater and precipitation water of Roorkee.

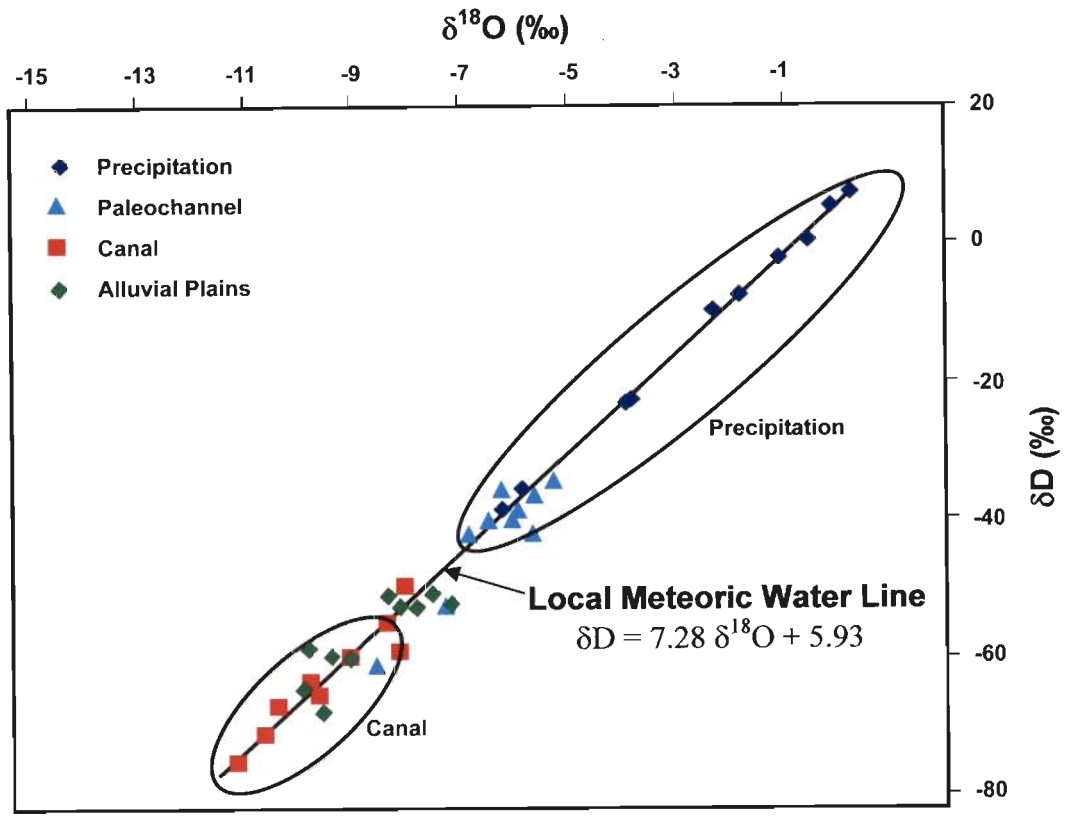

Figure 5.7: δ ^{18}O and δD characterization of the recharging sources and groundwater.

Table 5.8: Isotope data of groundwater samples over the study area.

Aquifer	Location Name	Sampling Date	$\delta^{18}O$	δD
Paleochannel	S1*	10.01.2007	-8.58	-60.61
	S2*	10.01.2007	-7.27	-52.52
	S3	10.01.2007	-6.86	-42.3
	S4	10.01.2007	-5.68	-41.75
	S5	10.01.2007	-6.51	-40.25
	S6	10.01.2007	-6.08	-39.91
	S7	10.01.2007	-5.97	-38.60
	S8	10.01.2007	-5.68	-36.71
	S9	10.01.2007	-6.29	-35.64
	S10	10.01.2007	-5.30	-34.31
Alluvial Plains	S11	11.01.2007	-9.62	-67.61
	S12	11.01.2007	-7.86	-52.4
	S13	11.01.2007	-9.89	-58.13
	S14	11.01.2007	-9.42	-59.55
	S15	11.01.2007	-8.36	-50.72
	S16	11.01.2007	-9.92	-64.57
	S17	11.01.2007	-9.09	-59.90
	S18	11.01.2007	-7.62	-51.05
	S19	11.01.2007	-7.26	-52.10
	S20	11.01.2007	-8.18	-52.50

** Near major distributary*

vi) Locations S1 to S10 are falling in the paleochannel. Among them, the isotopic ratio in groundwater at locations S3 to S10 lies closer to the average isotopic value of the precipitation. This indicates precipitation is the main component for groundwater recharge at these locations. Canal water component is pre-dominant for recharging groundwater reservoir at location S1 and S2 as they are nearer to Upper Ganga Canal/Main Basera Distributary and their isotopic ratio in groundwater is closer to canal water. The value of average isotopic ratio in groundwater sample is enriched away from Upper Ganga Canal/Main Basera Distributary or depleted towards the canal. This indicates that the influence of canal water to groundwater recharge decreases away from the canal and rainfall recharge component relatively increases. This also indicates

precipitation is the main component for groundwater recharge for paleochannel aquifers. Samples collected from locations (S11-S120) falling in the alluvial plains are depleted in comparison to samples falling in the paleochannel. Their isotopic ratio in groundwater is closer to the average value of canal water (Figure 5.7). This indicates that the alluvial plains aquifers are getting recharge by both canal and rainfall.

5.5 Groundwater Flow

Groundwater flow map has been generated to establish the groundwater flow direction. For this purpose, groundwater levels have been monitored in wells at 37 locations (12 on the paleochannel aquifers and 25 on the adjacent alluvium plains) over 2 years (2005-2006) for both pre- and post-monsoon period (Table 5.9). The precise locations (x, y, z co-ordinates) have been determined through differential GPS.

Average depth to water level below ground surface for each observation wells has been determined for both pre- and post-monsoon period. The reduced groundwater level for each well has been obtained by subtracting the value of depth to water level below ground surface to the ground height of the observation points. The longitudes/latitudes and ground height of each observation wells were obtained from differential GPS. The X, Y co-ordinates (i.e. longitude/latitude) of each well and their corresponding reduced groundwater level are stored as point attribute file in GIS. The file is then exported from GIS in the text (.txt) format, which is then used to generate a grid data using the 'Data operation' from the Grid menu in Surfer software by using Krigging interpolation method. The resultant grid thus produced has been used to generate reduced water level contour map and flow vector map using 'Contour Map' and 'Vector Map' operation from the main menu of the Surfer software. The vector spacing has been taken to be 20 m in both the X an

Y direction. Integrated interpretation has been made by combining information of paleochannel map, reduced water level contour map and flow direction map. The longitudes/latitudes and ground level (GL) height from mean sea level (MSL), and corresponding water table (WT) depth from GL of each observation wells are given in Table 5.9. The well location map, for which the groundwater flow direction maps have been generated, is shown in Figure 5.8a. The reduced groundwater level contour maps along with flow direction and paleochannel map for both pre- and post monsoon period are shown in Figure 5.8b and Figure 5.9. It has been observed that groundwater flows away from the paleochannel for both pre- and post-monsoon period. The typical contour pattern (convex downwards) in the paleochannel aquifer is interpreted to be due to its higher vertical hydraulic conductivity and porosity. This further indicates that recharging of groundwater through paleochannels would lead to gradually recharging the alluvial plains.

Table 5.9: Groundwater level data used in the present study.

Aquifers	Location ID	Ground height from msl (m).	Depth of WT (m) from GL			
			Pre-monsoon		Post-monsoon	
			2005	2006	2005	2006
Paleochannel	W1	255.35	5.90	6.30	5.70	5.80
	W2	253.67	4.53	4.53	3.86	3.88
	W3	254.45	7.54	7.56	7.10	7.10
	W4	250.16	4.70	4.76	4.56	4.57
	W5	250.03	3.92	4.00	3.91	3.95
	W6	248.37	5.79	5.81	4.49	4.51
	W7	241.12	6.60	6.64	6.48	6.52
	W8*	246.97	13.10	12.85	12.93	12.69
	W9*	246.96	14.82	14.84	14.46	14.48
	W10	242.71	8.23	8.23	7.56	7.60
	W11	237.85	8.90	9.00	8.74	8.78
	W12	239.08	6.04	6.12	5.60	5.66
Alluvium plains	W13	255.39	5.05	5.09	3.07	3.09
	W14	255.92	6.36	6.42	5.45	5.49
	W15	254.29	3.31	3.33	1.55	1.61
	W16	254.86	5.20	5.30	3.60	3.68
	W21	251.97	6.96	6.98	4.00	4.01
	W22	244.16	8.35	8.37	8.19	8.21
	W23	245.23	7.40	7.40	7.16	7.18
	W24	245.30	7.95	7.99	7.67	7.67
	W25	239.15	7.81	7.83	7.66	7.68
	W26	239.23	6.01	6.05	5.80	5.80
	W27	242.30	7.62	7.64	5.30	5.36
	W28	241.02	9.61	9.65	8.61	8.61
	W29	236.94	9.99	9.99	9.94	9.96
	W30	241.71	11.59	11.61	10.65	10.68
	W31	239.50	5.78	5.80	3.28	3.30
	W32	240.74	7.86	7.84	6.10	6.12
	W33	256.50	6.49	6.51	6.00	6.00
	W34*	253.63	3.42	3.44	2.79	2.81
	W35*	251.46	3.99	3.97	3.51	3.53
	W36*	249.00	4.00	4.00	4.00	4.00
	W37	250.70	10.76	11.78	11.46	11.48

* Locations near the distributary

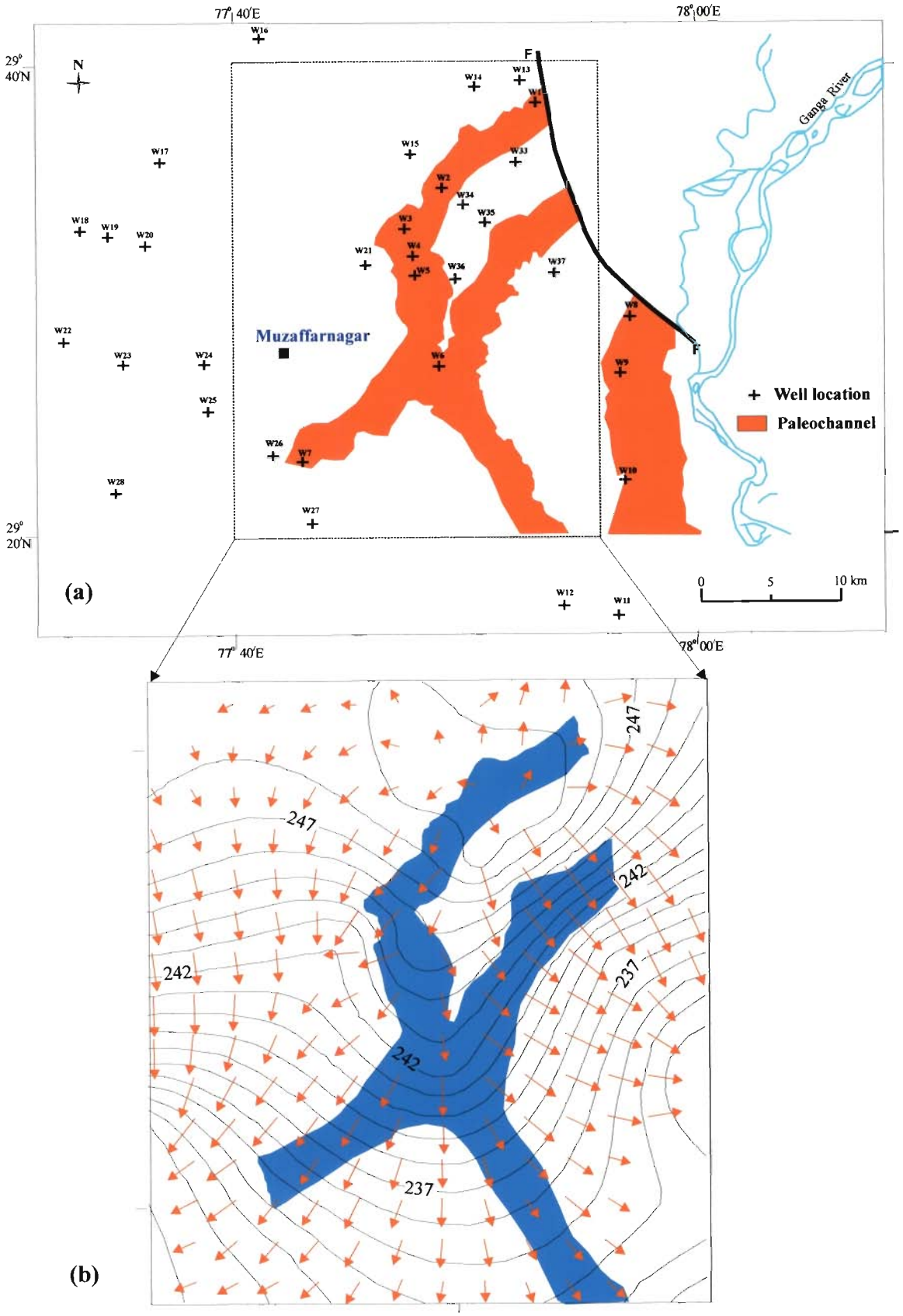

Figure 5.8: (a) Location map of wells; (b) Pre-monsoon reduced groundwater level contour and flow direction map.

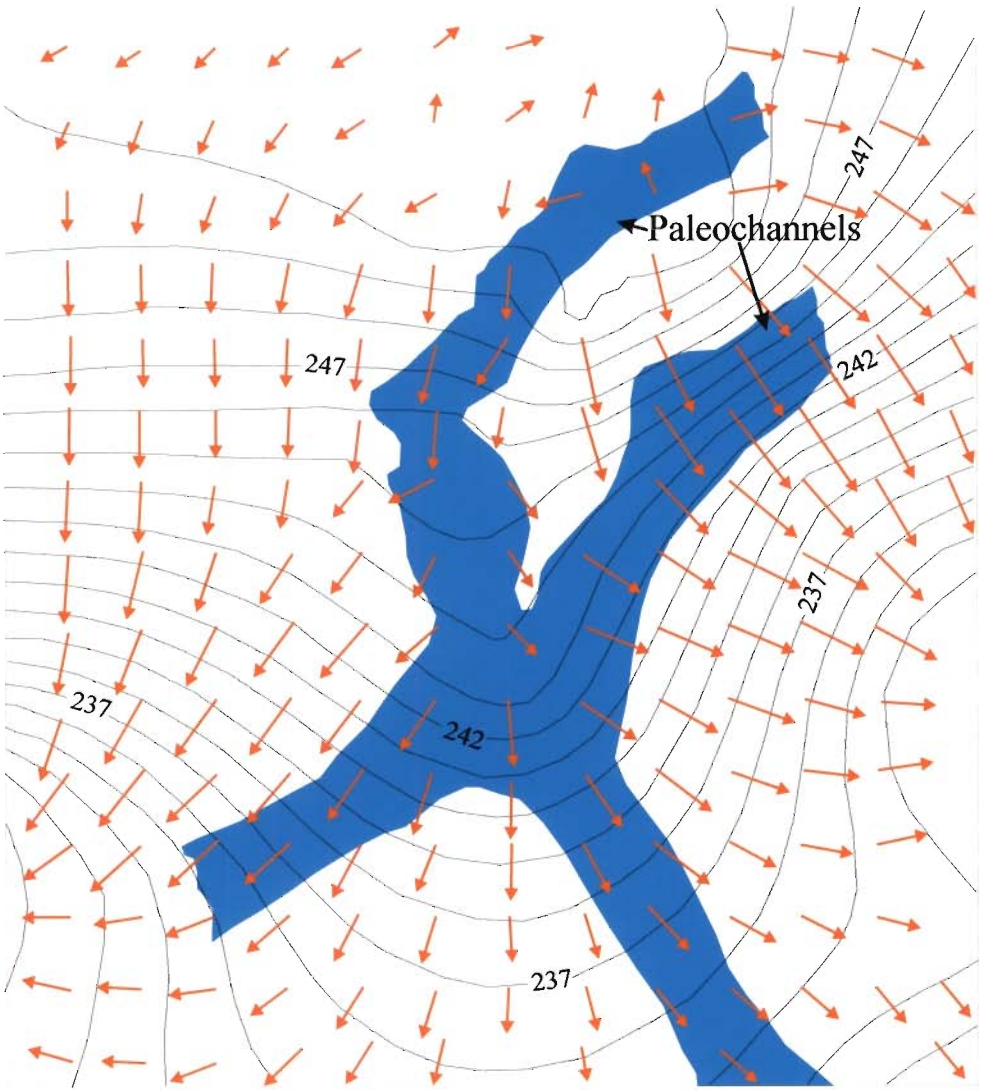

Figure 5.9: Post-monsoon reduced groundwater level contour and flow direction map.

Chapter 6

Delineation of Paleochannel Aquifer Geometry

6.1 Introduction

The study of aquifer geometry is important as it facilitates identification of areas with favourable aquifer disposition such as aquifer areal extent, thickness, and volume besides, aquifer boundaries and interconnectivity between adjacent aquifers. This information has implications in lateral groundwater movement, water exchange between adjacent aquifers, sea water intrusions, contaminant transport studies, and studies for artificial groundwater recharge (Tait et al., 2004; Srivastava, 2005; Samadder et al., 2007).

Well-log data provide information on lithologic variation with depth, and have been long used for generating sub-surface cross-sections. However, such interpretations have a limitation that the spatial (lateral) control as seen on surface is often not adequate. In this

study, remote sensing together with litholog data have been used for interpretating aquifer geometry, as remote sensing data provides valuable information on spatial (lateral) disposition of geological features such as soil, rock types, faults, landforms, drainage, water bodies etc. (Hendrix and Price, 1986; Gupta, 2003, Jaiswal et al., 2003).

As mentioned earlier, paleochannels are quite distinctly seen on the remote sensing images and have hydrogeologic characteristics suitable for artificial groundwater recharge (see Chapter5). Therefore, in this chapter, a systematic approach has been applied to construct paleochannel aquifer geometry and study its interconnectivity with the adjacent aquifers by using well-log and remote sensing data in an interpreted manner.

6.2 Methodology

Methodology for constructing paleochannel aquifer geometry and its interconnectivity with the adjacent aquifers includes — (a) base map preparation, (b) remote sensing image data processing, (c) paleochannel mapping, (c) litholog data analysis, and finally (d) data integration and interpretation (Figure 6.1). The base map preparation, remote sensing image data processing and paleochannel mapping has already been presented in Chapter 4. The following sections describe about the litholog data analysis and data integration and interpretation.

6.3 Litholog Data Analysis

Litholog data was collected from Tube Well Division of Uttar Pradesh and from field drilling operations in the study area (Section 3.4.1 and Section 3.4.2). Figure 6.2 shows the well locations from which litholog data have been used. The depth wise descriptions of some wells are given in Figure 6.3 to Figure 6.9. It has been observed that

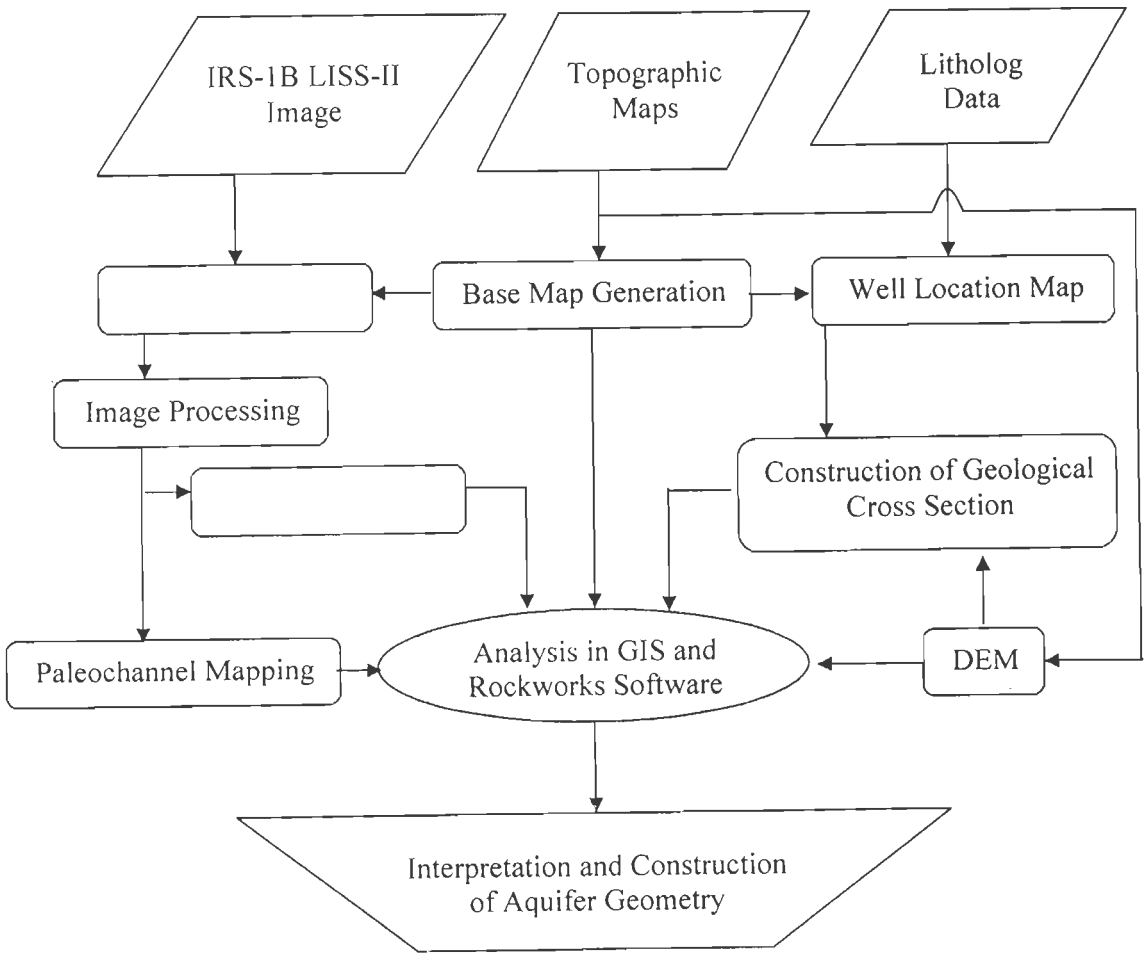

Figure 6.1: Flow diagram showing methodology for constructing aquifer geometry.

the paleochannel aquifer mainly consists of coarse sand occasionally mixed with pebbles, and boulders of varying sizes. On the other hand, the aquifers of the adjacent alluvial plains are mainly composed of medium to fine grained sand along with clay and kankar beds. A surficial clay layer (thickness 0.8-2 m), which is supposed to be responsible for high surface runoff, is present in the alluvial plains, whereas, it is generally absent over the paleochannels (Figure 6.3 to Figure 6.9).

6.4 Data Integration and Interpretation

Construction of subsurface lithological cross-section, construction of aquifer geometry, and final interpretation has been made by aggregating and synthesizing all the information - such as the base map, the CIR composite image, the paleochannel map, well location map, and the DEM.

The most of the bore logs collected from the Tuble Well Division of Uttar Pradesh are pertained to non-paleochannel area. They also have a large variation in strata penetrated, level of details, and lithological description. The existing lithologs are compared and standardised with respect to the observed field data and analyzed using Rockworks software.

For analysis of litholog data in Rockworks, the following inputs are required: location of the well-logs, log names, ground elevation of the corresponding wells, sub-surface lithologies and their respective depth from the ground level at which they occur.

Location of wells: The wells were located on the base map (by GIS overlay operation) and their corresponding latitude/longitude coordinates were found. The latitude/longitude coordinates for each location were converted into UTM coordinates by using 43N UTM zone through Rockwork.

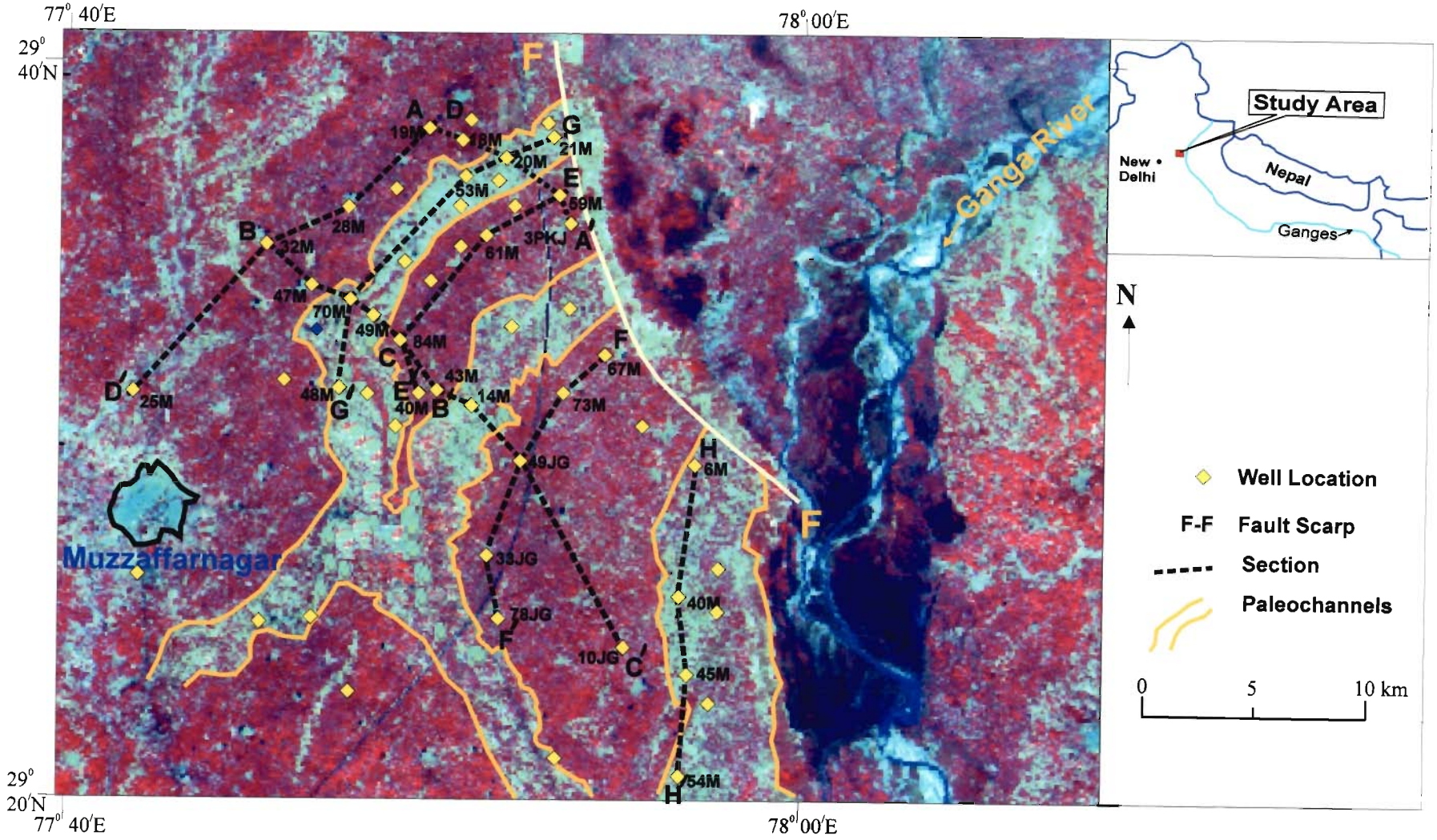

Figure 6.2: Well location marked on the Colour Infra-red Composite (R: NIR band; G: Red band; B: Green band), generated from the IRS-LISS-II (November, 1998) image data. Major locations, paleochannels and fault-scarp are also marked on the background.

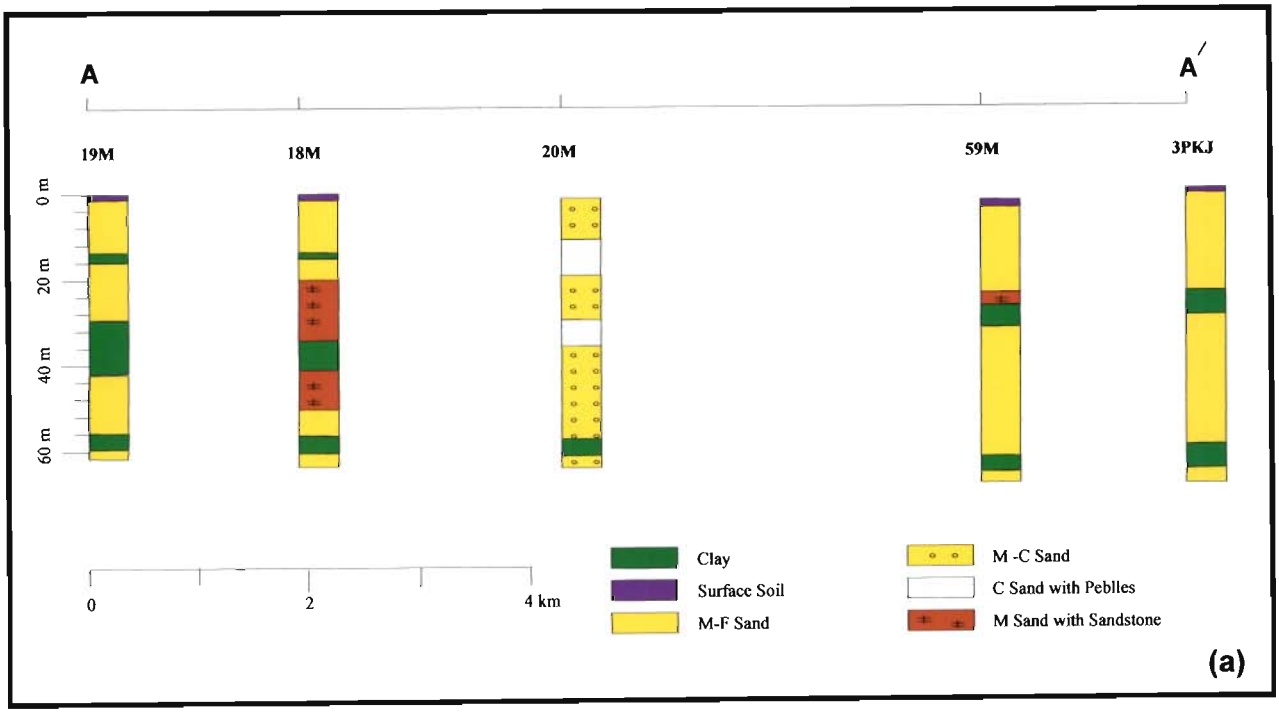

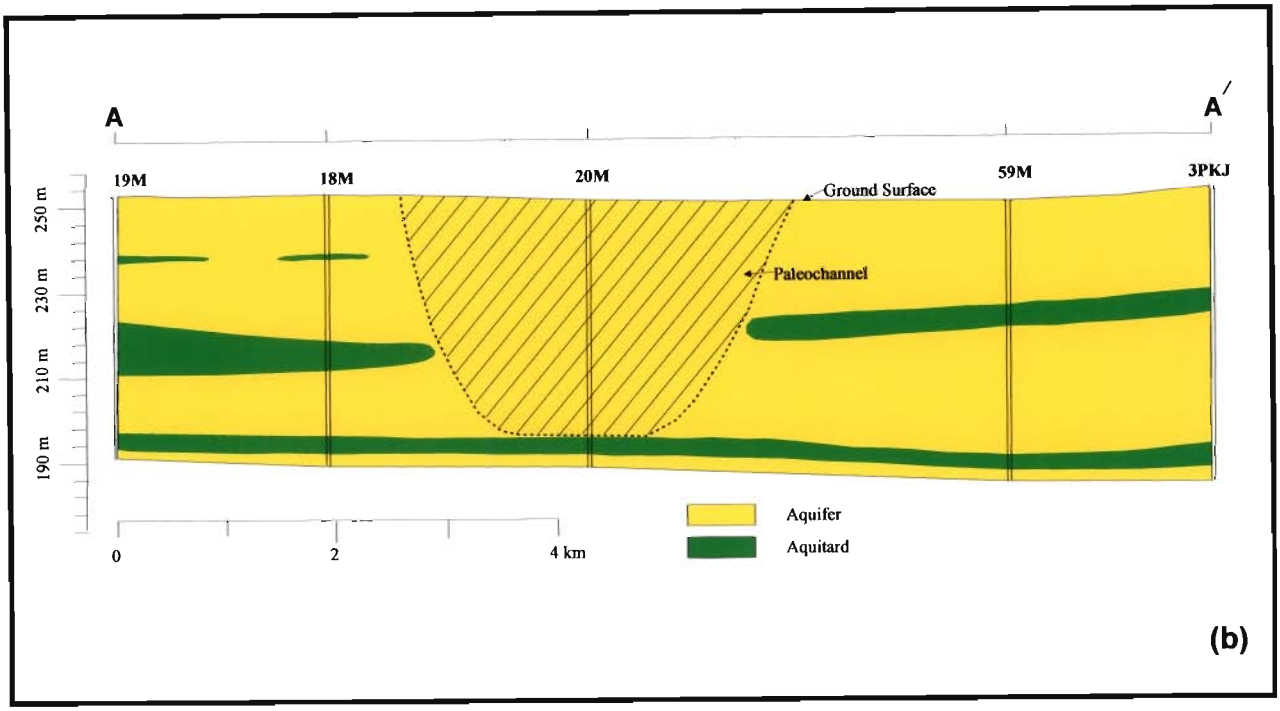

Figure 6.3: (a) Lithologic description of wells 19M, 18M, 20M, 59M and 3PKJ. (b) Interpreted geological section along A-A' through well Nos. 19M, 18M, 20M, 59M and 3PKJ (for section orientation see Figure 6.2). Note the paleochannel.

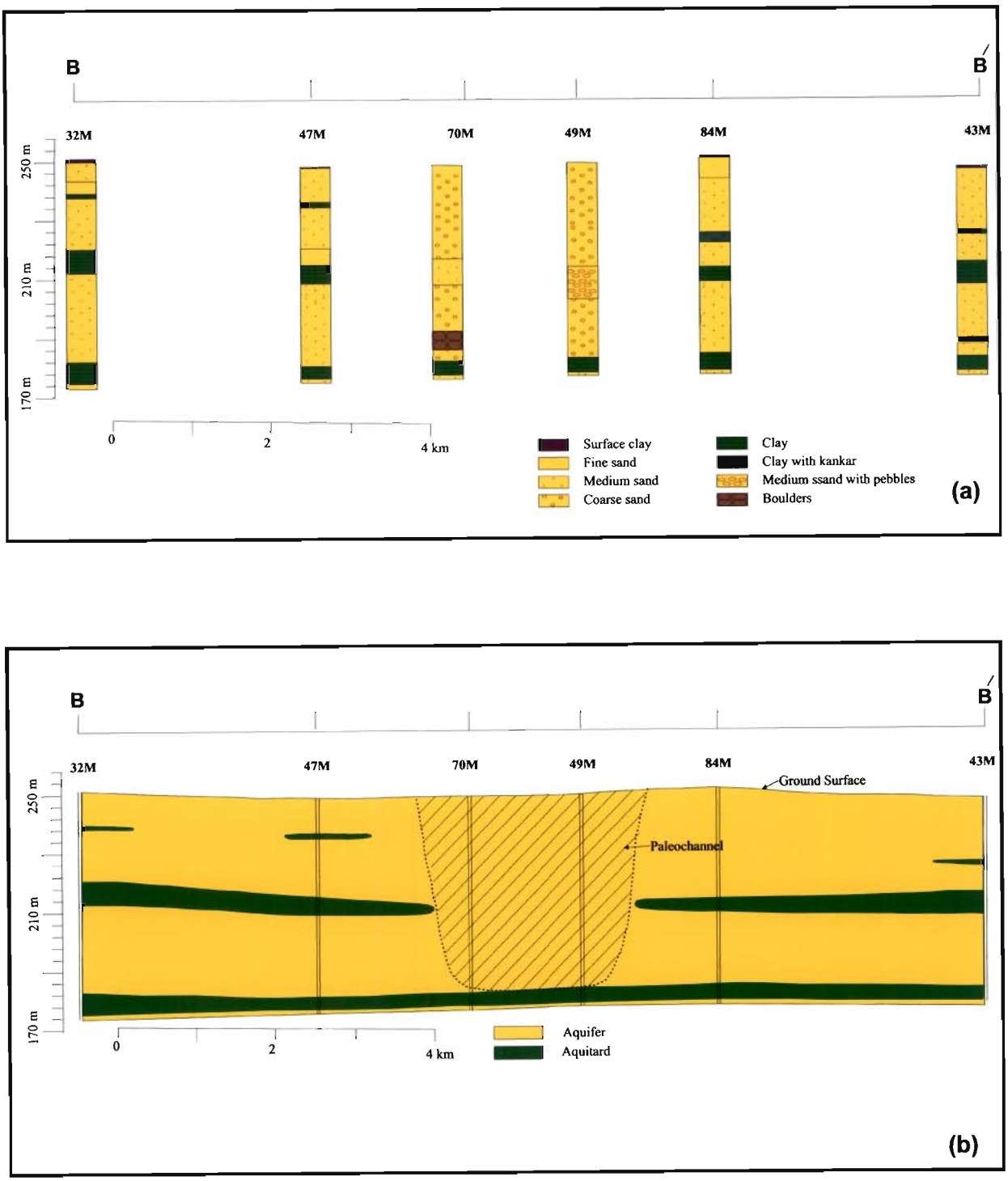

Figure 6.4: (a) Lithologic description of wells 32M, 47M, 70M, 49M, 84M and 43M. (b) Interpreted geological section along B-B′ through well Nos. 32M, 47M, 70M, 49M, 84M and 43M (for section orientation see Figure 6.2). Note the paleochannel.

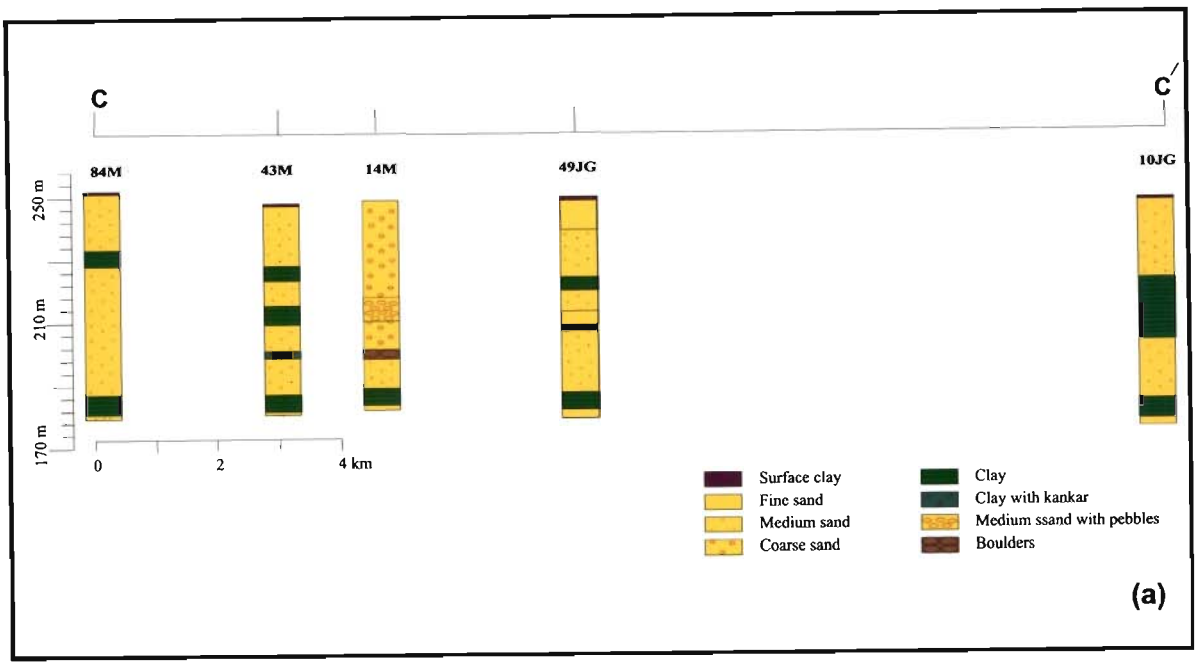

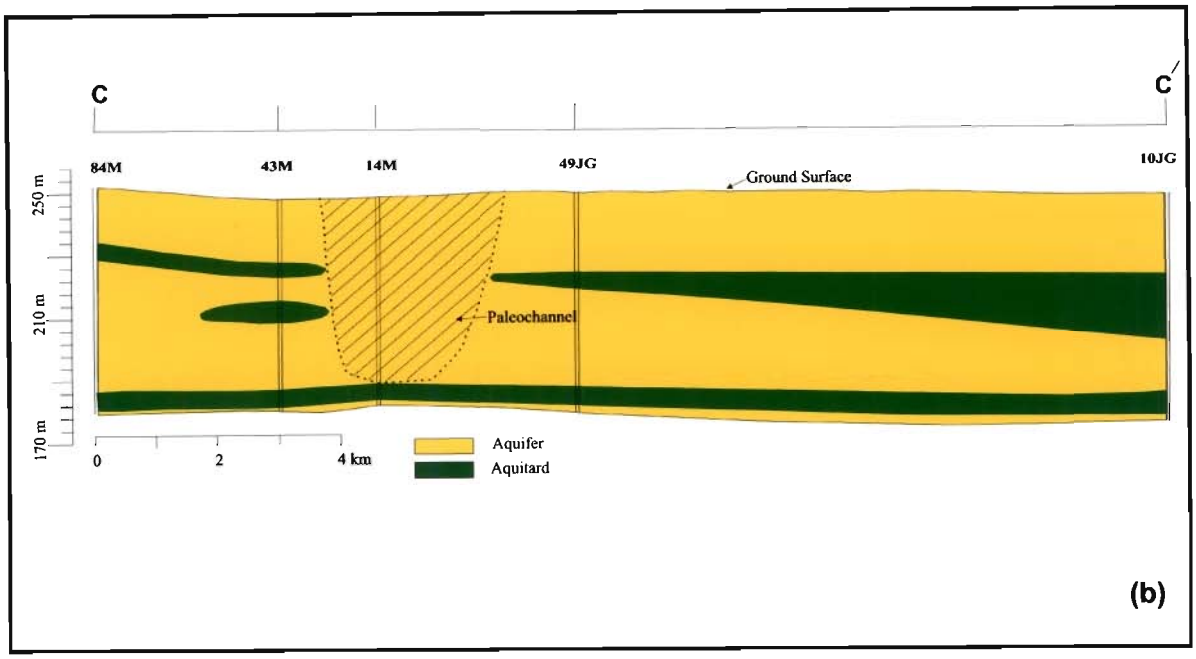

Figure 6.5: (a) Lithologic description of wells 84M, 43M, 14M, 69M and 10JG. (b) Interpreted geological section along C-C′ through well Nos. 84M, 43M, 14M, 69M and 10JG (for section orientation see Figure 6.2). Note the paleochannel.

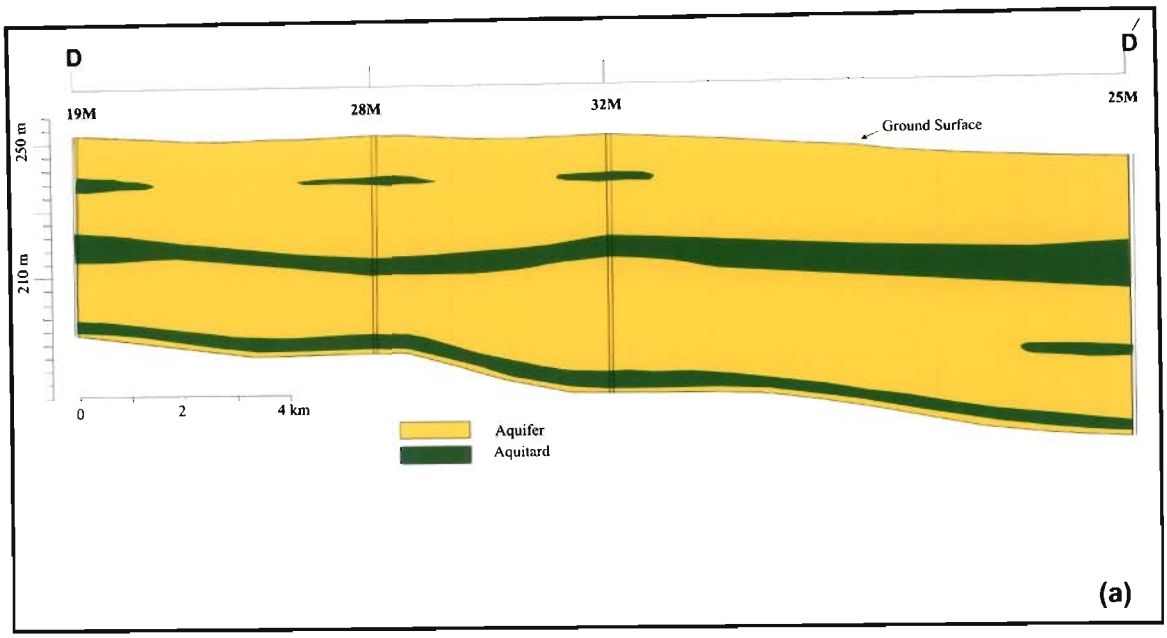

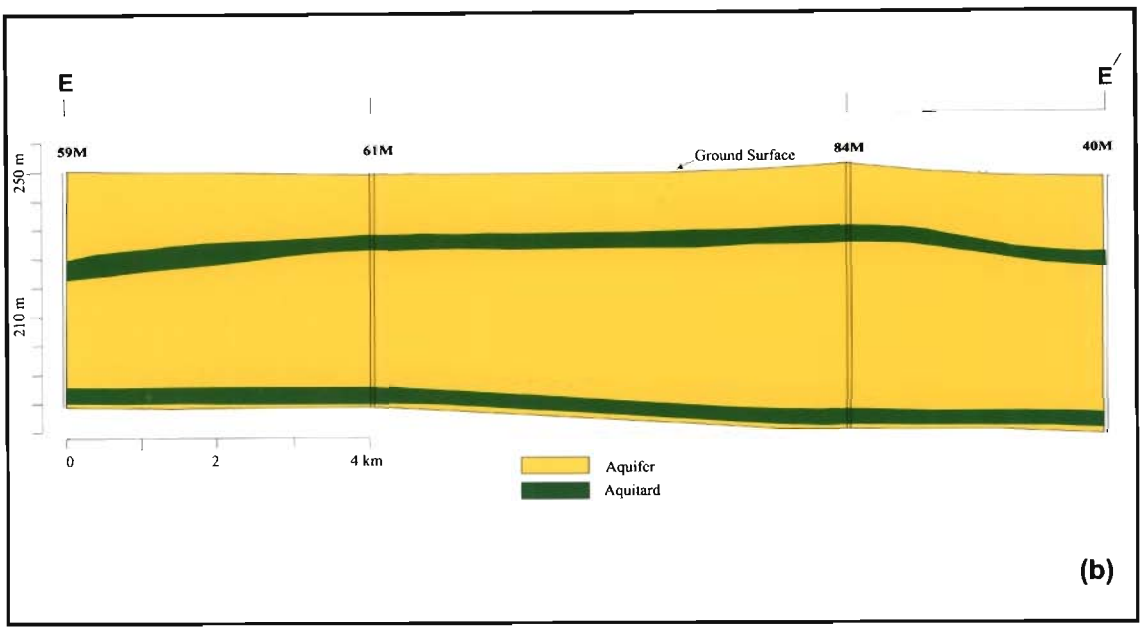

Figure 6.6: (a) Interpreted geological section along D-D′ through well Nos. 19M, 28M, 32M, and 25M.
(b) Interpreted geological section along E-E′ through well Nos. 59M, 61M, 84M and 40M. Line of section and well locations are shown in Figure 6.2.

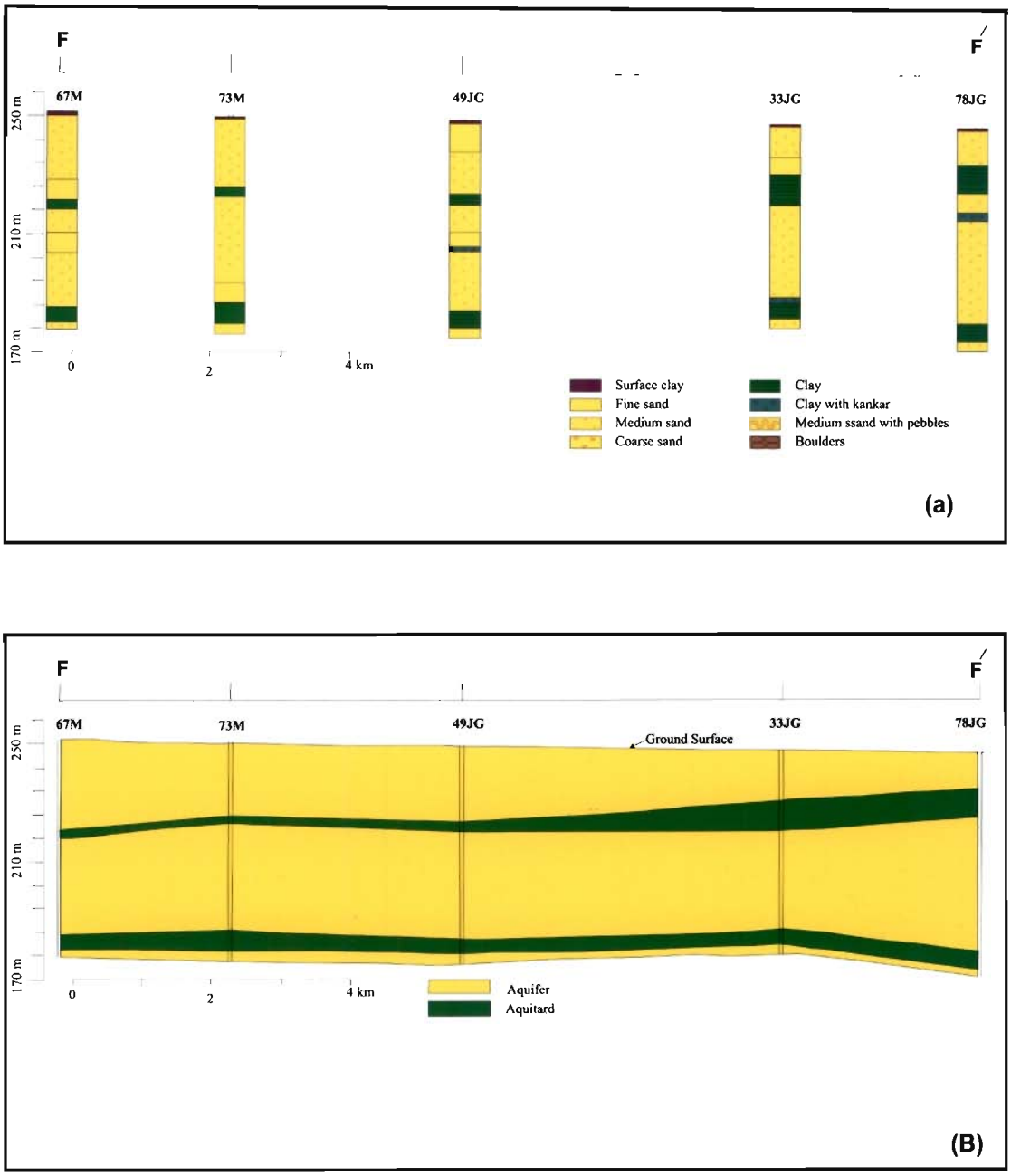

Figure 6.7: (a) Lithologic description of wells 67M, 73M, 49JG, 33JG and 78JG. (b) Interpreted geological section along F-F′ through well Nos. 67M, 73M, 49JG, 33JG and 78JG (for section orientation see Figure 6.2). Note the paleochannel.

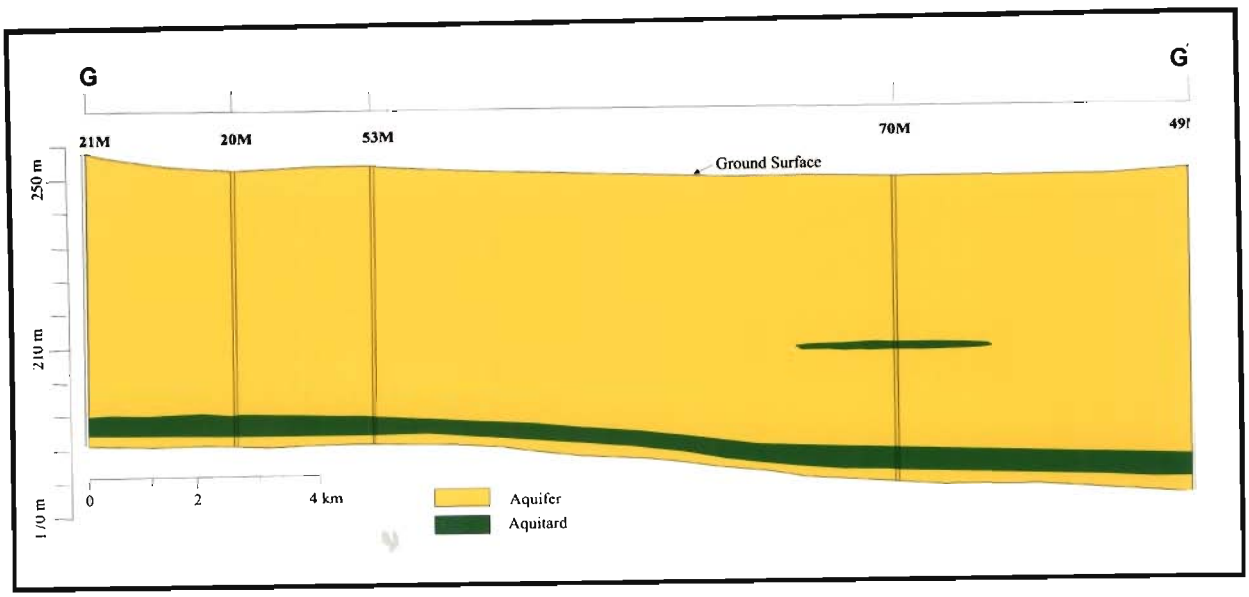

Figure 6.8: Interpreted geological section along G-G′ through well Nos. 21M, 20M, 53M, 70M and 49M (for section orientation see Figure 6.2).

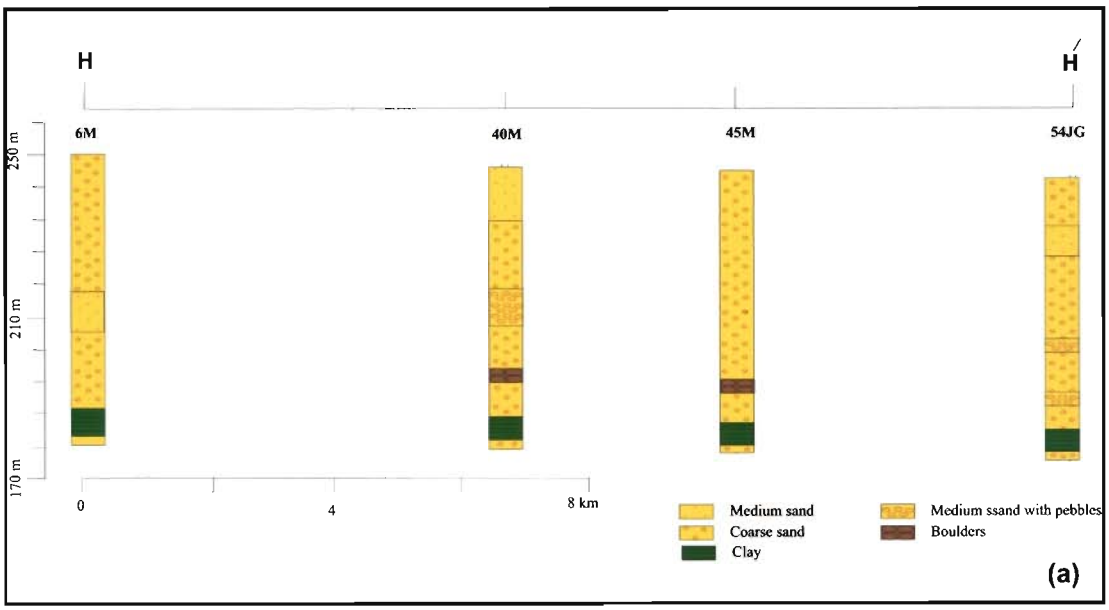

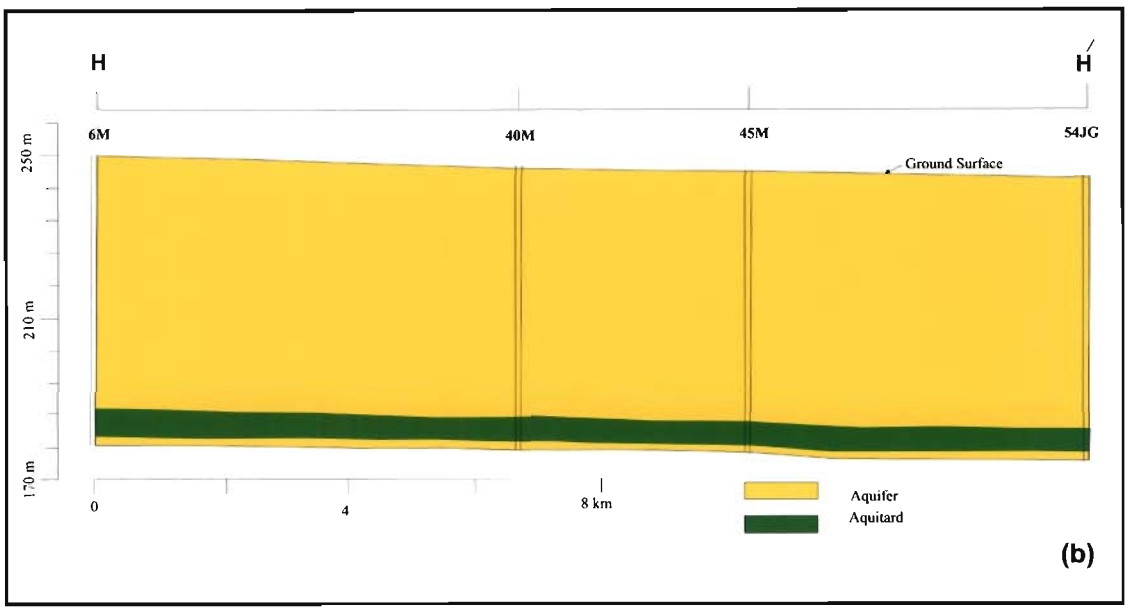

Figure 6.9: (a) Lithologic description of wells 6M, 40M, 45M and 54JG. (b) Interpreted geological section along H-H′ through well Nos. 6M, 40M, 45M and 54JG (for section orientation see Figure 6.2). Note the paleochannel.

Ground elevation: From the topographic map, a DEM has been generated; the wells were located on the DEM and the heights corresponding to the wells are determined by overlying the locations on the DEM.

All these informations, such as well location, name and corresponding surface height, UTM coordinates, and the sorted lithological information of the individual well including depth data of lithologies were entered into Rockworks for analysis and interpretation. The litholog data were sorted out and different lithological units were classified as aquifer and confining layers. After this, a well location map was displayed in Rockworks and single litholog for each well and numerous cross-sections between wells were constructed to aid interpretation.

6.5 Interpretation and Construction of Aquifer Geometry

The various data sets and maps, including the base map, the CIR composite image, and paleochannel map were converted into UTM coordinate system and imported into Rockworks. Interpretation has been done by aggregating and synthesizing all the information. Figure 6.2 shows the CIR composite in the background with well locations for which the litholog information has been used. Also shown are the lineament and paleochannels interpreted from remote sensing data.

Various cross-sections along strike of the paleochannel, across the paleochannel and within the paleochannel are studied and are critically analyzed for interpreting geometry and interconnectivity of the paleochannel aquifer with the adjacent alluvial aquifer. A few typical interpreted geological sections are given below (Figure 6.3 to Figure 6.9, horizontal and vertical scale is given along side of each profile):

Section 1: An interpreted geological section (A-A$^{/}$) through well Nos. 19M, 18M, 20M, 59M and 3PKJ is shown in Figure 6.3b. The width of the paleochannel is plotted from remote sensing data and the depth is from well-log data. It has been observed that a surface clay layer is present in all the wells except well no 20M which is within the paleochannel (Figure 6.3a). The thickness of surface clay layer varies from 0.5 to 1 m. In well Nos. 19M, 18M. 59M and 3PKJ a clay bed (5 to 8 m thick) is noted at about 30 m depth, but it is absent in the well Nos. 20M, which is in the paleochannel. Therefore, the clay bed is considered as a continuous layer passing through the well Nos. 19M, 18M, 59M and 3PKJ and pinching layer on either side of the paleochannel. Further, at a depth of about 55-60 m, a clay bed (of thickness 5 to 7 m) is noted in all the wells. Therefore, it is shown as a continuous clay layer below the paleochannel.

The first aquifer in the alluvial plains in this section is an unconfined and is composed of fine to medium sand with a number of lenses of clay and kankar. The clay lenses are conspicuous in boreholes no 19M and 18M. The depth range of this aquifer varies from 25 m to 33 m. The upper most aquiclude (clay) in this section starts from the bottom of the unconfined aquifer and extends upto a depth of 25 m in 3PKJ to 41 m in 19M. The thickness of this aquiclude is almost uniform. The second aquifer is confined in nature and is mainly composed of fine to medium grained sand along with some lenses of kankar. The depth of this aquifer ranges from 55 m to 62 m. The paleochannel aquifer is unconfined in nature and is mainly composed of medium to coarse grain sandy material along with boulder and pebbles beds. This paleochannel aquifer extends upto a depth of about 65 m and is well connected with the adjacent alluvial plains aquifers upto the depth.

Section 2: Another geological section B-B$^{/}$ has been constructed through well nos. 32M, 47M, 70M, 49M, 84M and 43M (Figure 6.4b). The width of the paleochannel is again plotted from remote sensing data and the depth is from well-log data. A surface clay layer (of thickness about 0.8 m) is present in all the wells except 47M and 70M, which are within the paleochannel. In well nos. 32M, 47M, 84M, and 43M, a clay bed of about 10 m thick, is present at a depth of about 32 m. But, it is absent in well nos. 70M and 49M which are in the paleochannel. Therefore, the clay bed is interpreted as a pinching layer on either side of the paleochannel. At a depth of about 65 m, a clay bed of thickness 8 m is noted in all the wells. Therefore, it is shown as a continuous clay layer below the paleochannel. Clay lenses (thickness less than 2 m) are also found in well nos. 32M, 47M, and 43M at a depth of about 10 m, 15 m, and 24 m below ground level respectively. The clay lenses present between the sandy formations are depicting semi-confined aquifer conditions.

The thickness of first aquifer in alluvial plains area varies from 28 to 32 m and is unconfined to semi-confined in nature. Whereas, the second aquifer having thickness of about 32 m is confined in nature. From the cross-section and grain size analysis, it has been observed that the paleochannel aquifer is mainly composed of coarse grained sandy material along with pebbles and boulder beds and are well connected with the adjacent two aquifer upto a depth of about 65 m. The adjacent aquifers are mainly composed of medium to fine grained sandy material along with lenses of clay and kankar.

Section 3: Sub-surface cross-section along C-C$^{/}$ is taken through well Nos. 84M, 43M, 14M, 69M and 10JG (Figure 6.5b). This section is also quite similar with the previously described two sections (i.e. section 1 and section 2). The first aquiclude

(clay layer) (thickness varies from 6-18 m) is shown as a pinching clay layer on either side of the paleochannel as it appears in all the wells at a depth of about 24 m below ground level except well no. 14M which is in the palochannel. A clay layer of thickness about 8 m is observed all the wells at a depth of about 65 m and is shown as a continuous clay bed passing through all the wells below the paleochannel. A clay lense is observed at a depth of about 35 m below ground level in the well no 43M. The depth of the paleochannel aquifer is about 65 m and is again found to be interconnected with the adjacent two aquifers.

Section 4: Figure 6.6a. represents an interpreted lithological profile (along section D-D$^{/}$) on the western bank of the paleochannel passing through well Nos. 19M, 28M, 32M, and 25M. The profile runs parallel to the strike of the paleochannel. It is evident from the section that the ground slope is from NE to SW. The thickness of surface clay varies from 0.8 m to 1.8 m. The first aquifer in this section is unconfined to semi confined in nature and consists of fine to medium grained sandy material with a number of lenses of clay and kankar. The clay lenses are conspicuous in boreholes no 19M, 28M and 32M. The depth range of this aquifer varies from 28 m to 35 m. The upper most aquiclude (clay) in this section starts from the bottom of the first aquifer and extends upto a depth of 42 m. The thickness of this aquiclude varies from 8-12 m. The second aquifer is confined aquifer and its depth ranges from 55-75 m. The clay layers or aquicludes fallow the general trend of ground slope.

Section 5: Another section E-E$^{/}$ parallel to the strike of the paleochannel on the eastern bank of the paleochannel is shown in Figure 6.6b. Like the section 4, the ground slope is from NE to SW and a surface clay layer of thickness of about 0.8 m is observed in all the wells. The first unconfined aquifer extends upto a depth about 25 m. The second

confined aquifer having thickness about 35 m extends upto depth of about 65-70 m. The two aquicludes having uniform thickness occur at a depth of about 25 m and 65 m respectively.

Section 6: Figure 6.7b is also an interpreted profile (along section F-F′) on the western bank of the paleochannel constructed through well Nos. 67M, 73M, 49JG, 33JG, and 78JG. The profile runs parallel to the strike of the paleochannel and the well-logs having a uniform pattern like previous sections (i.e. Sections 4 and Section 5).

Section 7 and Section 8: Section 7 (along G-G′) and Section 8 (along H-H′) have been constructed through wells which are on the paleochannel (Figure 6.8 and Figure 6.9b). The section G-G′ is constructed through well nos. 21M, 20M, 53M, 70M, and 49M whereas, the section along H-H′ is passing through well nos. 6M, 40M, 45M, and 54JG. Both the sections show ground slope NE to SW and the basement clay layer at depth about 65-70 m. It is also evident from the cross-section that the basement clay layer fallows the trend of the ground slope. The surface clay layer is absent in both the sections. The paleochannel aquifer is mainly composed of a very thick (65 m) course graine sandy materials along with pebbles and boulder beds. Clay lense is also present in well no 70M (Figure 6.8) at a depth of about 42 m.

Chapter 7

Natural Groundwater Recharge Estimation by Tracer Technique

7.1 Introduction

Estimation of natural groundwater recharge is very important for artificial groundwater recharge study and various groundwater applications such as groundwater budgeting and planning groundwater usage. Surface infiltration systems designed to provide artificial recharge of groundwater require permeable soils (sandy loam, sands, gravel) that must have relatively high recharge rate so that the water can be transmitted adequately. A proper understanding of soil moisture movement in the unsaturated zone is of importance in understanding and estimating the groundwater recharge. There are two components of recharge to groundwater: (i) vertical component, which includes precipitation and irrigation inputs, and (ii) lateral component, through the subsurface horizontal flow due to natural hydraulic gradient. In most of the cases, the major source of recharge to groundwater is due to precipitation. Conventional methods for estimating

groundwater recharge require large volume of hydrometeorological and hydrogeological data accumulated over a considerable time span, which is generally inadequately available, lacking or even unreliable in many cases (Jacobus et al., 2002; Scanlon et al., 2002; Mondal and Singh, 2004; Chand et al., 2005). Sometimes, based on the data from some representative basins, recharge rate may be suggested for similar water-bearing formations, where data are unavailable (CGWB, 1997). Though, such extrapolations may be also too farfetched. In view of the above needs and constraints, there has been an increasing emphasis on the use of isotopic and tracer techniques for soil moisture movement analysis and estimating groundwater recharge in the unsaturated zone. The advantage is that the tritiated water molecule, HTO, does not behave differently from the other water molecules in the ground water cycle. The health hazard in handling tritium is also negligible because of its emission of soft beta particles having maximum energies of only 18 KeV. Several workers (Zimmerman et al., 1967a, 1967b; Munnich 1968a, 1968b; Datta et al., 1973; Sharma and Gupta, 1987; Sukhija et al., 1996; Athavale and Rangarajan, 2000; Israil et al., 2004) have applied the tritium tagging methods for soil moisture movement analysis in unsaturated zones of different geological and climatological conditions. The methodology provides spot measurements of natural recharge and has been extensively used by various workers (Datta et al., 1973; Sukhija and Rama, 1973; Datta, 1975; Verhagen et al., 1979; Gupta and Sharma, 1984; Sukhija et al., 1996). Other methods, such as the chloride method and soil moisture method, have also been used to a limited extent (Allison and Hughes, 1978; Edmunds and Walton, 1980).

Although, the study area is a part of vast Indo-Gangetic Plains which are broadly categorized as an alluvial region, there exists variation in landforms with varying soil and hydrogeologic characteristics which are likely to control the recharge rate. Besides the

main channel of the Ganga River, there are two major landforms — paleochannels and alluvial plains in the area (Figure 7.1). So, in this chapter, groundwater recharge rate due to precipitation is estimated using tritium tagging technique in two major different landforms, viz. the paleochannels and the alluvial plains over the study area. The landform map generated from remote sensing (IRS-LISS-II multispectral sensor) data is used as a base map for selecting sites for tritium injection. Adequate field data (grain size distribution of soil samples, water table fluctuation etc.) has been used as ground truth for verifying and supporting the interpretations. Field hydrogeological characteristics of the paleochannel and the adjacent alluvial plains have already been discussed in Chapter 5. The following section describes methodology of the work (Figure 7.2)-site selection for tritium injection, field and laboratory experiment, and finally results.

7.2 Tritium Tagging

7.2.1 Site Selection

Keeping in view the aim of the present study to estimate natural groundwater recharge in the areas of two different landforms, sites for tritium injection have been selected using landform and paleochannel map generated from remote sensing data (Chapter 4). Fourteen experimental sites — eight within paleochannel and six on the alluvial plains, have been selected (Figure 7.1).

7.2.2 Injection of Tritium at the Selected Sites

Tritium injection experiment is performed during the pre-monsoon period (June 2006). At each selected site, five injections of 2 ml tritium of 40μ Ci/cc specific activity were made within a circle of 0.1 m radius (one at the center and the other four along the

circumference on the extremities of two mutually perpendicular diameters) at a depth of about 70 cm below ground level (Figure 7.3). A precise identification was given to each injection site. The holes were back-filled with the same soil after injecting tritium in order to reduce the direct loss of injected tracer due to evaporation and to avoid the direct entry of water.

7.2.3 Soil Sampling

The soil samples were collected just before injection (in June, 2006) and after about four months of injection (in October, 2006) at each 10 cm vertical soil column. Soil samples were collected layer by layer with the help of a hand auger of 2 inch diameter from ground surface to about 250 cm depth (Figure 7.4). The soil sample from each layer was carefully weighed and about 200 gm of the sample was collected in properly sealed polyethylene bottles so that there was no exchange of the moisture with the atmosphere.

7.3 Laboratory Experiments

The laboratory experiments consist of

a) Estimation of soil moisture content

b) Particle size analysis

c) Measurement of tritium counts in the soil samples.

7.3.1 Soil moisture content

The moisture content of the soil samples on wet weight basis was estimated by gravimetric method. Weight of each sample was determined by weighing the samples using electronic balance. After that, a small amount of soil sample (approximately 100 gm)

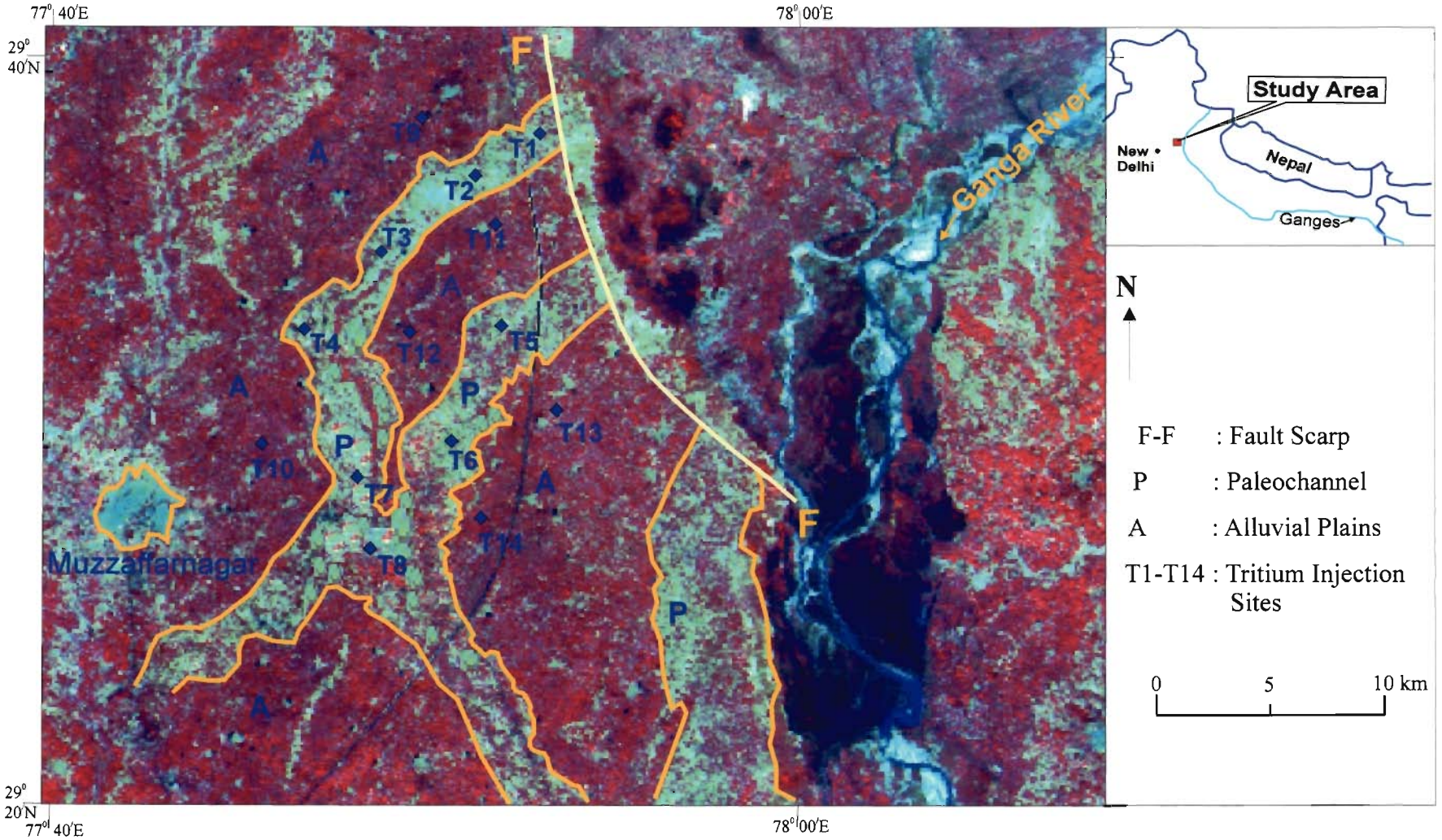

Figure 7.1: Location of tritium injection sites in paleochannels and alluvial plains,marked on the colour infra-red composite of IRS-LISS-II image data(NIR band coded in red colour; Red band coded in green colour; and Green band coded in blue colour).

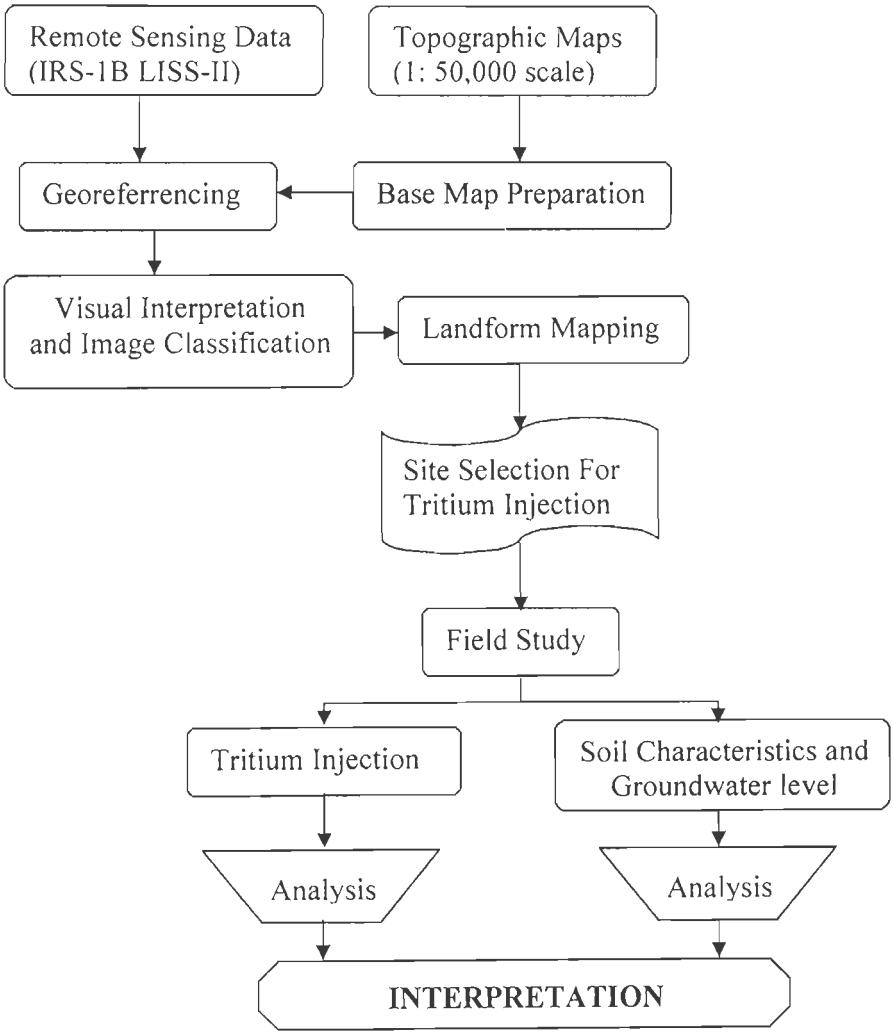

Figure 7.2: Flow diagram showing methodology adopted for estimating natural groundwater recharge using tritium tagging technique.

was kept in oven at 108^0 C for 24 hours to dry. Calculating the weight difference between wet and dry sample, the percentage of moisture content present in the soil sample was estimated. Bulk density for each soil sample was determined by dividing the wet weight of the sample by the volume of each sample, which was equivalent to the volume of hand auger of known diameter (2 inches) for 10 cm depth of soil column. Volumetric moisture content for each soil sample was estimated by multiplying the moisture content and bulk density of the soil.

7.3.2 Water Extraction from Soil Sample

Each soil sample was subjected to distillation to avoid volatile impurities being collected along with the water. The distillation was done at distillation counter at Nuclear Hydrology Laboratory of National Institute of Hydrology, Roorkee (Figure 7.4d). Water from each soil sample was extracted by simple distillation process and stored in the plastic/glass vials.

7.3.3Tritium Activity Measurement with LSC

Tritium activity was measured on liquid scintillation counter (LSC) (Model 'System 1409', Wallac Oy, Finland) at Nuclear Hydrology Laboratory of National Institute of Hydrology, Roorkee, India (Figure 7.4c). One ml of the soil water extracted from each 10 cm layer was mixed with 10 ml of scintillation cocktail 'W' (prepared by dissolving 10 gm of [2,5 -Diphenyl oxazole (PPO)], 0.25 gm of [(1,4- Di-2, (5-phenyloxazolyl)-Benzene) (POPOP) and 100 gm of Naphthalene in one liter of [1,4-Dioxane]). The function of the scintillation cocktail is to convert the energy of the radioactive decay particles into visible light photons, which can be detected by the scintillation counter. The amount of light photons being emitted from the vial is proportional to the energy of the particle. That is, the

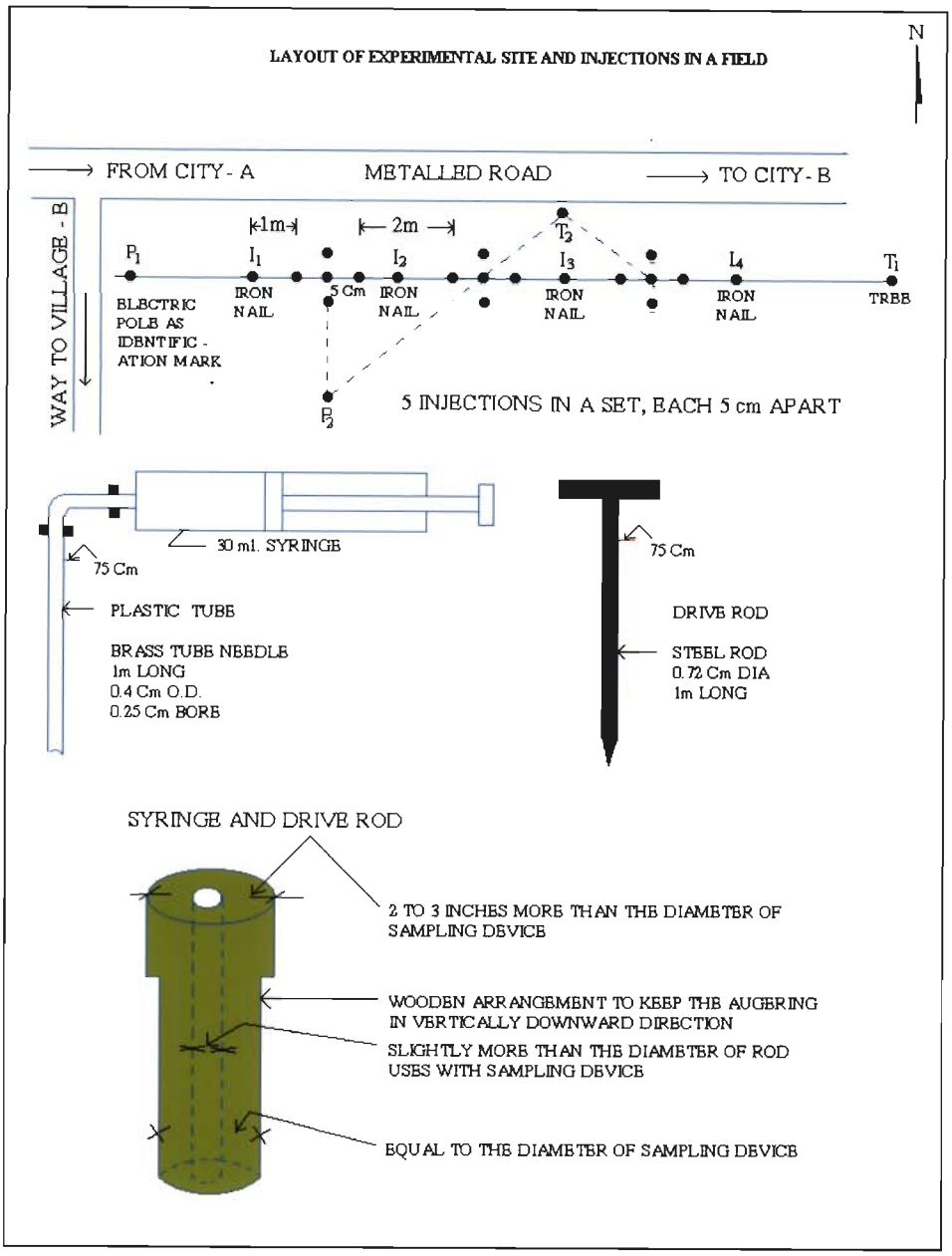

Figure 7.3: Systematic diagram of injection layout for artificial tritium injection at test sites (NIH).

Figure 7.4: (a) Tritium injection at selected site.
(b) Soil sampling during field investigation.
(c) Liquid scintillation counter at NIH (Model: WALLAC 1409).
(d) Soil moisture extraction set up.

higher the energy of a particle, the more solvent molecules it is able to excite and, therefore, more light is generated. These light photons are emitted from the liquid scintillation vial in all directions and is "directed" into the two photomultiplier tubes (PMT's) which convert the light into a measurable electrical pulse. The background activity in each scintillations vial containing 10 ml of cocktail was measured in liquid scintillation counter using easy count approach and background counts (counts per minute) were obtained by the system. One ml of tritiated water extracted from each soil sample was added to the each vial for which background activity was already measured with LSC.

The vials containing 1 ml of soil water extract and 10 ml of cocktail were placed in the counting chamber of the LSC in order and each sample was counted using easy count approach and consequently count rate (counts per minute or cpm) for each sample was obtained by the system. These count rates were corrected for background counts in order to get net tritium counts per minute. The values of volumetric moisture contents and net tritium count rate of different sites are tabulated in Annexure-I given last of the chapter.

7.4 Determination of Recharge to Groundwater

Munnich (1968a, 1968b) and Zimmerman et al. (1967a, 1967b) initiated the use of isotope technique to monitor the vertical movement of water. They assumed that the moisture flows in discrete layers in such a way that if any fresh water is added to the top surface of the soil, the infiltrated layer of the water pushes the older layer downward in the soil system and so on till the last layer of moisture reaches the saturated zone. This concept of water flow in unsaturated zone is known as the piston flow model. Thus, if a radio-isotope (say tritium) is tagged below the active root zone (below 70 cm) and not affected by solar heating, the tagged tritium will be mixed with the soil moisture available at that

depth and will act as an impermeable sheet. Therefore, water added to the top of the soil surface will infiltrate into the ground by pushing down the older water. Thus the shift in the tritium peak can be observed after some time.

The net tritium count rates for various sites were plotted as a histogram against the individual depth intervals, which shows position of the original and shifted peaks of the injected tritium. The movement of injected tritium and soil moisture at various test sites are shown in Figure 7.5 to Figure 7.7. The shift of the peak from original depth of injection of 70 cm was calculated. Percent recharge to the groundwater during time interval between injection of tritium and subsequent sampling (pre-monsoon to post-monsoon 2006) has been calculated using the following equation (Zimmerman et al. 1967a, 1967b):

$$R = Q_v \, d \, (100/P)$$

Where, *R*: the percentage of recharge to ground water

Q_v: the effective average volumetric moisture content in tritium peak shift region.

d : the shift of tritium peak in cm, and

p: precipitation and irrigation inputs in cm at the injection site. These two components are taken for the interval between injection and sampling. However, all the stations considered in this study are on non-irrigated patches.

The precipitation data was collected from the Groundwater Department, Uttar Pradesh, India. The rainfall distribution map was generated from Thiessen polygon method through GIS and subsequently the total monsoon (from the date of injection to the date of sampling) rainfall was calculated for each experimental site. The movement of injected tritium and soil moisture at various test sites are shown in Figure 7.5 to Figure 7.7 (Annexure-I). The computed recharge rates at various experimental sites, as determined from field cum laboratory data of tritium peak shift, average volumetric moisture content

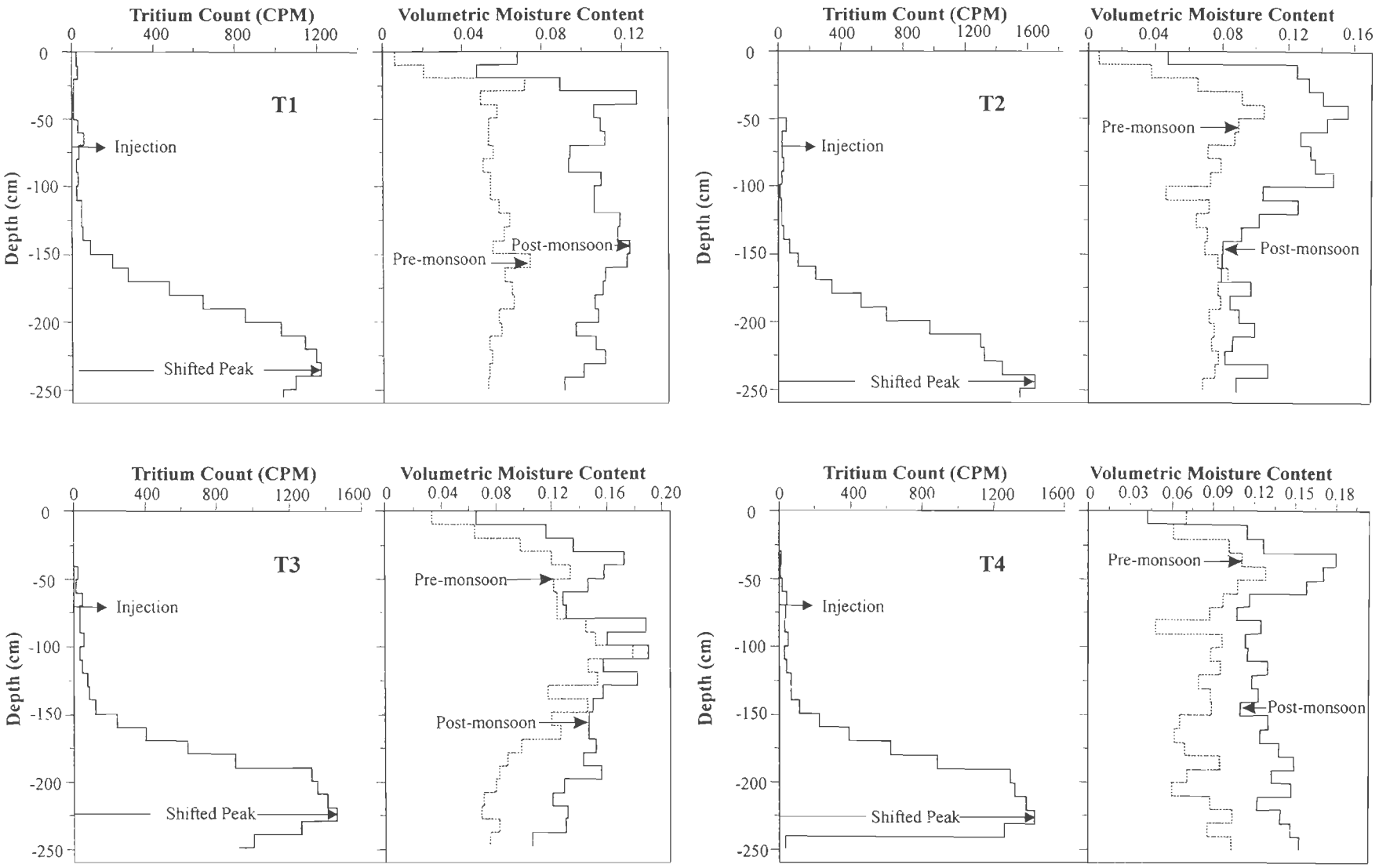

Figure 7.5: Movement of tritium peak and soil moisture for location T1-T4.

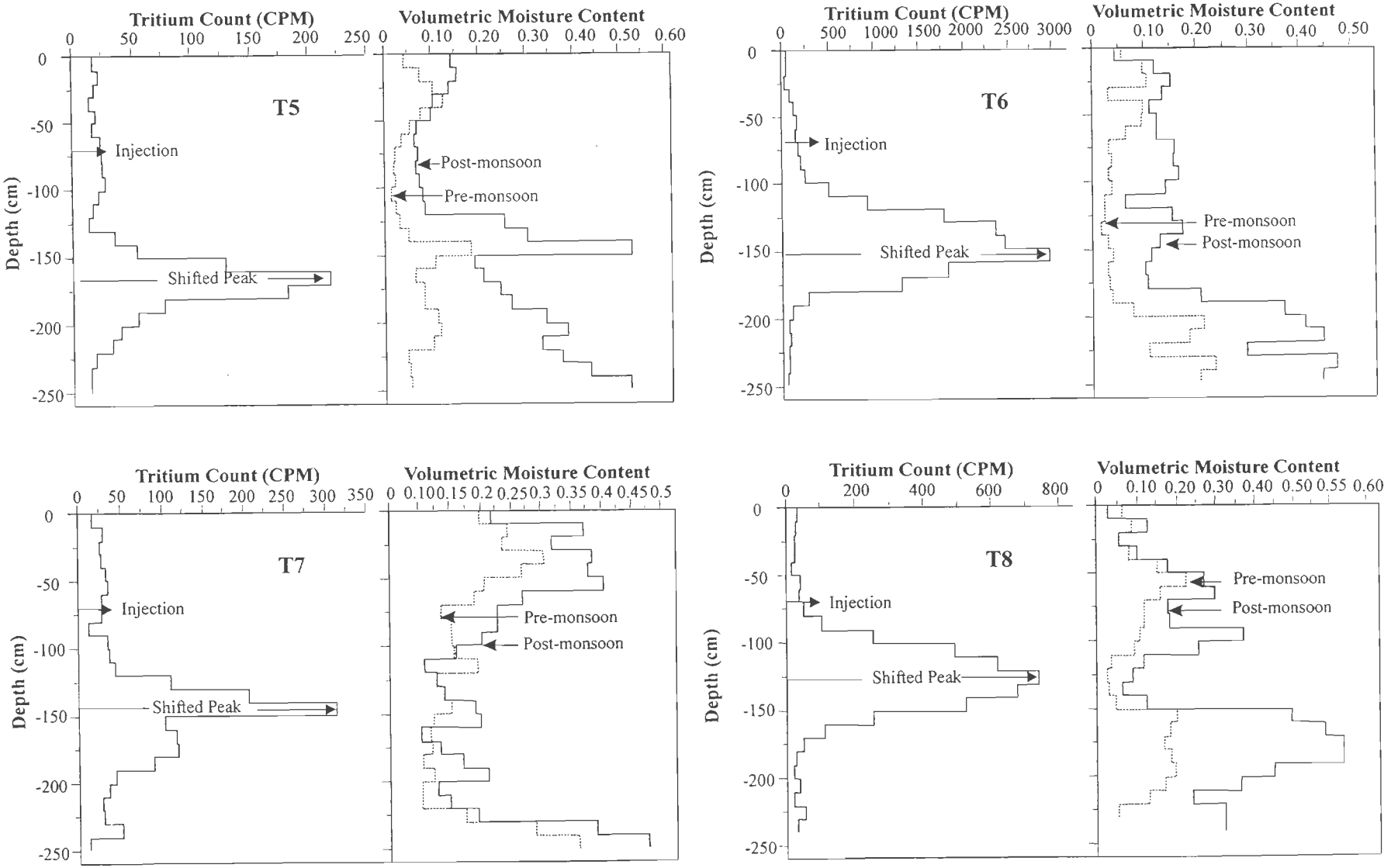

Figure 7.6: Movement of tritium peak and soil moisture for location T5-T8.

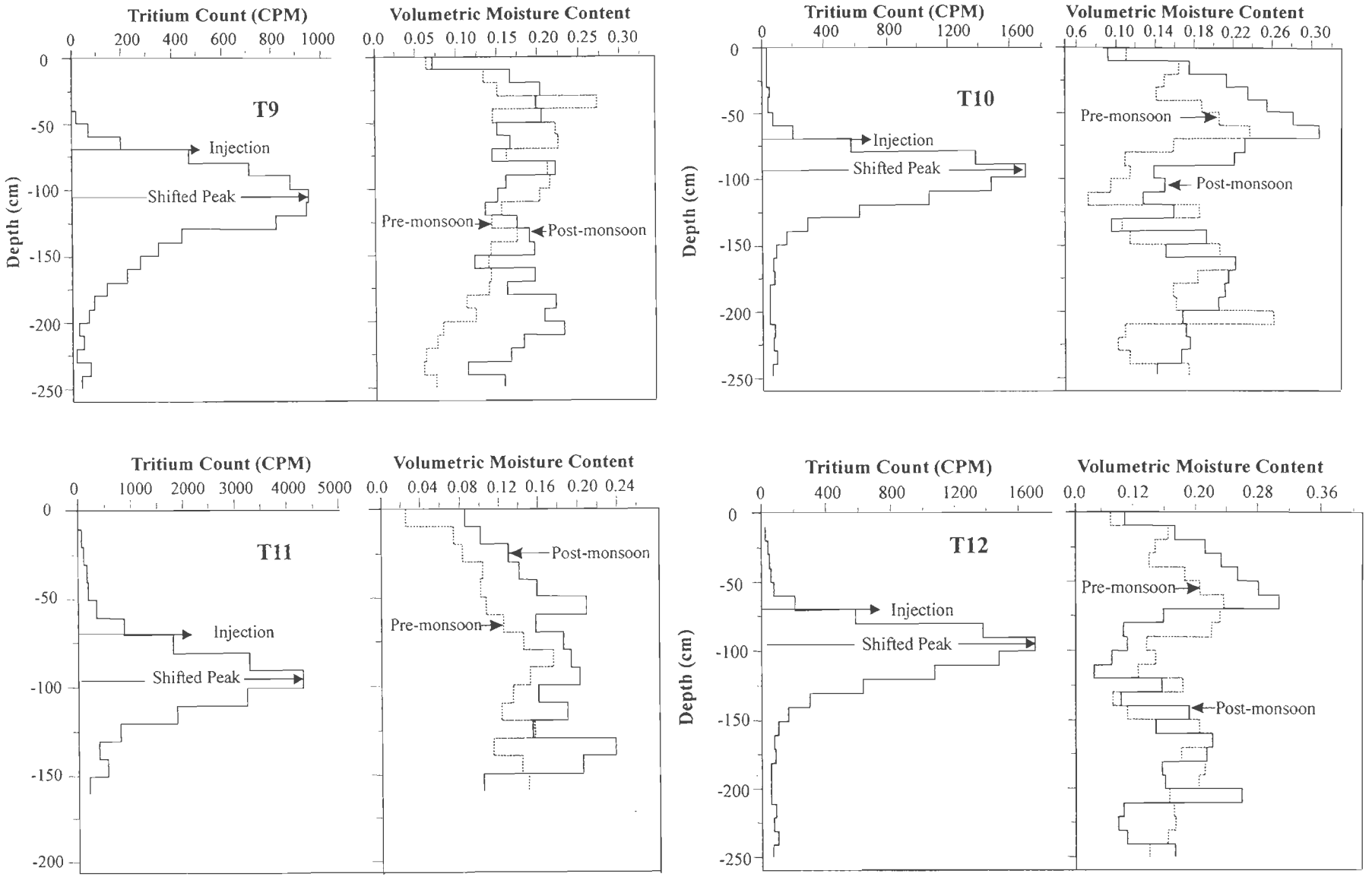

Figure 7.7: Movement of tritium peak and soil moisture for location T9-T12.

in peak shift region and precipitation (in the time interval of injection and sampling) are given in Table 7.1

Table 7.1: The percentage recharge to groundwater at various experimental sites due to monsoonal rain.

Location	Tritium Peak Shift (d) in cm	Average effective volumetric moisture content (Q_v) in peak shift region	Precipitation (cm) between injection time to sampling time	Recharge to groundwater (%)
(a) Paleochannel				
T1	165.0	0.077	67.3	18.9
T 2	175.0	0.079	67.3	20.4
T3	155.0	0. 099	67.3	23.0
T4	153.0	0.122	65.3	28.7
T5	95.3	0.189	67.3	26.8
T6	75.4	0.143	67.3	16.0
T7	75.2	0.151	67.3	17.0
T8	57.0	0.201	67.3	17.0
(b) Alluvial Plains				
T9	32.0	0.176	67.3	8.4
T10	30.8	0.184	67.3	8.4
T11	24.0	0.176	67.3	6.3
T12	30.8	0.196	67.3	8.9
T13	31.9	0.198	67.3	9.4
T14	39.9	0.187	67.3	11.0

7.5 Particle Size Analysis

Particle size distribution of soil samples collected form different sites was carried out by sieve analysis. The test results of the analysis for various sites are given in Annexure-II. Figure 7.8 represents the relationship between average sand content (%) and recharge rate for both the landform types.

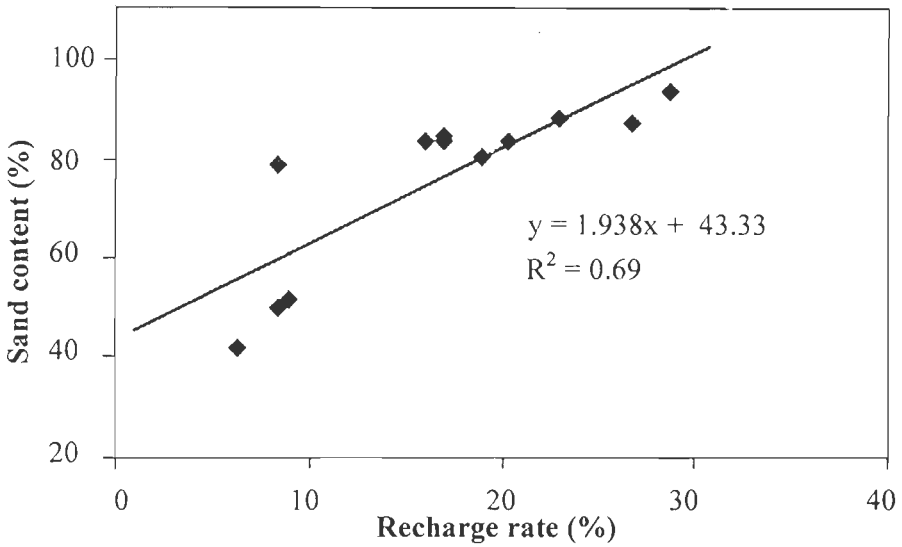

Figure 7.8: Relationship between average sand content (%) and corresponding recharge rate (%).

The groundwater levels at the adjacent wells of few tritium tagging sites were recorded at the time of tritium injection (pre-monsoon) and sampling (post-monsoon) (Table 7.2). The groundwater level fluctuations from the recorded sites have been plotted along with the percentage of recharge estimated from Tritium Tagging Technique (Figure 7.9).

7.6 Estimation of Specific Yield

In order to compute the areal average recharge from the point recharge values, Gupta and Sharma (1984) used a method. Thiessen polygons were drawn around the rain gauge stations corresponding to the various tritium tagging stations. Lastly, the areal average recharge was generated for each of these polygons by multiplying the water input, the fractional recharge and the area of the polygons.

Table 7.2: Specific yield estimated from tritium tracer technique.

Location	Fractional Recharge	Sand %	Water Level Fluctuation (m)	Specific Yield (%)
(a) Paleochannel				
T1	0.19	80.50	0.45	28.3
T2	0.20	83.80	0.52	25.8
T3	0.23	88.20	0.67	23.0
T4	0.29	93.70	1.21	16.8
T5	0.27	87.53	--	--
T6	0.16	83.33	--	--
T7	0.17	84.84	--	--
T8	0.17	83.49	--	--
(b) Alluval plains				
T9	0.084	49.80	0.41	13.7
T10	0.084	78.81		--
T11	0.063	41.90	0.40	10.6
T12	0.089	51.30	0.42	14.2
*T13	0.094	--	--	--
*T14	0.110	--	--	--

* Husasain, 2004

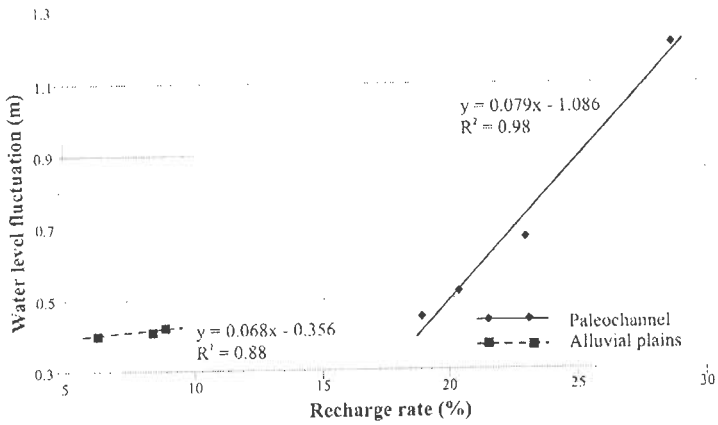

Figure 7.9: Relationship between water table fluctuation and corresponding recharge rate (%).

Using the water table fluctuation data in conjunction with the recharge estimates for the study period, the specific yield of unconfined aquifers for the individual polygon areas has been obtained using the following equation (Gupta and Sharma, 1984):

$$S = \frac{Q}{\partial h * A}$$

Where, S = specific yield

A = Area of thiessain polygon (m^2).

Q = Quantity of estimated recharge in the polygon area (m^3).

= A × Average fractional recharge × Rainfall in meter

∂h = Average water level fluctuation for the polygon area during the period of the tritium experiment (m).

For point location, Equiation-1 can be written as

$$S = \frac{\text{Average fractional recharge} \times \text{Rainfall in meter}}{\text{Average water level fluctuation during the period of the tritium experiment}}$$

Based on the above equation, specific yield values for few sites are estimated (Table 7.2). It has been observed that the paleochannel aquifer shows higher specific yields (16.8 to 28.3%) than that of adjacent shallow aquifer (specific yield is less than 14.2%). The average value of specific yield reported by Shakeel (1997) over the study area ranges from 13 to 26%. So, the specific yield values obtained by the combine use of tritium tracer along with relevant field data shows a good correlation with field data.

7.7 Results

The computed recharge rates at various experimental sites, as determined from field cum laboratory data of tritium peak shift, average volumetric moisture content in peak shift region and precipitation data are given in Table 7.1. The movement of injected tritium and soil moisture at various test sites are shown in Figure 7.5 to Figure 7.7. By comparing recharge rates with different landforms and their hydrogeologic characteristics (Chapter 6 and Table 7.1), it can be inferred that: (a) paleochannel area has relatively coarse grained material with sandy loam soil type and having high recharge rate of 17.0 to 28.7%, and (b) the upper layers of the alluvial plains have medium to fine grained sediments with silty loam soil type showing relatively low recharge rate (6.3 to 11.0 %).

Figure 7.8 represents the relationship between average sand content (%) and recharge rate for both the landform types. It is observed that the plot between percentage of average sand content and recharge rates shows a linear relationship In the paleochannel areas, the percentage of sand content is high (80.5-93.7%) and recharge rates are also high. On the other hand, in the alluvial plains, the sand content is lower (41.9-51.3 %) and recharge rates are also much lower.

Figure 7.9 shows relationship between water level fluctuation (m) and recharge rates (%). Although, the small numbers of the samples are a limitation and the study needs to be corroborated using a large number of sampling sites, but the two landforms are found to possess different regression characteristics. In the paleochannel areas, the water level fluctuations and recharge rates being much higher, as compared to the alluvial plains, where the water level fluctuations and the corresponding recharge rates are lower. Linear relationship between the groundwater table fluctuation and recharge percent shows that the vertical percolation constitutes the major component of recharge in the study area.

ANNEXURE-I

Volumetric soil moisture content and net tritium count rate at location T-1.

Depth (cm)	Volumetric moisture content (%)		Net tritium counts per minute
	Pre-Monsoon	Post-Monsoon	
0-10	0.0064	0.0681	22.0
10-20	0.0209	0.0476	31.4
20-30	0.0718	0.0896	11.8
30-40	0.0494	0.1275	14.2
40-50	0.0577	0.1060	11.4
50-60	0.0537	0.1094	28.2
60-70	0.0536	0.1117	60.6
70-80	0.0558	0.0939	35.4
80-90	0.0509	0.0934	27.2
90-100	0.0546	0.1095	30.0
100-110	0.0545	0.1063	22.4
110-120	0.0584	0.1065	47.2
120-130	0.0641	0.1190	47.0
130-140	0.0615	0.1180	52.4
140-150	0.0558	0.1238	89.2
150-160	0.0743	0.1227	199.0
160-170	0.0614	0.1118	276.4
170-180	0.0655	0.1106	479.0
180-190	0.0662	0.1065	644.4
190-200	0.0585	0.1079	850.0
200-210	0.0596	0.0968	1021.2
210-220	0.0540	0.1070	1136.8
220-230	0.0551	0.1114	1190.0
230-240	0.0538	0.1008	1216.6
240-250	0.0530	0.0911	1089.4

Volumetric soil moisture content and net tritium count rate at location T-2.

Depth (cm)	Volumetric moisture content (%)		Net tritium counts per minute
	Pre-Monsoon	Post-Monsoon	
0-10	0.0062	0.0476	9.0
10-20	0.0377	0.1252	20.6
20-30	0.0654	0.1322	6.0
30-40	0.0920	0.1405	18.8
40-50	0.1051	0.1558	8.0
50-60	0.0898	0.1435	53.4
60-70	0.0876	0.1273	25.4
70-80	0.0716	0.1332	31.2
80-90	0.0791	0.1361	34.6
90-100	0.0730	0.1472	25.4
100-110	0.0465	0.1048	13.0
110-120	0.0722	0.1260	20.4
120-130	0.0645	0.1022	21.8
130-140	0.0713	0.0920	36.0
140-150	0.0698	0.0807	72.8
150-160	0.0776	0.0805	125.8
160-170	0.0834	0.0797	237.6
170-180	0.0780	0.0978	340.8
180-190	0.0790	0.0847	528.6
190-200	0.0723	0.0904	691.8
200-210	0.0752	0.1001	968.8
210-220	0.0741	0.0866	1299.2
220-230	0.0777	0.0819	1318.0
230-240	0.0759	0.1077	1439.0
240-250	0.0684	0.0889	1650.8

Volumetric soil moisture content and net tritium count rate at location T-3.

Depth (cm)	Volumetric moisture content (%)		Net tritium counts per minute
	Pre-Monsoon	Post-Monsoon	
0-10	0.0334	0.0659	40.2
10-20	0.0640	0.1159	20.0
20-30	0.0975	0.1354	22.3
30-40	0.1202	0.1721	22.6
40-50	0.1335	0.1577	18.0
50-60	0.1219	0.1463	12.6
60-70	0.1234	0.1285	41.2
70-80	0.1238	0.1309	30.8
80-90	0.1444	0.1881	32.0
90-100	0.1512	0.1605	49.0
100-110	0.1786	0.1898	34.6
110-120	0.1464	0.1567	41.4
120-130	0.1528	0.1818	70.6
130-140	0.1175	0.1570	75.0
140-150	0.1458	0.1497	118.6
150-160	0.1200	0.1469	235.4
160-170	0.1263	0.1469	400.4
170-180	0.0983	0.1517	635.0
180-190	0.0881	0.1427	900.2
190-200	0.0824	0.1556	1318.5
200-210	0.0798	0.1289	1349.2
210-220	0.0708	0.12087	1408.0
220-230	0.0689	0.1309	1456.2
230-240	0.0818	0.1298	1260.2
240-250	0.0753	0.1056	1000.4

Volumetric soil moisture content and net tritium count rate at location T-4.

Depth (cm)	Volumetric moisture content (%)		Net tritium counts per minute
	Pre-Monsoon	Post-Monsoon	
0-10	0.0703	0.0424	42.2
10-20	0.0613	0.1150	14.0
20-30	0.1017	0.1268	23.8
30-40	0.1109	0.1798	22.6
40-50	0.1284	0.1705	19.0
50-60	0.1082	0.1583	11.6
60-70	0.0972	0.1168	42.2
70-80	0.0879	0.1072	35.8
80-90	0.0488	0.1251	34.8
90-100	0.0968	0.1141	48.0
100-110	0.0887	0.1161	33.6
110-120	0.0956	0.1298	40.4
120-130	0.0795	0.1192	71.6
130-140	0.0888	0.1235	73.0
140-150	0.0894	0.1105	120.6
150-160	0.0663	0.1309	230.4
160-170	0.0626	0.1256	398.4
170-180	0.0705	0.1393	634.0
180-190	0.0959	0.1499	898.2
190-200	0.0724	0.1341	1311.6
200-210	0.0610	0.1480	1337.2
210-220	0.0890	0.1241	1403.2
220-230	0.1051	0.1399	1453.2
230-240	0.0871	0.1479	1280.2
240-250	0.1045	0.1539	42.2

Volumetric soil moisture content and net tritium count rate at location T-5.

Depth (cm)	Volumetric moisture content (%)		Net tritium counts per minute
	Pre-Monsoon	Post-Monsoon	
0-10	0.0436	0.1426	18.2
10-20	0.0762	0.1553	22.9
20-30	0.1055	0.1394	19.6
30-40	0.1262	0.1056	15.2
40-50	0.1004	0.0798	20.4
50-60	0.0565	0.0699	17.6
60-70	0.0398	0.0668	24.9
70-80	0.0268	0.0730	25.6
80-90	0.0247	0.0711	26.3
90-100	0.0263	0.0756	29.2
100-110	0.0187	0.0847	23.5
110-120	0.0279	0.0873	18.7
120-130	0.0343	0.2570	15.0
130-140	0.0540	0.3072	35.9
140-150	0.1884	0.5313	55.4
150-160	0.1124	0.1946	130.7
160-170	0.0696	0.2125	219.9
170-180	0.0870	0.2485	183.2
180-190	0.0889	0.2733	78.9
190-200	0.1168	0.3466	56.1
200-210	0.1207	0.3933	41.7
210-220	0.1068	0.3382	34.3
220-230	0.0535	0.3807	21.3
230-240	0.0576	0.4423	17.1
240-250	0.0594	0.5293	16.8

Volumetric soil moisture content and net tritium count rate at location T-6.

Depth (cm)	Volumetric moisture content (%)		Net tritium counts per minute
	Pre-Monsoon	Post-Monsoon	
0-10	0.0584	0.0429	29.3
10-20	0.0980	0.1198	33.7
20-30	0.1055	0.1520	28.2
30-40	0.0314	0.1352	77.4
40-50	0.0976	0.1102	107.1
50-60	0.0973	0.1247	141.4
60-70	0.0642	0.1251	138.8
70-80	0.0326	0.1585	159.1
80-90	0.0379	0.1567	185.0
90-100	0.0324	0.1661	235.7
100-110	0.0382	0.1395	484.6
110-120	0.0256	0.0636	921.6
120-130	0.0240	0.1539	1783.8
130-140	0.0178	0.1740	2361.7
140-150	0.0299	0.1301	2455.7
150-160	0.0388	0.1136	2951.6
160-170	0.0305	0.1027	1812.2
170-180	0.0324	0.1061	1303.2
180-190	0.0385	0.2060	260.7
190-200	0.0786	0.370	1 80.0
200-210	0.2122	0.4114	42.0
210-220	0.1850	0.4461	59.7
220-230	0.1068	0.2946	43.7
230-240	0.2344	0.4716	50.0
240-250	0.2038	0.4441	24.3

Volumetric soil moisture content and net tritium count rate at location T-7.

Depth (cm)	Volumetric moisture content (%)		Net tritium counts per minute
	Pre-Monsoon	Post-Monsoon	
0-10	0.1987	0.2187	16.8
10-20	0.3730	0.2452	30.1
20-30	0.2381	0.3202	27.2
30-40	0.3062	0.3853	28.3
40-50	0.2683	0.3791	33.7
50-60	0.4060	0.2066	35.5
60-70	0.2714	0.1894	29.2
70-80	0.2282	0.1370	29.3
80-90	0.2283	0.1533	13.7
90-100	0.1545	0.2036	36.5
100-110	0.1593	0.1618	38.6
110-120	01964	0.1103	44.9
120-130	0.1298	0.1773	111.3
130-140	0.1433	0.1167	206.9
140-150	0.1928	0.1532	314.4
150-160	0.2014	0.1242	105.1
160-170	0.1191	0.1048	119.4
170-180	0.1230	0.1364	120.3
180-190	0.1086	0.1739	91.4
190-200	0.1285	0.2161	45.8
200-210	0.1066	0.1337	38.6
210-220	0.1064	0.1534	30.6
220-230	0.1786	0.1993	31.3
230-240	29.208	0.3954	53.3
240-250	36.596	0.4805	14.7

Volumetric soil moisture content and net tritium count rate at location T-8.

Depth (cm)	Volumetric moisture content (%)		Net tritium counts per minute
	Pre-Monsoon	Post-Monsoon	
0-10	0.0614	0.0236	35.6
10-20	0.1275	0.0870	32.4
20-30	0.7846	0.0547	28.2
30-40	0.1012	0.0795	27.2
40-50	0.1795	0.1530	20.0
50-60	0.2269	0.2717	45.9
60-70	0.1588	0.2968	41.7
70-80	0.1198	0.1786	53.1
80-90	0.1193	0.1850	106.6
90-100	0.1091	0.3734	257.7
100-110	0.0935	0.2590	494.8
110-120	0.0383	0.1190	621.7
120-130	0.0269	0.0930	744.0
130-140	0.0293	0.0656	680.7
140-150	0.0498	0.1277	531.0
150-160	0.2049	0.4986	259.6
160-170	0.1865	0.5835	116.4
170-180	0.1748	0.6307	56.6
180-190	0.1898	0.6326	34.6
190-200	0.2001	0.4554	30.3
200-210	0.1775	0.3707	49.0
210-220	0.1348	0.2476	29.0
220-230	0.0569	0.3283	64.5
230-240		0.3293	42.0

Volumetric soil moisture content and net tritium count rate at location T-9.

Depth (cm)	Volumetric moisture content (%)		Net tritium counts per minute
	Pre-Monsoon	Post-Monsoon	
0-10	0.0639	0.0713	22.4
10-20	0.1334	0.1664	0.0
20-30	0.1821	0.2039	9.4
30-40	0.2715	0.1990	0.0
40-50	0.1446	0.2051	19.6
50-60	0.2216	0.1499	67.2
60-70	0.2249	0.1670	197.4
70-80	0.1624	0.1445	470.4
80-90	0.2119	0.3223	712.4
90-100	0.2145	0.1609	872.8
100-110	0.2024	0.1501	948.2
110-120	0.1555	0.1349	939.4
120-130	0.1436	0.1743	819
130-140	0.1745	0.1892	438.6
140-150	0.1422	0.1958	347.4
150-160	0.1396	0.1214	650.8
160-170	0.1417	0.1962	221.4
170-180	0.1399	0.1620	140.0
180-190	0.1114	0.2218	88.4
190-200	0.1230	0.2078	66.8
200-210	0.0832	0.2315	27.2
210-220	0.0765	0.1819	46.4
220-230	0.0614	0.1667	17.2
230-240	0.0598	0.1133	74.6
240-250	0.0750	0.1580	38.0

Volumetric soil moisture content and net tritium count rate at location T-10.

Depth (cm)	Volumetric moisture content (%)		Net tritium counts per minute
	Pre-Monsoon	Post-Monsoon	
0-10	0.1106	0.0924	35.4
10-20	0.1741	0.1645	34.4
20-30	0.2129	0.1489	32.3
30-40	0.2339	0.1407	40.6
40-50	0.2541	0.1866	45.8
50-60	0.2811	0.2054	69.8
60-70	0.3072	0.2360	202.5
70-80	0.1582	0.2316	577.4
80-90	0.1086	0.2201	1375.9
90-100	0.1137	0.1375	1702.9
100-110	0.0939	0.1489	1476.6
110-120	0.0710	0.1267	1074.9
120-130	0.1577	0.1848	624.6
130-140	0.1056	0.0951	295.0
140-150	0.1917	0.1130	157.9
150-160	0.1493	0.2050	94.6
160-170	0.2218	0.2194	69.7
170-180	0.2143	0.1817	77.0
180-190	0.1571	0.2110	50.0
190-200	0.1597	0.2034	49.6
200-210	0.2606	0.1665	49.7
210-220	0.1082	0.1702	81.2
220-230	0.1017	0.1739	69.8
230-240	0.1133	0.1654	92.5
240-250	0.1734	0.1408	61.4

Volumetric soil moisture content and net tritium count rate at location T-11.

Depth (cm)	Volumetric moisture content (%)		Net tritium counts per minute
	Pre-Monsoon	Post-Monsoon	
0-10	0.0253	0.085118	104.8
10-20	0.0739	0.101476	126.8
20-30	0.0829	0.130095	104.8
30-40	0.1033	0.140576	166.0
40-50	0.1011	0.158760	183.0
50-60	0.1068	0.209530	352.4
60-70	0.1247	0.157272	878.4
70-80	0.1452	0.185593	1798.2
80-90	0.1753	0.192702	3279.2
90-100	0.1514	0.201712	4298.6
100-110	0.1343	0.159581	3235.6
110-120	0.1227	0.189425	1869.2
120-130	0.1561	0.153764	797.4
130-140	0.1139	0.237928	376.6
140-150	0.1431	0.205099	537.4
150-160	0.1491	0.103899	197.4

Volumetric soil moisture content and net tritium count rate at location T-12.

Depth (cm)	Volumetric moisture content (%)		Net tritium counts per minute
	Pre-Monsoon	Post-Monsoon	
0-10	0.0924	0.1106	35.4
10-20	0.1645	0.1741	34.4
20-30	0.1489	0.2129	32.3
30-40	0.1407	0.2339	40.6
40-50	0.1866	0.2541	45.8
50-60	0.2054	0.2811	69.8
60-70	0.2360	0.3072	202.5
70-80	0.2316	0.1582	577.4
80-90	0.2201	0.1086	1375.9
90-100	0.1375	0.1137	1702.9
100-110	0.1489	0.0939	1476.6
110-120	0.1267	0.0710	1074.9
120-130	0.1848	0.1577	624.6
130-140	0.0951	0.1056	295.0
140-150	0.1130	0.1917	157.9
150-160	0.2050	0.1493	94.6
160-170	0.2194	0.2218	69.7
170-180	0.1817	0.2143	77.0
180-190	0.2110	0.1571	50.0
190-200	0.2034	0.1597	49.6
200-210	0.1665	0.2606	49.7
210-220	0.1720	0.1082	81.2
220-230	0.1739	0.1017	69.8
230-240	0.1654	0.1133	92.5
240-250	0.1408	0.1734	61.4

ANNEXURE-II

Particle size distribution for site T1.

Sl. No.	Depth (m)	Sand % (2 mm-0.075 mm)	(Silt+Clay) % (<0.075 mm)
1.	0-50	71.1	28.9
2.	50-100	85.4	14.6
3.	100-150	82.6	17.4
4	150-200	85.8	14.2
5.	200-250	77.4	22.6
Average		**80.5**	**19.5**

Particle size distribution for site T2.

Sl. No.	Depth (m)	Sand % (2 mm-0.075 mm)	(Silt+Clay) % (<0.075 mm)
1.	0-50	74.9	25.1
2.	50-100	93.7	6.3
3.	100-150	83.8	16.2
4	150-200	87.7	12.3
5.	200-250	78.9	21.1
Average		**83.8**	**16.2**

Particle size distribution for site T3.

Sl. No.	Depth (m)	Sand % (2 mm-0.075 mm)	(Silt+Clay) % (<0.075 mm)
1.	0-50	84.8	15.2
2.	50-100	87.9	12.1
3.	100-150	88.6	11.4
4	150-200	89.3	10.7
5.	200-250	90.5	9.5
Average		**88.2**	**11.8**

Particle size distribution for site T4.

Sl. No.	Depth (m)	Sand % (2 mm-0.075 mm)	(Silt+Clay) % (<0.075 mm)
1.	0-50	89.8	10.2
2.	50-100	93.5	6.5
3.	100-150	94.6	5.4
4	150-200	95.2	4.8
5.	200-250	95.5	4.5
Average		**93.7**	**6.3**

Particle size distribution for site T5.

Sl. No.	Depth (m)	Sand % (2 mm-0.075 mm)	(Silt+Clay) % (<0.075 mm)
1.	0-50	88.06	11.93
2.	50-100	91.02	8.97
3.	100-150	83.87	16.12
4	150-200	85.74	14.25
5.	200-250	88.97	11.02
Average		**87.53**	**12.46**

Particle size distribution for site T6.

Sl. No.	Depth (m)	Sand % (2 mm-0.075 mm)	(Silt+Clay) % (<0.075 mm)
1.	0-50	89.06	10.93
2.	50-100	74.40	25.60
3.	100-150	82.33	17.67
4	150-200	87.90	12.10
5.	200-250	82.98	17.02
Average		**83.33**	**16.66**

Particle size distribution for site T7.

Sl. No.	Depth (m)	Sand % (2 mm-0.075 mm)	(Silt+Clay) % (<0.075 mm)
1.	0-50	76.49	23.50
2.	50-100	78.77	21.22
3.	100-150	86.29	13.71
4	150-200	92.46	7.54
5.	200-250	90.20	9.80
Average		**84.84**	**15.15**

Particle size distribution for site T8.

Sl. No.	Depth (m)	Sand % (2 mm-0.075 mm)	(Silt+Clay) % (<0.075 mm)
1.	0-50	93.4	6.60
2.	50-100	85.18	14.82
3.	100-150	86.38	13.62
4	150-200	73.96	26.04
5.	200-250	78.54	21.46
Average		**83.49**	**16.50**

Particle size distribution for site T9.

Sl. No.	Depth (m)	Sand % (2 mm-0.075 mm)	(Silt+Clay) % (<0.075 mm)
1.	0-50	26.5	73.5
2.	50-100	54.8	45.2
3.	100-150	52.2	47.8
4	150-200	56.9	43.1
5.	200-250	58.8	41.2
Average		**49.8**	**50.2**

Particle size distribution for site T10.

Sl. No.	Depth (m)	Sand % (2 mm-0.075 mm)	(Silt+Clay) % (<0.075 mm)
1.	0-50	83.05	16.94
2.	50-100	79.87	20.12
3.	100-150	80.08	19.92
4	150-200	86.59	13.61
5.	200-250	64.48	35.51
Average		**78.81**	**21.22**

Particle size distribution for site T11.

Sl. No.	Depth (m)	Sand % (2 mm-0.075 mm)	(Silt+Clay) % (<0.075 mm)
1.	0-50	28.4	71.6
2.	50-100	41.7	58.3
3.	100-150	48.6	51.4
4	150-200	46.8	53.2
5.	200-250	44.1	55.9
Average		**41.9**	**58.1**

Particle size distribution for site T12.

Sl. No.	Depth (m)	Sand % (2 mm-0.075 mm)	(Silt+Clay) % (<0.075 mm)
1.	0-50	31.3	68.7
2.	50-100	56.8	43.2
3.	100-150	55.2	44.8
4	150-200	55.8	44.2
5.	200-250	57.1	42.9
Average		**51.3**	**48.7**

Chapter 8

Source Water Availability and Recharge Planning

8.1 Introduction

In the foregoing chapters, it has been observed that the paleochannel aquifers are highly suitable hydrogeologically for artificial groundwater recharge in the area. In this perspective, it is important to estimate the allowable recharge of paleochannel aquifers, and availability of source water for artificial recharge. In this chapter, first, flow accumulation map has been generated from DEM through GIS. This is followed by estimation of surface runoff through Remote Sensing-GIS based Soil Conservation Service Curve Number (SCS-CN) method, and allowable recharge volume estimation of paleochannel aquifer. Finally, suggestion for planning/water budgeting for artificial recharge has been discussed. The methodology adopted is given in Figure 8.1.

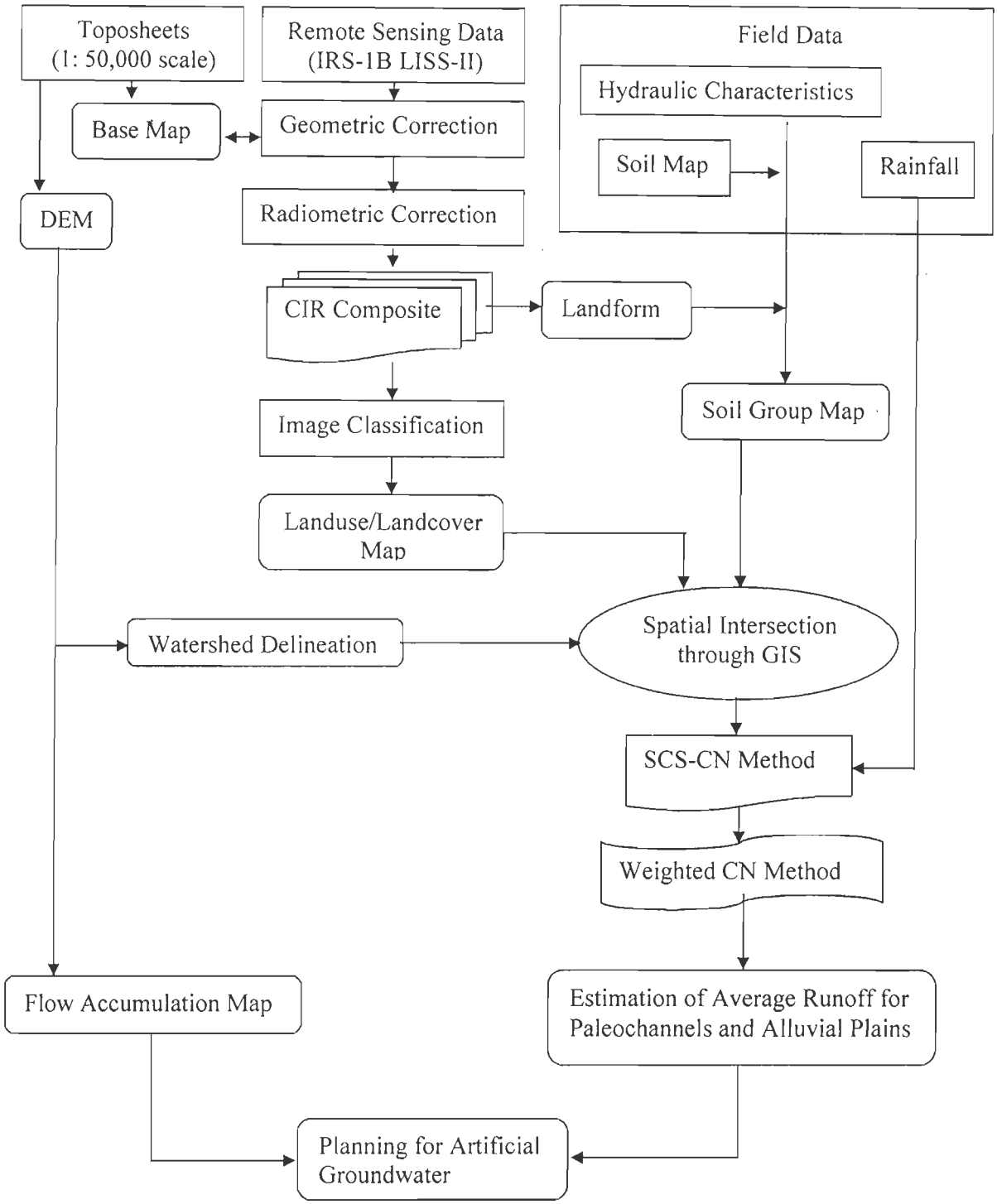

Figure 8.1: Flow diagram showing methodology adopted for source water estimation and planning for artificial recharge.

8.2 Flow Accumulation Map Generation

To generate the flow accumulation map, a DEM is required. DEM has been generated by the following steps (Figure 8.2):

i) Georeferencing of toposheets using a definite co-ordinate system.

ii) Digitization of point heights from toposheets.

iii) Incorporate point height from differential GPS survey.

iv) Generation of DEM using GIS interpolation (Krigging) method.

Using the above DEM, flow accumulation map and major watersheds have been delineated (using 'DEM Hydroprocessing' operations in ILWIS 3.3 software) (Figur 8.3 and Figure 8.4). The flow accumulation map contains cumulative hydrologic flow values that represent the number of input pixels which contribute water to the outlets (or sinks if these have not been removed); the outlets of the largest streams, rivers etc. will have the largest values. The flow accumulation map over the study area is shown in Figure 8.3.

8.3 Estimation of Surface Runoff through SCS-CN Method

Availability of source water is basically assessed in terms of non-committed surplus monsoon runoff, which as per the water source development scenario, can be utilized. Based on the available source water, planning is made for artificial recharge. The surface runoff can be estimated by analyzing the monsoon rainfall patterns, its frequency, number of rainy days, and maximum rainfall in a day and its variation in time and space. Application of conventional hydrological model for estimating runoff with parameters determined through ground truth measurement is highly time/labour consuming and economically unviable. Remote sensing data acquired from spaceborne platforms offers unique opportunities quickly and reliably with less cost and manpower for study of soils,

landuse/landcover and other parameters required for runoff modelling (Schultz, 1998). Several workers has estimated surface runoff by using remote sensing and GIS approach (Ragan and Jackson, 1980; Hill et al., 1987; Tiwari et al., 1991). Most of them prepared landuse/landcover map from remote sensing data and surface runoff was estimated by using this landuse/landcover map along with precipitation and simple mathematical formula through GIS. To date, most of the work on adopting remote sensing and GIS to runoff estimation has been with the SCS-CN model. In this study, rainfall runoff has been estimated by SCS-CN model through remote sensing and GIS approach. The methodology is as follows:

8.3.1 Database Generation

Data on landuse/landcover (LULC), hydrological soil group, and rainfall are required for estimating rainfall runoff by remote sensing-GIS based SCS-CN model.

8.3.1.1 Landuse/Landcover

The LULC is an important characteristic of the runoff process that affects infiltration, erosion and evapotranspiration. The infiltration, evapotranspiration and runoff vary from one land cover to another. For example, the area covered by forest comprises increased infiltration and reduced runoff components. The runoff yield is increased gradually from forest cover, grassland, farmland, barren land and urban built-up land (Yannian, 1990). In the present study, the remote sensing method was adopted for mapping spatial distribution of landuse/landcover in the study area.

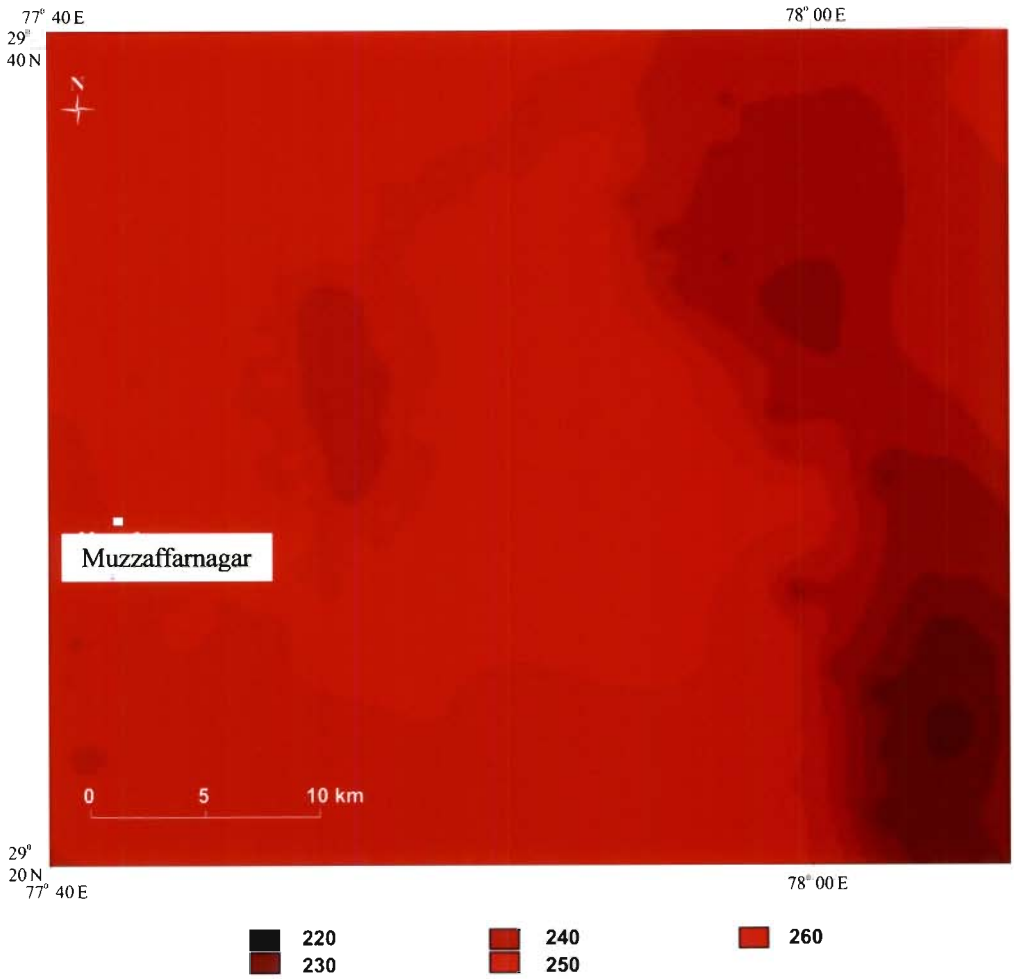

Figure 8.2: Digital Elevation Model (DEM) of the study area.

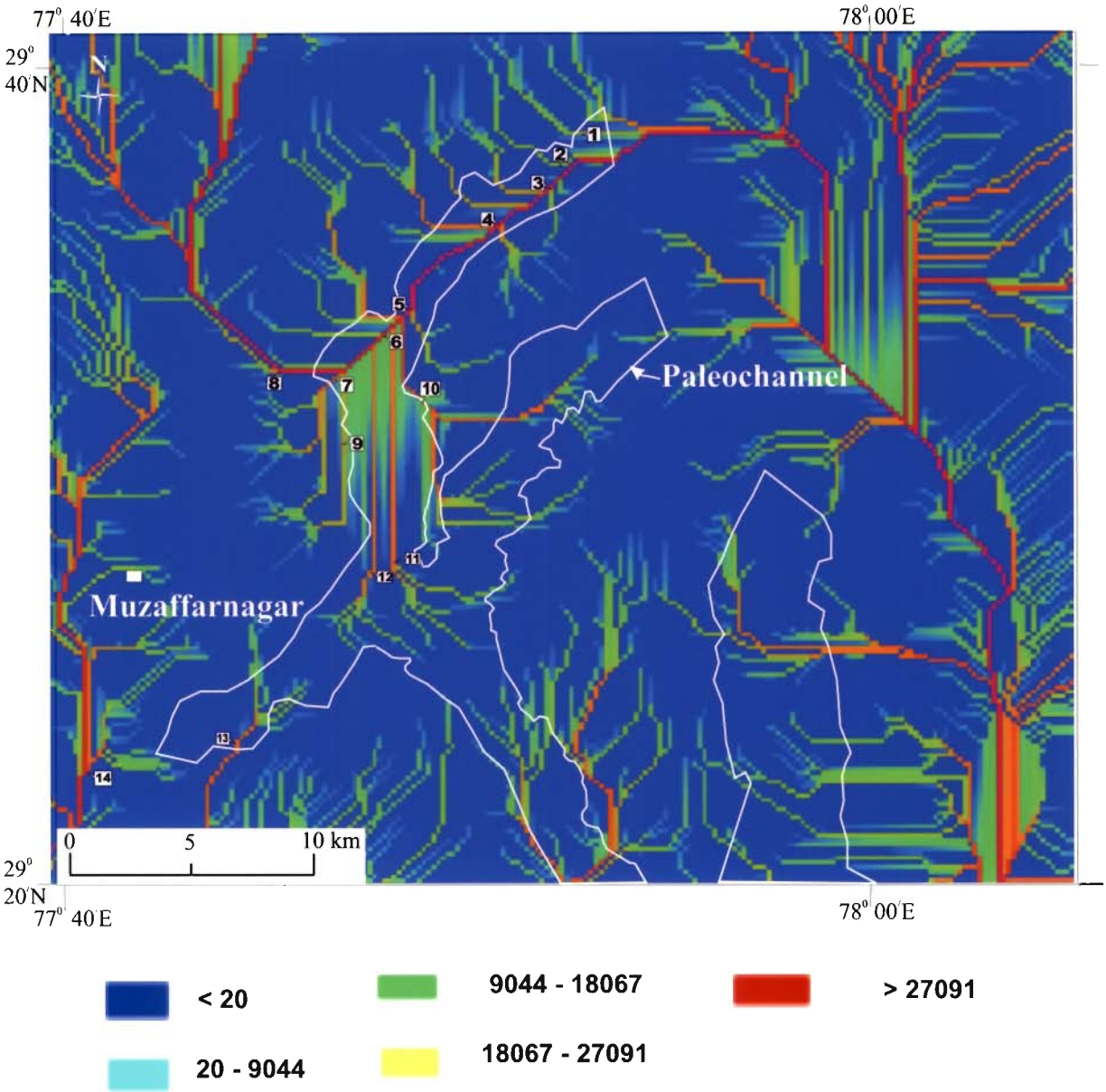

Figure 8.3: Flow accumulation map over the study area.

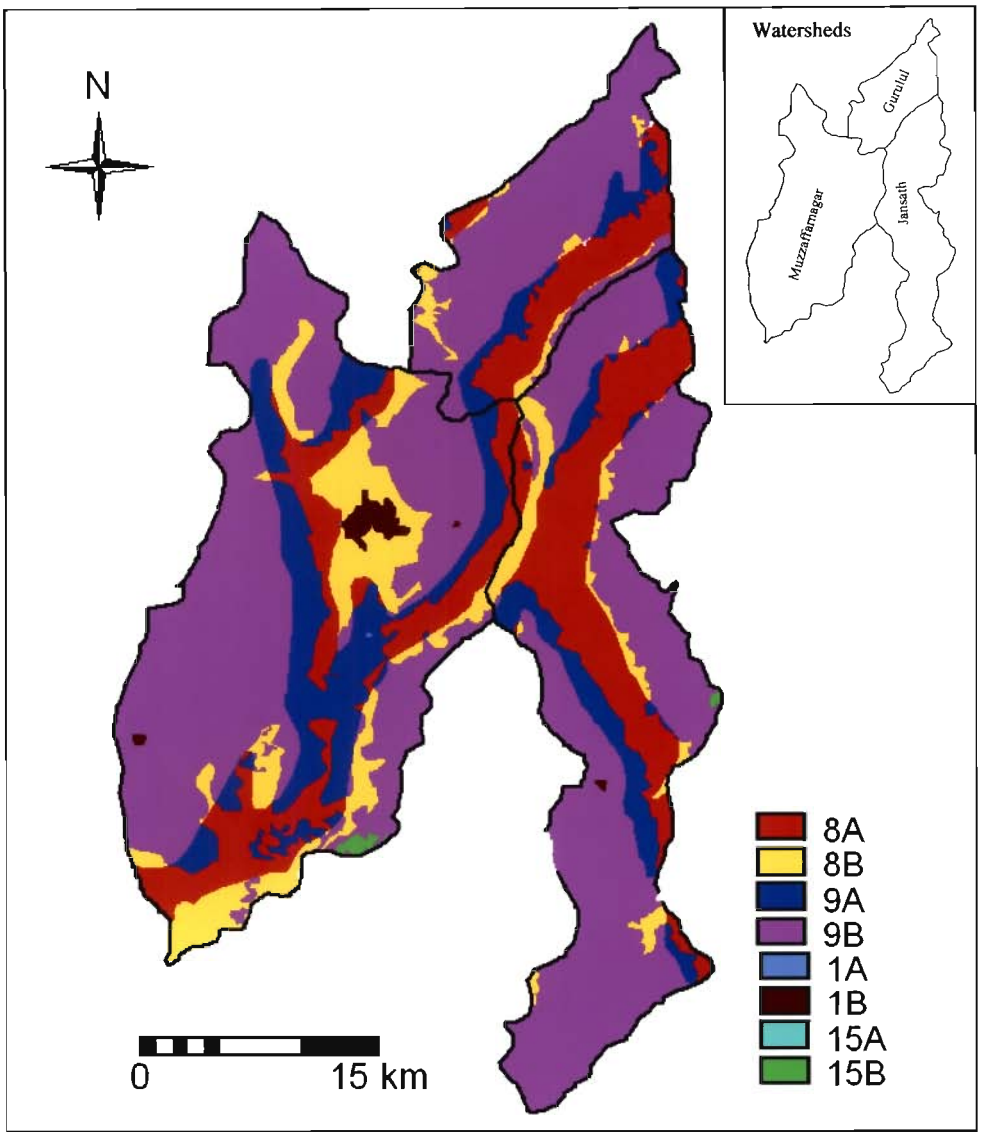

Figure 8.4: Combined map of landuse/landcover and hydrological soil group for three watersheds.

Several studies have been conducted to demonstrate the feasibility of interpreting the LULC categories from remotely sensed data and using the same data input parameters in a hydrologic modeling for estimating the runoff (Ragan and Jackson, 1980; Slack and Welch, 1980; Kathryn et al., 1986; Jackson et al., 1996). In the present study, the various landuse/landcover units were interpreted using digitally classified IRS-1B-LISS II data (as discussed in Chapter 4). The different LULC classes and their corresponding CN values are summarized in Table 8.1.

Table 8. 1: LULC and their corresponding CN values for different soil groups (Antecedent moisture condition II and Ia = 0.2S) (based on USDA-SCS, 1985).

Landuse/ Landcover Name	ID	CN values for different soil groups			
		A	B	C	D
Residential	1	77	85	90	92
Paleochannel	8	74	83	88	90
Agricultural land	9	66	74	80	82
Forest	15	45	66	77	83

8.3.1.2 Hydrological Soil Group

The initial infiltration and transmission of surface water into an aquifer system is a function of soil type and its texture. Loose soil structure, good aeration and high organic content in the soils enhance infiltration. The knowledge of soil cover and subsoil conditions is essential for prediction of runoff or recharge condition in a basin. Based on infiltration rate, texture, depth, drainage condition and water transmission capacity, the soils have been classified into different hydrological soil groups: A, B, C and D (Table 8.2, Chow et al., 1988; Viessman et al., 1989).

Table 8.2: Criteria for classification of hydrological soil group (Chow et al., 1988; Viessman et al., 1989).

Character	Hydrological Soil Group			
	A	B	C	D
Infiltration rate	High	Moderate	Slow	Very slow
Texture	Sand/Gravel	Moderately coarse to moderately fine	Moderately fine to fine	Clay
Depth	Deep	Moderately deep to deep	Moderately deep	Shallow over an impervious layer or clay pan or high water table
Drainage	Well to excess	Moderately well drained to well drained	Moderately drained to slow	Very slow
Water Transmision	High	Moderate	Slow	Very slow
Remarks	Low runoff potential	Moderate runoff potential	Moderate runoff potential	High runoff potential

Hydrological soil map of the study area has been generated from extensive field studies and some data derived from the soil map of Uttar Pradesh (UP) (National Bureau of Soil Survey and Land Use Planning, 1999). As stated earlier, there are two major landforms (viz. paleochannels and alluvial plains) present in the area, and they have relative significant differences in hydrogeological characteristics. Superimposition of the soil map over landform map indicates that generally, sandy loam occupies the paleochannel areas and silty loam occupies the agricultural land. This indicates that the paleochannel areas appear to have largely low runoff potential, whereas the agricultural areas may have moderate runoff potential. Thus, based on integrated information of landforms and soils, the study area has been divided into two regions of different hydrogeological

characteristics, called Soil Group A and Soil Group B. The spatial distribution of Soil Groups A and B on the three watershed of the study area is shown in Figure 8.5 and Table 8.3.

Table 8.3: Area of different soil group in watersheds.

Watersheds	Hydrological Soil Group	
	A (km^2)	B (km^2)
Gurukul	65.58	127.52
Muzzaffarnagar	147.64	281.39
Jansath	202.89	429.56
Total	416.11	838.47

8.3.2 SCS Curve Number Method for Runoff Estimation

In earlier decades, the runoff was estimated as a percentage of storm rainfall, where the percentage of runoff increases with the increase in rainfall. The SCS has developed a widely used runoff curve number procedure for estimating the runoff in which the effect of landuse/landcover, various soil cover types and antecedent moisture condition have been considered. If more than one land use or soil cover occurs in a basin, the composite curve number method was adopted (Anon, 1973). The basic assumption of the SCS curve number is that, for a single storm event, potential maximum soil retention is equal to the ratio of direct runoff to available rainfall. This relationship, after algebraic manipulation and inclusion of simplifying assumptions, results in the following equations (USDA-SCS, 1985), where, curve number represents a convenient representation of potential maximum soil retention (Ponce and Hawkins, 1996):

$$Q = \frac{(P - 0.2S)^2}{(P + 0.8S)}$$

where, Q is direct flow volume expressed as a depth, P is total rainfall, S is potential maximum soil retention.

Curve Number (CN) value is used to estimate potential maximum soil retention (S) by the following equation.

$$S = \frac{25{,}400}{CN} - 254 \quad \text{(water depth expressed in mm)}$$

The CN values were tabulated according to the National Engineering Handbook for various land covers and soil textures. These values were developed from annual flood rainfall–runoff data from the literature for a variety of watersheds, generally less than one square km in area (USDA-SCS, 1985). For runoff estimation in a basin, curve number (CN), potential maximum soil retention (S), initial abstraction (Ia) and antecedent moisture condition are required.

8.3.3 Spatial Intersection and Derivation of Curve Number

A major advantage of Geographic Information Systems (GIS) is the spatial analysis through intersection and manipulation. To obtain CN for each watershed, it is necessary to intersect the LULC and hydrological soil group in each watershed. For spatial intersection, the ILWIS software has been used in this study. Spatial intersections have been carried out for the three watersheds in the study area. The output with different LULC, hydrological soil groups and corresponding curve numbers (CN) for the three watersheds is shown in Figure 8.4 and Table 8.3.

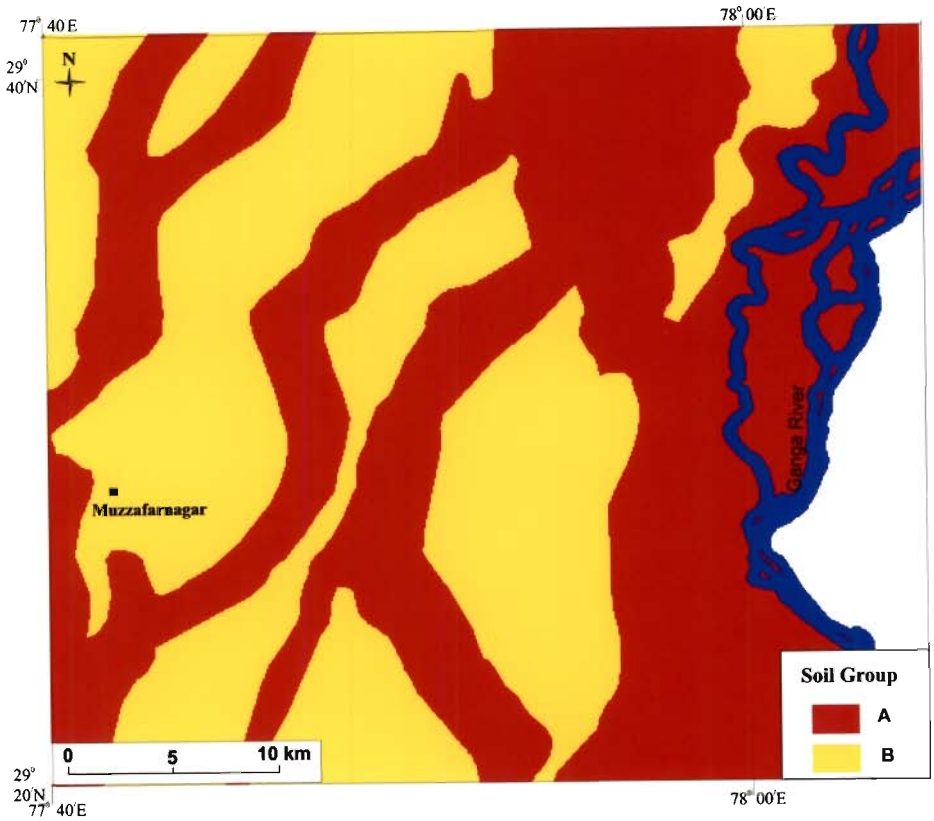

Figure 8.5: Hydrological soil group map of the study area.

Once the curve numbers have been identified for different land units, the weighted curve numbers were calculated for each watershed area in the following manner.

$$\text{Weighted curve number} = \frac{\sum (CN_1 \times a_1 + CN2 \times a_2 + \ldots\ldots + CN_n a_n)}{\sum a}$$

where, CN_1 is the curve number for particular land unit 1, a_1 is the area for that particular land unit 1, and $\sum a$ is the sum of the total watershed area

The weighted curve numbers for different watersheds are also given in Table 8.4.

Table 8.4: Values of weighted curve number, retention parameter and initial abstraction for different watersheds.

Water shed	LU/ LC-Id	Soil Group	Area (m^2) ($\times 10^6$)	CN	Weighted CN (AMC-II)	Retention parameter – S (mm)	Initial abstraction -I_a (mm)
Gurukul	8	A	44.9	74	77.02 ≈ 77	75.87	15.0
	8	B	1.0	88			
	9	A	19.7	66			
	9	B	117.9	80			
Jansath	1	B	3.9	85	73.78 ≈ 74	89.24	17.84
	8	A	105	74			
	8	B	26.8	83			
	9	A	42.5	66			
	9	B	253	74			
Muzzafarnagar	1	A	0.2	77	74.07 ≈ 74	89.24	17.84
	1	B	8.1	85			
	8	A	96.1	74			
	8	B	92.2	83			
	9	A	106.6	66			
	9	B	326.6	74			
	15	B	2.4	66			

After calculating the weighted curve number, the potential maximum soil retention (S) was calculated for each watershed by using the following formula:

$$S = \frac{25,400}{CN} - 254$$

The values of potential maximum soil retention (S) for different watersheds are also given in Table 8.4. After precipitation, initial abstractions (Ia) take place prior to surface runoff. Initial abstraction is a means of water losses due to plant interceptions, infiltration and surface storage. The standard assumption is that

$$Ia = 0.2S$$

The initial abstraction values have been calculated for each watershed (Table 8.4). If rainfall is greater than 0.2 S, then there is a possibility of runoff, else runoff will not take place. Hence, in this study, the rainfall events > 0.2S have been considered for further runoff estimation (Table 8.5). The daily rainfall data for 4 years from 2001 to 2004 were collected from the Groundwater Department for three rain gauge stations, namely Gurukul, Muzzaffarnagar and Jansath.

Table 8.5: Number of events generating surface runoff for different watersheds.

Watershed	No of Events for the year 2001- 2004			
	2001	2002	2003	2004
Gurukul	16	19	18	14
Jansath	19	20	22	16
Muzzaffarnagar	14	15	15	9

8.3.4 Estimation of Antecedent Moisture Condition (AMC)

AMC is a measure of the moisture content present at the time of surface runoff. The curve numbers valid for different AMC condition are different. To estimate AMC for each storm event, five previous day's daily rainfall data values are added and this total rainfall value is categorized into three levels—AMC I, AMC II and AMC III (as per USDA-SCS method), as given in Table 8.6. The AMC I refers to dry condition of soil, AMC II refers to

normal or average, and AMC III refers to wet condition of the watershed. Thus, the curve number (CN) corresponding to AMC I refers to the dry CN or the lowest runoff potential; the CN corresponding to AMC III refers to the wet CN or highest runoff potential, and the CN corresponding to AMC II stands for the average CN or the average runoff potential. In other words, higher the AMC, higher the CN, and higher the runoff potential of the watershed. In general, CN is calculated under normal condition (i.e. AMC II), and based on the previous five —days rainfall, the calculated CNs are adjusted.

Table 8.6 : Antecedent moisture condition classification (USDA–SCS, 1985).

Antcedent moisture condition	Rainfall range (mm)
I (dry)	< 36
II (normal)	36-53
III (wet)	>53

As for example, if the AMC is I (dry condition), the curve number is adjusted by using the following formula:

$$CN = 0.39 \times CN \times \exp(0.009 \times CN)$$

If the AMC is III (wet condition), the curve number is adjusted by using the following equation:

$$CN = 1.95 \times CN \times \exp(-0.00669 \times CN)$$

8.3.5 Runoff Estimation for the Watersheds

Runoff has been estimated by using "Weighted-Q' method. In this method, curve numbers for each landuse/landcover-soilgroup are calculated. Adjusted curve number (as per antecedent moisture conditions), and S value are also obtained for each

landuse/landcover-soil group and lastly Q (mm) for each event is calculated for every landuse/landcover-soilgroup seperately. Averaging the estimated runoff volume of 4 years, the average runoff for each landuse/landcover-soil group are calculated (Table 8.7). It has been observed that the paleochannel areas (landuse/landcover-soilgroup ID 8A and 8B) have generated low annual rainfall runoff, whereas, the alluvial plains have generated (landuse/landcover-soilgroup ID 8A and 8B) relatively higher rainfall runoff (Table 8.8).

Table 8.7: Average runoff depth for different landuse/landcover – soil group estimated by SCS–CN weighted method.

Water shed	LU/LC-Id	Soil Group	Runoff depth (mm) for year 2001-2004					
			2001	2002	2003	2004	Total	Average
Gurukul	8	A	15.1	143.7	131.3	6.9	296.9	74.2
	8	B	0.1	0.4	0.4	0.1	0.9	0.2
	9	A	7.6	52.6	45.4	5.3	110.9	27.7
	9	B	42.8	432.9	415.7	17.7	909.2	227.3
Jansath	1	B	0.5	0.9	0.9	0.2	2.5	0.6
	8	A	84.4	218.6	179.3	31.2	513.5	128.4
	8	B	32.3	63.2	57.4	12.9	165.7	41.4
	9	A	23.7	78.7	59.0	9.3	170.7	42.7
	9	B	203.4	526.9	432.2	75.2	1237.8	309.4
Muzzafarnagar	1	A	0.1	0.2	0.1	0.1	0.3	0.1
	1	B	1.3	9.6	9.5	0.5	20.9	5.2
	8	A	9.7	86.5	79.5	2.6	178.3	44.6
	8	B	13.5	103.4	101.2	4.4	222.5	55.6
	9	A	10.8	77.3	67.4	4.2	159.8	39.9
	9	B	32.9	293.9	270.1	8.9	605.9	151.5
	15	B	0.2	1.7	1.5	0.1	3.5	0.9

Table 8.8: Average annual runoff for paleochannel and alluvial plains for different watersheds.

Watersheds	Annual average rainfall runoff depth (m)	
	Paleochannel	Alluvial plains
Gurukul	0.07	0.25
Muzzafarnagar	0.10	0.19
Jansath	0.17	0.35

8.4 Estimation of Actual Allowable Recharge for the Paleochannel Aquifer

To effectively practice the artificial recharge in a basin, it is necessary to estimate the aquifer space available for recharge. The evaluation of the storage potential of sub-surface reservoirs is invariably based on the knowledge of three-dimensional data of aquifers, which includes their thickness and lateral extent. The availability of sub-surface storage space and its replenishment capacity further govern the extent of recharge. In this study the paleochannel aquifer dimension and its storage potential are estimated using remote sensing-GIS, litholog and field data. The estimation of storage potential of the paleochannel aquifer has involved the following steps:

(a) Estimation of areal extent of the paleochannel aquifer: The areal extent of the paleochannel aquifer is estimated from analysis in GIS. It has been found that the width of paleochannel varies from 3 to 5 km. In the present study, only one paleochannel (marked as P1 in Figure 4.6 in Chapter 4) has been considered for artificial groundwater recharge. The areal extent of this paleochannel is estimated through GIS as $(20{,}000 \times 2500) = 5 \times 10^7$ m^2.

(b) Estimation of thickness of the unsaturated zone: The unsaturated zone available for artificial recharge has been estimated from water level data. The average depth of water level below ground level is considered as the average thickness of the unsaturated zone. The post-monsoon water table depth from the surface in the paleochannel aquifer varies from 3.86 m to 14.46 m (Table 5. 9 of Chapter 5). Therefore, the average thickness of the unsaturated zone of the paleochannel aquifer is taken as 9.16 m. The entire thickness of 9.16 m can not be recharged, as it will lead to water logging into the area.

Therefore, a thickness of 2 m is left empty at the top. Hence, the average unsaturated thickness is taken as 7.16 m.

(c) Total volume of unsaturated zone: The total volume of the unsaturated zone available for artificial recharge in the paleochannel aquifer has been calculated by multiplying the areal extent and thickness of the unsaturated zone:

Total volume of the unsaturated zone available for artificial recharge = areal extent × thickness of the unsaturated zone = $5 \times 10^7 \times 7.16\ m^3 = 358 \times 10^6\ m^3$

(d) Estimation of total volume of allowable recharge: The total volume of water that is allowed to the paleochannel aquifer for artificial recharge is estimated by multiplying the total volume of the unsaturated zone available for artificial recharge with the average storage capacity of the paleochannel aquifer, i.e.,

Volume of total allowable recharge = Volume of the unsaturated zone available × storage coefficient.

The storage coefficient for the paleochannel aquifer is estimated as 0.25. Thus, the total allowable recharge for the paleochannel aquifer is $358 \times 10^6 \times 0.25\ m^3 = 89.5 \times 10^6\ m^3$.

Now, the volume of water required for arresting the decline of water table in the three watersheds in the study area has been estimated. This volume of water = Total area of watersheds × Average declining rate × Average storage coefficient. = $1154.6 \times 0.15 \times 0.2\ 10^6\ m^3 = 34.6 \times 10^6\ m^3$. Therefore, it can be inferred that the paleochannel aquifer has sufficient storage potential to arrest the declining trend of groundwater table through artificial recharge.

8.5 Planning for Artificial Recharge

For selection of sites for artificial recharge, the following criteria have been taken:

a) The site should have a high flow accumulation value from surface.

b) The site should be in the paleochannel or very nearest to the paleochannel.

c) The inlet should be of barren land so that construction of any recharge structures is possible.

Based on the source water availability, a three stage plan has been developed here for recharging the paleochannel aquifer reservoir.

First stage planning: As the agricultural activity within the paleochannel is quite thin, for the first stage, the sites for artificial recharge are selected within the paleochannel. 11 such suitable locations (shown as 1, 2, 3, 4, 5, 6, 7, 10, 11, 12 and 13 in Figure 8.3) are selected and their area of influence (i.e. number of pixel from which the runoff will be accumulated to the outlet point) and average annual runoff volume are given in Table 8.9. The average annual runoff volume has been calculated by multiplying the average annual runoff (m) (derived from SCS-CN method), number of pixels that are supposed to generate the runoff for the outlet point, and the pixel size (m^2).

Runoff volume for the particular outlet = Average annual runoff (m) × Number of pixels that are supposed to generate the runoff for the outlet point × Area of pixel (m^2).

From such an estimation, it has been inferred that about 1.5×10^6 m^3 runoff per annum would be available for artificial recharge at the above 11 selected sites. Hence, 33.1×10^6 m^3 of water is still required for artificial recharge for arresting the water table decline.

Second stage planning: For the second stage of planning, a few sites have been selected outside the paleochannel, but lying very close to the paleochannel, so that

carrying cost of water is minimal. Three such locations are selected and are shown as site 8, 9 and 14 on Figure 8.3 and their collective outputs per year are estimated as 1.4 $\times 10^6$ m^3. Thus, after first and second stages of planning, it is found that 31.7 $\times 10^6$ m^3 of water is still required for further recharge to arrest the decline water table. Hence, third stage of planning has been suggested.

Table 8.9: Annual average runoff volume for different locations.

Location ID	Number of pixel supposed to generate the runoff		Watershed from which runoff accumulated	Total annual runoff volume (m^3)
	Paleochannel	Alluvial plains		
1	4	227	Gurukul	22820.0
2	8	157	Gurukul	15940.0
3	217	604	Gurukul	66910.0
4	581	910	Gurukul	108430.0
5	223	1069	Gurukul	113590.0
6	969	529	Gurukul	81970.0
7	35	840	Gurukul	85050.0
8	Nil	9921	Gurukul	992100.0
9	16	256	Muzzafarnagar	20300.8
10	Nil	619	Jansath	871552.2
11	437	101	Jansath	43936.8
12	487	Nil	Muzzafarnagar	19480.0
13	436	143	Muzzafarnagar	28422.4
14	Nil	5405	Muzzafarnagar	415104.0

Third stage planning: In this stage, major canals and their distributaries are considered. Upper Ganga Cannal is present close to the paleochannel aquifer, and the paleochannel aquifer is well traversed by distributaries. Therefore, a detailed study of discharge through the main canal and their distributaries has been carried out. The water demand from the canal over the study area is quite high from the month of February to June, and it is minimum during the month of July to September. Even during the low demand period, the water is still available in the canal, which is not used for irrigation. Hence,

surplus water released from the main canal can be utilized to meet out the requirement for artificial recharge in the period July – September. The average discharge of the Upper Ganga Canal is 300 m^3/sec. So, the total discharge through the canal during the low demand period (i.e. July to September) is 2988×10^6 m^3. The requirement of water for artificial recharge after the second stage of planning is 31.7×10^6 m^3. Thus, the requirement is just 1% of the total canal discharge during the low demand period. So, it is suggested that 3 m^3/sec discharge from the canal during the period July – September may be diverted to meet the above requirements, to arrest the declining groundwater table through artificial recharge.

In this way, the paleochannel regions can be used for artificial groundwater recharge to arrest the falling groundwater table and manage water resources.

Chapter 9

Summary and Conclusions

The Indo-Gangetic plain is a land of fertile soil, moderate climate and generally abundant water. Groundwater is the main source of water supply for various purposes. However, over the years due to swelling population, increasing industrialization and expanding agriculture, the demand of water has multiplied. The average declining rate of groundwater table is estimated as 0.15 m $year^{-1}$ in the western part of Uttar Pradesh where the study has been carried out. Hence, there is a great need to evolve strategies to manage and artificially recharge groundwater resources in the area.

Research Objectives

In the present work, a systematic study has been taken up for developing a strategy to replenish groundwater artificially in the study area, lying in the western part of Indo-

Gangetic Plains. Such a work with the above specific objective not has been taken up in the area hitherto. The main objectives of the research work are as follows:

a) Application of Remote Sensing — GIS techniques to map spatial distribution of porous and permeable stretches which happen to be parts of paleochannels of the Ganga river.

b) Evaluation of hydrogeological characteristics of paleochannel-aquifers and also the adjacent alluvial plains.

c) Estimation of allowable recharge volume of the rechargeable aquifer.

d) Estimation of source water availability and planning for artificial recharge.

Data and Software Used

The following data sets collected from various sources have been used in this study:

(a) Remote sensing data: IRS-1B-LISS II (November, 1998) data.

(b) Ancillary data: (i) Survey of India toposheets at 1: 50,000 scale; (ii) Soil map from National Bureau of Soil Survey and Land Use Planning; (iii) Data such as specific yield, storage coefficient etc., collected from various groundwater organisations.

(c) Field Data: Extensive field work has been carried out during the period July 2004 to July 2007 for conducting drilling operation, soil sample collection, water sample collection, field experimentation for tritium injection, ground water level monitoring and differential GPS survey. The field surveys have yielded data on various hydrogeological characteristics such as soil texture, subsurface lithological information, hydraulic conductivity, vertical hydraulic conductivity, recharge rate, recharge source, and groundwater flow direction.

The remote sensing data has been processed by using ERDAS Imagine-8.7 software. The GIS analysis has been carried out using ILWIS-3.3 and ARC GIS and R2V software. Litholog data analysis has been carried out by using ROCKWORKS-2006 software.

Study Area

The study area is located in the western part of the vast Indo-Gangetic Plain (Muzaffarnagar and Saharanpur districts in Uttar Pradesh) in India and lies between latitudes $29^0 10'$ N to $29^0 50'$N and longitudes $77^0 30'$ E to $78^0 10'$ E with total geographic area of approximately 3000 km^2. It is quite devoid of any significant topographic features, exhibiting the characteristics of a typical river flood plain. The area slopes gently from north to south, at an average gradient of less than 0.38 m km^{-1}. Hydrogeologically it comprises extensive, multiple alluvial aquifer systems, composed of unconsolidated to semi-consolidated deposits of sand, clay and calcium carbonate concretions (locally known as kankar) that constitute a good groundwater reservoir system.

Data Processing and Analysis

In order to fulfil the research objective, the following broad methodological steps have been followed:

Data analysis and processing has involved image processing of remote sensing data and laboratory analysis of collected samples. A base map has been prepared from the Survey of India Topographic maps by scanning, geo-referencing, mosaicking and digitizing. All the data layers have been co-registered with the base map. Point data

obtained from field and laboratory experiment are properly placed on the base map and finally various information have been obtained using GIS tools.

Analysis in GIS environment has involved data synthesis and analysis through GIS. Particular emphasis has been given on various hydrogeological characteristics of paleochannel aquifer for artificial groundwater recharge by combining use of remote sensing and field data through GIS. Finally, an attempt has been made to assess the quantity of surface water that is likely to be available for recharge purposes.

Results and Analysis

(I) Paleochannel Mapping: The important aspect for developing an artificial recharge scheme is to demarcate the area that is suitable hydrogeologically as well as socio-economically. The study area physiographically exhibits the characteristics of a river flood plain. Among the physiographic units, the paleochannel deposits are particularly striking for artificial groundwater recharge and are very clearly seen on the remote sensing (IRS-1B LISS-II) image. They appear as zones of high permeability and rather poor both in vegetation and surface soil moisture. They have sinuous/serpentine shape and are significantly different from the rest of the alluvial deposits. For artificial recharge study, it becomes essential to delineate the paleochannels courses. In this study, major paleochannels have been delineated from remote sensing (IRS-1B-LISS-II multispectral sensor) and field data.

IRS-1B LISS-II sensor data has been used as the primary data source to implement the supervised classification for generating landuse/landcover (LULC) map. Six LULC classes - agricultural land, paleochannel, dry streams, water body, built-up area, and marshy land have been chosen and a LULC map has been generated with an overall

accuracy of 87.9% using Maximum Likelihood Classifier (MLC). A 3 × 3 pixels majority filter has been applied, which assigns the most dominant class to the central pixel to remove the stray pixels and to generate a smooth image. Finally, integrating information from CIR composites, LULC map, and extensive field observations, paleochannels have been traced and a paleochannel map has been generated.

In the study area, three major paleochannels generally N–S trending and exhibiting broadly successive shifting and meandering pattern have been deciphered. All of these paleochannels in this study area are located to the west of the present–day course of the river Ganga. The paleochannel courses are very wide (2-5 km) suggesting their formation by a large river and thus, it can be inferred that the Ganga River has been shifted from the west to the east. The paleochannels can be traversed about 60-80 km on the satellite image. Field observations have revealed that the soils in the paleochannels are composed mailny coarse sand. High permeable, porous, coarse grained materials possessing high infiltration rate is responsible for rather poor agricultural activity in the paleochannel area.

(II) Litholog data analysis: Well-log data give the sub-surface lithological information with depth. 50 lithologs over the study area obtained from field drilling operation and some from Groundwater Division of Uttar Pradesh have been analysed to determine the aquifer depth and carry out litholog correlation. The sub-surface formations/materials have been classified depth–wise as: coarse sand, medium sand, fine sand, and clay. It has been observed that the paleochannel aquifer mainly consists of coarse sand occasionally mixed with pebbles, and boulders of varying sizes. On the other hand, the adjacent alluvial plains aquifers are mainly composed of medium to fine grained sand along with clay and kankar beds. It has been also observed that the surficial clay layer (thickness 0.8-2 m), which is

supposed to be responsible for high surface runoff, is present in the alluvial plains, whereas, it is generally absent over the paleochannels.

(III) Delineation of paleochannel aquifer geometry: An attempt has been made to interpret and delineate aquifer geometry by integrating satellite sensor and litholog data. The litho-log data were sorted out and different lithological units were classified as aquifer and confining layers. Construction of subsurface lithological cross-section, construction of aquifer geometry, and final interpretation has been made by aggregating and synthesizing all the information - such as the base map, the CIR composite image, paleochannel map, well location map, and the DEM.

The first aquifer in the alluvial plains is an unconfined to semi-confined in nature and consists of fine to medium sand with a number of lenses of clay and kankar. The thickness of this aquifer varies from ≈ 25 m to ≈ 33 m. The upper most aquiclude (clay) starts from the base of the unconfined aquifer and extends upto a depth of ≈ 41 m. The thickness of this aquiclude varies from 5-8 m. The second aquifer is confined in nature and mainly consists of fine to medium grained sand along with some lenses of kankar. The thickness of this aquifer ranges from 55 m to 70 m.

The paleochannel aquifer is unconfined and is mainly composed of coarse grain sandy material along with boulder and pebbles beds. This paleochannel aquifer extends upto a depth of about 55-65 m and is well connected with the adjacent alluvial plains aquifers.

(IV) Hydrogeological characteristics: Hydrogeological characteristics of the paleochannel and the adjacent alluvial plains become important for implementing artificial recharge. The following hydrogeologic characteristics have been considered:

- *Soil texture analysis*: Twenty (20) surface soil samples, collected from sites located on both the paleochannels and alluvial plains, have been subjected to grain size analysis to yield information on soil texture. From the mechanical analysis of soil samples in the laboratory, the percentage for each of the soil fractions (sand, silt and clay) were determined. The percent of each the soil fractions (sand, silt and clay) are plotted on the USDA textural triangle. It has been found that in the area of paleochannels, the percentage of sand varies from 58.3 to 78.6 and that of silt and clay varies between 7.0 to 29.1 and 7.3 to 16.3 respectively. On the other hand, in the areas of alluvial plains, the sand percent varies between 15.1 to 28.8, whereas silt and clay percentage is between 51.9 to 69.3 and 11.8 to 24.2 respectively. This shows that the paleochannels comprise dominantly sandy loam type of soil, on the other hand, the alluvial plains are characterised by silty loam type of soil.

- *Vertical hydraulic conductivity*: A series of 17 observation wells systematically sited on the paleochannel and its either flanks have been drilled and sampling has been carried out for collecting lithological information at different depths. Grain size analysis has been carried out for all the 82 samples collected from different locations and at various depths during drilling. The grain size distributions have been plotted on lognormal graph paper to obtain grading curve for each sample. D_{10} has been calculated for each sample form the grading curve and subsequently bulk hydraulic conductivity has been determined using Hazen (1911) equation. In paleochannel aquifer, the D_{10} values range from 0.21 to 0.33 mm, whereas, in alluvial plains, it is 0.14 to 0.18 mm. The estimated bulk hydraulic conductivity for selected core samples at different depths ranges from 30 to 75.3 m/day for samples falling in the paleochannel. On the other hand, the alluvial plain aquifer shows

lower vertical hydraulic conductivity with values from 13.5 to 22.3 m/day. The hydraulic conductivity of boulder and pebble beds is considered as more than 100 m/day.

- *Natural recharge rate and specific yield*: The natural groundwater recharge rate due to precipitation has been estimated using tritium tagging technique in the two major different landforms, viz. the paleochannels and the alluvial plains. The methodology of the work involves - site selection for tritium injection, followed by field and laboratory experimentation, computation of recharge rate and specific yield. The paeochannel and landform map generated from remote sensing (IRS-LISS-II multispectral sensor) data has been used as a base map for selecting sites for tritium injection. Thirteen experimental sites – 6 within paleochannel and 7 on the adjacent alluvial plains have been selected. Comparison of recharge rates and hydrogeologic characteristics in different landforms indicates that: (a) paleochannel area has coarse grained soil (sandy loam) and has high recharge rate of 18.9 to 28.7%, and (b) the alluvial plains have medium to fine grained soil (silty loam) and relatively low recharge rate (6.3 to 8.9 %).

The groundwater levels in the wells adjacent to tritium tagging sites were recorded in June (pre-monsoon) and October (post-monsoon) 2006. Again, the two landforms are found to possess different regression characteristics, in the paleochannel areas, the water level fluctuations and recharge rates being much higher, as compared to the alluvial plains. A linear relationship between the groundwater table fluctuation and recharge percent shows that the vertical percolation constitutes the major component of recharge in the area. It has been observed that the paleochannel aquifer shows higher specific yields (16.8 to 28.3%) than the adjacent shallow aquifer (specific yields < 14.2%). The specific yields computed by this method are found to be quite similar to the values computed by conventional methods.

▫ *Stable isotope analysis and recharge source*: In the present study, the stable isotopes of groundwater samples from the first unconfined aquifer have been analysed using Dual Inlet Mass Spectrometer at the National Institute of Hydrology, Roorkee (India). Samples were collected from three different sources namely, precipitation (at NIH), groundwater (from 11 sites- 5 in the paleochannel and 6 in the alluvial plains aquifer), and the adjacent Ganga Canal. It has been observed that, the isotopic ratio ($\delta^{18}O$) in groundwater at locations falling within the paleochannel ranges from – 6.86 to – 5.68, which are closer to the average isotopic value of the precipitation. This indicates precipitation is the main component for groundwater recharge for paleochannel aquifers. On the other hand, samples falling in the alluvial plains are depleted ($\delta^{18}O$ ranges from -9.92 to -7.27) in comparison to samples falling in the paleochannel. Their isotopic ratio in groundwater is closer to the average value of the canal water. This indicates that the alluvial plains aquifers are getting recharge by both canal and rainfall. The value of average istotopic ratio in groundwater sample gets enriched away from the Upper Ganga Canal (Main Basera Distributary) or depleted towards the canal. This indicates that the influence of canal water to groundwater recharge decreases away from the canal and rainfall recharge component relatively increases.

▫ *Groundwater flow*: Groundwater levels have been monitored in wells at 37 locations (12 on the paleochannel aquifers and 25 on the adjacent alluvium plains over 2 years (2005-2006) for both pre- and post-monsoon period. The precise location (latitudes and longitudes) and the height of the ground surface from mean sea level of such wells have been determined through differential GPS. Integrated interpretation has been made by combining information of paleochannel map, reduced water level contour map and flow direction map. It has been observed that groundwater flows away from the paleochannel

for both pre- and post-monsoon period. The typical contour pattern (convex downwards) in the paleochannel aquifer is interpreted to be due to its higher hydraulic conductivity and porosity. This further indicates that if groundwater is recharged through paleochannels, it will slowly recharge the alluvial plains.

- *Rainfall runoff*: The USDA-SCS method has been used to estimate runoff in three watersheds of the study area. For this purpose, landuse/landcover data has been generated from remote sensing images and soils type map has been generated from extensive field studies and soil map of Uttar Pradesh (UP) (National Bureau of Soil Survey and Land Use Planning, 1999). The antecedent moisture condition (AMC) has been considered from the previous 5 days rainfall data. The rainfall-runoff for the three watersheds (namely Gurukul, Jansath and Muzzaffarnagar) has been estimated from the above data sets. It has been observed that the paleochannel area shows lower rainfall- runoff, whereas, the alluvial plains show relatively higher rainfall runoff, as expected.

(V) Planning for artificial recharge: For this purpose, firstly, the paleochannel aquifer dimension and its storage potential have been estimated from using remote sensing data, litholog data and field data using GIS environment. The total allowable recharge for one of the paleochannel aquifer has been studied here and is estimated as 89.5×10^6 m^3. On the other hand, the volume of water required for arresting the decline of groundwater table over the three watersheds is estimated as 34.6×10^6 m^3. Thus, it can be stated that the paleochannel aquifers have sufficient storage capacity to arrest the declining trend of water table through artificial recharge.

Thereafter, flow accumulation map has been generated from DEM in GIS. In combination of flow accumulation map and average rainfall runoff, the suitable points for artificial recharge have been selected and their average annual runoff (for artificial

recharge) has been estimated. The following criteria are adopted for selection of artificial recharge sites: (a) the site should have a high flow accumulation value from surface, (b) the site should be on the paleochannel or near to the paleochannel, and (c) the site be of such landuse that construction of any recharge structures is possible.

Based on the above data sets and source water availability consideration, a three stage plan has been suggested for recharging the paleochannel aquifer reservoir:

First stage planning: As the agricultural activity within the paleochannel is thin, the sites have been selected within the paleochannel in the first stage. Eleven such suitable locations have been selected and their areas of influence and average annual runoff volume have been estimated. From such estimation, it has been inferred that about 1.5 $\times 10^6$ m^3 water is available for artificial recharge in the selected sites annually.

Second stage planning: Based on the criteria described above, three points/sites adjacent to the paleochannels have been selected so that the carrying cost of water is minimal. Their collective outputs per year is estimated as 1.4×10^6 m^3.

So, after first and second stage of planning, it has been observed that 31.7×10^6 m^3 of water needs to be imported for recharging the aquifer to arrest the declining water table.

Third stage planning: In this stage, major canals and distributaries are considered. The Upper Ganga Canal is found to present close to the paleochannel aquifer and it is well accessible to the paleochannel aquifer through various distributaries. So, a detailed study of discharge through the main canal and distributaries and the water demand for irrigation is considered. It has been found that the water demand over the study area is quite high from the month of February to June, and it is minimum during the month of July to September. It is proposed that surplus water from the main canal may be

utilized for meet out the requirements for artificial recharge. The average discharge of the Upper Ganga Canal is 300 m^3/sec. It is estimated that barely 1% of discharge during the lean demand months (July-September) would be sufficient to meet the requirements for artificial recharge purposes.

Major Contributions

As an overview, the major contributions of the study are site–specific in the sense that extensive stretches of paleochannels of the Ganga river have been delineated, and it has been shown for the first time that their hydrogeological characters are quite different from the rest of adjoining alluvial plains. Besides, a few contributions can be also considered as methodology innovations.

In brief, the following may be considered as important contributions of the study:

1. Delineation of wide (4-6 km) and extensive (60-80 km long) stretches of paleochannels of the Ganga Plains; the paleochannels are sinuous/serpentine shaped and are characterized by low surface moisture and extremely sparse to poor vegetation.
2. An innovative procedure has been developed to integrate drilling and remote sensing image data for delineating sub-surface aquifer geometry. The aquifers are interpreted to possess spatial variation in geometry and occasional vertical displacements along normal faults.
3. The paleochannels comprise of dominantly coarse sand with occasional pebbles, and extend upto a depth of 50–60 m below the surface, which is responsible for very high hydraulic conductivity (30–75.3 m/day).

4. The tritium tagging data indicates that the recharge rate is much higher (upto 28.7%) in the areas of paleochannels than in the areas of general alluvial plains (upto 8.9%). Further, specific yield is found to be 16.8–28.3% in the paleochannel aquifers, as compared to <14.2% in the alluvial shallow aquifers.
5. The groundwater contour map exhibits typical convex downwards pattern in the paleochannel aquifer areas for both pre- and post-monsoon data sets; this indicates higher hydraulic conductivity and porosity in the paleochannel region. This further shows that if groundwater is recharged through paleochannels, it will slowly recharge the alluvial plains too.
6. Considering the various aspects, an integrated three–stage planning using rainfall runoff water and barely 1% of the canal discharge in the lean water demand period (July-September), has been suggested – that would be sufficient to meet the requirement of artificial recharge and arrest the declining groundwater table in the study area.

The above are important findings, as it has been widely believed and accepted that the Indo-Gangetic Plains comprise vast stretches of alluvium possessing laterally near–uniform hydrogeological/sedimentological characteristics, and only vertical variation in clay/silt/sand content of sediments leads to significant changes in hydrogeological behaviour. Delineation of major paleochannels (2-5 km wide and 60-80 km long) generally N–S trending and extending upto depth of 60 m below ground level, having very different hydrogeological characteristics, acting as almost conduits of very high vertical and lateral hydraulic conductivity – are important new site–specific findings.

References

Abu-Taleb, M., (1999) The Importance of Artificial Groundwater Recharge in Water Management Policy Analysis, In: *Proceedings of the Regional Seminar on Potential of Artificial Recharge of Groundwater*, University of Jordan, Amman, Jordan.

Allison, G. B. and Hughes, M. W., (1978) The Use of Environmental Chloride and Tritium to Estimate Total Recharge to an Unconfined Aquifer, *Australian Journal of Soil Research*, 16, 181-195.

American Society of Civil Engineers, (2001) Standard Guidelines for Artificial Recharge of Ground Water, *American Society of Civil Engineers,* ASCE, EWRI/ASCE 34-01.

Anbazhagan, S., Ramasamy, S. M. and Edwin, J. M., (1997) Artificial Recharge Studies through Remote Sensing in Central Part of Tamil Nadu, India, *IEEE*, 29-31.

Anbazhagan, S., Aschenbrenner, F. and Knoblich, K., (1999) Geographic Information System for Artificial Recharge Study in Germany, *IEEE*, 2380-2382.

Anbazhagan, S., Ramasamy, S. M and Das Gupta, S., (2005) Remote Sensing and GIS for Artificial Recharge Study, Runoff Estimation and Planning in Ayyar basin, Tamil Nadu, India, *Environmental Geology*, 48, 158–170, *DOI 10.1007/s00254-005-1284-4.*

Anderson, J. M., Hardy, E. E., Roach, J. T. and Witmert, R. E., (1976) A Land Use Classification System for Use with Remote Sensing Data, *U. S. Geological Survey Professional Paper*, No. 964, Washington DC: Government Printing Office.

Anon, (1973) A Method for Estimating Volume and Rate of Runoff in Small Watersheds, Technical Paper No. 149, *Soil Conservation Service*, USDA- SCS, Washington, D.C.

Aronoff, S., (1989) Geographic Information Systems: A Management Perspective, *WDL Publications*, Ottawa.

Arora, M. K. and Agarwal, K., (2002) A Computer Program for Sampling Design to Assess Image Classification Accuracy, *Photogrammetry Journal of Finland*, 18(1), 33-43.

Athavale, R. N. and Rangarajan, R., (2000) Annual Replenishable Groundwater Potential of India - An Estimate Based on Injected Tritium Studies, *Journal of Hydrology*, 234, 38-53.

Australian Water Resources Council, (1982) Guidelines for the Use of Reclaimed Water for Aquifer Recharge, Series Editor: Council, Australian Water Resources Series Title: Water Management, Series. No. 2 (Australian Government Publishing Service, Department of National Development and Energy).

Barksdae, H. C. and Debuchanne, G. D., (1946) Artificial Recharge of Productive Groundwater Aquifers in New Jersey, *Economic Geology*, 41, 726.

Batchelor, C. H., Rama, M. R. and James, A. J., (2000) Karnataka Watershed Development Project, Water Resources Audit, KWAD Murray and Tredoux , KWAD Report, 17.

Beeby-Thompson, A., (1950) Recharging London's Water Basin, *Timer Review Industry*, 20–25.

Bhowmic, A. N., (1992) The Prospect of Geophysical Surveys for Artificial Recharge Studies in Granitic Terrain – A futuristic Approach, In: *Proceeding on Workshop on Artificial Recharge of Groundwater in Granitic Terrain*, Bangalore, India, 46-64.

Bobba, A. G., Bukata, R. P. and Jerome, J. H., (1992) Digitally Processed Satellite Data as a Tool in Detecting Potential Groundwater Flow Systems, *Journal of Hydrology*, 131(1-4), 25–62.

Bourgeosis, P. O., (1972) Notes on Developing Ground Water, *Water and Pollution Control*, 110(10), 24-28.

Bouwer, H., (1996) Issues in Artificial Recharge, *Water Science and Technology*, 33, 381-390.

Bouwer, H., (2002) Artificial Recharge of Groundwater: Hydrogeology and Engineering, *Hydrogeology Journal*, 10, 121-142.

Brown, R., B., (1990) Soil Texture, Fact sheet SL-29, Soil and Water Science Department, Florida Cooperative Extension Service, Institute of Food and Agricultural Sciences, University of Florida.

Carver, R. E., (1971) Procedure in Sedimentary Petrology, *Wily-Interscience*, Division of John Wiley & Sons.

Census of India, (1991) *http://www.indiastat.com/india/Villages/village_population.asp.*

Census of India, (2001) Final Population Totals, Series-8, Published by Director of Census Operations, Delhi.

Central Ground Water Board (CGWB), (1997) Groundwater Resources Estimation Methodology, Report of the Groundwater Resources Estimation Committee, *Ministry of Water Resources*, India.

Central Ground Water Board (CGWB), (2000) Guide on Artificial Recharge to Groundwater, *Ministry of Water Resources*, New Delhi, India.

Central Ground Water Board (CGWB), (2000) Evaluation of Impact of Central Sector Artificial Recharge Scheme on Ground Water System (8th plan), *Central Ground Water Board*, India.

CGWB/UNESCO, (2000) Rainwater Harvesting and Artificial Recharge to Groundwater - A guide to follow, *Central Ground Water Board,* India, *UNESCO, IHP Programme.*

Chand, R., Hodlur, G. K., Prakash, M. R., Mondal, N. C. and Singh, V. S., (2005) Reliable Natural Recharge Estimates in Granitic Terrain, *Current Science*, 88, 821-824.

Chavez, P. S. Jr., (1988) An Improved Dark Object Subtraction Technique for Atmospheric Correction of Multispectral Data, *Remote Sensing of Environment*, 24, 459-479.

Chowdhury, A., Jha, M. K. and Machiwal, D., (2003) Application of Remote Sensing and GIS in Groundwater Studies: An Overview, *Proceedings of the International Conference on Water & Environment (WE-2003)*, Ground Water Pollution, 15–18 December, 2003, M.P., India, 39–50.

Chow, V. T., Maidment, D. R. and Mays, L. W., (1988) Applied Hydrology, *McGraw Hill*, NewYork.

Clarke, R., (1991) Water: The International Crisis, *Earthscan Publications Ltd.*, London, 193p.

Cochran, R., (1981) Artificial recharge and its potential for Oklahomas Ogallala Aquifer, *Oklahoma Water Resources Board*, Oklahoma.

Craig, H., (1961a) Standards for Reporting Concentrations of Deuterium and Oxygen-18 in Natural Waters, *Science*, 133, 1833-1834.

Craig, H., (1961b) Isotopic Variations in Meteoric Waters, *Science*, 133, 1702-1703.

Csaplovics, E., (1998) High Resolution Space Imagery for Regional Environmental Monitoring – Status Quo and Future Trends, *International Archives of Photogrammetry & Remote Sensing*, 32(7), 211-216.

Datta, P. S., Goel, P. S. and Rama Sangal, S. P., (1973) Groundwater Recharge in Western Uttar Pradesh, *Proceedings of Indian Academy of Sciences*, LXXV, 1-12.

Datta, P. S., (1975) Groundwater Recharge Studies in the Indo-Gangetic Alluvial Plains Using Tritium Tracer, Ph. D Thesis (unpublished), Indian Institute of Technology Kharagpur, India.

Deckers, F. and Te Stroet, C. B. M., (1996) Use of GIS and Database with Distributed Modeling. In: *Abbott MB, Refsgaard JC (Eds),* Distributed Hydrological Modeling, Kluwer Academic Publishers, Dordrecht, 215–232.

DeVantier, B. A. and Feldman, A. D., (1993) Review of GIS Applications in Hydrologic Modeling, *Journal of Water Resources Planning and Management*, ASCE,119(2), 246–261.

de Villiers, M., (2000) Water: The Fate of Our Most Precious Resource, *Mariner Books*, Houghton, Mifflin, Boston.

Edet, A. E., Okereke, C. S., Teme, S. C. and EsuE, O., (1998) Application of Remote Sensing Data to Groundwater Exploration: a Case Study of the Cross-river State, Southeastern Nigeria, *Hydrogeology Journal*, 6, 394–404.

Edmunds, W. M. and Walton, N. R. G., (1980) A Geochemical and Isotopic Approach to Recharge Evaluation in Semi-arid Zone; Past and Present, *International Atomic Energy Agency*, Vienna, STI/PUB/547, 47-68.

Elango, L. and Arrikkat, S., (1998) Groundwater Recharge Studies in Ongur Subbasin, South India using Geographical Information System, In: *Proceedings of the 3rd International Conference on Hydroinformatics*, 24–26 August 1998, Copenhagen, Denmark, 1, 505–510.

Engman, E. T. and Gurney, R. J., (1991) Remote Sensing in Hydrology, *Chapman and Hall*, London, 225p.

Falkenmark, M. and Lundqvist, J., (1997) World Freshwater Problems – Call for a New Realism, *UN/SEI*, New York/Stockholm, 53p.

Faust, N., Anderson, W. H. and Star, J. L., (1991) Geographic Information Systems and Remote Sensing Future Computing Environment, *Photogrammetric Engineering and Remote Sensing*, 57(6), 655–668.

Fetter, C. W., (1994) Applied Hydrogeology: Englewood Cliffs, New Jersey, Prentice-Hall, 691p.

Foody, G. M., Campbell, N. A., Trodd, N. M. and Wood, T. F., (1992) Derivation and Applications of Probabilistic Measures of Class Membership from Maximum Likelihood Classification, *Photogrammetric Engineering & Remote Sensing*, 58, 1335-1341.

Foody, G. M., (2002) Status of Land Cover Classification Accuracy Assessment, *Remote Sensing of Environment*, 80, 185-201.

Gale, I., Neumann, R., Calow, R. and Moench, M., (2002) The Effectiveness of Artificial Recharge of Groundwater: A Review, British Geological Survey Commercial Report CR/02/108N.

Ghosh, R., Goel, R. K., Lole, B. S., Singh, T. P., Sastry, K. L. N., Patel, J. G., Vanikar, Y. V., Thakker, P. S. and Navalgund, R. R., (1993) District Level Planning - A Case Study for the Panchmahals District Using Remote Sensing and Geographic Information System Techniques, *International Journal of Remote Sensing*, 14, 3163-3168.

Gogu, R. C., Carabin, G., Hallet, V., Peters, V. and Dassargues, A., (2001) GIS-based Hydrogeological Databases and Groundwater Modeling, *Hydrogeology Journal*, 9, 555–569.

Goodchild, M. F., (1993) The State of GIS for Environmental Problem-solving. In: *Goodchild MF, Parks BO, Steyaert LT (eds)*, Environmental Modeling with GIS, Oxford University Press, New York, 8–15.

Gossel, W., Ebraheem, A. M. and Wycisk, P., (2004) A very Large Scale GIS-based Groundwater Flow Model for the Nubian Sandstone Aquifer in Eastern Sahara (Egypt, northern Sudan and eastern Libya), *Hydrogeology Journal*, 12(6), 698–713.

Goyal, S., Bharadwaj, R. S. and Jugran, D. K., (1999) Multicriteria Analysis using GIS for Ground Water Resource Evaluation in Rawasen and Pilli watersheds, U.P., India, *www.GISdevelopment.net.*

Gupta, R. P., (2003) Remote Sensing Geology, 2nd Edition, *Springer-Verlag*, Berlin-Heidelberg, Germany, 655p.

Gupta, S. K. and Sharma, P., (1984) Radioactive Tracer in Groundwater Hydrology of Sabarmati Basin, Western India: A Case Study, *Paper IAEA-SM-270/71P*, Extended Synopsis Volume, Vienna, 157-161.

Hadithi, M. A., Shukla, D. C. and Israil, M., (2003) Evaluation of Groundwater Resources Potential in Ratmau-Pathri Rao Watershed Haridwar District, Uttaranchal, India using Geo-electrical, Remote Sensing and GIS Techniques, In: *Proceedings of the International Conference on Water and Environment (WE-2003)*, Bhopal, India, Ground Water Pollution, 123–125.

Harter, T., (2003) Groundwater Sampling and Monitoring, University of California, Division of Agriculture and Natural Resources, Publication 8085, FWQP Reference Sheet 11.4.

Hazen, A., (1911) Discussion—Dams on Sand Foundations: In Transactions, *American Society of Civil Engineers*, 73, 199p.

Heilman, J. L. and Moore, D. G., (1981) Groundwater Applications of the Heat Capacity Mapping Mission, *Satellite Hydrology*, AWRA, Minneapolis, MN, 446–449.

Hendrix, W. G. and Price, J. E., (1986) Application of Geographic Information Systems for Assessment of Site Index and Forest Constraints, *Proceedings of the GIS workshop*, ASPR, Falls Church Vernia, 368-377.

Hill, J. M., Singh, V. P. and Aminian, H., (1987) A Computerised Data Base for Flood Prediction Modelling, *Water Resource Bulletin*, American Water Resources Association, 23, 21-27.

Hillel, D., (1982) Introduction to Soil Physics, *Academic Press Inc.*, Harcourt Brace Jovanovich Publishers, San Diego, 365p.

Hinton, J. C., (1996) GIS and Remote Sensing Integration for Environmental Applications, *International Journal of Geographical Information Systems*, 10(7), 877–890.

Huisman, L. and Olsthoorn, T. N., (1983) Artificial Groundwater Recharge, *Pitman*, Boston.

Israil, M., Mufid al-hadith, Singhal, D. C. and Kumar, B., (2004) Groundwater-recharge Estimation Using Surface Electrical Resistivity Method in the Himalayan Foothill Region, India, *Hydrogeology Journal*, DOI 10.1007/s10040-004-0391-8.

Jacobus, J., de Vries. and Simmers, I., (2002) Groundwater Recharge: An Overview of Processes and Challenges, *Hydrogeology Journal*, 10, 5-17.

Jackson, J. J., Ragan, R. M. and Shubinski, R. P., (1996) Flood Frequency Studies on Ungaged Urban Watersheds using Remotely Sensed Data, In: *Proceedings of the Natural Symposium on Urban Hydrology*, University of Kentucky, 3–9.

Jain, V., and Sinha, R., (2003) River Systems of the Ganga Plains and their Comparison

with Siwaliks: A Review, *Current Science*, 84 (8), 1025-1033.

Jaiswal, R. K., Mukherjee, S., Krishnamuthy, J. and Saxena, R., (2003) Role of Remote Sensing and Geographic Information System Techniques for Generating of Ground Water Prospect Zones Towards Rural Development - An Approach, *International Journal of Remote Sensing*, 24, 993-1008.

Jensen, J. R. (1996) Introductory Digital Image Processing-A Remote Sensing Perspective, 2nd Edition, *Prentice-Hall*, New Jersey, US, 379p.

Jha, M. K., Chowdhury, A., Chowdary, V. M. and Peiffer, S., (2006) Groundwater Management and Development by Integrated Remote Sensing and Geographic Information Systems: Prospects and Constraints, *Water Resource Management, DOI 10.1007/s11269-006-9024-4.*

Jha, M. K. and Peiffer, S., (2006) Applications of Remote Sensing and GIS Technologies in Groundwater Hydrology: Past, Present and Future, *Bayreuther Forum Ökologie*, 112.

Kamal, A., (1999) Hydrogeolgical Zonation of Groundwater Aquifer in parts of Saharanpur and Hardwar Districts - An Integrated Approach through Remote Sensing and GIS Techniques (unpublished), Dissertation Thesis, University of Roorkee, India, 85p.

Kamaraju, M. V. V., Bhattacharya, A., Reddy, G. S., Rao, G. C., Murthy, G. S. and Rao, T. C. M., (1995) Groundwater Potential Evaluation of West Godavari District, Andhra Pradesh State, India – A GIS Approach, *Ground Water*, 34(2), 318–325.

Karanth, K. R., (1963) Groundwater Assessment, Development and Management, *Tata Mcgraw Hill*, New Delhi.

Kathryn, F. C., Thomas, W., Gardne, R. and Gar, Y. W. P., (1986) Digital Analysis of the Hydrologic Components of Watersheds Using Simulated SPOT Imagery, Hydrologic Application of Space Technology, *Proceedings of the CocoaBeach Workshop*, Florida, IAHS160, 355–365.

Krishnamurthy, J. and Srinivas, G., (1995) Role of Geological and Geomorphological Factors in Groundwater Exploration: A Case Study using IRS-LISS-II Data, *International Journal of Remote Sensing*, 7, 2595-2618.

Krishnamurthy, J., Kumar, N. V., Jayaraman, V. and Manivel, M., (1996) An Approach to Demarcate Groundwater Potential Zones through Remote Sensing and a Geographic Information System, *International Journal of Remote Sensing*, 17(10), 1867–1884.

Kumar, S., Parkash, B., Manchanda, M. L. and Singhvi, A. K., (1996) Holocene Landform and Soil Evolution of the Western Gangetic Plains: Implications of Neotectonics and Climate, *Z. Geomorph. N.F.*, Suppl.-Bd 103, 283-312.

Lachassagne, P., Wyns, R., B´erard, P., Bruel, T., Ch´ery, L., Coutand, T., Desprats, J-F. and Strat, P. L., (2001) Exploitation of High-yields in Hard-rock Aquifers: Downscaling Methodology Combining GIS and Multicriteria Analysis to Delineate Field Prospecting Zones, *Ground Water*, 39(4), 568–581.

Libby, W. F., (1946) Atmospheric Helium Three and Radiocarbon from Cosmic Radiation, *Physical Review*, 69, 671-672.

Lillesand, T. M. and Kiefer R. W., (1999) Remote Sensing and Image Interpretation, *John Wiley and Sons*, New York, 724p.

Loague, K. and Corwin, D. L., (1998) Regional-scale Assessment of Non-point Source Groundwater Contamination, *Hydrological Processes*, 12(6), 957–966.

Mather, P. M., (1999) Computer Processing of Remotely-Sensed Images: An Introduction, 2nd Edition, *Willey*, Chichester, UK, 306p.

Meijerink, A. M. J., (1974) Photohydrological Reconnaissance Survey, *International Institute for Areal Survey and Earth Sciences (ITC)*, Enschede, Neatherland.

Meijerink, A. M. J., (2000) Groundwater, In: *Schultz GA, Engman ET (Eds)*, Remote Sensing in Hydrology and Water Management, Springer, Berlin, 305–325.

Mithal, R. S., Singhal, B. B. S. and Bajpai, I. P., (1973) Groundwater Conditions on Gangetic Alluvium of Uttar Pradesh, *Proceedings of International Symposium on Development of Groundwater Resources*, Madras, India, 53-61.

Mohindra, R., Prakash, B. and Prasad, J., (1992) Geomorphology and Pedology of the Gandak Megafan and Adjoining Areas in the Middle Gangetic Plains, India, *Earth Surface Proceedings on Landforms*, 17, 643-663.

Mondal, N. C. and Singh, V. S., (2004) A New Approach to Delineate the Groundwater Recharge Zone in Hard Rock Terrain, *Current Sciences*, 87, 658-662.

Munnich, K. O., (1968a) Moisture Movement Measured by Isotope Tagging, *In: Guide Book on Nuclear Techniques in Hydrology*, International Atomic Energy Agency, Vienna, 112-117.

Munnich, K. O., (1968b) Use of Nuclear Techniques for the Determination of Groundwater Recharge Rates, *In: Guide Book on Nuclear Techniques in Hydrology*, International Atomic Energy Agency, Vienna, 191-197.

Musa, K. A., Akhir, J. M. and Abdullah, I., (2000) Groundwater Prediction Potential Zone in Langat Basin using the Integration of Remote Sensing and GIS, *www.GISdevelopment.net.*

Myers, V. I. and Moore, D. G., (1972) Remote Sensing for Defining Aquifers in Glacial Drift, In: *Proceedings of the 8th International Symposium on Remote Sensing of the Environment*, Environmental Research Institute of Michigan, Ann Arbor, MI, 715–728.

Nakata, T., (1982) A Photometric Study of Active Faults in Nepal Himalayas, *Journal of Nepal Geological Society*, 2, 67-80.

Narang, R. S. and Virmani, S. M., (2001) Rice-Wheat Consortium for the Indo-Gangetic Plains, *http://www.rwc.cgiar.org/new/docs/CPS-11.pdf.*

National Bureau of Soil Survey and Land Use Planning, (1999) Soil Map of Uttar Pradesh, Sheet No.1, Scale 1: 500,000.

National Institute of Hydrology (NIH), (1986) Hydrogeological Investigation in Sabarmati and Mahi Basins and Coastal Saurahtra using Radioisotopes and Chemical Tracers - A Report, NIH, Roorkee, India.

National Institute of Hydrology, (1998) Review of Artificial Recharge Practices, *National Institute of Hydrology Roorkee (India)*, Jal Vigyan Bhawan, SR-5/97-98.

National Institute of Hydrology (NIH), (2000) Study of Soil Moisture Movement and Recharge to Groundwater due to Monsoon Rains and Irrigation using Tritium Tagging Technique in Saharanpur District, NIH, Roorkee, India, Report No. CS/AR-23/1999-2000.

Navalgund, R. R. and Kasturirangan, K., (1983) The Remote Sensing Satellite – A Program Overview, In: *Proceedings of Indian Academy of Sciences; Engineering – Sciences – Remote Sensing – III*, 6, 313-336.

Navalgund, R. R., (2001) Remote Sensing – Basics and Applications, *Resonance: Journal of Science Education*, 51-60, *http://www.ias.ac.in/resonance/Dec2001/pdf/Dec2001 p51-60pdf.*

Nefedov, K. E. and Popova, T. A., (1972) Deciphering of Groundwater from Aerial Photographs, *Amerind*, New Delhi.

O'Hare, M. P., Fairchild, D. M., Hajali, P. A. and Canter, L. W., (1982) Artificial Recharge of Ground Water, Status and Potential in the Contiguous United States, *Norman*, Oklahoma.

Pandy, M. P., Raghava, R. and Raju, T. S., (1963) Groundwater Resources of Tarai-Bhabar Belts and Intermontane Doon Valley of Western Uttar Pradesh, *Exploratory Tubewells Organization*, Ministry of Food and Agriculture, India.

Ponce, V. M. and Hawkins, R. H., (1996) Runoff Curve Number: Has it Reached Maturity?, *Journal of Hydrologic Engineering*, 1(1), 11–19.

Ponce, V. M., Pandey, R. P. and Kumar, S., (1999) Groundwater Recharge by Channel Infiltration in El Barbon Basin, Baja California, Mexico, *Journal of Hydrology*, 214, 1-7.

Pyne, R. D. G., (1995) Groundwater Recharge and Wells: a Guide to Aquifer Storage Recovery, *Lewis Publishers*.

Ragan, R. M. and Jackson, T. J., (1980) Runoff Synthesis Using Landsat and SCS Model, *Journal of Hydraulic Division*, ASCE, 106(HY5), 667-678.

Raghunath, H. M., (2003) Groundwater, 2nd Edition, *New Age International (P) Ltd.*, New Delhi, Bangalore, Guwahati, Hyderabad, Kolkata, Lucknow, Mumbai, 563 pp.

Raiverman, V., Kunte, S. V. and Mukherji, A., (1983) Basin Geometry, Cenozoic Sedimentation and Hydrocarbon Prospects in Northwestern Himalaya and Indo-Gangetic Plains, *Petroleum Asia*, 6, 66-97.

Ramalingam, M. and Santhakumar, A. R., (2002) Case Study on Artificial Recharge using Remote Sensing and GIS, *www.GISdevelopment.net.*

Ramasamy, S. M. and Anbazhagan, S., (1997) Criteria and Techniques of Detecting Site- specific Mechanisms for Artificial Recaharge – A Case Study from Ayyar Basin, India, *Journal of Geological Society of India*, 50, 449-456.

Rao, M. B. R., (1973) The Subsurface Geology of Indo-Gangetic Plains, *Journal of Geological Society of India*, 14, 217-242.

Richards, J. A. and Jia, X., (1999) Remote Sensing Digital Image Analysis: An Introduction, 3rd Edition, *Springer-Verlag*, Heidelberg, Germany, 363p.

Romani, S., (1998) On the Technique of Water Conservation and Artificial Recharge Adopted in the Drought Affected Jhabua District of M.P., *Bhujal News*, 3(1).

Ross, M. A. and Tara, P. D., (1993) Integrated Hydrologic Modeling with Geographic Information Systems, *Journal of Water Resources Planning and Management*, ASCE 119(2), 129–141.

Salama, R. B., Tapley, I., Ishii, T. and Hawkes, G., (1994) Identification of Areas of Recharge and Discharge using Landsat-TM Satellite Imagery and Aerial Photography Mapping Techniques, *Journal of Hydrology*,162(1– 2),119–141.

Samadder, R. K., Kumar, S. and Gupta, R. P., (2007) Conjunctive Use of Well-log and Remote Sensing Data for Interpreting Shallow Aquifer Geometry in Ganga Plains, *Journal of the Geological Society of India*, 69, 925-932.

Sander, P., Chesley, M. M. and Minor, T. B., (1996) Groundwater Assessment using Remote Sensing and GIS in a Rural Groundwater Project in Ghana: Lessons Learned, *Hydrogeology Journal*, 4(3), 40–49.

Sanjeevi, S., (1996) Morphology of Dunes of the Coromandel Coast of Tamil Nadu: A Satellite Data Based Approach for Coastal Landuse Planning, *Landscape and Urban Planning*, 34, 189-195.

Sanjeevi, S., Vani, K. and Lakshmi, K., (2001) Comparison of Conventional and Wavelet Transform Techniques for Fusion of IRS-1C LISS-III and PAN Images, In: *Proceddings of ACRS 2001 – 22nd Asian Conference on Remote Sensing*, 21(12), 2345-2352.

Saraf, A. K. and Chaudhury, P. R., (1998) Integrated Remote Sensing and GIS for Groundwater Exploration and Identification of Artificial-recharge Sites, *International Journal of Remote Sensing*, 19(10), 1825-1841.

Sastri, V. V., Venkatachala, B. S., Bhandari, L. L., Raju, A. T. R. and Datta, A. K. (1971) Tectonic Framework and Subsurface Stratigraphy of Ganga Basin, *Journal of Geological Society of India*, 12(3), 222-233.

Scanlon, B. R., Healy, R. W. and Cook, P. G., (2002) Choosing Appropriate Techniques for Quantifying Groundwater Recharge, *Hydrogeology Journal*, 10(1), 18-39.

Schultz, G. A., (1993) Application of GIS and Remote Sensing in Hydrology. In: *Kovar K, Nachtnebel HP (Eds)*, Application of Geographic Information Systems in Hydrology and Water Resources Management, IAHS Pub. No. 211, 127–140.

Schultz, G. A., (1998) Remote Sensing in Hydrology, *Journal of Hydrology*, 100, 239-265.

Shahid, S. and Nath, S. K., (2002) GIS Integration of Remote Sensing and Electrical Sounding Data for Hydrogeological Exploration, *Journal of Spatial Hydrology*, 2(1), 1–10.

Shakeel, M., (1997) An Integrated Approach for Evolution of Hydraulic Properties of Alluvial Aquifer, Ph. D Thesis (unpublished), Department of Hydrology, IIT Roorkee, India.

Shanmugam, P. Ahn, Y. H., Sanjeevi, S. and Manjunath, A. S., (2003) Integration of ERS- 2 SAR and IRS- 1D LISS-III for Improved Coastal Wetland Mapping, *Korean Journal of Remote Sensing*, 19(5), 351-361.

Shanmugam, P. and Sanjeevi, S., (2002) Analysis and Evaluation of Speckle Suppression Algorithms as Applied to Radar Images, *International Geoscience and Remote Sensing Symposium (IGARSS 2002)*, Ontario, Canada, July 9-13, 1-3.

Sharma, P. and Gupta, S. K., (1987) Isotopic Investigation of Soil Water Movement: A Case Study in the Thar Desert, Western Rajasthan, *Hydrological Sciences Journal*, 32, 469-483.

Sikdar, P. K., Chakraborty, S., Adhya, E. and Paul, P. K., (2004) Landuse/landcover Changes and Groundwater Potential Zoning in and around Raniganj Coal Mining Area, Bardhaman District, West Bengal: A GIS and Remote Sensing Approach, *Journal of Spatial Hydrology*, 4(2), 1–24.

Singh, A. K. and Prakash, S. R., (2002) An Integrated Approach of Remote Sensing, Geophysics and GIS to Evaluation of Groundwater Potentiality of Ojhala Sub-watershed, Mirjapur District, U.P., India, *www.GISdevelopment.net*.

Singh, A. K., Raviprakash, S., Mishra, D. and Singh, S., (2002) Groundwater Potential Modeling in Chandrapraha Subwatershed, U.P. using Remote Sensing, Geoelectrical, and GIS, *www.GISdevelopement.net* .

Singh, R. P., Agma, R. N. and Tyagi, K. K., (1983) Water Balance of Hindon-Yamuna Doab, *Groundwater Investigation Organization (GWIO)*, Roorkee Division, T.M. No. 148; GUA (R-1).

Singhai, S. K., Parkash, B. and Manchanda, M. L., (1991) Geological and Pedological Evolution of Haryana Satate, *Bulletine of Oil and Natural Gas Commission*, 28, 37-60.

Singhal, D. C. and Gupta, B. L, (1966) Analysis of Pumping Test Data from Well in the Indo-Gangetic Alluvium of India and its Bearing on the Aquifer Characteristics, *Journal of Hydrology*, 4, 121-140.

Sinha, R., Khanna, M., Jain, V. and Tandon, S. K., (2000) Mega-geomorphology and Sedimentation History of Parts of Ganga-Yamuna Plains, *Current Science*, 82, 562-566.

Sinha, R., Navada, S. V., Chatterjee, A., Kumar, S., Mitra, A. and Nair, A. R., (2000) Hydrogen and Oxygen Isotopes Analysis of Antarctic Lake Waters, Schirmacher Oasis, East Antarctica, *Current Science*, 78 (8), 992-995.

Sinha, R., Sanjoy, D. and Dikshit, O., (2002) GIS-Assisted Mapping of Catchment-scale Erosion and Sediment Sources in Alaknanda Valley, Garhwal Himalaya, India, *Zeitschrift fur Geomorphologie (Annals of Geomorphology)*, 46/2, 145-165.

Sinha, R., Jain, V., Prasad Babu, G. and Ghosh, S., (2005) Geomorphic Characterization and Diversity of the Fluvial Systems of the Gangetic Plains, *Geomorphology*, 70/3-4, 207-225.

Slack, R. B. and Welch, R., (1980) Soil Conservation Service Runoff Curve Number Estimates from Landsat Data, *Water Resource Bulletin*, 16, 887–893.

Srivastava, A., (2005) Aquifer Geometry, Basement-topography and Groundwater Quality around Ken Graben, India, *Journal of Spatial Hydrology*, 2(2), 1-7.

Srivastava, H., Patel, P. and Navalgund, R. R., (2006) Incorporating Soil Texture in Soil Moisture Estimation from Extended Low-1 Beam Mode RADARSAT-1 SAR Data, *International Journal of Remote Sensing*, 27, 2587–2598.

Stafford, D. B., (1991) Civil Engineering Applications of Remote Sensing and Geographic Information Systems, *ASCE*, New York.

Sukhija, B. S. and Rama, (1973) Evaluation of Groundwater Recharge in the Semi-arid Regions of India Using Environmental Tritium, *Proceedings of Indian Academy of Sciences*, 77, 279-292.

Sukhija, B. S., Nagabhushanam, P. and Reddy, D. V., (1996) Groundwater Recharge in Semi-arid Regions of India: An Overview of Results Obtained Using Tracers, *Hydrogeology Journal*, 4, 51-71.

Tait, N. G., Davison, R. M., Whittaker, J. J., Leharne, S. A. and Lerner, D. N., (2004) Borehole Optimization System (BOS) - A GIS Based Risk Analysis Tool for Optimizing the Use of Urban Groundwater, *Environmental Modeling and Software*,19, 1111-1124.

Tiwari, K. N., Kumar, P., Sebastian, M. and Pal, D. K., (1991) Hydrological Modeling for Runoff Determination, *Water Resources Development*, 7(3), 178-184.

Tandon, S. K., Gibling, M. R., Sinha, R., Singh V., Ghazanfari, P., Dasgupta, A., Jain, M. and Jain, V., (2006) Alluvial Valleys of the Gangetic Plains, India: Causes and Timing of Incision. In: *Incised Valleys in Time and Space*, SEPM Special Publication No. 85, 15-35.

Taylor, G. C., (1959) Groundwater Provinces of India, *Economic Geology*, 54, 683-697.

Teeuw, R. M., (1995) Groundwater Exploration using Remote Sensing and a Low-cost Geographical Information System, *Hydrogeology Journal*, 3(3), 21–30.

Todd, D. K., (1959) An Noted Bibliography on Artificial Recharge of Groundwater through 1954, U.S.G.S Water Supply Paper, 1477, 115.

Todd, D. K., (1980) Groundwater Hydrology, 2nd Edition, *John Wiley & Sons*, New York, 535p.

Todd, D. K. and Mays, L. W., (2005) Groundwater Hydrology, 3rd Edition, *John Wiley & Sons*, New York, 636p.

Travaglia, C. and Ammar, O., (1998) Groundwater Exploration by Satellite Remote Sensing in the Syrian Arab Republic, *www.fao.org* (accessed on June 25, 2003).

Tsakiris, G., (2004) Water Resources Management Trends, Prospects and Limitations, *Proceedings of the EWRA Symposium on Water Resources Management: Risks and Challenges for the 21st Century*, 2–4 September 2004, Izmir, 1–6.

Tsihrintzis, V. A., Hamid, R. and Fuentes, H. R., (1996) Use of Geographic Information Systems (GIS) in Water Resources: a Review, *Water Resources Management*, 10, 251–277.

Tzimopoulos, C., (1989) The Artificial Recharge of Groundwater: A Solution by Successive Variations of Steady Sates, *Water Resources Management*, 3, 231-239.

United Nations, (1975) Ground-Water Storage and Artificial Recharge, *United Nations Natural Resources/Water Series*, 2.

Urey, H. C., (1947) The Thermodynamic Properties of Isotopic Substances, *Journal of American Chemical Society*, 562-581.

USDA-SCS, (1985) National Engineering Handbook, Section 4 - Hydrology, Washington, D. C., USDA-SCS.

van de Griend, A. A., Camillo, P. J. and Gurney, R. J., (1985) Discrimination of Soil Physical Parameters, Thermal Inertia and Soil Moisture from Diurnal Surface Temperature Fluctuations, *Water Resources Research*, 21, 997–1009.

Vasanthakumaran, T., Shyamala, R. and Sridhar, K., (2002) Role of Remote Sensing and GIS in Identifying Artificial Recharge Zones of Upper Kolavarnar River Basin, Tamil Nadu, *www.GISdevelopment.net.*

Verhagen, B., Smith, T., McGeorge, P. E. and Dziembowski, I., (1979) Tritium Profiles in Kalahari Sand as a Measure of Rainwater Recharge, *Proceedings on Isotope Hydrology*, IAEA, Vienna, 733-749.

Viessman, J. R. W., Lewis, G. L. and Knapp, J. W., (1989) Introduction to Hydrology, 3rd Edition, *Harper and Row*, Singapore, 780p.

Waters, P., Greenbaum, P., Smart, L. and Osmaston, H., (1990) Applications of Remote Sensing to Groundwater Hydrology, *Remote Sensing Review*, 4, 223–264.

Watkins, D. W., McKinney, D. C., Maidment, D. R. and Lin, M. D., (1996) Use of Geographic Information Systems in Groundwater Flow Modeling, *Journal of Water Resources Planning and Management*, ASCE, 122(2), 88–96.

Wright, A., and Toit, Irene du., (1996) Artificial Recharge of Urban Wastewater, the Key Component in the Development of an Industrial Town on the Arid West Coast of South Africa, *Hydrogeology Journal*, 1, 118-129.

Yannian, Y. U., (1990) Hydrologic Effects of Forest, The Hydrological Basis for Water Resources Management, *Proceedings of the Beijing Symposium*, IAHS, Publication No. 197, 413–423.

Zhang, H., Haan, C. T. and Nofziger, D. L., (1990) Hydrologic Modeling with GIS: An Overview, *Applied Engineering in Agriculture*, ASAE, 6(4), 453–458.

Zimmerman, U., Ehhalt, D. and Munnich, K. O., (1967a) Soil Water Movement and Evapotranspiration: Changes in Isotopic Components of Soil Water, In: *Isotopes in Hydrology*, Proceedings Symposium, Vienna, 567-585.

Zimmerman, U., Munnich, K. O. and Roether, W., (1967b) Downward Movement of Soil Moisture Traced by Means of Hydrogen Isotopes, In: *Glenn ES (ed) Isotope techniques in the hydrologic cycle*: American Geophysical Union, Geophysical Monograph, 11, 28-36.

Internet Resource:

http://*www.nrsa.gov.in*